



^b
**UNIVERSITÄT
BERN**

Graduate School for Cellular and Biomedical Sciences
University of Bern

The Role of Stress in Neuropathophysiological Mechanisms of Functional Neurological Disorders

PhD Thesis submitted by

Samantha Weber

for the degree of

PhD in Neuroscience

Supervisor

Prof. Dr. med. Selma Aybek

Department of Neurology

Faculty of Medicine of the University of Bern

Co-advisor

Prof. Dr. Christopher Pryce

Department of Psychiatry, Psychotherapy & Psychosomatics

Faculty of Medicine of the University of Zurich

Accepted by the Faculty of Medicine, the Faculty of Science and the Vetsuisse
Faculty of the University of Bern at the request of the Graduate School for
Cellular and Biomedical Sciences

Bern,

Dean of the Faculty of Medicine

Bern,

Dean of the Faculty of Science

Bern,

Dean of the Vetsuisse Faculty Bern

Acknowledgements

This PhD has been an inspirational and instructive journey, where I grew beyond myself, met many inspirational people, and found so much joy in developing new ideas and projects. I am very grateful for every experience I made, every adventure I had, and every person who supported and joined me on this journey.

Firstly, I would like to thank my supervisor Prof. Dr. med. Selma Aybek. Thank you for giving me this amazing opportunity and experience. Being an inspirational and strong woman to whom I can look up to, you have taught me more than just “being a good scientist”. You have always supported me, never had a doubt about me, pushed me beyond what I thought I could do, but most importantly made me enjoy every (scientific) moment of my PhD. I admire you as my supervisor, but even more as a person. You are very kind, intelligent, respectful, fair, and always late. Thank you for everything!

I would like to thank to my co-advisor Prof. Dr. rer. nat. Christopher Pryce for his engagement, the interesting scientific discussions, and his constructive feedback on my project. You have taught me to always critically question my results, and you have made me a better scientist. I would like to thank Prof. Dr. med. Michele Tinazzi for his dedication, his external evaluation of my project and his kind feedback. Moreover, a special thank goes to Prof. Rupert Bruckmaier for his excellent mentorship far beyond the requirements of the graduate school. Thank you for being available when help was needed, for your expertise on the analyses, and for your supportive and kind personality.

A very special thank goes to my colleague and partner in ~~erime~~ research Janine (the Schänu) Bühler. Thank you for the great teamwork throughout our PhDs, thank you for complementing me, thank you for being my inner voice of sanity, thank you for being the biceps to my (very weak) coracobrachialis, and thank you for having made me enjoy every (non-scientific) moment of my PhD. What has started as colleagues, has turned into friendship and I hope we will always remember our great time we had together in the FND Lab.

I would like to also thank all the other lab members I have met during this time. A special thank goes to Giorgio A. Vanini. With your calm and relaxing attitude, you have taught us so much more than only the difference between Tagliatelle and Orecchiette. Many thanks go to Salome Heim for being the first friend I made in the FND Lab. Thank you for your refreshing nature. A special thank also goes to Dr. Serafeim Loukas, who has taught me so much and has helped me with all the analysis of my projects.

I also want to express my gratitude to Prof. Dimitri Van De Ville and Dr. Thomas Bolton for always supporting me, whenever help was needed. I also would like to thank to Samuel Stettler and the whole team of the translational imaging centre. Thank you for creating such a relaxed, and happy mood during our measurement sessions, for all the free coffee, and for all the funny moments.

Not to forget, I want to thank to all the healthy volunteers and patients who kindly participated in our studies. Especially, I want to thank all the numerous patients with FND. It was a pleasure to meet every single of you and to see how enthusiastically you all participated in our studies! Thank you all for giving me the feeling that this work counts and that I can contribute.

Lastly, I want to thank my family and friends. Specifically, to my mother. You are great, funny, and the coolest mom ever! Thank you for that you have supported me in every step of my life. A special last thank goes to my boyfriend Joaquín Peñalver de Andrés. Thank you for walking this journey together, for sharing each of the good, but also bad moments, and for your unconditional support.

Abstract

Functional neurological disorders (FND) comprise the appearance of diverse neurological symptoms without an underlying classical neurological condition. “Medically unexplained neurological symptoms” have been stigmatized for a long time, and patients were often not been taken serious in their suffering. As historically FND has often been explained as a psychogenic disorder, underpinning the importance of psychological stress, contemporary models aim at integrating a multifactorial origin of FND by means of a biopsychosocial or stress-diathesis model unifying neuroscientific, psychological, and biological concepts in FND. Nowadays, FND is considered a neuropsychiatric disorder, and various risk factors could be identified, reliable clinical signs have been validated, and successful treatment options have been developed. Notwithstanding the enormous effort that has been devoted to identifying *why* and *how* FND develops, a satisfactory model of underlying pathophysiological mechanisms of FND remain elusive, and thus, objective biomarkers are lacking.

To fill this gap, this thesis aimed at connecting the questions on *why* and *how* FND emerges by studying the neurological, psychological, and physiological aspects of stress and unifying them within the context of a stress-diathesis model for FND. As such, potential biomarkers are investigated, and novel concepts of potential pathophysiological mechanisms are discussed.

First, the robustness and generalizability of resting-state functional magnetic resonance imaging (fMRI) was tested and evaluated in a multi-centre setting, as this has previously been suggested to serve as a potential positive imaging-based biomarker for FND. Second, stress biomarkers were examined and how they potentially relate to psychological and neurological correlates of FND. Third, large-scale functional brain network dynamics and their possible implication in the clinical presentation of symptoms were analysed.

The findings presented in this thesis demonstrate the applicability as well as the persisting technical limitations of resting-state fMRI as an imaging-based biomarker for FND. Further, it could be shown that FND patients have a flattened cortisol awakening response – a common biomarker for psychosocial stress – which was associated to emotional neglect as a precipitating risk factor for FND. Moreover, volumetric brain alterations have been identified in FND and their hypothetical role as predisposing factor was discussed. Lastly, distinct dynamic functional alterations encompassing the salience and limbic network were identified in FND patients, which appeared to correlate with symptom severity and stress biomarkers.

To conclude, the findings are discussed in the context of pre-existing pathophysiological models for FND and introduce novel points of view. Furthermore, the limitations of this work are thoroughly evaluated, and future directions and their applications are addressed. Lastly, the clinical importance and contribution to the field is comprehensively highlighted.

Altogether, the findings presented in this thesis support and expand previous literature by 1) demonstrating the predictive power of imaging-based biomarkers, 2) identifying potential

abnormalities in the biological stress axis within a standardized setting and discussing their novelty in the framework of the stress-diathesis model, and 3) firstly adopting a spatio-temporal network analysis in FND and reflecting on its neurophysiological relevance. In summary, this thesis supports a stress-diathesis model of FND and highlights potential psychological, neurological, and physiological attributes in the pathophysiological mechanisms of FND.

Contents

Abstract	vii
1 General Introduction	1
1.1. Functional neurological disorders.....	2
1.2. Functional neurological disorders and stress: a comprehensive view on <i>why</i> the symptoms develop	4
1.3. Functional neurological disorders and functional brain alterations: mechanistic insights on <i>how</i> the symptoms develop	10
1.4. Overview of the Thesis	13
2 Multi-centre Classification using Resting-state Functional Connectivity	26
2.1. Introduction.....	28
2.2. Materials and methods	30
2.3. Results.....	36
2.4. Discussion.....	43
3 A Biopsychological approach to the Stress-Diathesis Model	51
3.1. Introduction.....	53
3.2. Materials and methods	54
3.3. Results.....	59
3.4. Discussion.....	68
3 Dynamic Functional Connectivity	76
4.1. Introduction.....	78
4.2. Materials and methods	80
4.3. Results.....	84
4.4. Discussion.....	89
5 General Discussion and Outlook	98
5.1. Recap Thesis Background and Aims	99

5.2. General Findings of the Thesis	100
5.3. General Limitations and Future Directions.....	104
5.4. Contribution to the field.....	106
5.5. Conclusion	108
List of Tables	111
List of Figures	114
References	122
Curriculum Vitae	139
List of Publications.....	143
Declaration of Originality.....	146
Appendix A Supplementary Material for Chapter 2.....	148
Appendix B Supplementary Material for Chapter 3.....	167
Appendix C Supplementary Material for Chapter 4.....	190

List of Abbreviations and Acronyms

AAL	Automatic anatomic labelling (atlas)
ACC	Anterior cingulate cortex
ACTH	Adrenocorticotrophic hormone
AUC	Area-under-the-curve
BDI	Beck's depression inventory
CAP	Co-activation pattern
CAR	Cortisol awakening response
CGI	Clinical global impression (score)
CRF	Corticotropin-releasing factor
CTQ	Childhood trauma questionnaire
DAN	Dorsal attention network
DBC	Diurnal baseline cortisol
DBCC	Diurnal baseline cortisol concentration
dIPFC	Dorsolateral prefrontal cortex
DMN	Default mode network
DSM-5	Diagnostic and Statistical Manual of Mental Disorders 5 th Edition
ECN	Executive control network
FC	Functional connectivity
FDR	False-discovery rate
FWE	Family-wise error
fMRI	Functional magnetic resonance imaging
FND	Functional neurological disorders
HC	Healthy controls
HPA	Hypothalamus-pituitary-adrenal (axis)
IPL	Inferior parietal lobule
MRI	Magnetic resonance imaging
Nac	Nucleus accumbens
PACC	Post-awakening cortisol concentration
PAG	Periaqueductal gray
PCC	Posterior cingulate cortex
PLSC	Partial least squares correlation
PNES	Psychogenic non-epileptic seizures
PPPD	Persistent postural perceptual dizziness
PTSD	Post-traumatic stress disorder
ROI	Region-of-interest
S-FMDRS	Simplified version of the psychogenic movement disorder rating (scale)
SMA	Supplementary motor area
SOA	Sense of agency

STAI	State-trait anxiety inventory
SVD	Single value decomposition
SVM	Support vector machine (classifier)
TEC	Traumatic experiences checklist
TIV	Total intracranial volume
TPJ	Temporo-parietal junction
VBM	Voxel-based morphometry

CHAPTER 1

General Introduction

1.1. Functional neurological disorders

Functional neurological disorder (FND; conversion disorder; historically referred to as *hysteria*) is a debilitating and common neurological condition at the crossroads between neurology and psychiatry. Across the different subtypes of FND, patients often present with various neurological symptoms such as motor symptoms (e.g., tremor, weakness, gait disorder), sensory symptoms, psychogenic non-epileptic seizures (PNES), functional cognitive disorder, or persistent perceptual postural dizziness (Bennett et al., 2021; Hallett et al., 2022; Stone and Carson, 2015). In addition, patients can present with substantive symptom overlaps with a comorbid neurological disorder (e.g., stroke, multiple sclerosis, Parkinson's disease) and develop different symptoms throughout the course of their disease (Mckenzie et al., 2011). Amongst others, typical hallmark of functional neurological symptoms are inconsistency during distraction (Espay and Lang, 2015) or variability of the symptoms during neurological examinations (Hallett, 2015), paroxysmal akinesia or hyperkinesia (Espay et al., 2018a), or sensory loss unrelated to the dermatome map of innervation (Stone and Vermeulen, 2016). The symptoms, however, cannot be explained by traditional neurological diseases (Espay et al., 2018a) and were often categorized to as *medically unexplained* (Stone et al., 2009b). The symptoms, however, appear to be the product of underlying functional brain alteration (Drane et al., 2020; Perez et al., 2021), of which traditionally a psychogenic origin has been attributed (Kanaan and Craig, 2019). Nonetheless, the exact underlying pathophysiological mechanism remains unidentified (Voon et al., 2016).

Despite of '*functional/psychological*' being the second most common diagnosis in outpatient neurology clinics in the UK (J. Stone et al., 2010a), patients often undergo multiple time- and cost-consuming tests (Stephen et al., 2021) and clinical examinations to rule out an underlying organic lesion, neurological diseases, or other comorbid conditions (Espay et al., 2009; LaFaver et al., 2020). Even though accurate diagnostic criteria are nowadays well established (Bennett et al., 2021; Daum et al., 2015), clinicians themselves are still afraid of misdiagnosing patients (Walzl et al., 2019), suspect feigning (MacDuffie et al., 2021), or simply do not feel comfortable of addressing FND as a '*psychogenic*' diagnosis to their patients (Kanaan et al., 2009). In addition, patients often suffer from comorbidities such as fatigue, pain, as well as panic-, mood-, or anxiety disorders (Carson and Lehn, 2016). As a consequence, neurologists often acknowledge the severity of the patients' suffering, but do not feel responsible for their psychological concerns, what would force them to work outside of their field of expertise (Kanaan et al., 2009). On the contrary, patients feel insecure and not taken serious (Crimlisk et al., 2000), which often worsens their symptoms, as then an early diagnosis and corresponding treatment is often delayed (Gelauff et al., 2014).

The limited understanding of the pathophysiological mechanisms, the diverse symptom presentations, the physical- and psychological comorbidities, the unbearable suffering of patients, and the high socioeconomic burden highlight the need of advancing the understanding of FND as a disorder but also its significance as a diagnosis.

1.1.1. A historical view on functional neurological disorders

First records on FND predate 4000 years ago. Ancient Egyptians reported on convulsive symptoms presumably caused by spontaneous movements of the uterus (Tasca et al., 2012). Almost 2000 years later, Hippocrates – traditionally referred to as the *father of medicine* – reported on symptoms similar to those nowadays observed in FND. *Hysteria* – as he called the disease – was solely attributed to women caused by an unsatisfactory sexual life, which further caused the uterus to migrate – resulting in convulsions, tremors, anxiety, or paralysis. As such, the body part affected by the symptoms were explained as in where in the body the uterus was roaming (King, 1993; Tasca et al., 2012).

During the 18th century, the work on *Hysteria* was resumed by Pierre Briquet who shifted the aetiology of *Hysteria* away from female sexual frustration and towards a disease of the nervous system. Briquet theorized that the symptoms resulted from the suffering of the part of the brain responsible for emotional impressions and sentiments (Mai and Merskey, 1981).

In the late 19th century, Jean-Martin Charcot – known for his exceptional work on *Hysteria* – postulated that the symptoms might be produced by a *dynamic neurological lesion* triggered by emotional trauma (Aybek, 2019; Harris, 2005). Moreover, he firstly confirmed male hysteria (Harris, 2005). Research in FND took a turn as Sigmund Freud and Josef Breuer – founders of *psychoanalysis* - defined FND as a disorder of a psychological origin. They assumed that the repression of insufferable psychological-, or emotional distress from conscious awareness lead to the expression as – or conversion into – bodily symptoms (Kanaan, 2016; Nemiah, 1996), giving rise to the term *conversion disorder*. Moreover, these stressors were often assumed to be of sexual or physical nature (Roelofs and Pasmán, 2016).

As in the 20th century neurology and psychiatry were split in two distinct medical fields of expertise (Baker et al., 2002) – and with its division separated the mind from the body – FND was left behind in the ditch. Together with the traumatic aftermath of the world wars and their relevance for medicine, neurologists simply lost their interest in FND, and research in the field was put on hold (Fend et al., 2020). With the upcoming of functional magnetic resonance imaging (fMRI) in the late 20th century, neurology and psychiatry were united again in FND, which in turn regained its deserved attention in research (Raynor and Baslet, 2021). Suddenly, intrinsic differences in brain function could be studied (Aybek and Vuilleumier, 2016) and a new line of research developed trying to not only understand *why* but also *how* symptoms in FND develops (J. Stone et al., 2010b).

1.2. Functional neurological disorders and stress: a comprehensive view on *why* the symptoms develop

With Freud establishing FND as a *psychogenic* disorder, psychological stress or trauma became a critical requirement for the diagnosis of FND. Consequently, high interest has been devoted to study the role of psychological stress and trauma history in FND. Accordingly, sexual abuse (Betts and Boden, 1992), together with physical abuse (Alper et al., 1993) was firstly associated to PNES patients and to other FND subtypes (Roelofs et al., 2005, 2002; Spinhoven et al., 2004). Moreover, they linked severity and frequency of childhood abuse to symptom severity. Similarly, symptom onset and severity could be connected to recent adverse social-occupational life events with a partial link to early childhood physical and sexual abuse (Roelofs et al., 2005), highlighting the importance of type but also timing of trauma.

A substantial proportion of patients however, did not report on psychological stressors or past trauma, and consequently their causal role in the development of FND had to be questioned (Nicholson et al., 2011; Jon Stone et al., 2010). The diagnostic criteria for FND were thus reformulated in the 5th Edition of the *Diagnostic and Statistical Manual of Mental Disorders* (DSM-5), shifting from psychological stress and trauma as a prerequisite to a precipitating risk factor (American Psychiatric Association, 2013). Hence, the mind-body dualism of that symptoms are either the result of a psychiatric disorder or a neurological disease was resolved for FND (Cretton et al., 2020) and the disorder was newly defined a *neuropsychiatric* condition, linking psychological stressors and trauma as a risk factor – and not a requirement anymore – to the aetiology of FND. In this regard, recent models aim to integrate a multifactorial origin of FND investigating the neuropathophysiological mechanisms by means of a biopsychosocial model, unifying knowledge from neuroscience, psychology as well as biology to advance the understanding of FND (Cretton et al., 2020; Keynejad et al., 2019).

1.2.1. The role of trauma in functional neurological disorders

Adverse (early) life events have recurrently been reported in FND (Kanaan and Craig, 2019; Karatzias et al., 2017; Reuber et al., 2007; Roelofs and Pasman, 2016), traditionally highlighting the role of sexual (and physical) abuse during childhood. A recent meta-analysis on 34 studies comparing traumatic life events in FND patients to those in HCs and psychiatric control patients, indeed, confirmed an increased frequency of childhood and adult adverse life events and abuse in FND patients, as compared to other psychiatric conditions. On the contrary, it also highlighted once more the large number of patients who did not report on a particular trauma history (ranging from 14 to 77% across 13 studies). Denial or a memory- or recall bias, however, could not be excluded. Rather unexpectedly, the analysis also identified emotional neglect to be much stronger associated with the development of functional neurological symptoms, and thus weakened the dominating role of sexual abuse in the suspected aetiology

of FND (Ludwig et al., 2018). Similarly, a systematic review on 133 studies identified physical injury in 37% of the patients prior to symptom onset (Stone et al., 2009a). Interestingly, physical trauma was associated with late-onset of FND, whereas early-onset was rather linked to childhood sexual abuse (Morsy et al., 2021; Myers et al., 2021; Stone et al., 2009a). Alongside with psychological stressors, physical injuries (and correspondingly, inflammatory reactions) as precipitating risk factor opened the debate on how biology needs to be integrated in the disease model of FND.

Functional- and structural imaging studies intensively investigated the relationship between traumatic life events, symptom presentation and brain functional- and structural abnormalities in FND. Aybek and colleagues were the first to link recall of autobiographic traumatic memories to aberrant brain function in FND patients (Aybek et al., 2014a). While recalling traumatic events with escape potential¹, increased activity was found in the right supplementary motor area (SMA), the right temporo-parietal junction (TPJ), and the left dorsolateral prefrontal cortex (dlPFC). During the same condition, decreased activity was found in hippocampal and parahippocampal regions. Moreover, post-hoc functional connectivity (FC) analysis revealed an increased connectivity between the SMA and the left amygdala. The dlPFC is involved in executive functions (Grier, 2005; Hoffmann, 2013) such as the cognitive regulation of emotions (Dixon et al., 2017), and – together with the SMA (Nachev et al., 2008) – involved in motor planning and selection of action sequences based on internal and external cues. On the other hand, the hippocampal- and parahippocampal regions are essential for declarative and episodic memories (Natu et al., 2019), whereas the amygdala is a key region for emotion processing; Both regions are key hubs of the limbic network and amygdalar-hippocampal circuits thus play a key role in emotion-associated memory processing (Yang and Wang, 2017). Aybek and colleagues (Aybek et al., 2014a) could therefore firstly show that memories of traumatic events directly affect brain function in FND patients. Namely, reduced hippocampal activity might be a neural correlate of memory suppression, whereas the enhanced connectivity between the amygdala and the SMA might reflect increased arousal to emotional stress, which further modulates motor preparation and thus might represent a neural correlate of physical symptom presentation in FND. Nevertheless, preliminary results on memory suppression using a neuropsychiatric test battery did not reveal that patients suppressed negatively valenced memories. An impairment in declarative emotional memory thus, could not yet be identified in FND patients (Brown et al., 2014).

In a subsequent study, increased activity was found in the amygdala, the peri-aqueductal gray (PAG) matter, the dlPFC, the SMA, and the cingulate cortex in response to negatively

¹ Escape potential in traumatic events refers to having a secondary gain of being ill (Feinstein, 2011). As such, it is defined as the extent to which a subsequent disease after an adverse event might reduce the stressful effect of the event itself. An exemplification of a traumatic event with escape potential describes when a spouse threatens to divorce, and the subsequent illness of the individual might prevent the spouse from ending the relationship.

valenced (fearful and sad) faces (Aybek et al., 2015). Particularly via its connection to the amygdala, the PAG is a key region involved in motor reactions towards threatening stimuli (LeDoux et al., 1988). The results of these studies could once more link abnormal emotion regulation to motor dysfunctions in FND patients. In a similar study setting, neural responses to fearful and happy faces were compared between HC, functional- and essential tremor (Espay et al., 2018c), as well as between HC, functional- and organic dystonia (Espay et al., 2018b). Increased activity in the paracingulate cortex was found in functional tremor patients as compared to HC, as well as reduced primary motor regions (i.e., precentral gyrus) activation as compared to essential tremor. Moreover, decreased activity in motor regions as well as the insula were found in functional dystonia patients compared to both groups. The insula is an important hub of the salience network and involved in conscious and unconscious emotion processing as well as emotional awareness and interoception (Gu et al., 2013). Emotional awareness refers to the conscious (but also subconscious) processing of affective stimuli, whereas interoception refers to the perception of the body's state closely related to its emotional state (Gu et al., 2013). Hereafter, these studies confirmed an emotional-stimulus dependent alteration of brain networks involved in emotion processing as well as motor preparation and execution.

Abnormal emotion regulation was firstly directly linked to motor output in patients in a study in which the participants were asked to maintain a grip force while pleasant and unpleasant images were shown (Blakemore et al., 2016). Differently than in HC, patients showed an amplified force towards unpleasant images, together with increased activity in the hippocampus and the posterior cingulate cortex (PCC). The PCC and the hippocampus are thought to be involved in self-reflective behaviour (Brewer et al., 2013), and their aberrant activity was attributed to enhanced evaluation of visual stimuli as emotionally relevant. To recap, it was firstly shown that psychological stressors in patients might modulate voluntary motor actions.

Further, an aberrant neural response of cortico-limbic structures to stress was found during a psychosocial stress test, in which patients were asked to perform difficult math problems under time pressure and receiving negative feedback on their performance. As such, this study design allowed to directly observe brain function in response to acute stress situations. An increased neural response to psychosocial stress was found in the dorsomedial prefrontal cortex (dmPFC) and the left hippocampus, together with a reduced response in the dlPFC and the right hippocampus (Balachandran et al., 2021). It has been shown previously, that especially a decreased PFC and hippocampal activation has an inhibitory effect on the autonomic and endocrine stress response (Pruessner et al., 2008; Wheelock et al., 2016). Moreover, hippocampal deactivation disinhibits the hypothalamus-pituitary-adrenal (HPA) axis, triggering the stress response (e.g., cortisol secretion from the adrenal glands) (Pruessner et al., 2008; Wheelock et al., 2016). As such a direct link was established between aberrant brain activity, emotional hyperarousal, and the biological stress response.

While most studies investigated the relationship between psychosocial stress and functional brain abnormalities in FND within a task-based setting, similar results were also achieved in a resting-state setting, during which participants did not perform a specific task, and were asked to lay as calm as possible in the scanner. As such, using step-wise FC analyses on resting-state data of FND patients, Diez and colleagues identified enhanced functional propagation from primary motor areas to the amygdala, the insula, the cingulate cortex, as well as the TPJ (Diez et al., 2019). Moreover, functional propagation profiles of the insula and the amygdala correlated with symptom severity and could predict clinical improvement after a six-months follow-up. Comparatively in a seed-based analysis, connectivity between the right amygdala (seed) and the right middle frontal gyrus was reduced in FND patients and could be correlated to age of onset as well as symptom severity in FND (Spagnolo et al., 2020). Similarly, physical trauma in FND patients could be linked to aberrant connectivity profiles in limbic (amygdala-hippocampus), paralimbic (cingulo-insular and ventromedial prefrontal), as well as sensorimotor cortices (Diez et al., 2020). Interestingly, these connectivity profiles were not observed in psychiatric control patients with similar trauma scores as the FND cohort.

While functional MRI studies are abundant in FND, only few studies investigated structural aberrancies in relation to trauma, stress, and symptom presentation. As such, women with FND ($N = 18$) showed an inverse relationship between childhood abuse and a reduce brain volume in the insula (Perez et al., 2017a). In the full cohort ($N = 23$), a significant inverse relationship was found between number of traumatic events in FND patients and reduced volume in the hippocampus (Perez et al., 2017a). Comparatively, increased cortical thickness was found in premotor cortex of hemiparetic FND patients, which further positively correlated with symptom severity (Aybek et al., 2014b). Likewise, reduced cortical thickness in the anterior cingulate cortex (ACC) was found to be negatively associated to somatoform dissociation symptoms in motor FND patients (Perez et al., 2018).

In summary, increased amygdalar reactivity and increased limbic-motor, as well as altered cortico-limbic connectivity patterns have consistently been found in task-based, as well as resting-state fMRI studies in relation to stress and adverse life events. These regional abnormalities and alterations in FC can be associated to an altered social-emotional cognition, impaired interoceptive- and emotional awareness, as well as abnormal emotion-motion interactions in FND (Pick et al., 2019). These patterns might represent a maladaptive reaction to stress, could be related to the disorder itself (state) or might represent a predisposing vulnerability trait derived from preceding traumatic life events (Kozłowska, 2007; Roelofs and Pasma, 2016). The exact mechanisms or a potential causal relationship between trauma history, emotional arousal, and brain structural- and functional abnormalities, however, remain to be discovered.

1.2.2. Biological stress in functional neurological disorders

While the neural response to psychological stress and previous trauma has extensively been studied in FND, only little has been done focusing on the biological implications of stress. Previous results – especially on increased amygdalar reactivity to stress (see previous chapter) – suggests that patients find themselves in a hyperarousal state. Yet only little is known about the biological underpinnings of stress and its corresponding biomarkers of a potential hyperarousal state in FND. Responses to stress can be mediated twofold: 1) through a rapid sympathetic response mediated by the autonomic nervous system, and 2) through a slower response mediated by the HPA axis. Autonomic sympathetic stress responses mediated through biological messengers such as adrenaline and can be measured by means of an increase in heart rate, blood pressure, and respiratory frequency, as well as pupil dilatation, sweating, etc. (Gibbons, 2019). The hypothalamus, the pituitary gland, and the adrenal glands correspond to the three main anatomical structures regulating the adaptive (slow) response to stress (Smith and Vale, 2006), and will be further elucidated in Chapter 1.4.2.4. Activation of the HPA axis eventually leads to glucocorticoid synthesis and secretion of stress hormones such as cortisol. Cortisol itself can be measured non-invasively in the saliva and proved itself a reliable biomarker to study stress (Hellhammer et al., 2009; Wust et al., 2000).

Studying stress biomarkers in FND could advance the understanding of stress-related pathophysiological mechanisms, and a more detailed comprehension on the attributed effects from preceding stressful life events or predisposing factors might be obtained. As such, Bakvis and colleagues could show that PNES patients have a positive attentional bias towards threatening stimuli during an emotional Stroop task (Bakvis et al., 2009a), with an even stronger effect in patients with a history of sexual abuse. Correspondingly, the authors detected a decreased heart rate variability compared to HC, which was previously associated with poor emotion regulation (Ruiz-Padial et al., 2003). In summary, it was shown that patients were hypervigilant towards threatening stimuli together with an abnormal autonomic stress response. Likewise, increased heart rate and lower heart rate variability was found in children with FND during different task settings including a resting-state condition, an auditory attention task, and an emotional face-processing task during electro-encephalography measures (Kozłowska et al., 2017b, 2015). Some patients experienced a non-epileptic seizure during the data acquisition, which was accompanied with higher baseline heart rate, lower heart rate variability and exceptionally high resting respiratory rates, as compared to the other (non-seizure) patients (Kozłowska et al., 2015). Moreover, patients had a higher amplitude of event-related potentials to the emotionally-neutral auditory stimulus during the attention task (Kozłowska et al., 2017b), indicating a hyperarousal state in FND patients which can be linked to – or precede – the functional symptoms.

The same authors further identified a blunted cortisol awakening response (CAR²) in children with FND (Chung et al., 2022) measured at wake-up and 30 minutes later. Moreover, subjective stress and adverse childhood events negatively correlated with the CAR. Here, a potential HPA dysfunction was firstly shown in children with FND, which might contribute to physical symptoms such as fatigue (due to a disturbed circadian rhythm). These results might represent a long-term maladaptive habituation to stress, which might substantially contribute to the development of FND by increasing the patients' vulnerability to stress.

Similar results were found in a study comparing serum levels of different stress hormones between 6 pm to 8 pm in 15 PNES patients to 60 HC with and without history of abuse. Patients with PNES showed lower basal levels of cortisol compared to HC with sexual abuse but not compared to HC without a history of sexual abuse (Winterdahl et al., 2017). Interestingly, PNES patients were found to have higher levels of adrenocorticotropic hormone (ACTH), which is known to stimulate glucocorticoid synthesis and secretion in the adrenal glands. Contradictorily, increased basal diurnal cortisol, and no significant differences in morning cortisol was found in an earlier study (Bakvis et al., 2010), during which saliva samples were collected throughout two consecutive days in a domestic setting. Cortisol levels were particularly elevated in PNES patients with a history of sexual abuse. In a further study on 33 motor FND patients and age-, and gender matched HC, however, no significant differences in morning cortisol levels, nor diurnal cortisol levels could be detected (Maurer et al., 2015). The subjects of this study were hospitalized overnight and woken-up the next day by the nursing staff. Participants could potentially have woken-up prior to the wake-up time given by the nursing staff, which could have affected the cortisol awakening response. Moreover, in 24% of the subjects, disease duration was less than a year and no changes in HPA axis activity might indicate a long-term adaptive process throughout the course of the disease.

As compared to measures at rest, two studies examined the stress response in motor FND patients (Apazoglou et al., 2017), as well as in PNES patients (Bakvis et al., 2009a) using the Trier Social Stress Test (TSST). In both studies, patients exhibited a response to psychosocial stress that was comparable to the stress response of HC indicating a functioning adaptation to psychosocial stress situations. The motor FND patients in particular showed also higher levels of cortisol during the stress test (Apazoglou et al., 2017), whereas no differences were found in PNES patients (Bakvis et al., 2009a). Lastly, Apazoglou and colleagues also investigated basal cortisol levels and patients showed overall increased levels in cortisol during the afternoon (Apazoglou et al., 2017), and were related to the number of adverse life events. These findings are consistent with the previous results of Bakvis and colleagues (Bakvis et al., 2010).

² The cortisol awakening response (CAR) describes the rapid increase in cortisol upon awakening, which occurs naturally and maintains a crucial role in diverse homeostatic processes of the body (e.g., gluconeogenesis, immune system, mobilization, consciousness, alertness) (Clow et al., 2010; Pruessner et al., 1997; Wust et al., 2000).

In summary, previous results on cortisol as a marker of stress in FND were often inconsistent and exhibited a large heterogeneity. However, in many of the here mentioned studies, a potential association between HPA axis dysfunction and traumatic life events could be established, which suggests a certain role in the symptom presentation of FND.

Apart from the large heterogeneity across studies, the significance of a dysfunctional stress response in the symptom production or pathogenesis of FND is not yet clear. In other studies on stress-related disorders, chronic stress was often associated with neuroanatomical changes (i.e., reduced volumes), particularly in regions with high glucocorticoid receptor concentration such as the prefrontal cortex, the hippocampus or the amygdala (Lupien et al., 2018; McEwen, 2017). Accordingly, it was suspected that chronically elevated levels of cortisol might exhibit a neurotoxic effect on these regions (Conrad, 2008; Lupien et al., 2018). This hypothesis has particularly been studied in trauma survivors with post-traumatic stress disorder (PTSD), whereat a decreased hippocampal volume could be detected (Heim et al., 2000; Herman, 2013; Yehuda and Ph, 2001; Yehuda and Seckl, 2011).

While the relationship between psychological stress and functional- and structural brain abnormalities has been extensively studied, no studies so far identified a link between biological stress markers and these abnormalities in FND. Studying biological stress markers in conjunction with neurological-, and psychological hallmarks of FND could advance the understanding on disease mechanisms in FND.

1.3. Functional neurological disorders and functional brain alterations: mechanistic insights on *how* the symptoms develop

Throughout history, multiple attempts have been made on explanatory theories on the mechanisms of the sudden onset of neurological symptoms in the assumed absence of a structural cause. Consequently, clinicians often suspected feigning of symptoms, as a result of being unable to identify a causal reason for the symptoms (MacDuffie et al., 2021). With the emerging of neuroimaging techniques, the neural correlates of functional neurological symptoms could firstly be described by comparing neural activity during the attempted movement of the affected body parts with the activity occurring during the movement of the unaffected parts (Marshall et al., 1997; Tiihonen et al., 1995). Instead of activating the premotor regions as a response to voluntarily attempted movement of the affected limb, orbitofrontal regions, as well as the ACC were activated, which were suspected to exert an inhibitory effect on motor regions and motor initiation, eventually causing functional paralysis. Similarly, distinct brain activation patterns were identified in subsequent studies, in which functional symptoms were compared with simulated symptoms in HC (Stone et al., 2007), or when motor imagery was compared between affected and non-affected sides in FND patients (de Lange et al., 2008, 2007). Particularly, the ventromedial prefrontal cortex showed enhanced activity

during motor imagery of the affected hand. The ventromedial prefrontal cortex is part of the default mode network (DMN), and normally reduces its activity during demanding cognitive tasks, but is active during self-referential mental activity (Gusnard et al., 2001). An increased ventromedial prefrontal cortex activity in patients was thus attributed to enhanced self-monitoring in patients with FND (de Lange et al., 2008). These results were further confirmed in a study investigating motor initiation and inhibition in a patient with left-sided paralysis (Cojan et al., 2009). Furthermore, the authors identified increased FC between the ventromedial prefrontal cortex, the PCC and the precuneus with the right motor cortex, revealing that increased self-reflective processes in patients might negatively interact with motor pathways. These first findings showed that symptoms of patients are not the product of feigning but are rather associated with a dysfunction in *motor initiation*, partially driven through increased self-monitoring processes.

Subsequent studies, in which patients had to judge either when they felt the urge to move (attention to motor intention) or when they actually moved (attention to movement), confirmed impaired awareness of voluntary motor intention in FND patients (Baek et al., 2017; Edwards et al., 2011). Baek further associated the impaired attention to awareness with increased activity in the dlPFC, and the SMA, and reduced activity in the right inferior parietal lobule. Moreover, FC at rest was reduced between the right inferior parietal cortex and prefrontal structures but increased between premotor regions (Baek et al., 2017). Particularly, the reduced connectivity in fronto-parietal networks points towards an impairment already upstream of motor intention and action selection, and is thought to be involved in the inhibition of already ongoing motor programs (Brass et al., 2005). In line with this, it could be shown that voluntary, straight movements of functional tremor patients worsened when attention was explicitly shifted towards a visual feedback, but improved with a shift of the attention to different aspects of the movement, e.g., increasing its velocity (Huys et al., 2021). Therefore, locating the attention on the visual feedback of the movements itself might interfere with the implicit (“automatic”) execution of a motor program by replacing it with an explicit control of movement, which is then normally less smooth and less well performed (Wulf, 2013).

The voluntary – or involuntary – *control of movements* in patients with FND was also previously addressed in a study during which brain activity of patients was examined in the very same moment they experienced their motor symptoms, i.e., tremor (Voon et al., 2010b). Brain activity during symptom occurrence was compared to the brain activity when patients were asked to mimic their tremors. As compared to the activation during the voluntarily mimicked symptoms, a hypoactivation in the right TPJ was found during the involuntarily experienced symptoms. A subsequent resting-state study further identified decreased FC between the right TPJ and sensorimotor regions, the insula and the SMA (Maurer et al., 2016). The right TPJ represents a key node for multimodal integration of information (Eddy, 2016; Sepulcre et al., 2012), and is of particular importance in the computational comparison between internal prediction models and external states, and is often associated to the sense of agency (SoA), i.e., the sense of being in control over one’s own actions (Haggard, 2017). Enhanced

activation of the TPJ was associated with greater incongruence between the internal model (feedforward) and external events (sensory information) (Spengler et al., 2009), and thus a reduced SoA. In summary, these findings emphasize that functional symptoms might arise as a pathology of the attentional network rather than – or in combination with a dysfunction of the motor system.

Misdirected attention, increased self-monitoring and a reduced SoA in FND can be reflected by the basis of a hierarchical Bayesian model, in which the brain is thought to make predictions on sensory inputs (posterior) based on precise internal models (priors) (Edwards et al., 2012; Friston, 2010). A mismatch between the posterior and the prior is defined as the prediction error and leads to a constant update of the internal model in terms of integrating the feedback from the environment, and thus increasing the precision of the prior. The concept of altered attention regarding self-reflective processes was firstly illustrated in a Bayesian framework by Pareés and colleagues conducting a study in which tremors of functional and organic patients were objectively assessed using wrist actigraphy, as well as subjectively rated by the patients themselves. FND patients were found to over-report on their daily tremor-frequency in comparison to organic tremor patients (Pareés et al., 2012). In a subsequent study, FND patients were found to perform particularly worse during a visuomotor task in which the executed movements could be pre-planned with a high precision (precise priors), than compared to when external noise was added (high prediction error) (Pareés et al., 2013). The results of these studies were interpreted as patients overweighting their priors to the extent that their motor performance relies mostly on prior expectancy rather than external sensory inputs (posterior). The sensation of the symptoms was therefore strongly influenced by the belief (prior) on the severity of the symptoms. Consequently, when turning the attention towards symptoms, the prior expectancy on the symptoms gets increased strong enough to cause an abnormal motor behaviour. Consequently, the misinterpretation of the prediction error by higher-order regions then leads to an abnormal SoA. In line with this theory, patient's symptoms often improve, when attention is drifted away from the symptoms (Espay and Lang, 2015; Huys et al., 2021), hence reducing the weight of the priors. Such an attentional shift towards overweighting the priors, might possibly be explained by judging new sensory input based on past (negative) experience, such as e.g., a preceding physical injury or psychological trauma (Pareés et al., 2012). A more recent perspective on the Bayesian model for FND (Fiorio et al., 2022) also proposed nocebo-like mechanisms which increase prior beliefs in FND patients through misdirected attention towards the expected sensory inputs. The nocebo effect describes the appearance or worsening of symptoms upon administration of a sham treatment within a negative psychosocial environment (Benedetti, 2013). The nocebo effect is thought to result from a top-down attentional process which involves the expectations of a possible negative outcome (Fiorio et al., 2022, 2012). Moreover, it is suggested that the nocebo effect can be learned in the form of a classical conditioning (Van den Bergh et al., 2002), as such that expectations on a negative outcome can trigger the somatic sensation (Beissner et al., 2015). In addition, anxious personality traits might favour the nocebo effect (Planès et al., 2016), due to

a tendency to stronger emphasize on negative outcomes (Barsky, 2002). Taken together, nocebo-like mechanisms might be involved in the development of FND symptoms in the form of increasing prior beliefs (weight) on somatic symptoms through a maladaptive attentional process induced by a negative psychosocial context (Fiorio et al., 2022).

In brief, FND is not caused by a single malfunctioning brain region, but rather depicts a large-scale brain network dysfunctions involving different neural networks and neuroscientific concepts with a direct effect on symptom production (Aybek and Vuilleumier, 2016; Demartini et al., 2021; Drane et al., 2020; Perez et al., 2021, 2012; Pick et al., 2019). In sum, patients were found to have impairments in 1) emotion processing, awareness and interoception – involving the salience and limbic network (as discussed in the previous chapter), 2) attention – involving fronto-parietal networks, as well as 3) motor intention and self-agency – involving fronto-parietal and sensorimotor pathways.

Uncovering the distinct neural activation and aberrant FC patterns in FND, and further connecting them to dysfunctional neuroscientific concepts and symptom production, has set path towards investigating their clinical utility and their potential as biomarkers. Apart from the well-established positive clinical signs for FND (Daum et al., 2015; Stone and Carson, 2015), objective (data-based) biomarkers could monitor disease progression, predict treatment responses, or could add an additional diagnostic certainty (Thomsen et al., 2020). As such, numerous studies identified neural correlates of patient-reported symptom severity or duration of symptoms (Diez et al., 2021, 2019; Jungilligens et al., 2021; Perez et al., 2017a), or predicted treatment outcome based on functional imaging data (Espay et al., 2019; Faul et al., 2020). Lastly, Wegrzyk firstly applied a multivariate classification approach to resting-state data of motor FND patients aiming at distinguishing them from healthy controls in a predictive, diagnostic setting solely based on their FC (Wegrzyk et al., 2018). With an accuracy of almost 70%, this study showed feasibility and a potential clinical applicability of using imaging-based biomarkers as an additional objective rule-in test for the disorder.

In summary, impairments in diverse networks have been identified and integrative models on symptom production in FND emerged across the last decades. Moreover, neural correlates of FND could be linked to the clinical presentations of patients and showed their potential as prognostic and diagnostic biomarker for FND.

1.4. Overview of the Thesis

FND is a long-known disorder, nonetheless, for long time neglected in research and clinical practice. Research in the field has advanced tremendously throughout the last decades, but underlying pathophysiological mechanisms remain unclear. In the framework of a biopsychosocial model, the role of different precipitating, predisposing, and perpetuating risk factors were commonly assessed and examined. To answer the question on *why* FND develops, research highlighted the role of precipitating childhood adversities and identified a potential dysfunction in the biological stress regulation. To answer the question on *how* FND develops,

research often focus on aberrant functional brain networks and neuroscientific concepts as assessed with various neuroimaging techniques, with which distinct functional abnormalities could be linked to abnormal 1) emotion processing, emotion-motion interactions and interoception, 2) attention, and 3) self-agency and motor planning and intention. This thesis aims at connecting the research on the questions on the *how* and the *why* by means of studying the role of stress in conjunction with functional- and structural brain abnormalities in patients with FND. Studying the neurological-, biological-, and psychological aspects of FND could thereby advance the conception of its pathophysiological mechanisms.

1.4.1. Scope and Aims of the Thesis

The aim of this thesis was to study stress as a risk factor in FND patients and to evaluate its relationship to neurological- and psychological correlates of FND. Based on the well-established literature presented in Chapter 1, we set out the following goals:

- 1. Aberrant functional connectivity can be defined as a positive imaging-based biomarker of FND:** In order to establish validity and feasibility of a previously published classification approach (Wegrzyk et al., 2018) within a world-wide multi-centre setting, three different validation steps were implemented. The first goal of the study was the replication of previous results within different FND datasets collected at other centres (intra-centre cross-validation step). Secondly, the robustness of a multi-centre classification approach was assessed by pooling the data of these centres together (pooled cross-validation step). Thirdly, the generalizability of the method was evaluated by using data from each single centre once as test set after training on the data from the other centres (inter-centre cross-validation step). Successfully distinguishing FND patients from HC sets path towards a clinical application.
- 2. Dynamic functional alterations in FND patients may underlie the fluctuating symptoms of FND:** Analysing not only spatial but also temporal features of brain functional abnormalities might provide important mechanistic insights to the aetiology of FND. As such, this study identified dynamic functional aberrancies of the limbic network in FND and examined their spatial and temporal characteristics. Furthermore, the relationship between dynamic brain network alterations and clinical scores were assessed in order to deepen the understanding of dynamic brain states in FND and to examine their role in the pathophysiological mechanisms underlying the symptom production in FND.
- 3. Chronic stress relates to experience-dependent neurophysiological changes and might play a role in the pathophysiology of FND:** Inspired by previous literature on stress and hyperarousal symptoms in FND, this study set out to assess the daytime

cortisol profile in FND patients. As such, it was hypothesized that patients will show increased basal activity of the HPA axis indexed by cortisol levels. Furthermore, the relationship between aberrant HPA axis function, preceding trauma and structural- and functional brain alterations was assessed in order to clarify the biological relevance of stress in FND.

The hypotheses of this thesis were tested in two experiments. During the first experiment, resting-state fMRI data were collected retrospectively in four distinct functional movement disorder centres. The results of this study are detailed in Chapter 2. In a second experiment, multimodal data from FND patients and age- and gender matched healthy controls (HC) were acquired in a cross-sectional experiment. Participants were asked to collect nine saliva samples throughout the day in order to assess their diurnal cortisol levels. Further, participants completed questionnaires on subjective stress, depression, anxiety, childhood trauma, and traumatic life events. A structural MRI was acquired from each participant. Additionally, resting-state brain activity of each participant was acquired during a six-minute resting-state functional MRI. Patients further underwent a neurological examination. The results of this study are detailed in Chapter 3 and Chapter 4.

This thesis thus advances the knowledge on pathophysiological mechanisms in FND at two different levels. First, this study identified potential links between the *why* and the *how* axes, a line of research that has never been followed before. Second, the identification of possible biological and/or imaging-based biomarkers enables the translation of objective diagnostic and prognostic quantitative data into the clinical daily routine, not to replace the clinical diagnosis but to further strengthen it.

1.4.2. Applied Methods

In the following sections, a short introduction to each of the methods used in this thesis will be given. It will cover the principles of computing the static resting-state FC derived from functional MRI data and its graph-based embedding into vector space in order to integrate the data into a machine-learning based approach. Furthermore, dynamic FC, or more specifically co-activation pattern (CAP) analysis will be covered, which offers a new approach to study functional brain dynamics. Ultimately, an overview will be given on the biological stress system in humans along with the different measures that can be calculated derived from salivary cortisol.

1.4.2.1. Brain Network Analyses

Functional magnetic resonance imaging (fMRI) gained attention as a potential non-invasive tool to study brain function and identify imaging-based biomarkers for

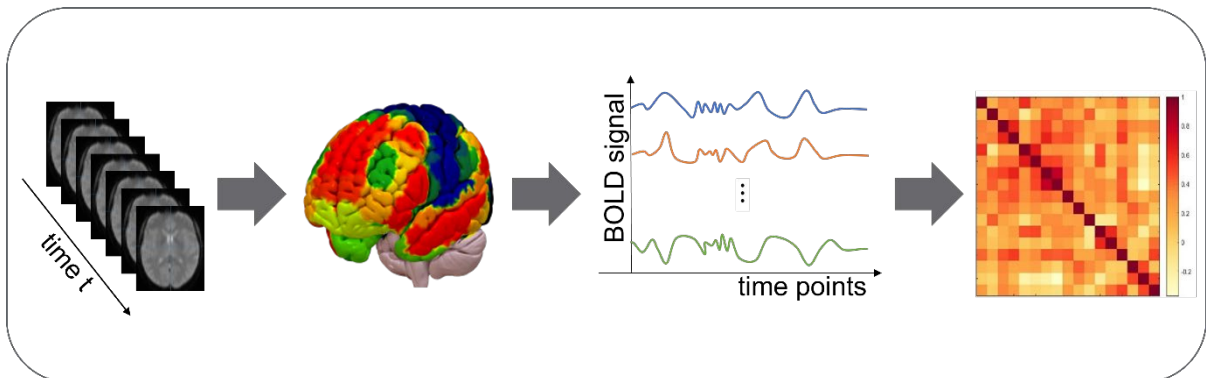


Figure 1.1: Schematic overview of calculation of functional connectivity. 3D functional brain volumes are acquired across a specific measurement period t and parcellated according to predefined ROIs or network atlases. Region/network-averaged BOLD signal is extracted and temporal cross-correlations (i.e., functional connectivity) is calculated. Whole-brain functional connectivity can be represented using a correlation matrix (functional connectivity matrix).

neuropsychiatric disorders (Takamura and Hanakawa, 2017). During an fMRI acquisition the blood oxygen level dependent (BOLD) signal is measured reflecting neural responses to metabolic changes in the brain (Logothetis, 2003). The very first fMRI studies investigated fluctuations of the BOLD signal in response to externally controlled stimuli or tasks (task-based fMRI), offering – for instance - a possibility to study certain brain regions involved in a particular cognitive function (Heeger and Ress, 2002; Ogawa et al., 1990). Furthermore, it could be shown that brain regions do not exhibit isolated activation but rather show a simultaneous temporal activation, which is often highly correlated between distinct brain regions. This so-called *functional connectivity* between brain regions was defined as “the temporal correlation of neurophysiological events between spatially separated brain regions” (Friston et al., 1993). Interestingly, Biswal and colleagues firstly introduced the idea of studying the brain at rest (Biswal et al., 1995), and identified spontaneous brain activity in volunteers that were measured under fMRI and were instructed to relax and to not think of anything in particular. These spontaneous fluctuations – predominantly occurring in low frequency ranges (< 0.1 Hz) – were interpreted as ongoing cognitive processes (Biswal et al., 1995, 1997). Nowadays, so-called resting-state fMRI approaches are widely used in research on neuropsychiatric disorders, as it is relatively easy applicable, does not require a complex set-up, and is less demanding for the patient in comparison to task-based approaches (Greicius, 2008; Takamura and Hanakawa, 2017). Up to now, multiple fMRI-based methodological approaches exist, with the aim to map behavioural differences and symptom presentation of patients to underlying functional brain abnormalities (Sokolov et al., 2019; van den Heuvel and Hulshoff Pol, 2010). In the scope of this thesis, (static) resting-state FC and – derived from it - a whole-brain graph analytical approach, as well as a dynamic FC approach will be discussed in more details.

When acquiring a resting-state fMRI, the participants are usually instructed to rest calmly in the scanner, to not fall asleep, and to not think of anything in particular. During the acquisition time, a time series of functional 3D volumes is acquired, at which each individual volume represents a snapshot of the brain activity at timepoint t . FC can be computed using a

voxel-wise, seed-based or atlas-based approaches, and is commonly calculated using Pearson’s correlation coefficient. Voxel-wise approaches are widely used in multivariate analyses such as independent component analysis (ICA) (Allen et al., 2011). During seed-based FC approaches, FC (temporal cross-correlation) is computed between a predefined region-of-interest (ROI, i.e., *seed*) and the remaining voxels in the brain (Fox et al., 2005; Lv et al., 2018). Seed-based connectivity analyses are particularly helpful when prior knowledge of functional brain alterations is given (Sokolov et al., 2019). During atlas-based approaches, the functional volumes are first parcellated into predefined brain regions or brain networks (Tzourio-Mazoyer et al., 2002; Yeo et al., 2011) and the FC is calculated between all pairs of regions at which the signal within a region represents the averaged signal of the voxel laying within the predefined region (Smith et al., 2011; Sokolov et al., 2019; van den Heuvel and Hulshoff Pol, 2010). Pairwise FC can then be represented using a correlation (FC) matrix with each cell representing the temporal correlation between two regions of interest, Figure 1.1.

Resting-state FC can further be represented using an undirected graph $G = (V, E)$, consisting of a set of vertices and edges. The vertices V thus correspond to each individual ROI, whereas the edges E represents the connectivity, i.e., correlation coefficient, between two vertices (Achard et al., 2006; Richiardi et al., 2010). Complex properties of the functional brain network can be derived using a graph-based approach, such as e.g., the nodal degree, describing the number of connections of each individual node (see Chapter 2, 2.2.7.1. Most discriminative connections). A highly connected node is then often referred to as *hub*. Figure 1.2 represents a simple example of the brain network organization using a graph-based approach.

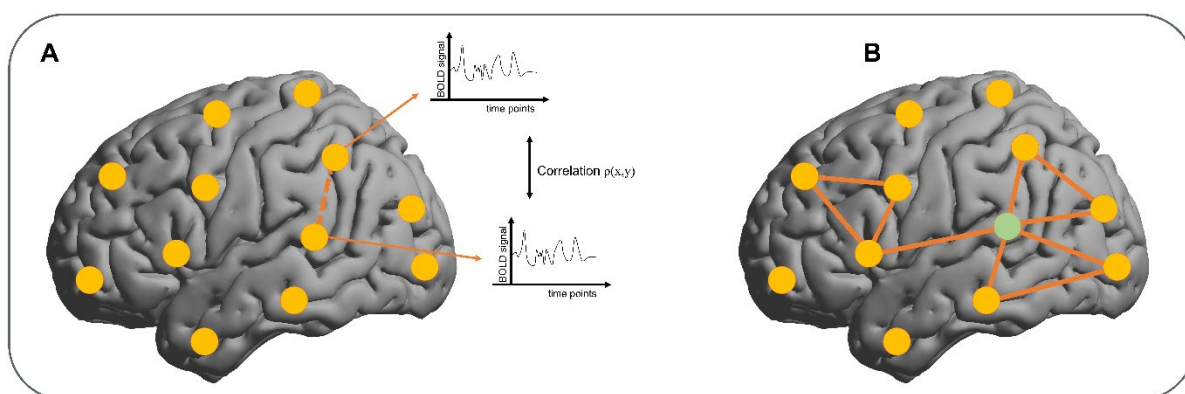


Figure 1.2: Schematic representation of the functional connectivity network. (A) Pearson’s correlation coefficient can be calculated between two individual graphs as a measure of functional connectivity. (B) The functional brain network can be represented as a graph consisting of a set of vertices (orange circles) and edges (orange lines). Highly connected nodes are referred to as hubs (green circle).

Assessing FC between voxels or spatially distinct brain regions thus represent a *static* approach, summarizing the cross-correlation across the whole acquisition time and thus assuming that the activity remains constant over time. Brain activity, however, has been found to show fluctuations over shorter periods of time (Brembs, 2021; Chang and Glover, 2010), highlighting the importance of time-resolved analyses (i.e., dynamic FC). Recently, various

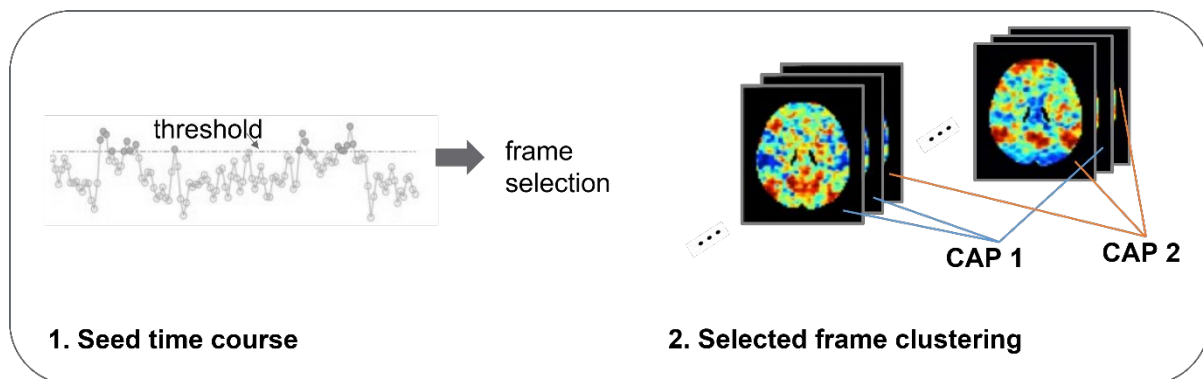


Figure 1.3: Schematic representation of co-activation pattern (CAP) analysis. CAPs are derived by selecting those volumes that highly co (de-)activate with the selected seed(s). The selected seeds are further grouped into different brain states using a temporal clustering approach. (Adapted from (Sokolov et al., 2019))

methods have been established to study the temporal dynamics of the resting brain (for review: Preti et al., 2017). Dynamic FC approaches therefore can be used to identify different brain states and their temporal characteristics (e.g., relative occurrence of individual brain states), at which a brain state is defined as the synchronous firing of a group of neurons in the same frequency (Brown, 2006). In the framework of this thesis, a co-activation pattern (CAP; Liu et al., 2018; Liu and Duyn, 2013) based analysis approach was adapted (Chapter 4). On a conceptual level, only a few fMRI volumes or “frames” are thought to be sufficient to identify seed-based FC maps or networks (Tagliazucchi et al., 2016). During a first step thus, one or multiple seeds are defined and only a reduced number of volumes are selected, which strongly (de-)activate with the seed. Second, a temporal clustering approach is applied to the selected volumes yielding the representative brain states (Liu et al., 2018; Preti et al., 2017), Figure 1.3.

1.4.2.2. Machine Learning

In the last decades, machine learning algorithms gained interest as a complementary tool for the analysis of neuroimaging data. Among the multiple existing algorithms, Support Vector Machine (SVM) classifiers are the most popular, as they are comparably simple in application, can operate with high dimensional data, and still require only a low computational load (Janardhanan et al., 2015). SVM are *supervised* learning algorithms, at which a discriminative model is built autonomously, that best separates the different groups within a dataset given prior knowledge about the group labels (e.g., controls versus patients). During an evaluation-, or test step, the discriminative model will be applied to a naïve dataset in order to make accurate predictions about the group labels (Russel and Norvig, 2009).

In the scope of this thesis (Chapter 2: Multi-centre Classification using Resting-state Functional Connectivity), a non-linear classification was implemented by mapping FC features into a high-dimensional space using a graph-based approach (Richiardi et al., 2011, 2010), building a hyperplane that separates the two groups optimally according to their FC features

(Cortes and Vapnik, 1995; Russel and Norvig, 2009). As such, the features of each subject are defined as a vector containing the different FC values across the whole brain. During the initial so-called training step, a discriminative model is built by assigning a *weight* to each feature, with higher weights representing a greater contribution to the model. The subsequent evaluation step was performed using a leave-one-out (LOO) cross-validation approach. During the LOO cross-validation approach, the classification is repeated N -times with N representing the number of subjects in the dataset. During each fold, the model is built using $N-1$ subjects, and tested/evaluated on the left-out subject.

The accuracy of the model can be calculated as the percentage of overall subjects correctly classified. Moreover, sensitivity (true-positive rate), specificity (true-negative rate) and area-under-receiver-operating-characteristic curve (AUC) were computed. Statistical significance was assessed using permutation testing, at which the classification was performed 1000-times with randomly permuted class labels (i.e., FND patients and HC), in order to estimate the likelihood of the results to be observed by chance.

In other neuropsychiatric or affective disorders, applying machine learning approaches to neuroimaging data could provide a potential clinically significant way of identifying new biomarkers (Hahn et al., 2010; Nakano et al., 2020; Nunes et al., 2020; Patel et al., 2015; Xia et al., 2018), predicting individual treatment responses (Jiang et al., 2018; Redlich et al., 2016), or evaluating personalized treatment strategies (Liu et al., 2012).

Thereby, machine learning-based approaches bring new possibilities to study underlying structural and functional brain network dysfunctions in a diagnostic and/or prognostic way, and are widely used and applied using different models and imaging modalities (for review: Gao et al., 2018). Nevertheless, those methods are still at an exploratory stage and face several technical challenges - by way of example, how to handle the heterogeneity of the imaging data - which in turn affects comparability between different studies.

Together with the large clinical heterogeneity of neuropsychiatric disorders such as FND, studies using machine learning algorithms are often limited by the small sample size of the individual data set. Small sample sizes have often been associated with insufficiently controlling for overfitting, resulting in high classification performance on the training set, but poor performance on the validation set (i.e., poor generalizability; Vabalas et al., 2019). Importantly, the appropriate model must be carefully selected and built, and evaluation of the model must be accompanied by a proper cross-validation strategy, in order to evaluate its generalizability to naïve, unseen data (Erickson et al., 2017; Russel and Norvig, 2009). Moreover, performance of classification approaches using multi-centre data need to be evaluated in order to generalize across centres and symptom types.

1.4.2.3. Voxel-based Morphometry

Voxel-based morphometry (VBM) is a computational approach in neuroimaging to assess statistical differences in grey matter tissue (Ashburner and Friston, 2000). To do so, the

individual T1-weighted (“anatomical”) MR images are segmented into the different tissue types such as grey matter, white matter, or cerebrospinal fluid etc. At its simplest, segmentation is achieved by overlapping the anatomical image with tissue probability maps, which give the probability of any voxel belonging to a certain tissue. The segmented anatomical images are then further mapped into a common template space (Ashburner and Friston, 2005) in order to account for inter-individual differences (normalization). Lastly, the normalized, segmented images are smoothed using an isotropic Gaussian kernel. Each voxel contains now the average grey matter concentration from itself and its surrounding voxels. Spatial smoothing makes the voxels more Gaussian and can compensate for inaccurate spatial normalization (Ashburner and Friston, 2000).

To assess group differences, a voxel-wise parametric test can be applied to the images. Most commonly, a general linear model (GLM) is used (Friston et al., 1994), which allows to further account for confounding factors such as e.g., age or gender. To account for voxel-wise multiple comparisons, an appropriate correction is applied. Figure 1.4 provides a graphical representation of the VBM workflow.

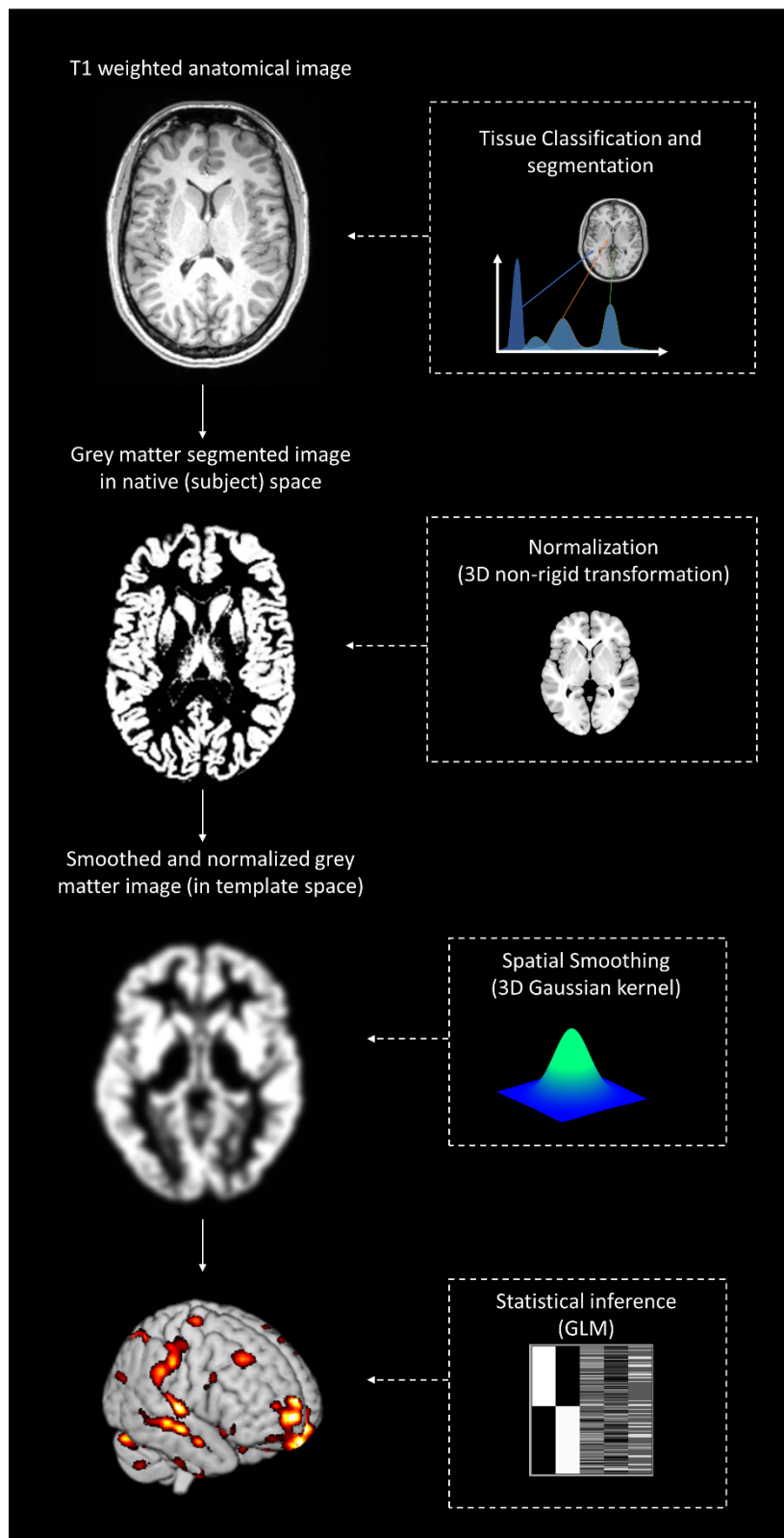


Figure 1.4: Workflow voxel-based morphometry. The T1-weighted anatomical image is first segmented, then normalized to a standard (template) space, and smoothed using a Gaussian kernel. Statistical inference is made upon voxel-wise comparison of grey matter using a general linear model (GLM).

1.4.2.4. Cortisol

The hypothalamic-pituitary-adrenal (HPA) axis is one of the main regulatory systems for stress. As a response to stress, hypophysiotropic neurons in the paraventricular nucleus of the hypothalamus secrete corticotropin-releasing factor (CRF), which binds to its receptor in the pituitary gland, resulting in the release of adrenocorticotropic hormone (ACTH). Blood-circulating ACTH targets the adrenal cortex, where it promotes the release of cortisol (Smith and Vale, 2006). The HPA-axis itself is regulated through a negative feedback triggered by increased levels of circulating cortisol (McEwen, 2017; Smith and Vale, 2006), Figure 1.5.

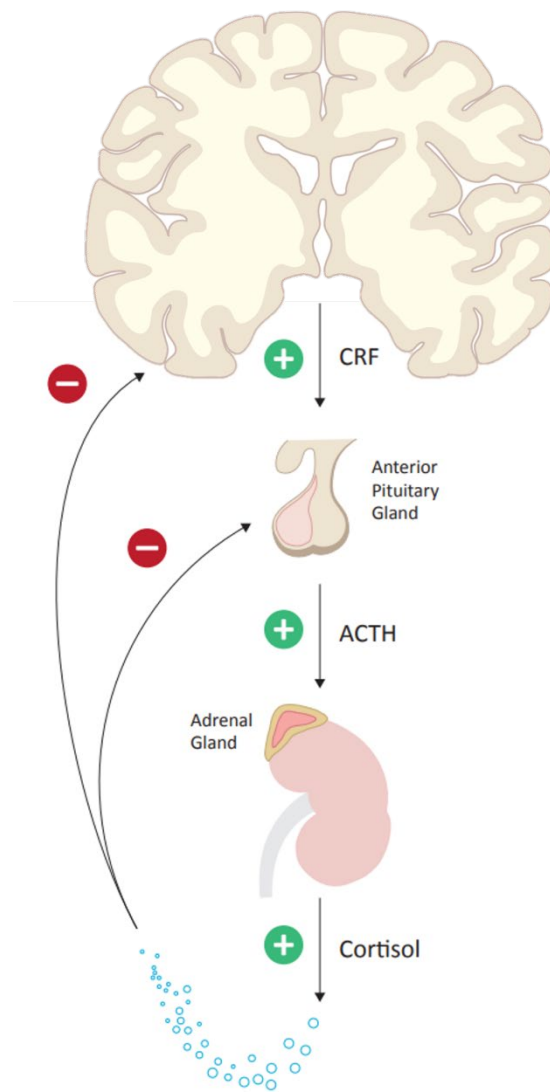


Figure 1.5: Schematic representation of HPA Axis. Corticotropin-releasing factor (CRF) is released in the paraventricular nucleus of the hypothalamus, resulting in the secretion of adrenocorticotropic hormone (ACTH) in the pituitary gland, subsequently triggering cortisol release from the adrenal glands.

A dysfunctional regulation or activation of the HPA-axis was frequently found to contribute to the development of stress-related pathologies (McEwen, 2017; Munk et al., 1984). Generally, cortisol acts systemically and is not only secreted in response to stress. Cortisol receptors are abundant in the body and involved in numerous homeostatic processes, such as glucose homeostasis or the immune response (Kadmiel and Cidlowski, 2013; Oakley and Cidlowski, 2013). Cortisol secretion is thus strictly regulated within the body. Importantly, the HPA-axis also follows a circadian rhythm with a peak of cortisol secretion in the morning upon awakening (cortisol awakening response, CAR) and low levels towards the afternoon/night (Oster et al., 2017), Figure 1.6. The CAR is defined as the rapid dynamic increase in cortisol secretion across the first 30 to 45 minutes upon awakening (Pruessner et al., 2003; Stalder et al., 2016).

Correspondingly, specially cortisol – as the end effector of the HPA axis - has often been used as a biomarker in stress research (Hellhammer et al., 2009; Wust et al., 2000). More specifically, the CAR as a hallmark for proper HPA-axis function has been found to show distinctive associations with psychosocial-, and health-related parameters (Adam et al., 2017; Pruessner et al., 2003). Moreover, environmental noise and the adaptive response of the HPA-axis has been found to be reflected by the CAR with a high accuracy and high intraindividual stability (Wust et al., 2000). Deviations from the typical CAR peak are further assumed to be associated with maladaptive neuroendocrine processes to long-term stress (Clow et al., 2004; Stalder et al., 2010), making it the perfect trait biomarker to study stress-related disorders. However, cortisol itself is also very susceptible to various trait- and state factors such as age, sex, but also medication, smoking, or hormonal contraception (Schlotz et al., 2011), which need to be carefully addressed during the analysis.

In 2016, expert consensus guidelines (Stalder et al., 2016) were published, formulating clear guidelines on sampling protocols, participant instructions and adherence, accounting for covariates, as well as statistical considerations when reporting and interpreting the CAR. In the framework of this thesis, salivary cortisol data was assessed by adhering strictly to the consensus guidelines with regards to the study design, and statistical analysis. Methodological considerations are further explained in Chapter 3, as well as in Appendix B, Supplementary Material for Chapter 3.

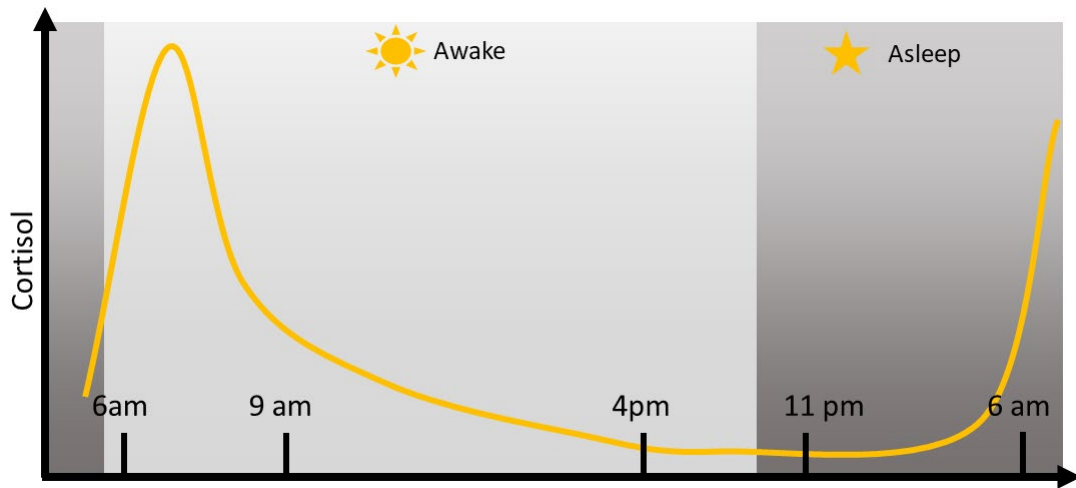


Figure 1.6: Graphical illustration of the circadian rhythm of cortisol. The initial peak in the morning, 30 to 45 minutes upon awakening represents the cortisol awakening response. During the afternoon, the cortisol levels are low.

Multi-centre Classification using Resting-state Functional Connectivity

This chapter is published as:

*Weber, S., Heim, S., Richiardi, J., Van De Ville, D., Serranová, T., Jech, R., Marapin, R.S., Tijssen, M.A.J., Aybek, S. Multi-centre classification of functional neurological disorders based on resting-state functional connectivity. NeuroImage: Clinical 35, 2022
<https://doi.org/10.1016/j.nicl.2022.103090>*

Contribution:

I was involved in the conceptualization, experimental design, project administration and coordination with the other centres together with my supervisor Prof. Dr. med. Selma Aybek. Together with a former colleague (Salome Heim), I collected the data from centre II. I performed the pre-processing and analysis of all the demographic- and imaging data. I developed and programmed the three validation-steps based on previous literature. I implemented the quality control steps under supervision of Prof. Dimitri Van De Ville and PD Jonas Richiardi. I wrote the original draft of the manuscript, coordinated correspondence with the Journal and revised the manuscript.

Abstract

Patients suffering from functional neurological disorder (FND) experience disabling neurological symptoms not caused by an underlying classical neurological disease (such as stroke or multiple sclerosis). The diagnosis is made based on reliable positive clinical signs, but clinicians often require additional time- and cost consuming medical tests and examinations. Resting-state functional connectivity (RS FC) showed its potential as an imaging-based adjunctive biomarker to help distinguish patients from healthy controls and could represent a “rule-in” procedure to assist in the diagnostic process. However, the use of RS FC depends on its applicability in a multi-centre setting, which is particularly susceptible to inter-scanner variability. The aim of this study was to test the robustness of a classification approach based on RS FC in a multi-centre setting.

This study aimed to distinguish 86 FND patients from 86 healthy controls acquired in four different centres using a multivariate machine learning approach based on whole-brain RS FC. First, previously published results were replicated in each centre individually (intra-centre cross-validation) and its robustness across inter-scanner variability was assessed by pooling all the data (pooled cross-validation). Second, we evaluated the generalizability of the method by using data from each centre once as a test set, and the data from the remaining centres as a training set (inter-centre cross-validation).

FND patients were successfully distinguished from healthy controls in the replication step (accuracy of 74%) as well as in each individual additional centre (accuracies of 73%, 71% and 70%). The pooled cross validation confirmed that the classifier was robust with an accuracy of 72%. The results survived post-hoc adjustment for anxiety, depression, psychotropic medication intake, and symptom severity. The most discriminant features involved the angular- and supramarginal gyri, sensorimotor cortex, cingular- and insular cortex, and hippocampal regions. The inter-centre validation step did not exceed chance level (accuracy below 50%).

The results demonstrate the applicability of RS FC to correctly distinguish FND patients from healthy controls in different centres and its robustness against inter-scanner variability. In order to generalize its use across different centres and aim for clinical application, future studies should work towards optimization of acquisition parameters and include neurological and psychiatric control groups presenting with similar symptoms.

2.1. Introduction

Functional neurological disorders (FND) describe the presence of neurological symptoms not caused by a classical neurological disease (American Psychiatric Association, 2013) but related to brain dysfunctions (Drane et al., 2020). Patients can experience a wide range of neurological symptoms, most frequently motor (e.g., weakness or abnormal movements), sensory (e.g., numbness), or attacks of clouded consciousness which are sometimes accompanied by convulsions (Brown, 2016; World Health Organization, 1993). Nowadays, the diagnosis of FND is made on the basis of positive clinical signs (Daum et al., 2015; Stone and Carson, 2015), and less emphasis is put on an exclusion process (i.e., not identifying an underlying explanatory neurological disease). Indeed, even if there is no gold standard against which to compare the validity of these signs, several recent studies have shown excellent specificity for several bedside clinical signs (Daum et al., 2015; Espay et al., 2018a; Syed et al., 2011). However, due to heterogeneity of FND symptoms and a broad spectrum of potential differential diagnosis, specialists often request multiple time- and cost-consuming additional tests to rule out an underlying organic lesion or comorbid condition (Espay et al., 2009), even if they were convinced of the diagnosis based on their initial clinical evaluation (Espay et al., 2018a). This highlights the need to identify an adjunctive positive biomarker to support clinicians in their daily clinical routine. Such a marker could allow rapid confirmation of the clinical diagnosis, rather than engaging in a long and exhaustive process of excluding all evoked differential diagnoses.

In the search for new biomarkers in neuropsychiatric disorders, resting-state (RS) functional magnetic resonance imaging (fMRI) has gained growing attention as a promising and easily applicable tool (Greicius, 2008). Resting-state fMRI allows studying blood oxygen dependent level (BOLD) signal fluctuations in the brain under resting condition and therefore does not depend on the patient's active participation. Furthermore, inter-regional correlations of temporal fluctuations are thought to reflect FC between spatially distinct brain regions. Therefore, RS fMRI can reveal important information about underlying neuropathophysiological changes in functional networks of patients (Sokolov et al., 2019; Takamura and Hanakawa, 2017; van den Heuvel and Hulshoff Pol, 2010). Even though task-based fMRI studies are predominant in FND, RS studies in FND were able to confirm findings from task-based studies and identified consistent results. Amongst the existing RS studies, (1) increased limbic connectivity to motor control areas (Baek et al., 2017; Maurer et al., 2016; van der Kruijs et al., 2012), (2) aberrant connectivity from the right temporoparietal junction (TPJ) to sensorimotor regions (Diez et al., 2019; Hassa et al., 2017; Maurer et al., 2016; Mueller et al., 2022; Wegrzyk et al., 2018), as well as (3) altered connectivity from memory-related temporal structures (Longarzo et al., 2020; Monsa et al., 2018; Szaflarski et al., 2018) were identified.

In parallel, the application of machine learning algorithms offers a complementary tool for RS fMRI data analysis. Moreover, machine learning approaches have shown to be robust and

sensitive to disease-specific alterations in functional and structural medical images (Erickson et al., 2017). As such, its value has been demonstrated in several neurological diseases and heterogenous psychiatric disorders by successfully distinguishing patients from healthy controls based on RS FC (for review see (Nielsen et al., 2020)).

In the field of FND, our previous study (Wegrzyk et al., 2018) showed promising results with regards to accurately distinguishing FND from healthy controls (HC). We applied a multivariate classification approach based on whole-brain RS FC aiming at discriminating motor FND patients from healthy controls in a predictive setting. Similarly, in another study the seizure-subtype of FND (psychogenic non-epileptic or functional seizures) was successfully classified against healthy controls, based on RS FC (Ding et al., 2013) and T1-weighted structural MRI data (Vasta et al., 2018). Even though real-life use of such a biomarker will need control groups with similar symptoms to FND and not only healthy controls, these studies provided a strong rationale to continue the validation of such classification algorithms. Indeed, most bedside positive signs for FND are specific and reliable, but neuroimaging classification based on machine learning might provide a future clinical tool in the form of an additional rule-in test against other neurological and psychiatric diseases and disorders.

The translation of neuroimaging data from bench to bedside has always been challenging due to the clinical heterogeneity (Espay et al., 2018a; Galli et al., 2020) and within-group differences of neuropsychiatric disorders (i.e., FND patients), and consequently its limited generalizability within and between patient populations (Stone et al., 2011). Importantly, overcoming the problem of low generalizability requires large samples, which includes patients with different symptom types and symptom severities, and preferably from different centres. Furthermore, establishing RS FC as an adjunctive positive biomarker for FND requires its applicability within and across different centres, i.e., different symptom types and symptom severity, consequently increasing the sample size and the heterogeneity of the dataset, which might benefit the classification performance. The next step towards a clinical application therefore includes the validation of multivariate classification approaches in different datasets (i.e., with regard to FND subtypes or scanners), and to assess their performance when using multi-centre data.

To bridge this gap, we set out to further evaluate the classification performance of our previously published classification approach (Wegrzyk et al., 2018) through three different validation steps (Dyrba et al., 2013; Nunes et al., 2020; Rozycki et al., 2018). First, our aim was to replicate the previous results by applying the method in additional datasets collected at other centres (intra-centre cross-validation step) and test its robustness when used in a multi-centre setting by pooling the data of these centres together (pooled cross-validation step). Our second aim was to assess the generalizability of the method by using data from each single centre once as test set after training on the data from the other centres (inter-centre cross-validation step). Successfully distinguishing FND patients from HC in a multi-centre setting could set path towards a clinical application by including neurological and psychiatric controls with similar symptoms (but other diagnoses) in future studies.

2.2. Materials and methods

2.2.1. Participants

Data were collected retrospectively from four different European University Neurology Departments: i) Geneva (Switzerland, previously published in (Wegrzyk et al., 2018)), ii) Bern (Switzerland), iii) Prague (Czech Republic, previously published in (Mueller et al., 2022)) and iv) Groningen (The Netherlands, previously reported in (Marapin et al., 2021, 2020)). Board-certified neurologists confirmed the diagnosis of FND according to DSM-5 (World Health Organization, 1993) and using positive signs (Stone and Carson, 2015). We included FND patients with motor and sensory symptoms (F44.4 and 44.6), with functional seizures (F44.5), and mixed symptom type (F44.7). For movement disorders (F44.4), clinically definite and documented diagnoses according to (Gupta and Lang, 2009) were included. Exclusion criteria were a current neurological disease or disorder (other than FND), alcohol or drug abuse, pregnancy or breast-feeding, and contraindication for MRI scanning. The studies were approved by local ethics committees at each of the centres, i.e., the ethics committee of the University Hospitals of Geneva (CER 14-088), the Competent Ethics Committee of the Canton Bern (SN_2018-00433), the Ethics Committee of the General University Hospital in Prague (approval number 26/15) and the Medical Ethical Committee of the Amsterdam University Medical Center, location AMC, the Netherlands (identification number MEC10/079). All subjects provided written informed consent.

The dataset included 220 MRI scans from patients suffering from FND and age- and sex-matched HC. Data from 21 subjects were excluded due to too high motion artefacts (see section 2.3), and 10 subjects were excluded due to insufficient quality of the functional data (slice artefacts in frontal and/or parietal regions). To maintain an equal number of age- and sex matches, the equivalent age- and sex match of each excluded subject was discarded as well ($n = 17$), in order to have a well-balanced dataset (Dyrba et al., 2013; Nielsen et al., 2020). We confirmed matched ages within and between the centres using a type III - ANOVA with factor group and centre. The remaining 172 MRI scans included data from 86 patients and their 86 age- and sex-matched healthy controls (Table 2), correspondingly, it needs to be underlined that - as compared to the previous work - two healthy controls were excluded from the original dataset of centre I in order to have equal number of subjects in both groups. Similarly, as compared to the dataset in (Marapin et al., 2021, 2020), two subjects were excluded due to motion artefacts along with their corresponding age- and sex match).

2.2.2. Data Acquisition

Mood disorders are known comorbidities in FND patients (Carson and Lehn, 2016). Therefore, anxiety and depression scores, as well as psychotropic medication (i.e., benzodiazepines, neuroleptics, antidepressants, antiepileptics, and opioids) are commonly

assessed in studies on FND patients. Accordingly, centre I, II, and III collected behavioural data of patients and controls on anxiety and depression using the Spielberg State-Trait Anxiety Inventory (STAI, Spielberger et al., 1983) and the Beck's Depression Inventory (BDI, Beck, 1961). Centre IV collected behavioural data on anxiety and depression in patients using the Beck's Anxiety Inventory (BAI, Beck et al., 1988) and the Beck's Depression Inventory (BDI, Beck, 1961). Symptom severity was evaluated using the Clinical Global Impression (CGI) score (0 = no symptoms to 5 = very severe symptoms) in centre I; using the CGI score (0 = no symptoms to 7 = very severe symptoms) in centre II and IV; and using the Simplified Version of the Psychogenic Movement Disorder Rating Scale (S-FMDRS, Nielsen et al., 2017) in centre III. CGI scores with different scales were converted into the same scale. S-FMDRS scores were converted into CGI scores (see Appendix A, Supplementary Material for Chapter 2). Differences in symptom severity between centres (CGI score) were analysed using one-way ANOVA.

Functional and structural MRI data were all acquired on 3-Tesla units using different MRI manufacturers, machines and protocols. Acquisition parameters for the fMRI data of each centre are summarized in Table 2.1. In one centre (centre IV), fMRI data were based on fast field single echo planar imaging (FEEPI), whereas in the others, it was based on whole-brain single shot multi-slice BOLD echo-planar imaging (EPI). Structural scans were obtained using a T1-weighted Magnetization Prepared Rapid Gradient-Echo (MPRAGE) image in centre I, II, and III; and using a T1 weighted turbo field echo (TFE) image in centre IV.

2.2.3. MR pre-processing

Data were pre-processed and analysed using MATLAB (R2017b, MathWorks Inc., Natick, USA). Each centre was pre-processed individually. An adapted version of the previous pre-processing pipeline from (Wegrzyk et al., 2018) based on the Statistical Parametric Mapping version 12 (SPM12) tools (<https://www.fil.ion.ucl.ac.uk/spm/software/spm12/>) was used, including: functional realignment and co-registration of the mean functional image to the structural image, and segmentation of the structural image into grey matter, white matter, and cerebrospinal fluid. The functional images were additionally checked for excessive head motion using the framewise displacement (FD) method of Power and colleagues (Power et al., 2014). Mean FD and number of volumes above threshold of $> 0.5\text{mm}$ were calculated per subject. A type III – ANOVA was used to evaluate differences in motion artefacts for the factors group and centre. Then, for each subject an individual structural brain atlas based on the AAL atlas (Tzourio-Mazoyer et al., 2002) was built using a customized version of the IBASPM toolbox (Aléman-Gomez, Y.M.-G., Melie-Garcia and Valdés-Hernandez, 2006). From the AAL atlas, we used 88 regions (whole atlas without the cerebellum and pallidum (due to signal drop-out), same as in (Wegrzyk et al., 2018)). The individual structural atlas was mapped onto the native resolution of the functional data. Furthermore, region-averaged time-series were extracted and motion parameters, as well as the average signal from the white matter and the cerebrospinal

fluid were regressed out (Richiardi et al., 2011; Wegrzyk et al., 2018). The region-averaged time-series were Winsorized to the 95th percentile to reduce the effect of outliers and linearly detrended. For optimization purposes of the first validation step (see Chapter 2.2.5. Classification), the region-averaged time-courses were either bandpass filtered (0.01-0.08 Hz) or wavelet subband filtered (Richiardi et al., 2011) (see Appendix A, Supplementary Material for Chapter 2 for further details and explanations on the pre-processing pipelines).

Table 2.1: Scanner acquisition parameters.

Centre	Model	Manufacturer	TR [s]	TE [ms]	Acquisition time [min]	Volumes	flip angle [°]	Voxel size[mm ³]
I	Magnetom TrioTim	Siemens	2	20	05:08	150	80	3.0 x 3.0 x 2.5
II	Magnetom Prisma	Siemens	2	20	05:08	150	80	3.0 x 3.0 x 2.5
III	Magnetom Skyra	Siemens	2	30	10:16	300	90	3.0 x 3.0 x 3.0
IV	Philips Intera Medical Systems	Philips	2	30	07:30	225	70	3.5 x 3.5 x 3.5

Abbreviations: TR: repetition time; TE: echo time

2.2.4. Resting-State Functional Connectivity Modelling

Pairwise Pearson correlation coefficients between each pair of atlas regions were calculated for each subject to obtain a correlation matrix (number of regions x number of regions) (Smith et al., 2011). The correlation coefficients were Fisher-Z transformed to make the connectivity matrices Gaussian. The Fisher-Z transformed connectivity matrices of each centre were then connection-wise Z-scored to normalize the data with regard to centre, which acts as a site harmonization. To evaluate the effectiveness of the normalization, we analysed within- and between centre and group effects of FC differences between each pair of regions using n-way ANOVA before and after normalization. For each subject, the upper triangular part (without the diagonal) of the correlation matrix was extracted and lexicographically organized in a two-dimensional feature representation, which was used further as input feature vectors for the classifier. The feature vector of each subject therefore contained $[(88 \times 87)/2] = 3828$ features. The exact procedure can be found in (Richiardi et al., 2011, 2010).

2.2.5. Classification

To perform a binary classification, a Support Vector Machine (SVM) classifier with a linear Kernel function and L2 regularization was used, which learned a discriminative function that separated the two groups as accurately as possible. The SVM implementation for MATLAB of the LIBSVM package (Chang, C.-C. and Lin, 2011) (software available at <https://www.csie.ntu.edu.tw/~cjlin/libsvm/>) was used, where the C parameter was set at 1. The classification process includes two main steps: 1) training and testing of the model and 2)

evaluation of the model. In order to estimate the performance of our model, we chose three cross-validation approaches adapted and similarly implemented as in (Dyrba et al., 2013) and (Nunes et al., 2020):

- (1) **Intra-centre cross-validation:** Each dataset was evaluated individually by separating training and test set by using an N -fold leave-one-out (LOO) cross-validation approach, where n represents the number of subjects. For each iteration, $N-1$ subjects were used as training data and the remaining subject was used as test data. This was repeated until each subject within a centre was used once to test the classification performance. During this intra-centre cross-validation, we therefore replicated the results in centre I, and validated its applicability in three other datasets originating from three separate centres (centre II-IV).
- (2) **Pooled cross-validation:** All the data of the four centres were pooled and separated in a training set and a testing set by using the N -fold LOO cross-validation approach again. The classifier was trained on $N-1$ subjects, including all subjects of the four centres, and tested on the remaining subject. This was repeated until each subject from each centre was used once to test the classification performance. During this pooled cross-validation, we evaluated the classifiers performance when working with data that arise from different scanners introducing a scanner-specific variability.
- (3) **Inter-centre cross-validation:** The data from $S-1$ scanners were used as a training set and the data from each remaining single centre was used once as a testing set. During this inter-centre cross-validation, we investigated if the learned linear SVM model can be applied to data from an unknown scanner and therefore evaluated its generalization power.

This setting poses great challenges due to the many sources of uncontrolled variance across scanners and datasets (Abraham et al., 2017; Noble et al., 2017). We thus further examined the classification performance when gradually transferring subjects from the test set to the training set. Doing so, the test set is not fully naïve to the potential centre-specific bias introduced in the inter-centre cross-validation setting. This procedure, however, can help to understand the impact of scanner-specific bias to the classification performance. We iteratively transferred data from two subjects (one HC and one FND) from the test set to the training set to examine the learning curve. In each iteration, two more subjects were transferred from the test set to the training set until a maximum number of 28 subjects (i.e., 14 HC, 14 FND) was transferred. Namely, 28 subjects represent the maximum number of subjects that can be transferred in order to have at least two remaining subjects in the test set.

In each setting, the classification performance was calculated as the average performance across all folds. Figure 2.1 gives an overview of the three different validation steps (for a detailed description, see Appendix A, Supplementary Material for Chapter 2).

2.2.6. Evaluation

To evaluate the classifier's performance, accuracy, sensitivity, specificity, as well as the area under receiver operating characteristic curve (AUC) were computed. The accuracy provides information about the overall performance of the classifier with respect to both groups and was defined as $accuracy = (TP + TN)/N$ where TP is the number of true positives (patients correctly classified as patients), and TN is the number of true negatives (controls correctly classified as controls), and n is the total number of subjects. The sensitivity is the true positive rate and the specificity the true negative rate, i.e., $sensitivity = TP/(TP+FN)$, $specificity = TN/(TN+FP)$, where FN and FP refer to the number of false negatives and false positives, respectively. The AUC assesses the probability of correctly classifying a random pair of patient and control. It reflects test accuracies as follows: AUC = 1 refers to perfect accuracy, AUC between 0.7 – 0.9 refers to moderate, AUC between 0.5 – 0.7 = refers to low and, AUC = 0.5 is uninformative. To assess the significance of the classification, we performed permutation testing, i.e., the classification was repeated 1000 times using its null distribution with the group labels (patients/control) randomly permuted.

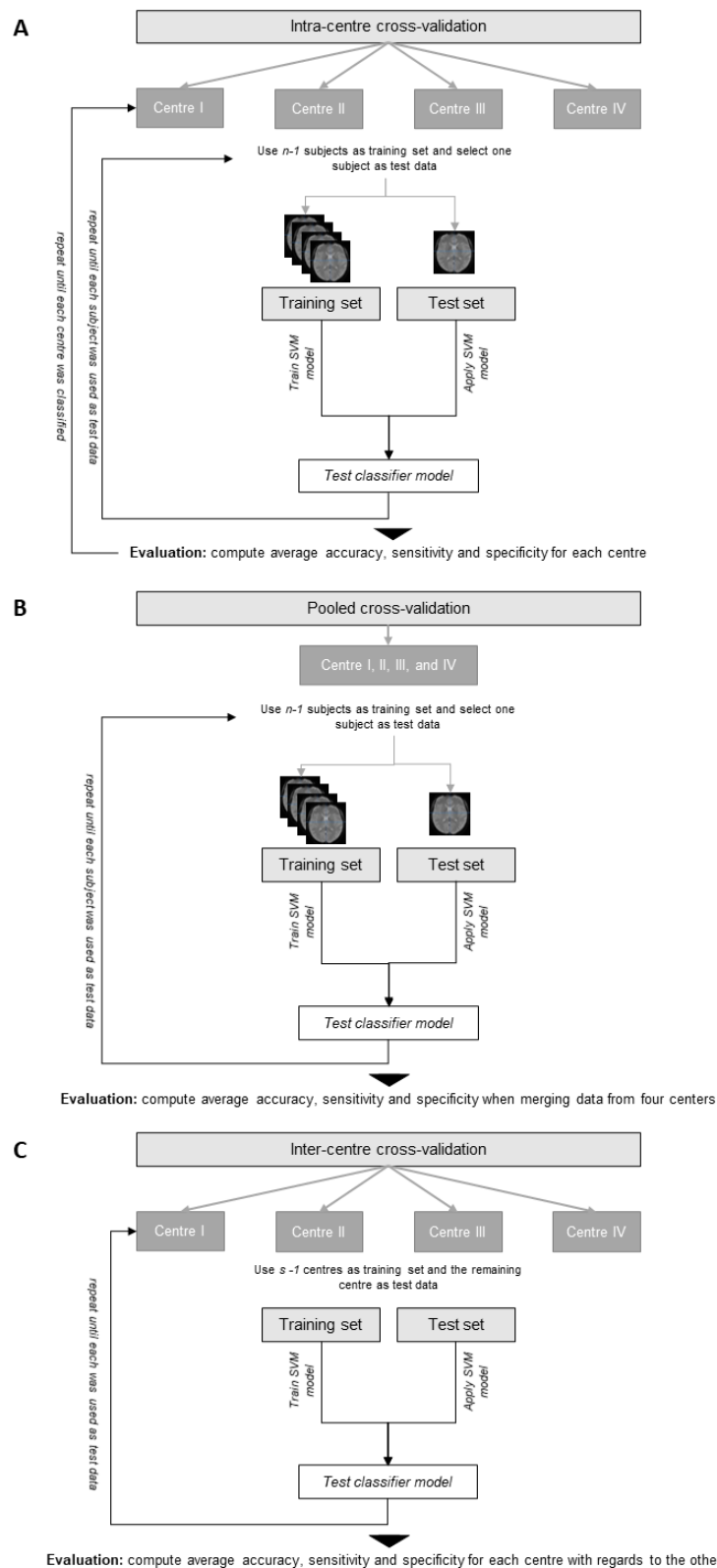


Figure 2.1: Flow chart of the three cross-validation approaches. Flow chart including (A) intra-centre cross-validation, (B) pooled cross-validation, and (C) inter-centre cross-validation. Throughout the training, a leave-one-out cross-validation (LOOCV) approach was applied.

2.2.7. Post-hoc analyses

2.2.7.1. Most discriminative connections

To shed light on which brain areas may be linked to the pathophysiology of FND and common across all four centres, we focussed the post-hoc analyses on the validation steps which pooled all the data from the four centres (step 2: pooled cross-validation). In order to explore the connections that were most discriminative to distinguish patients and controls, we analysed the highest weights assigned by the classifier to the different functional connections (i.e., correlation coefficients).

Within these most discriminative connections, we then further identified those regions that appeared with the highest frequency. From this set of regions, we analysed the connectivity differences between patients and controls by exploring whether these regions were hypo- or hyper-connected in patients versus controls. For this purpose, we calculated the mean connectivity between the corresponding pairs of regions for each group (healthy controls and FND patients).

2.2.7.2. Impact of anxiety, depression, medication, and clinical score on classification performance

In order to verify that our results were not driven by potential confounding factors like anxiety (STAI), depression (BDI), psychotropic medication (yes/no), and clinical scores/symptom severity (CGI), we used a logistic regression analysis (using *glm* function in R, which automatically removes missing data from regression analysis). Specifically, we test whether the aforementioned factors could predict if a subject was classified correctly or not (yes/no). We tested each factor individually and in combination.

2.3. Results

2.3.1. Demographic and clinical data

Data from 86 FND patients and 86 age- and sex-matched healthy controls, arising from four different centres were included in this study. All patients and 71 HC completed the Beck's Depression Inventory (BDI, (Beck, 1961)); 71 patients and 71 HC completed the State-Trait Anxiety Inventory (STAI-S, (Spielberger et al., 1983)). Two patients of centre II were not rated using CGI. Demographic and clinical data are presented in Table 2.2. There was no significant difference in age between centres and groups. One-way ANOVA on symptom severity (CGI scores) identified a significant effect of factor centre. Post-hoc Tukey's honestly significant difference (Tukey's HSD) showed that the difference in symptom severity between centre I and

IV ($P = 0.02$), between centre II and IV ($P = 0.001$) and centre III and IV ($P = 0.011$) were statistically significant, meaning centre IV had more severe cases than the three other centres.

FND symptom type was similar between centre I to III with a majority of abnormal movement (F44.4) diagnosis (see Table 2.2 for details) as well as functional seizures (F44.5) or mixed (F44.7) whereas centre IV had exclusively abnormal movements (F44.4) cases.

Table 2.2: Demographic and clinical characteristics of the four centres.

	Centre I		Centre II		Centre III		Centre IV	
	FND ($N = 23$)	HC ($N = 23$)	FND ($N = 24$)	HC ($N = 24$)	FND ($N = 24$)	HC ($N = 24$)	FND ($N = 15$)	HC ($N = 15$)
Age, mean (SD), years	42.4 (13.9)	41.8 (13.3)	39.8 (13.2)	35.5 (13.3)	42.6 (10.6)	44.3 (9.41)	40.8 (12.2)	40.7 (13.2)
Sex (females/males)	21/2	20/3	14/10	16/8	21/3	21/3	7/8	8/7
Disease severity (CGI, median, quantile)	2 [0.5 – 3]	<i>NA</i>	1 [1 – 2]	<i>NA</i>	1 [1 – 2]	<i>NA</i>	3 [2 – 3]	<i>NA</i>
Psychotropic medication intake (yes/no)	14/9	0/23	6/18	1/23	11/13	7/17	<i>NA</i>	<i>NA</i>
Symptom type ^a	12 weakness 4 seizures 2 gait disorder	<i>NA</i>	11 weakness 3 seizures 12 gait disorder	<i>NA</i>	18 weakness 1 seizures 4 gait disorder	<i>NA</i>	3 tremor 13 myoclonus	<i>NA</i>
BDI score, mean (SD)	11.3 (5.18)	6.44 (6.27)	11.0 (11.7)	3.54 (3.82)	18.0 (14.9)	11.8 (13.1)	8.33 (8.41)	<i>NA</i>
STAI-S score, mean (SD)	60.6 (13.8)	60.7 (15.1)	73.5 (23.0)	64.5 (17.1)	90.7 (28.4)	84.0 (22.7)	<i>NA</i>	<i>NA</i>
BAI score, mean (SD)	<i>NA</i>	<i>NA</i>	<i>NA</i>	<i>NA</i>	<i>NA</i>	<i>NA</i>	17.2 (13.3)	<i>NA</i>

Data from centres I and IV are not the exact same data as used in the previous publications, due to the exact age- and sex match. Abbreviations: *FND*: functional neurological disorders, *HC*: healthy controls, *BDI*: Beck's Depression Inventors, *STAI*: State-Trait Anxiety Inventory, *CGI*: Clinical Global Impression Score ranging from 0 = none, 1 = mild, 2 = moderate, 3 = severe, 4 = very severe, *SD* = standard deviation, *NA* = not applicable.

^aPatients can present with more than one symptom type.

2.3.2. Framewise displacement

FD measures showed a significant main effect of *centre* ($F(3,164) = 5.5210$, $P = 0.001$). Post-hoc multiple comparison of means showed that the difference between centre I and centre III ($P < 0.0001$) and centre IV ($P = 0.0006$), as well as between centre II and centre III ($P =$

0.0002) and IV ($P = 0.008$) were statistically significant (Appendix A, Supplementary Material for Chapter 2, Figure A.2), meaning that centres III and IV had more motion artefacts as compared to centre I and II.

2.3.3. Replication and Robustness of Classification Approach

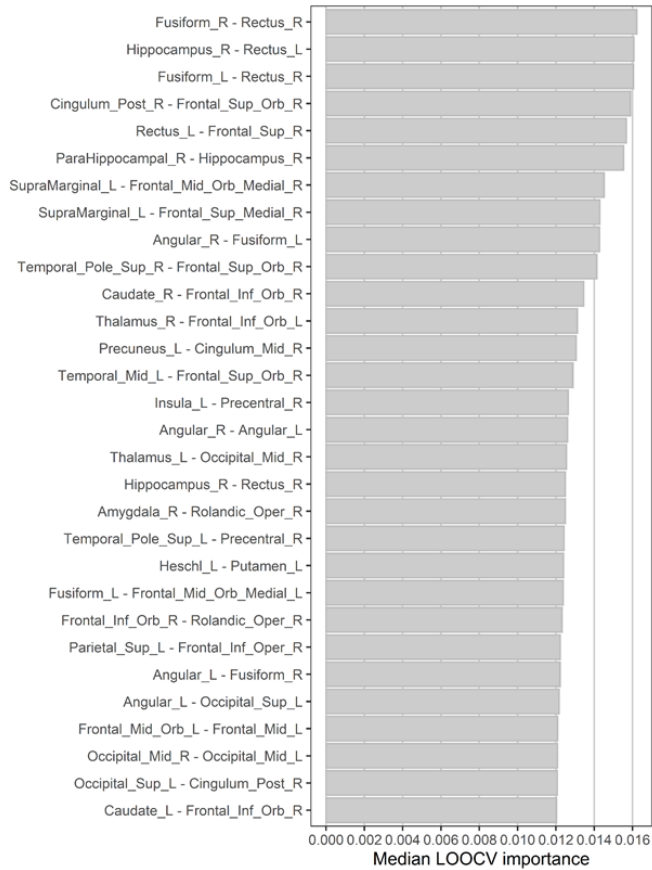
- (1) *Replication*: Applying the method from (Wegrzyk et al., 2018) on the slightly modified sample size (see Chapter 2.2.1. Participants) found very similar values: accuracy of 73.9% (published 68.8%), as well as a highly balanced sensitivity of 69.6% (published 68%), specificity of 78.3% (published 69.6%), and with AUC of 0.86.
- (2) *Intra-centre cross-validation*: The exact same method, when applied to centres II, III and IV, yielded accuracies ranging from 70 – 72.9% ($P = 0.02 – 0.001$). Equivalently, the sensitivity and specificity were balanced (sensitivity: 70.8 – 79.2%, specificity: 66.7 – 70.8), and their diagnostic abilities - indicated by the AUC - were moderate to good in all three centres (see Table 2.3 for details).
- (3) *Pooled cross-validation*: When data from the four centres were pooled, a significant classification accuracy of 71.5% (sensitivity: 67.4%, specificity 75.6%, AUC: 0.79, $P = 0.003$, see Table 2.3 for details) was found. We present below the list of most discriminative features with their SVM weights, the confusion matrix, and the receiver operating characteristic (ROC) curve and of the pooled cross-validation in Figure 2.2.

A visual representation of accuracy, sensitivity, specificity across all centres, and ROC curve of the intra-centre- and inter-centre cross-validation can be found in Appendix A, Supplementary Material for Chapter 2, Figure A.3 and Figure A.4.

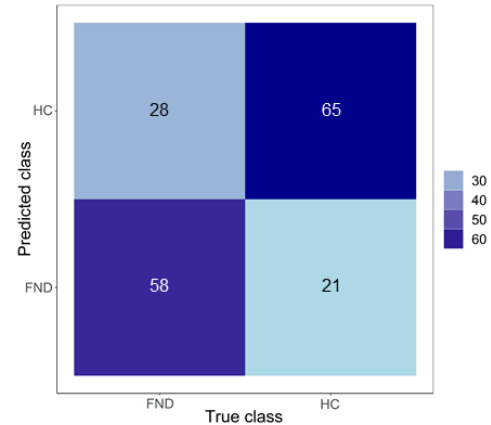
Table 2.3: Classification performance of the intra-centre and pooled validation steps on the four different centres.

Centre	Accuracy (%)	Specificity (%)	Sensitivity (%)	AUC	P -value
<i>Intra-centre cross-validation</i>					
I	73.9	78.3	69.6	0.86	0.001
II	72.9	66.7	79.2	0.73	0.002
III	70.8	70.8	70.8	0.67	0.002
IV	70	66.7	73.3	0.75	0.02
<i>Pooled cross-validation</i>					
	71.5	75.6	67.4	0.79	0.003

A Most discriminative features



B Confusion matrix



C ROC curve (AUC: 0.79)

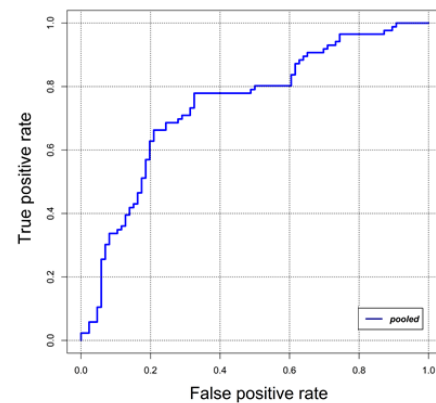


Figure 2.2: Classification results of the pooled cross-validation. (A) Overview over the 30 most discriminative features to distinguish FND from HC representing the weights assigned by the classifier (Median LOOCV importance). LOOCV refers to leave-one-out cross-validation. (B) Confusion matrix for the pooled cross-validation. (C) The receiver operating characteristics (ROC) curve, and area-under-the-curve (AUC) for the pooled cross-validation.

2.3.4. Post-hoc analyses

2.3.4.1. Most discriminative connections

In the pooled cross-validation, regions such as the hippocampus, the bilateral angular gyrus, the cingulate cortex, bilateral frontal regions and the bilateral supramarginal gyrus were most frequently found within the most discriminative connections. When exploring the connectivity differences between patients and controls in the regions yielding the most discriminative connections, we identified increased connectivity in patients between:

- the hippocampus and temporal regions (e.g., right superior temporal gyrus and middle temporal pole), the cingulate cortex, and the bilateral precuneus
- the bilateral angular gyrus and sensorimotor regions (e.g., postcentral gyrus), the bilateral fusiform gyrus, and the left superior occipital gyrus

- (c) right cingulate cortex and right frontal regions (e.g., orbitofrontal gyrus) and the right thalamus

Similarly, we identified decreased connectivity in patients between

- (a) the right hippocampus and right frontal regions (e.g., inferior orbitofrontal gyrus), subcortical regions (e.g., bilateral parahippocampal gyrus and bilateral amygdala) and subcortical structures (left putamen)
- (b) the anterior cingulate cortex and the right caudate
- (c) the right and left amygdala
- (d) left supramarginal gyrus and frontal regions (e.g., orbitofrontal and middle frontal gyrus)

For visualization purposes, regions yielding the most discriminative connections for the pooled cross-validation are presented in Figure 2.3 (the corresponding figure for each single centre can be found in Appendix A, Supplementary Material for Chapter 2, Figure A.6). A figure displaying hyper- and hypoconnectivity between the regions yielding the most discriminative connections can be found in Appendix A, Supplementary Material for Chapter 2, Figure A.5. Data were visualized using BrainNet Viewer (Xia et al., 2013). Mean FC in controls and patients between pairs of regions showing most discriminative FC of the pooled cross-validation can be found in the Appendix A, Supplementary Material for Chapter 2, Table A.2).

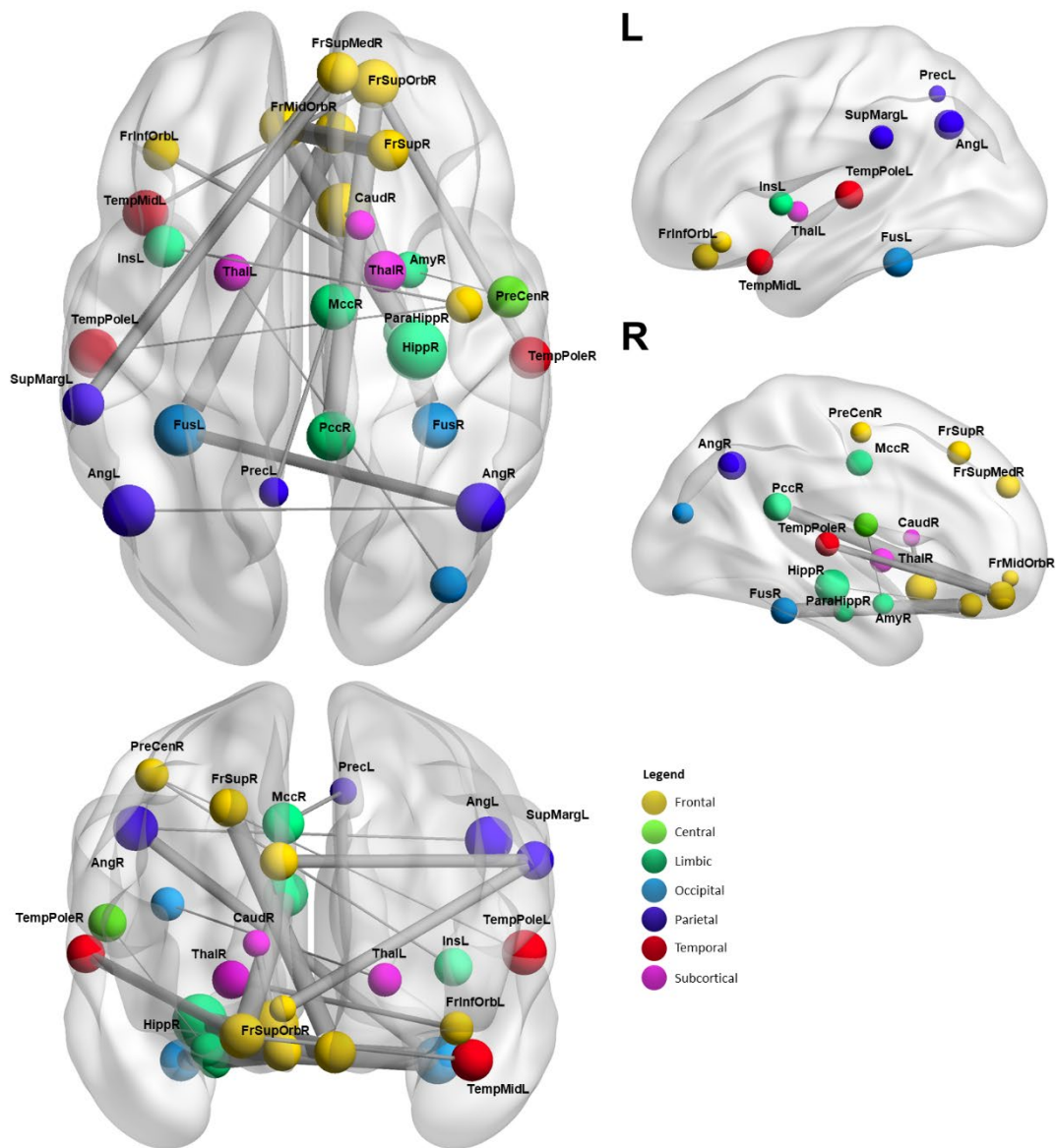


Figure 2.3: Regions yielding the most discriminative connections of the pooled classification based on the AAL atlas. Size of the nodes correspond to nodal degree, respectively occurrence within the most discriminative connections. Colour of the nodes corresponds to different lobes of the AAL. Thickness of edges correspond to SVM weights. Thicker edges therefore indicate higher SVM weights, respectively higher discrimination power. The mean functional connectivity values corresponding to this figure can be found in Appendix A, Supplementary Material for Chapter 2, Table A.2. The figures corresponding to each single centre can be found in Appendix A, Supplementary Material for Chapter 2, Figure A.6.

2.3.4.2. Logistic regression of anxiety, depression, medication, and clinical scores

Whether a subject was classified correctly or not (yes/no) could not be predicted by anxiety, depression, medication and clinical scores - neither in the intra-centre nor in the pooled cross-validation setting (Appendix A, Supplementary Material for Chapter 2, Table A.3). These potential confounding factors thus did not drive the classification performances.

2.3.5. Generalizability to multi-centre data

- (1) *Inter-centre cross-validation*: When data from each single centre were used once to test the classifier and data from the remaining three centres were used to train the classifier, we found classification accuracies ranging from 37.5 – 50% (sensitivity: 37.5 – 56.5%, specificity: 33.3 – 54.2%), below chance level. Correspondingly, the AUC was below chance (see Table 2.4 for details).
- (2) *Centre normalization of functional connectivity data*: After normalization (see section 2.3), n-way ANOVA on the different connections with factor *group* and *centre*, corrected for multiple comparisons using false discovery rate (FDR), showed only a significant effect of factor group in 287 connections. No centre nor interaction effect was found. After normalization, FC thus only differed between groups (FND and HC), but no centre effect remained.
- (3) *Adapting the inter-centre cross-validation*: By gradually transferring two subjects (1 HC and 1 FND) from the test set to the training set, we observed an improvement of the overall classification performance to the level of the intra-centre and pooled cross-validation. However, after the transfer of approximately 16-20 subjects, the model started overfitting the results. The different learning curves of accuracy, sensitivity, and specificity of the four centres are presented in the Appendix A, Supplementary Material for Chapter 2, Figure A.7).

Table 2.4: Classification performance of the inter-centre cross-validation step on the four different centres.

<i>Inter-centre cross-validation</i>					
Centre	Accuracy (%)	Specificity (%)	Sensitivity (%)	AUC	<i>P</i> -value
Test set: I	50	43.5	56.5	0.46	0.1
Test set: II	37.5	33.3	41.7	0.43	1.0
Test set: III	45.8	54.2	37.5	0.41	1.0
Test set: IV	46.7	46.7	46.7	0.48	1.0

2.4. Discussion

2.4.1. Classification

In line with our first aim, these results show that classification of RS fMRI brain images with a machine learning algorithm (Wegrzyk et al., 2018) could be successfully replicated in three separate samples stemming from different recruiting centres. This means that, overall, this method can successfully distinguish FND patients from healthy controls with accuracies at or above 70% (centre I: 73.9% / II: 72.9% / III: 70.8% / IV: 70.0%). Importantly, these results confirm that the method provides an accurate and robust classification of FND patients and healthy controls within different MRI scanners – as the four centres had different manufacturers and acquisition parameters – when the models are trained at each site. It also shows robustness against clinical heterogeneity, because the FND populations of the four centres were not identical in terms of symptom type and severity. Namely, centre IV included only functional movement disorders (F44.4), whereas centre I to III included mixed (F44.7) cohorts. Patients included in centre IV rated their symptoms as more severe compared to the FND patients included in the other centres.

To strengthen this first validation step, we examined if the classification approach is also robust when merging the data from all four centres together. Therefore, we ran the exact same analysis in a second validation step by pooling all the data together, this yielded a similarly high classification accuracy of 71.5%. Similar results have been found among diverse neurological and psychiatric conditions (for review: Nielsen et al., 2020; Orrù et al., 2012). This strongly suggests that machine learning is an appropriate and robust tool to detect differences in FC in FND patients and HC. Furthermore, despite the clinical heterogeneity and potential inter-centre confounding factors (e.g., inter-scanner variability), the classifier yielded high classification accuracies. Using a post-hoc logistic regression analysis, we could additionally show that neither anxiety, depression, psychotropic medication intake, nor clinical scores had an impact on classification performance. These results indicate that our model probably discriminated between patients and controls based on features specific to the underlying FND pathology (i.e., aberrant FC) and not the clinical comorbidities, nor the symptom severity of FND patients. The underlying changes in FC – independent of symptom type and severity - might represent a FND specific trait, rather than a state. To further verify what these FND specific traits are, however, it is of utmost importance to compare the classification performance against other patient groups with similar symptoms but different diagnoses (e.g., other neurological disorders and/or psychiatric controls). Moreover, it must be considered that other predisposing factors might potentially drive the classification performance. Namely, the aetiology of FND is multifactorial. For instance, genetic risk factors or preceding traumatic life events are thought to affect the pathophysiological mechanisms of FND (Hallett et al., 2022). Particularly, traumatic life experiences and childhood adversities are known risk factors with average odds ratio between 2 – 4 (Ludwig et al., 2018). Moreover, functional and structural alterations have been detected

in FND patients in the context of trauma exposure, particularly in regions pointed out by the pooled analysis such as the cingulate cortex, insula, and the hippocampus (Aybek et al., 2015, 2014a; Diez et al., 2020; Maurer et al., 2016; Perez et al., 2017a). To the best of our knowledge, this is the first study using multi-centre data of FND patients including different symptom types and symptom severity for a multivariate classification approach. Moreover, machine learning algorithms seem to be robust enough against different symptom types and severity scores, as represented in our results.

In line with our second aim, we evaluated the generalizability of this classification approach by examining whether data from a naïve centre can be correctly classified when applying a model that has been trained on data from the three other centres. Even though we normalized with respect to centre, this third validation step showed that individual classification accuracies did not exceed chance level. Compared to the pooled validation, this step introduced scanner bias of the left-out centre only during the testing, whereas during the pooled cross-validation setting the scanner bias was already included in the training set. This suggests that variance introduced by inter-scanner variability is too high to be overcome using inter-centre cross-validation and might be substantially different from variance introduced by other confounding factors such as comorbidities or symptom severity. With our post-hoc adaptation of the inter-centre cross-validation setting, in which we gradually transferred subjects from the test set to the training set in order to introduce centre-specific scanner bias already during the training, we observed a gradual increase in overall classification performance. This observation strengthens our assumption of that inter-scanner variability plays a critical role and cannot be overcome in our inter-centre cross-validation setting. Indeed, inter-scanner variability is a well-known bias for multi-centre RS fMRI data (Noble et al., 2017; N. Zhao et al., 2018) that yet has to be overcome. Specifically for multi-centric fMRI graph data, not only functional, but also structural imaging data has been shown to influence graph representation, as fMRI data is parcellated according to the structural MRI data (Castrillon et al., 2015). Neither did regressing out the site substantially aid the classification (Castrillon et al., 2015). Alternatively, our sample size might be too small to properly capture sufficient variation within each site (whether subject-driven or related to technical factors) to generalize to completely unseen sites. Another study on multi-site resting-state connectivity classification for Autism spectrum disorder showed that, given sufficient subjects in the training set (between 280 and 500 depending on inclusion criteria), inter-site performance could reach intra-site performance, but that this was not the case at smaller sample sizes (Abraham et al., 2017). The assumption that a sample size may be too small, can be strengthened by the fact that after normalizing the data, no significant centre effect remained.

In summary, a multi-centre scenario increases the sample size (i.e., in our second validation step) and consequently the heterogeneity of the sample, which might benefit the classification performance. On the contrary, it introduces systematic inter-scanner variability (“site bias”) which is unrelated to the underlying disorder of interest and thus might complicate the discriminative power (Abdulkadir et al., 2011). Consequently, there are only a few studies

investigating the applicability of multi-centre classification based on RS FC. In line with our findings, equivalently good classification performances were achieved in pooled multi-centre classification settings using a SVM classifier based on RS FC e.g., for autism spectrum disorder ($N = 240$ subjects, accuracy = 79%; Chen et al., 2016), for mild cognitive impairment ($N = 367$ subjects, accuracy = 72%; Teipel et al., 2017), as well as for major depressive disorder ($N = 358$ subjects, accuracy = 73%; Nakano et al., 2020). The latter also investigated robustness against site bias on classification using a leave-one-site-out cross-validation (LOSO-CV; equivalent to our inter-centre cross-validation). Comparable with our results, their LOSO-CV did not succeed in classifying major depressive disorder in a fully unknown dataset.

The inter-scanner variability clearly limited the classification performance and generalizability when data from a specific scanner was only used for testing but not during the training. Combining data from different modalities, has been found to be one solution to overcome the limitations of multi-centre RS fMRI (Zhuang et al., 2019). For instance, high classification accuracies were achieved in pooled as well as LOSO-CV combining T1-weighted (structural/anatomical) images with RS FC from patients with frontotemporal dementia and healthy controls (Donnelly-Kehoe et al., 2019). Accordingly, the successful classification of functional seizures based on structural imaging data (Vasta et al., 2018) would suggest employing multi-modal data of FND patients for future classification approaches when working towards a clinical application. Furthermore, previous studies attempted to identify and characterize inter-scanner variability and how they influence fMRI data (Dansereau et al., 2017; Friedman et al., 2006). As such, classification was found to be improved by site harmonization methods (Nakano et al., 2020; Yamashita et al., 2019; Yu et al., 2018). Site harmonization approaches, however, still face methodological challenges: Recent studies raised concerns that site harmonization methods might interfere with analytical methods (Chen et al., 2022), depend on choice of atlas (Yu et al., 2018), or can be substantially impacted by the use of fMRI acquisition parameters (Mori et al., 2018; Yamashita et al., 2019). Apart from using site harmonization approaches, promising results have also been found when applying unsupervised machine learning algorithms such as deep learning. Although they are computationally more complex, they appeared to be robust against site differences (Dewey et al., 2019; Zeng et al., 2018). At last, a feature selection could be implemented in order to reduce the high dimensionality of our feature vectors (Guyon et al., 2003). However, the aim of this project was to examine the generalizability of the previously applied method on different movement disorders/FND centres, rather than developing the best possible machine learning approach suitable for a multi-centre setting. Nevertheless, this could be the goal of future additional validation studies.

2.4.2. Connectivity patterns

Upon visualization of the most discriminative weights of individual connections, we could evaluate their individual contribution to the overall classification. Our study identified regions

as most discriminative that indeed were commonly reported in the literature, such as the cingulate cortex (Aybek et al., 2015; Baek et al., 2017; Blakemore et al., 2016; Marapin et al., 2020), right temporal regions (i.e., the temporoparietal junction, TPJ) (Aybek et al., 2014a; Espay et al., 2018b; Maurer et al., 2016), the amygdala (Aybek et al., 2015; Morris et al., 2017; Voon et al., 2011), the insula (Espay et al., 2018b; Stone et al., 2007; Voon et al., 2011), the inferior frontal gyrus (IFG, Espay et al., 2018b) or the dorsolateral prefrontal cortex (dlPFC, Aybek et al., 2014; Voon et al., 2016, 2011). However, feature weights need to be interpreted with caution, as a machine learning algorithm values the utility for classification, rather than the clinical relevance of a feature (Nielsen et al., 2020; Nunes et al., 2020). Therefore, one should not infer upon the potential underlying mechanisms of a disorder, but rather examine the weights for their potential pathophysiological validity. As such, our results provided connectivity patterns that are particularly interesting to further construe: connections including 1) the angular- and supramarginal gyri, to sensorimotor regions and 2) cingular- and insular cortex, to hippocampal regions. The angular and supramarginal gyrus are located within/bordering the temporo-parietal junction (TPJ), a key structure for FND. Abnormal interaction between the TPJ and sensorimotor regions has been repeatedly found in FND patient and is thought to be associated with their impaired sensory prediction signal (i.e., the sense of agency) (Perez et al., 2012; Voon et al., 2010b). Similarly, RS-fMRI study in FND identified decreased connectivity from the TPJ to sensorimotor regions (Maurer et al., 2016), to the precuneus (Mueller et al., 2022), and between the TPJ, motor regions, cingulate cortex and insula (Diez et al., 2019), as well as decreased connectivity between the right inferior parietal cortex to the dlPFC and the anterior cingulate cortex (Baek et al., 2017) supporting the theory of impaired sensorimotor integration and impaired sense of agency. On the other hand, the cingular- and insular cortex, and hippocampal regions belong – amongst others - to the limbic network and are considered to be part of the emotion-cognition integrative system (Pessoa, 2008). Altered connectivity in FND in limbic regions have been associated with abnormal frontal lobe emotional control and emotion-motion interactions (Aybek et al., 2014a; Monsa et al., 2018). In particular, aberrant hippocampus activity was found in response to aversive stimuli in task-based fMRI using emotional stimuli (Aybek et al., 2014a; Blakemore et al., 2016; Szaflarski et al., 2018). Moreover, increased FC was found between the cingulate cortex, precuneus, and the ventromedial prefrontal cortex during a motor task (Cojan et al., 2009). Similarly, RS fMRI studies on FND identified increased connectivity from parahippocampal structures to the right superior temporal gyrus (Longarzo et al., 2020) and to the middle- and inferior temporal gyrus (Szaflarski et al., 2018), increased connectivity between the hippocampus and default mode network (DMN) related regions (Monsa et al., 2018), as well as increased FC from the amygdala to the dlPFC (Morris et al., 2017). Alterations in RS FC in these regions thus support previous findings on task-based fMRI stating an impaired emotion regulation in FND (Aybek et al., 2015, 2014a; Espay et al., 2018b).

2.4.3. Towards a clinical application

Excellent sensitivity and specificity (between 80-100%) has been found for bedside clinical signs (Daum et al., 2015; Espay et al., 2018a; Syed et al., 2011). However, these maneuvers may still face several limitations, including a lack of gold standards against which to compare them and unblinded assessments in most studies along with other methodological issues such as a poor description of how the diagnosis of FND was made. Additional diagnostic procedures might support the clinical diagnostic process. With regard to a multivariate classification approach applied within a clinical setting, an accuracy of 70% might not present a final solution. The setting of classifying patients against healthy controls does not represent the clinical need and limits the generalizability of these results to clinical application at this stage. For daily clinical routine, one should rather aim at distinguishing a functional symptom from identical/similar neurological and psychiatric symptoms, and not from a healthy control. The potential applicability of such a machine learning approach would be for example to assist screening of patients in the emergency department in cases of ambiguous neurological symptoms or could provide more details in difficult cases. Therefore, rather than replacing a clinical diagnosis, it might provide additional diagnostic support in the form of additional rule-in tests. A patient with a functional disorder could easier be identified as such - in addition to the bedside clinical signs - and could be directly referred to a specialist, before undergoing multiple medical tests and examinations (Espay et al., 2009). Besides, the medico-legal context highlights the importance of identifying an adjunctive positive biomarker in order to help distinguishing FND from intentionally produced neurological symptoms as observed in malingering or factitious disorders in which patients fabricate their symptoms or simply are feigning or lying about their symptoms (Colombari et al., 2021). Therefore, to test the power against differential diagnoses, it is of utmost importance – as a next step - to classify FND patients against similar psychiatric patients, trauma patients or against neurological patients with the same or similar symptoms (e.g., dystonia, essential tremor, Parkinson's disease, or multiple sclerosis). In summary, machine learning algorithms could thus further support differential diagnoses and optimize treatment prevention and patient management. However, diagnostic utility is only provided if these results can be replicated in other patients with the same or similar symptoms, but different diagnoses.

2.4.4. Limitations and future directions

This study has several limitations. Even though data from four different centres were used, the sample size is small compared to other multi-centre classification studies using multi-centre data bases, such as the Alzheimer's Disease Neuroimaging Initiative (ADNI) (Jack et al., 2008) or the Autism Brain Imaging Data Exchange (ABIDE) project (Di Martino et al., 2014). To date, a large, multi-centre database sharing imaging data of FND patients unfortunately does

not exist. Small sample sizes have been associated with higher reported accuracies without properly controlling for overfitting (Vabalas et al., 2019). We avoided overfitting by perfectly matching our groups within- and between centres and by applying a leave-one-out cross-validation approach, which is a powerful tool against overfitting and recommended in small samples (Vabalas et al., 2019). Accordingly, our results of the intra-centre and pooled cross-validation are comparatively high with significant accuracies and highly balanced sensitivities and specificities. Nevertheless, a multi-centre database would bring the advantage of adjusting scanner protocols on each centre and scanner type and would thus provide comparably high data quality and low inter-scanner variability. Thereby, multi-centre imaging studies must be planned carefully with regards to scanner hardware and software, implementation of an appropriate quality assurance program to properly validate and monitor data, and application of proper site standardization methods (for recommendations see Glover et al., 2012).

A second limitation is the use of only one atlas with 90 cortical- and subcortical regions. As for now, the purpose of this project was to validate the previously published method across different centres, no changes were made to the pre-processing pipeline. Despite involving a higher computational load, a more fine-grained parcellation (e.g., Glasser atlas (Glasser et al., 2016)) or a voxel-wise approach could detect different information (Eickhoff et al., 2018), and may aid the future development of an adjunctive imaging-based biomarker. On the contrary, using an approach with a higher spatial resolution also bears the risk of overfitting or missing important information due to the comparable high amount of probably uninformative features (Erickson et al., 2017).

A third limitation is that centres III and IV were found to have higher head motion than centres I and II, what might negatively affect FC (Van Dijk et al., 2012). The significant results obtained in intra-centre and pooled-centre validation, however, indicate that even patients known to have a lot of movements (Centre III and IV had more motor subtypes of FND F44.4) can be correctly classified. For future studies, subjects should be strictly advised to lay calmly, and their head should be fixed using foam cushions. Ideally, prospective motion correction techniques including motion-tracking cameras or a pilot tone approach (Ludwig et al., 2021) could be used to further improve data quality in this respect.

A last limitation is that clinical data were not uniformly collected and used different scales (CGI, S-FMDRS scales), which meant that scales needed to be adjusted. Including symptom severity in our post-hoc logistic regression analysis is therefore not optimal, as the transformation we have done from S-FMDRS to CGI is intuitive but not validated. Similarly, as anxiety and/or depression scores were collected using different questionnaires (STAI, BDI or BAI), the regression analysis showing no influence of mood on the classification performance should be interpreted with caution until future studies confirm this with prospectively collected uniform clinical data. Together with the uneven distribution of symptom types, we cannot fully account for it with good reliability. From a technical point of view, a future project should aim at balancing the different symptom types, so that a data-driven machine learning approach would learn to recognize those patients as well who are normally

underrepresented in a clinical setting. To overcome the problem of different symptom type distribution, patients could also be stratified according to their symptom types and/or include the clinical data (e.g., CGI) into the model (Patel et al., 2015). In order to achieve this in a multi-centre setting, it would be necessary that the same clinical data and psychiatric comorbidities are collected using the same clinical scores and identical questionnaires in each centre. Additionally, data on traumatic life events or childhood adversities should be collected, in order to assess the potential influence on functional brain aberrancies.

2.4.5. Conclusion

In summary, multi-centre RS FC has shown its potential to distinguish FND patients from HC. These findings set the ground for future research on adjunctive biomarkers for FND as the method will need to be improved regarding its generalizability regarding inter-scanner variability and the heterogeneity of symptoms, comorbidities, and severity of symptoms. To provide diagnostic utility, future studies must investigate the classification power when classifying FND patients against classical neurological diseases and/or psychiatric disorders as this would represent a closer setting to the clinical daily routine and could be used as a decision support method for the clinical diagnosis. Importantly, not to replace the clinical diagnosis, but to provide additional rule-in criteria for the diagnosis instead.

A Biopsychological approach to the Stress-Diathesis Model

This chapter is published as:

Weber, S., Bühler, J., Vanini, G., Loukas, S., Bruckmaier, R., Aybek, S. Identification of biopsychological trait markers in functional neurological disorders. Brain, 2022

<https://doi.org/10.1093/brain/awac442>

Contribution:

I was involved in the conceptualization, experimental design, and project administration. Together with my colleague Janine Bühler, we planned the study execution and collected the data. I was responsible for the proper storage of biological data and coordinated the biological analysis with Prof. Rupert Bruckmaier. I performed the pre-processing and analysis of all the demographic-, biological-, and imaging data. I wrote the original draft of the manuscript, coordinated correspondence with the Journal and revised the manuscript.

Abstract

Stress is a well-known risk factor to develop a functional neurological disorder, a frequent neuropsychiatric medical condition in which patients experience a variety of disabling neurological symptoms. Only little is known about biological stress regulation, and how it interacts with predisposing biological and psychosocial risk factors. Dysregulation of the hypothalamic-pituitary-adrenal axis in patients with functional neurological disorders has been postulated but its relationship to preceding psychological trauma and brain anatomical changes remains to be elucidated. We set out to study the hypothalamic-pituitary-adrenal axis analysing the cortisol awakening response and diurnal baseline cortisol in 86 patients with mixed functional neurological symptoms compared to 76 healthy controls. We then examined the association between cortisol regulation and the severity and duration of traumatic life events. Finally, we analysed volumetric brain alterations in brain regions particularly sensitive to psychosocial stress, acting on the assumption of the neurotoxic effect of prolonged cortisol exposure. Overall, patients had a significantly flatter cortisol awakening response ($P < 0.001$) and reported longer ($P = 0.01$) and more severe ($P < 0.001$) emotional neglect as compared to healthy controls. Moreover, volumes of the bilateral amygdala and hippocampus were found to be reduced in patients. Using a partial least squares correlation, we found that in patients, emotional neglect plays a role in the multivariate pattern between trauma history and hypothalamic-pituitary-adrenal axis dysfunction, whilst cortisol did not relate to reduced brain volumes. This suggests that psychological stress acts as a precipitating psychosocial risk factor, whereas a reduced brain volume rather represents a biological predisposing trait marker for the disorder. Contrarily, an inverse relationship between brain volume and cortisol was found in healthy controls, representing a potential neurotoxic effect of cortisol. These findings support the theory of reduced subcortical volumes representing a predisposing trait factor in functional neurological disorders, rather than a state effect of the illness. In summary, this study supports a stress-diathesis model for functional neurological disorders and showed an association between different attributes of trauma history and abnormalities in hypothalamus-pituitary-adrenal axis function. Moreover, we suggest that reduced hippocampal- and amygdalar volumes represent a biological ‘trait marker’ for functional neurological disorder patients, which might contribute to a reduced resilience to stress.

3.1. Introduction

Functional neurological disorders (FNDs) represent a frequent medical condition (Bennett et al., 2021; Carson and Lehn, 2016; Hallett et al., 2022) in which typical symptom presentation (Aybek and Perez, 2022; Espay et al., 2018a), diagnostic criteria (American Psychiatric Association, 2013), and multimodal treatment options (Bennett et al., 2021; Hallett et al., 2022; LaFaver, 2020) are well established, but only little is known about the underlying neuropathophysiological mechanisms causing the diverse symptoms (Drane et al., 2020). Recent pathophysiological models focus on a multifactorial origin of FND in the framework of a stress-diathesis model (Ingram and Luxton, 2005; Monroe and Cummins, 2015) (from the ancient Greek term “diathesis” = predisposition) integrating predisposing, precipitating and preceding risk factors (Cretton et al., 2020; Hallett et al., 2022; Reuber et al., 2007), and evaluate state versus trait markers of the disorder (Conejero et al., 2022; Perez et al., 2021). Studying biopsychosocial vulnerability factors is thus of utmost importance and could further explain the development of FND symptoms in a subgroup of (biologically) vulnerable individuals with certain psychosocial risk factors (Cretton et al., 2020; Keynejad et al., 2019).

Negative life events have recurrently been reported in FND (Kanaan and Craig, 2019; Karatzias et al., 2017; Reuber et al., 2007; Roelofs and Pasma, 2016), traditionally highlighting the role of sexual and physical abuse during childhood as preceding risk factor (Reuber et al., 2007; Roelofs et al., 2005; Roelofs and Pasma, 2016). Moreover, severity and frequency of childhood abuse could be linked to symptom severity (Roelofs et al., 2002). Similarly, symptom onset and severity could be connected to recent adverse social-occupational life events with a partial link to early childhood physical and sexual abuse (Roelofs et al., 2005), highlighting the importance of type but also timing of trauma. In this regard, a recent meta-analysis confirmed an increased frequency of childhood and adult adverse life events and abuse in FND patients compared to healthy controls (HC) and psychiatric control patients (Ludwig et al., 2018). Additionally, emotional neglect was identified to be much stronger associated with the symptom development, and thus weakened the dominating role of sexual abuse in the suspected aetiology of FND (Ludwig et al., 2018).

Neuroimaging studies intensively investigated the relationship between traumatic life events, symptom presentation and brain functional- and structural abnormalities in FND. As such, structural alterations in limbic and motor regions could be associated to childhood abuse and symptom severity (Aybek et al., 2014b; Perez et al., 2018, 2017b), whose effect was even more pronounced in women (Perez et al., 2017a). Similarly, an aversive emotional-stimulus dependent alteration of cortico-limbic and limbic-motor brain networks, involving regions such as the hippocampus (Aybek et al., 2014a; Balachandran et al., 2021; Diez et al., 2020), the amygdala (Diez et al., 2020, 2019), the supplementary motor area (SMA, Aybek et al., 2014a) and the prefrontal cortex (PFC, Aybek et al., 2014a; Balachandran et al., 2021) have been identified in FND. Noteworthy, hippocampal deactivation is suggested to disinhibit the hypothalamus-pituitary-adrenal (HPA) axis, triggering a stress response (Pruessner et al., 2008;

Wheelock et al., 2016), resulting in the release of stress hormones such as cortisol (Smith and Vale, 2006). HPA-axis alterations – as for example observed under chronic stress – have been associated with neuroanatomical changes, particularly in the hippocampus, the amygdala, or the PFC (Lupien et al., 2018; McEwen, 2017) which was attributed to a potential neurotoxic effect of glucocorticoids (Conrad, 2008; Lupien et al., 2018).

In FND, some studies suggested that patients have prominent hyperarousal, as stress markers of the autonomic nervous system were found to be increased (Bakvis et al., 2009a; Kozłowska et al., 2017b, 2015). Only few studies, however, analysed cortisol in FND (Apazoglou et al., 2017; Bakvis et al., 2010, 2009a; Chung et al., 2022; Maurer et al., 2015; Winterdahl et al., 2017), – as a measure of the adaptive (slow) stress response (Smith and Vale, 2006) – and the results were inconsistent. As such, decreased morning (Chung et al., 2022) and basal diurnal (Winterdahl et al., 2017) cortisol were reported, in contrast to no differences (Maurer et al., 2015) or increased basal diurnal cortisol compared to levels in HC (Apazoglou et al., 2017; Bakvis et al., 2010). This is explained essentially by methodological issues: studies were conducted using small sample sizes, focusing on only one particular symptom type, or within different test settings, potentially biasing the results (Stalder et al., 2016). This highlights the need to study the role of biological stress in relation to its neurological-, and psychological correlates, which could advance the understanding of pathophysiological mechanisms in FND and could generalize previous findings.

We set out to study alterations in the HPA-axis in a transdiagnostic approach across a large cohort of FND patients with mixed symptoms in a standardized domestic setting, to minimize biases of experimental setting. We adapted a transdiagnostic approach, as this efficiently targets the commonalities across the different symptom types. The primary aim was to assess the cortisol awakening response in FND compared to HC. The secondary aim was to evaluate the relationship between HPA-axis dysfunction, volumetric brain alterations and preceding trauma, and to discuss their potential role as predisposing (trait) versus precipitating factors.

3.2. Materials and methods

3.2.1. Participants

The study was conducted at the University Hospital Inselspital Bern, Switzerland. We included data of 86 FND patients with motor (F44.4) and sensory symptoms (F44.6), with functional seizures (F44.5), mixed symptom type (F44.7), and persistent postural-perceptual dizziness (PPPD). Board-certified neurologists confirmed the diagnosis of FND according to DSM-5 (American Psychiatric Association, 2013) and using positive signs (Stone and Carson, 2015). We included 76 age- and sex matched HC. Due to COVID-19 pandemic regulations in the hospital, no HC older than 65 years were allowed to be invited, and thus FND patients older than 65 years were not matched. Exclusion criteria were: 1) major neurological comorbidities, 2) a current severe psychiatric condition (acute suicidality, active psychotic symptoms), 3) alcohol or drug abuse, 4) pregnancy or breast-feeding, 5) contraindications for MRI and 6)

insufficient language skills. The study was approved by the Competent Ethics Committee of the Canton Bern (SNCTP000002289) and conducted according to the Declaration of Helsinki. All subjects provided written informed consent.

3.2.2. Saliva Samples

Saliva samples were collected according to the consensus guidelines of Stalder (Stalder et al., 2016), concerning design and strategies to control for adherence, and to account for covariates. All participants were instructed in an initial face-to-face appointment and received written take-home instructions and a self-reported diary. We assessed smoking habits, and for female participants information about their menstrual cycle and intake of hormonal contraceptives, as they represent potentially confounding factors of cortisol secretion (Pruessner et al., 1997; Stalder et al., 2016; Wust et al., 2000). Saliva was collected within a domestic setting, and a sampling date convenient for the participant was set. A reminder was sent by e-mail the evening prior to the sampling date. Participants were asked to collect nine saliva samples throughout the day by chewing for 2 minutes on a cotton swab (Salivette collection devices, Sarstedt, Rommelsdorf, Germany). Samples were taken directly upon awakening, 15-, 30- 45- and 60 minutes post awakening and further at 2-, 3-, 4- and 5 p.m. Participants were instructed to complete the five samples before breakfast and to refrain from heavy meals, fruits or fruit juices, coffee, carbonated soft drinks, chewing gum, smoking, teeth brushing or strenuous physical activities during the sampling in the morning and 45-60 minutes prior to sampling in the afternoon. Participants were instructed to note their wake-up time, any deviations from the sampling time and potential confounds in their self-reported diary. Participants were free to wake-up naturally or using an alarm clock and to follow their daily routine as usual. Saliva samples were collected the next day, centrifuged (10 min at 3900 rpm and room temperature) and frozen at -20 °C.

3.2.3. Demographic, Behavioural, and Clinical Characteristics

Symptom severity was evaluated using the Clinical Global Impression (CGI) score (zero = no symptoms to seven = among the most extremely ill patients) and the Simplified Version of the Functional Movement Disorder Rating Scale (S-FMDRS, Nielsen et al., 2017). Duration of symptoms was calculated from onset of symptoms to date of the study inclusion (in months). Use of psychotropic medication (i.e., benzodiazepines, opioids, antidepressants, neuroleptics, and antiepileptics), as well as corticosteroid medication were recorded. Mood was assessed using the Spielberg State-Trait Anxiety Inventory (STAI, Spielberger et al., 1983) and the Beck's Depression Inventory (BDI, Beck, 1961). Sleep quality of the night prior to saliva sampling was assessed using item four and five of the Leeds Sleep Evaluation Questionnaire (LSEQ, Shahid et al., 2011).

3.2.4. Traumatic Life Events

Traumatic life experiences were measured using the Traumatic Experiences Checklist (TEC, Nijenhuis et al., 2002). The TEC is a 29-item self-reported questionnaire which assesses the presence of diverse physical, emotional, and sexual traumata including age, relationship to the perpetrator, and the self-reported impact of the respective trauma. The TEC was scored using the syntax available at <http://www.enijenhuis.nl/tec>. Based on the syntax we computed 1) the overall number of experienced traumata (sum of all items), 2) six individual trauma severity subscores (determined by subjective impact and age of trauma for emotional neglect, emotional abuse, physical abuse, sexual harassment, sexual abuse, and bodily threat), and 3) developmental composite scores calculating experienced trauma according to the age ranges of 0 to 6 years, 7 to 12 years, 13 to 18 years and > 19 years. Additionally, we computed duration and relationship to the perpetrator for each trauma subscore. The duration of trauma was calculated using the maximum duration within those questions belonging to each trauma subscore. The relationship to the perpetrator was coded into categorical variables being one: inner-family circle (parents, siblings, partner), two: outer-family circle (relatives), three: friends and acquaintances, four: strangers. Additionally, to focus on trauma occurring only during childhood, we used the Childhood Trauma Questionnaire (CTQ, Bernstein et al., 1998); a 25-item self-reported questionnaire which assesses childhood trauma across five domains including emotional- and physical abuse and neglect, and sexual abuse.

3.2.5. Saliva samples analysis

Salivary cortisol was analysed by a commercial saliva-specific competitive enzyme immunoassay (cELISA, Salimetrics, Newmarket, United Kingdom). The manufacturer states a functional sensitivity of 0.28 ng/mL, and cross-reactivity for 14 endogenous and synthetic steroids is reported to be <1% each. The assay had been used according to the protocol provided by the manufacturer. Intra- and inter-assay coefficients of variation were 4.5% and 4.8%, respectively.

3.2.6. Neuroimaging data acquisition and pre-processing

To investigate neuroanatomical differences between patients and controls, we used a voxel-based morphometry approach. Anatomical images were acquired for all subjects except of three FND patients and three HC. MRI sequence and pre-processing is detailed in the Appendix B, Supplementary Material for Chapter 3.

3.2.7. Statistical analysis

3.2.7.1. Behavioural data

Statistical analyses were performed using *R* software (version 4.1.2.) and MATLAB (R2017b, MathWorks Inc., Natick, USA). Questionnaire data were tested for normality using Shapiro-Wilk's test. Normally distributed data were analysed using two-sample *t*-test, highly skewed data using Wilcoxon rank sum test. Questionnaires with subscores were corrected for multiple comparisons using false discovery rate (FDR). Categorical data were analysed using Chi-squared test (sex) and Fisher's exact test (menstrual cycle and relationship to perpetrator (TEC)). To determine significance alpha-level was set at $P < 0.05$.

3.2.7.2. Biological data

We analysed two metrics to assess cortisol levels: the cortisol awakening response (CAR) and the diurnal baseline cortisol (DBC).

The CAR describes the rapid increase in cortisol secretion across the first 30 to 45 minutes upon awakening and thus, represents the dynamic changes of cortisol secretion occurring upon awakening (Pruessner et al., 2003; Stalder et al., 2016). It has been shown that the intraindividual stability is relatively high and subtle changes in HPA-axis function regarding environmental noise can be detected with high accuracy (Wust et al., 2000). To assess group cortisol differences in the CAR, a repeated measures ANOVA was used on the fitted data of the five morning samples (wake-up until 60 min post-awakening) using a linear mixed model with fixed effects of factor group and timepoint, and using age, sex, smoking, wake-up time, BDI, STAI, hormonal contraception, corticosteroid medication, psychotropic medication, menstrual cycle, menopause, and sleep quality as covariates of no interest (Pruessner et al., 1997).

The DBC represents the dynamic changes of cortisol throughout the afternoon (from 2 p.m. to 5 p.m.). To analyse the DBC, the same analysis was performed as in the CAR using the four samples in the afternoon. For the analyses of the CAR and the DBC, we excluded data from eight FND patients and nine HC as they did not properly adhere to the saliva sampling protocol with either missing samples ($N = 3$) and/or delays ($N = 16$) (strict sampling accuracy margin of $\Delta t > 5$ min for post-awakening samples and $\Delta t > 15$ min for afternoon samples (Stalder et al., 2016)).

As we were interested in examining the multivariate pattern of correlation between cortisol and other variables (see below), single estimates of the CAR and the DBC were calculated using area-under-the-curve (AUC) based measures, as recommended in methodological consensus guidelines (Fekedulegn et al., 2007; Stalder et al., 2016). As such, the post-awakening cortisol concentration (PACC) and the diurnal baseline cortisol concentration (DBCC) were computed. The PACC describes the summed cortisol concentration across the first five samples in the

morning. The DBCC represents the cumulated cortisol concentration of the four afternoon samples. As a measure for the PACC and DBCC, the AUC with respect to ground (AUC_G) was calculated. Additionally, as a (static) measure for the CAR, the AUC with respect to increase (AUC_i) was calculated on the five morning samples (CAR_i , Stalder et al., 2016). AUC-based measures were calculated according to Pruessner (Pruessner et al., 2003). Three subjects were excluded for calculating the AUC-based measures due to missing samples. Subjects reporting delays were included, as the AUC formula can account for sampling delays (see Appendix B, Supplementary Material for Chapter 3 and Figure B.1 for more details). All analyses were repeated in females only Figure B.9.

3.2.7.3. Imaging data

To analyse between group differences of cortical volumes, we firstly applied a general linear model on the smoothed whole-brain anatomical images within SPM12. Second, given the *a priori* hypothesis of the hippocampus and the amygdala being particularly vulnerable to anatomical changes in the context of chronic stress (Lupien et al., 2018; McEwen, 2017), we analysed volumetric differences in those two regions. As such, we performed two region-of-interest (ROI) analyses using the corresponding ROI masks, derived from the automatic anatomic labelling atlas 3 (AAL3, Rolls et al., 2020). Whole-brain, as well as ROI analyses were corrected for multiple comparisons using a family-wise error (FWE) rate at $P < 0.05$, and total intracranial volume (TIV), age, sex, depression, and anxiety were added to the analysis as covariates of no-interest. Lastly, we extracted subject-wise estimates of the mean ROI volumes for external analyses. All analyses were repeated in females only Appendix B, Supplementary Material for Chapter 3, Figure B.10, Table B.6.

3.2.8. Multivariate pattern of correlation

In a last step, we applied partial least squares correlation (PLSC, Krishnan et al., 2011; McIntosh and Lobaugh, 2004) to evaluate multivariate patterns of correlation between behavioural data (trauma scores), cortisol AUC_G and AUC_i measures (CAR_i , PACC, DBCC), and volumetric data (mean ROI volume) in FND patients and healthy controls. For the PLSC analysis, only those subjects were included of which salivary cortisol (FND = 84, HC = 75) and imaging data (FND = 83, HC = 73) were complete. Data was standardized and a correlation matrix was calculated between the two sets of variables. To find individual weights of the corresponding data tables (cortisol data, volumetric data, trauma scores), a single value decomposition (SVD) was applied on the correlation matrix. The SVD leads to different correlation components consisting of a set of design weights and outcome weights (salience), indicating the strength of contribution of each weight to the multivariate pattern. The weights were used to calculate two sets of latent variables as such that the covariance was maximized. Significance was evaluated by permutation testing (5000 permutations). Stability of the weights

was assessed using bootstrapping (200 bootstrapping samples). PLSC allows for examining the relationship between multiple variables with different attributes. We used the publicly available PLS toolbox for MATLAB (https://github.com/FND-ResearchGroup/myPLS_SL.git), the use of which has already been described in other studies (Loukas et al., 2021; Zöllner et al., 2019).

We conducted three individual PLSC analyses; First, we used the cortisol values as design variables, and TEC severity scores, developmental scores, duration of trauma, and relationship to the perpetrator as outcome variables to evaluate multivariate pattern of correlation of trauma history and HPA-axis dysfunction. Second, we used the volumetric data of the whole-brain, as well as hippocampus and the amygdala alone (normalized for TIVs) as design variables, and age, sex, and cortisol values as outcome variables to evaluate the multivariate pattern of correlation between cortisol and changes in brain volume. Lastly, we evaluated in patients only the relationship of the aforementioned factors with clinical data (i.e., symptom severity, and duration of symptoms), Appendix B, Supplementary Material for Chapter 3 Figure B.6, Figure B.7 and Figure B.8.

3.3. Results

3.3.1. Clinical, behavioural, and demographic characteristics

Data from 86 FND patients and 76 age- and sex matched HC were included in this study. Demographic, behavioural, and clinical data are presented in Table 3.1. The most common symptom types were sensorimotor deficit (38.7%), gait disorder (21.5%), and/or tremor (14.6%). Level of diagnostic certainty for functional seizure patients were: seven probable, three clinically established, and four documented, according to diagnostic criteria of LaFrance.(Lafrance et al., 2013) Five patients were currently under corticosteroid medication, four of them only in a topical form (nasal spray) used irregularly on demand, and one patient was under oral prednisone medication. Patients using sprays resigned from using them on the day of saliva collection. FND patients and HC significantly differed in their smoking habits (more smokers in FND), their BDI, and STAI scores (more depression and anxiety in FND).

Table 3.1: Demographic, behavioural, and clinical data

	FND (N = 86)	HC (N = 76)	Statistics
Age, mean (SD), years, [range]	37.7 (14.2), [17 – 77]	33.1 (10.9), [18 – 62]	<i>ns</i>
Sex (females/males)	64/22	55/21	<i>ns</i>
Hormonal Contraception (yes/no)	27/37	18/37	<i>ns</i>
Menopause (yes/no)	14/50	10/45	<i>ns</i>
Menstrual Cycle ^a	15 anovulation	10 anovulation	Two-sided, $P = 0.05$ *
	10 follicular	3 follicular	
	22 luteal	33 luteal	
	2 menstruation	1 menstruation	
	7 ovulation	3 ovulation	
Smoker (yes/no)	33/53	8/68	$\chi^2(1) = 15.2, P < 0.0009$ ***
Disease severity (CGI, median, quantile)	2 [1 – 4]	NA	
Disease severity (S-FMDRS, median, quantile)	6 [2 -12.75]	NA	
Duration of illness (in months)	75 (166)		
Symptom type ^b	45 sensorimotor		
	25 gait disorder		
	17 tremor		
	12 myoclonus		
	13 seizures	NA	
	8 dystonia		
	7 PPPD		
	5 speech disorder		
	2 functional deafness		
	1 functional vision loss		
ICD-10 Classification ^c	63 F44.4		
	7 F44.5		
	30 F44.6	NA	
	8 F44.7		
	6 PPPD		
Psychotropic medication	14 benzodiazepines		
	29 antidepressants		
	6 neuroleptics	0/76	
	9 antiepileptics		
Corticosteroids (yes/no)	5/81	0/76	
BDI score, mean (SD)	14.4 (9.96)	4.59 (6.28)	$Z = -7.61, P < 0.0001$ ***
STAI-S score, mean (SD)	37.2 (10.9)	32.1 (7.67)	$t(156.68) = 3.22, P = 0.002$ **
LSEQ, mean (SD)	0.422 (0.169)	0.455 (0.15)	<i>ns</i>

^aMenstrual cycle was indeterminable in 8 patients and 5 healthy controls (natural irregularity or continuous intake of hormonal contraception)

^bPatients can present with several symptom types

^cDiagnosis of mixed FND (F44.7) was given when F44.4, F44.5, and F44.6 was present

$P^{***} < 0.001, P^{**} < 0.01, P^* < 0.05.$

3.3.2. Trauma

3.3.2.1. Traumatic Life Events

- (1) Overall number of experienced traumata (TEC): FND patients experienced significantly more total traumatic events compared to HC (reported as mean \pm SD: FND 6.78 ± 4.37 , HC 4.21 ± 4.22 , $Z = 4541$, $P < 0.001$), Figure 3.1,A.
- (2) Trauma severity scores (TEC): FND patients reported significantly more emotional neglect (FND 5.26 ± 6.32 vs. HC 2.4 ± 4.68 , $Z = 4247$, $P = 0.002$), Figure 3.1,B.
- (3) Developmental composite scores (TEC): FND patients reported significantly more traumata occurring in the age range from 0 to 6 (FND 3.43 ± 4.87 vs. HC 2.08 ± 3.93 , $Z = 3810$, $P = 0.43$) from 7 to 12, (FND 4.71 ± 4.81 vs. HC 3.07 ± 4.17 , $Z = 3962$, $P = 0.043$) and > 19 years old (FND 2.9 ± 4.03 vs. HC 1.26 ± 2.24 , $Z = 3840$, $P = 0.01$), Figure 3.1,C.
- (4) Duration of trauma (TEC): FND patients reported a longer duration of emotional neglect as compared to HC, i.e., 4.5 years longer (FND 6.95 ± 1.2 years vs. HC 2.36 ± 0.6 years, $Z = 3984$, $P = 0.01$), Figure 3.1,D. No significant differences were found with respect to duration of trauma for the other subscores.
- (5) Relationship to the perpetrator (TEC): In FND patients, emotional neglect occurred more often through members of the inner-family circle (two-sided, $P = 0.006$). No significant differences were found in the other subscores.

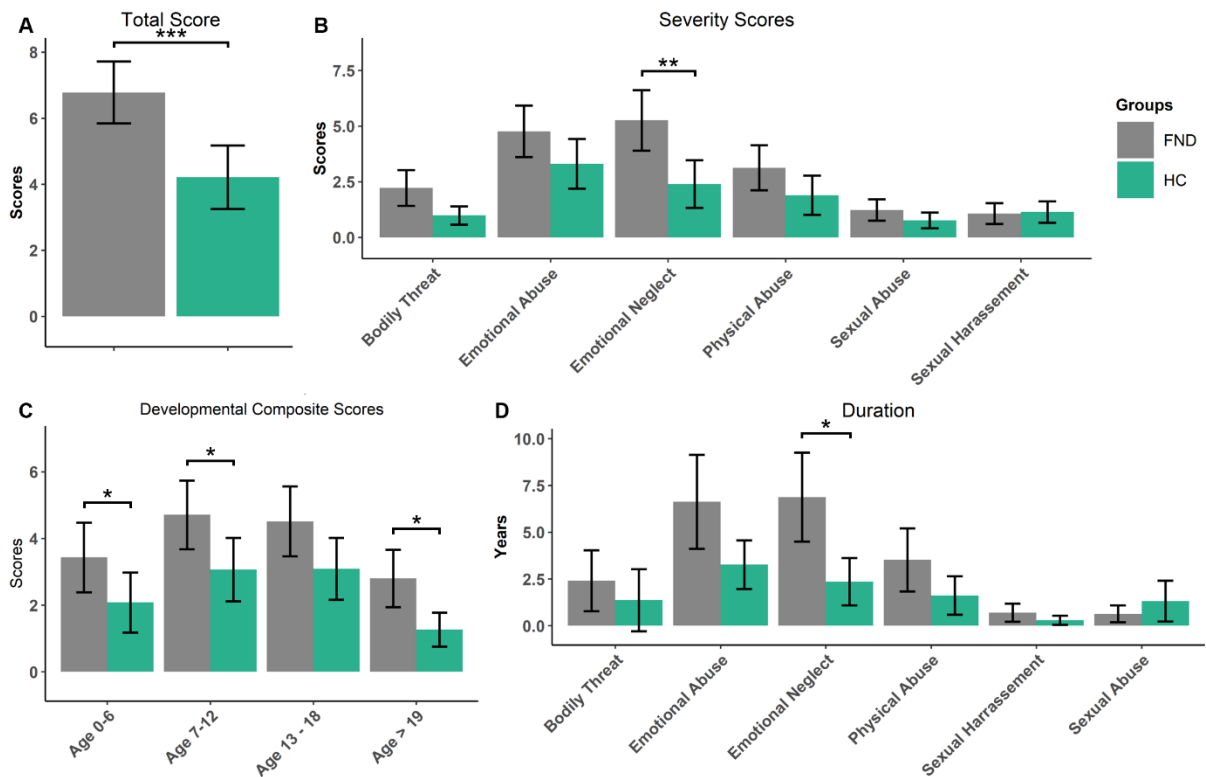


Figure 3.1: Traumatic Life Events. (A) For visualization purposes, means and confidence intervals of overall number of experienced traumata (ranging from 0 to 29). (B) Means and confidence intervals of six trauma severity scores (determined by subjective impact and age of trauma, ranging from 0 to 13 for emotional neglect, emotional abuse, physical abuse, sexual harassment, and sexual abuse or from 0 to 24 for bodily threat). (C) Means and confidence intervals of developmental composite scores (across trauma subscores). (D) Means and confidence intervals of duration of trauma. Significance codes: $P^{***} < 0.001$, $P^{**} < 0.01$, $P^* < 0.05$. Results are FDR-corrected.

3.3.2.2. Childhood Trauma

FND patients reported significantly more childhood emotional abuse (reported as mean \pm SD: FND 10.1 ± 5.1 , HC 8.2 ± 4.2 , $Z = 4028$, $P = 0.02$), emotional neglect (FND 11.1 ± 5.1 , HC 8.8 ± 4.2 , $Z = 4194$, $P = 0.009$), physical abuse (FND 7.3 ± 4.0 , HC 5.9 ± 2.0 , $Z = 3875$, $P = 0.03$), and physical neglect (FND 7.7 ± 3.1 , HC 6.79 ± 2.83 , $Z = 3935$, $P = 0.03$), Appendix B, Supplementary Material for Chapter 3, Figure B.2.

3.3.3. Salivary Cortisol

A significant main effect of group was found for the CAR ($F(1,680) = 28.81$, $P < 0.0001$) with lower levels in FND than HC. Post-hoc multiple comparisons between group and timepoints, showed that FND patients and HC significantly different in their cortisol levels at

timepoints 30' upon awakening, and almost reached significance at timepoint 15'-, 45'-, and 60' upon awakening ($P = 0.052$), Figure 3.2. No significant differences were found in the DBC.

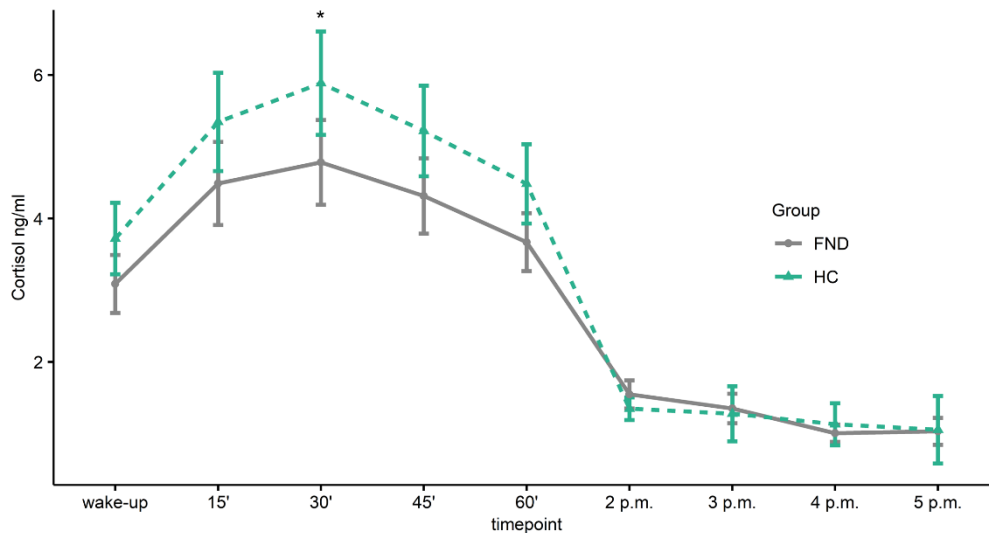


Figure 3.2: Cortisol Profile of FND patients and healthy. Mean and confidence intervals of daytime cortisol profile in FND patients and HC. Significance code: $P^* < 0.05$.

3.3.4. Volumetric brain alterations in FND patients

On a whole-brain level, significant group differences were found between FND patients and HC in five clusters at thresholds of $P_{FWE} = 0.05$, Figure 3.3, A and Table 3.2. These clusters included the following regions with decreased volumes in FND compared to controls: Left superior temporal gyrus, left gyrus rectus, bilateral amygdala, hippocampal- and parahippocampal gyri, as well as dorsolateral prefrontal gyri.

In line with the results on a whole-brain level, we confirmed our *a priori* hypothesis of a reduced hippocampal- and amygdalar volume in FND patients using an inclusive brain mask at thresholds of $P_{FWE} = 0.05$, Figure 3.3, B, Appendix B, Supplementary Material for Chapter 3, Table B.1 and Table B.2. Upon extraction of ROI volumes for external analyses, we found that the hippocampus, as well as amygdala volume were significantly smaller in FND patients compared to HC ($F(1,614) = 102, P < 0.001$). Post-hoc Tukey's HSD test revealed a significant difference between FND patients and HC in 1) the left hippocampus ($P < 0.001$), 2) the right hippocampus ($P < 0.001$) (Figure 3.3, B, upper panel), 3) the left amygdala ($P = 0.016$), and 4) the right amygdala ($P = 0.025$) (Figure 3.3, B, lower panel).

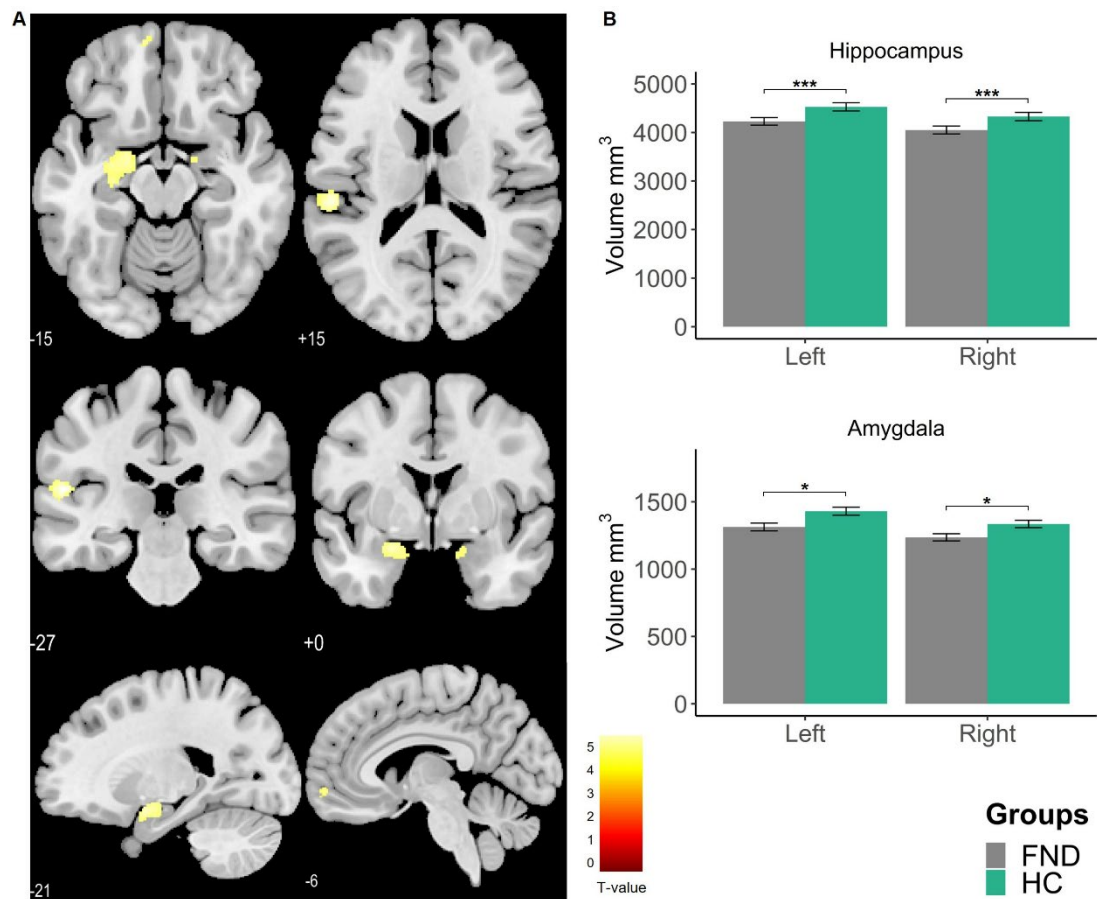


Figure 3.3: Results of voxel-based morphometry analysis. (A) Differential effect of voxel-wise comparison (HC > FND) with smaller grey-matter volume in FND in the hippocampus, parahippocampal gyri, amygdala, and dorsolateral frontal gyri. **(B)** Differential effect of mean ROI volume using a hippocampal mask (upper panel) and amygdala mask (lower panel) with smaller grey matter volume in FND. For both analyses, total intracranial volume (TIV), age, sex, depression (BDI), and anxiety (STAI) were added as covariates, thresholded on whole-brain level at $P_{FWE} < 0.05$. Significance codes: $P^{***} < 0.001$, $P^{**} < 0.01$, $P^* < 0.05$. A model corrected only for TIV, age, and sex can be found in the Appendix B, Supplementary Material for Chapter 3, Figure B.3, Table B.3.

Table 3.2: Whole-brain voxel-based morphometric results with total intracranial volume (TIV), age, sex, depression (BDI), and anxiety (STAI) as covariates of no interest.

Cluster-level			Peak-level			Peak coordinates in MNI Space			Cerebral regions
P_{FWE}	P_{FDR}	Cluster extent	P_{FWE}	P_{FDR}	Peak voxel Z-score	x,y,z {mm}			
0.001	0.084	255	0.002	0.506	5.248	-54 -27 14		Left superior temporal gyrus	
0.000	0.004	633	0.004	0.506	5.122	-15 3 -24		Left parahippocampal	
			0.006	0.667	4.996	-23 -1.5 -18		Left amygdala	
			0.017	0.875	4.783	-29 -17 -14		Left hippocampus	
0.006	0.553	82	0.004	0.506	5.117	0 62 -26		Left gyrus rectus	
0.008	0.553	69	0.014	0.875	4.831	15 3 -24		Right parahippocampal	
			0.035	0.917	4.607	17 -6 -15		Right amygdala	
0.009	0.553	61	0.019	0.875	4.753	-11 59 -15		Left superior frontal gyrus	
			0.026	0.897	4.680	-6 59 -7.5		Left dorsolateral prefrontal gyrus	

3.3.5. Relationship between Trauma and Cortisol

To evaluate relevance of experienced trauma on the single estimates of the cortisol measures (CARi, PACC and DBCC) in FND patients and HC, we first conducted a behavioural PLSC including TEC severity scores, developmental scores, duration of trauma, and relationship to the perpetrator as outcome variables. One PLSC component was found to be statistically significant based on the permutation testing ($P = 0.033$). The outcome and cortisol saliences of the previously mentioned component are shown in Figure 3.4. Yellow highlighted weights indicate that they were found to be robust (with the green dots representing the cortisol salience weights) and can be interpreted similarly to correlation coefficients as the data was standardized. Based on the PLSC results, a significant positive correlation was found in patients between the morning cortisol values (CARi, PACC) and the relationship to the perpetrator of physical abuse – meaning that the more familiar (inner-family circle) the perpetrator was, the higher the cortisol values. A significant negative correlation was found in patients between the morning cortisol values (CARi, PACC) and 1) the duration, and 2) severity of emotional neglect – meaning that the longer and more severe the emotional neglect, the lower the cortisol values. In HC, a positive correlation was found between cortisol values and 1) trauma occurring during late adolescence and 2) adulthood – meaning that the more trauma happened during late adolescence and adulthood, the higher the peak cortisol levels.

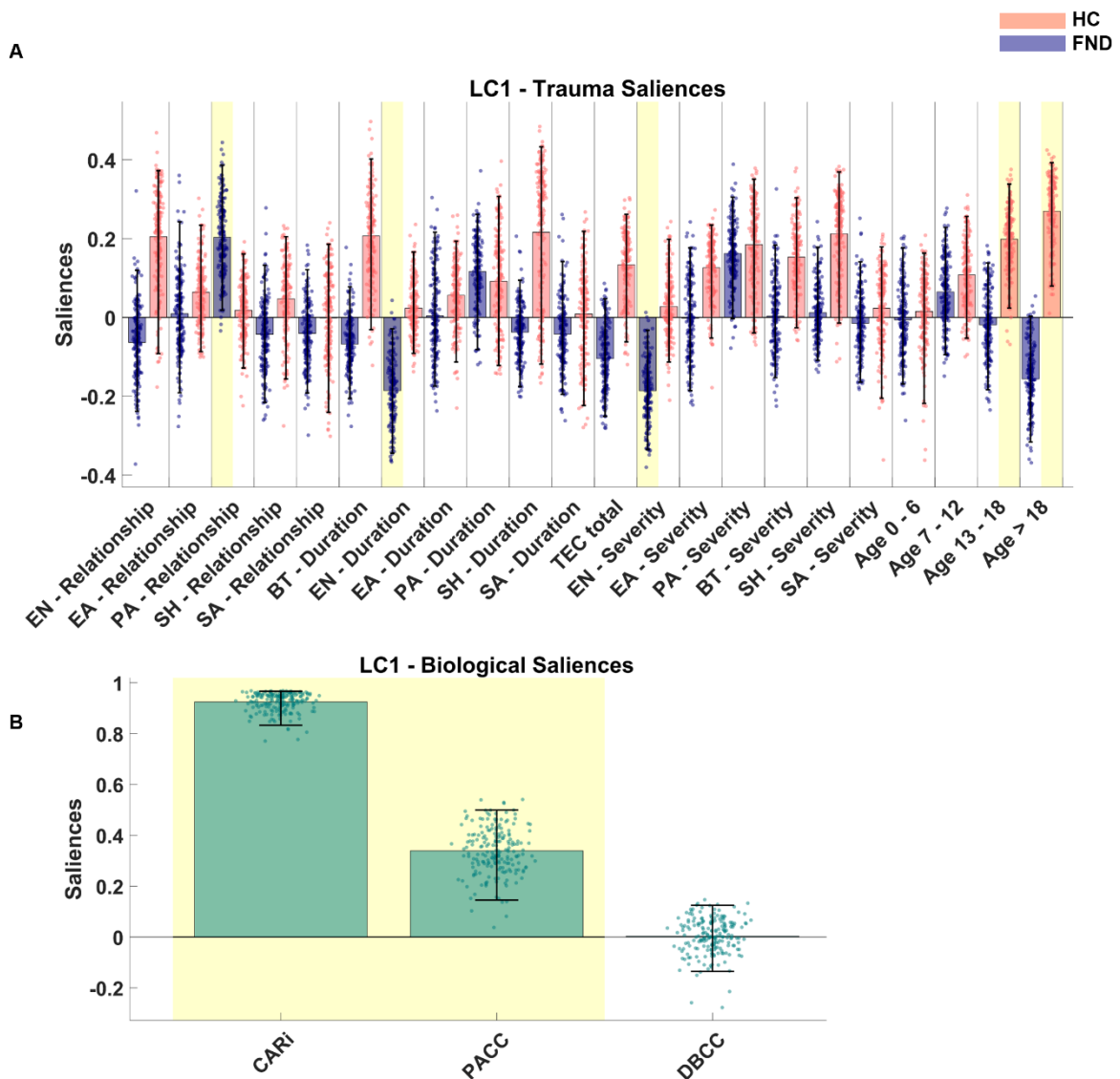


Figure 3.4: Partial least squares correlation (PLSC) results of the different cortisol measures (CARI, PACC, DBCC) in FND patients and healthy controls. The outcome (A) and cortisol saliencies (B) of the significant PLSC component ($P = 0.033$) are presented. 5th to 95th percentiles of bootstrapping are indicated in the error bars and yellow highlighted bars indicate robustness. The height of the bar corresponds to the saliency weight to the multivariate correlation pattern and can be interpreted similarly to correlation coefficients as the data was standardized. The permutation null distribution and the bootstrap mean percentiles are reported in Appendix B, Supplementary Material for Chapter 3, Figure B.4, Table B.4. Abbreviations: EN = Emotional neglect; EA = Emotional abuse; PA = Physical abuse; SH = Sexual harassment; SA = Sexual abuse; BT = Bodily threat.

3.3.6. Relationship between Cortisol and Brain Volume

To examine the potential relationship between single estimates of the cortisol measures (CAR_i, PACC and DBCC) and changes in whole-brain, respectively hippocampal- and amygdalar volumes in FND patients and HC, we conducted a PLSC including cortisol values as outcome variables and imaging data as design variables. No significant PLSC components were found when using the cluster volumes from the whole-brain analysis as design variables. When using the results from our ROI analysis (i.e., hippocampal and amygdalar volume), one PLSC component was found to be statistically significant (permutation testing, $P = 0.021$). The outcome and imaging saliences are shown in Figure 3.5.

Based on this PLSC analysis, a significant negative correlation was found only in HC between the brain volumes of the bilateral hippocampus and the bilateral amygdala and 1) the age – meaning that the older the subject, the smaller the brain volume – and 2) CAR_i – meaning the smaller the brain volume, the higher the cortisol levels. No multivariate pattern of correlation between brain volumes and cortisol data was found in FND patients.

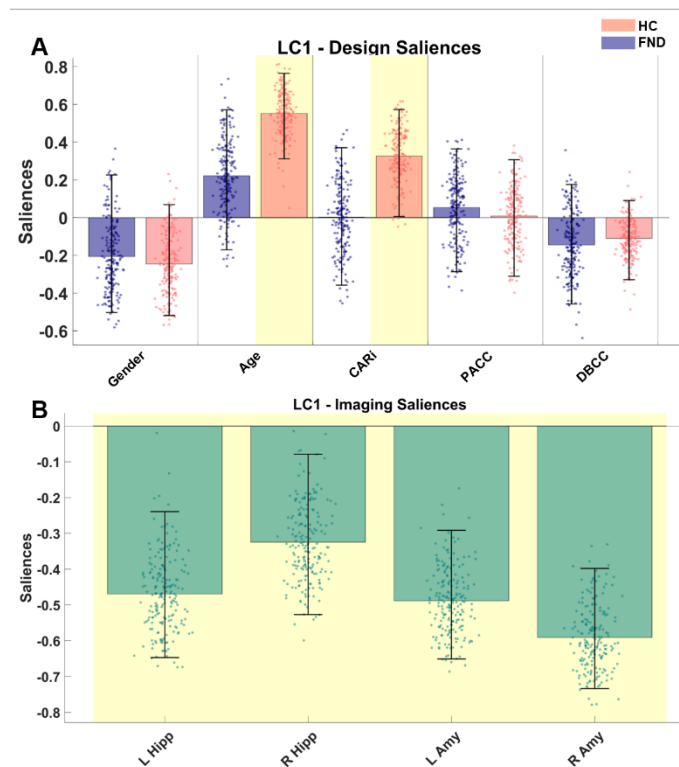


Figure 3.5: Partial least squares correlation (PLSC) results of the imaging data (hippocampal and amygdalar volumes) in FND patients and healthy controls. The outcome (A) and imaging saliences (B) of the significant PLSC component ($P = 0.021$) are presented. 5th to 95th percentiles of bootstrapping are indicated in the error bars and yellow highlighted bars indicate robustness. The height of the bar corresponds to the salience weight to the multivariate correlation pattern and can be interpreted similarly to correlation coefficients as the data was standardized. The permutation null distribution and the bootstrap mean percentiles are reported in Appendix B, Supplementary Material for Chapter 3, Figure B.5.

3.3.7. Relationship with Symptom Severity in FND

No significant multivariate correlation was identified in patients, when using symptom severity as outcome variable, and trauma scores, single estimates of cortisol measures, or brain volumes, independently, as design variables, Appendix B, Supplementary Material for Chapter 3, Figure B.6, Figure B.7 and Figure B.8.

3.4. Discussion

Our findings provide biopsychological evidence for the stress-diathesis model in FND (state versus trait). We identified a reduced cortisol awakening response in a transdiagnostic approach in FND patients. Moreover, we linked the potential HPA-axis dysregulation to prolonged preceding emotional neglect, pointing towards a long-term process resulting in a maladaptive HPA-axis sensitization. Lastly, we identified anatomical changes in the superior frontal gyrus, the superior temporal gyrus, the hippocampus, and the amygdala. In FND, however, reduced cortical volumes were not associated with cortisol – what would have pointed towards a potential neurotoxic effect, nor with symptom severity – what could have explained a state related change. These findings put in question whether the here found results represent a direct state effect of FND, a biological trait factor, or a combination of both as will be further discussed below. A schematic representation of the here discussed results are displayed in Figure 3.6.

Only few studies investigated cortisol levels and the stress response in FND patients. Consistent with our results, Chung (Chung et al., 2022) detected a blunted CAR in 32 children with FND (mixed symptoms) assessed using two saliva samples in the morning (at wake-up and 30 min later), which were partially collected in a domestic setting. Likewise, a study in 15 female functional seizure patients identified lower serum cortisol levels in the morning as compared to HC with a history of abuse (Winterdahl et al., 2017). Contradictorily, a study in which 33 motor FND patients and 33 HC were hospitalized overnight, no difference in morning cortisol levels were found (Maurer et al., 2015). This discordance might be explained by the testing conditions: a non-familiar environment (e.g., hospitalization (Maurer et al., 2015)) might introduce alterations in cortisol levels that covary with psychosocial factors and might not represent the clinical status of patients (Stalder et al., 2016, 2010). Consistent with our results, no group differences in the basal diurnal cortisol levels were found in 19 functional seizure patients (Bakvis et al., 2009a), nor in motor FND patients ($N = 16$ (Apazoglou et al., 2017), $N = 33$ (Maurer et al., 2015)). Contrarily, a group effect with higher basal diurnal cortisol levels in the afternoon was found in motor FND (Apazoglou et al., 2017), mainly driven by stress, as well as in functional seizure patients (Bakvis et al., 2010), mainly driven by experienced sexual abuse. Lastly, cortisol secretion was studied in response to stress. Using the Trier Social Stress Test, two studies reported a comparable stress response in FND patients as

to HC indicating a normal adaptation to social stress situations (Apazolou et al., 2017; Bakvis et al., 2009a). In summary, previous results on cortisol in FND show a large heterogeneity, mainly explained by methodological issues: each of the studies was conducted in a different setting (stress test (Apazolou et al., 2017; Bakvis et al., 2010, 2009a) versus no stress test and domestic setting versus hospitalized (Chung et al., 2022; Maurer et al., 2015; Winterdahl et al., 2017)), assessing different measures of cortisol (i.e., morning versus basal versus stress response), which in most cases prevents a direct comparison between results. Our transdiagnostic approach has the advantage of having a large sample with mixed symptoms, which ensures a better generalizability in comparison to previous studies focused on small subgroups of FND patients.

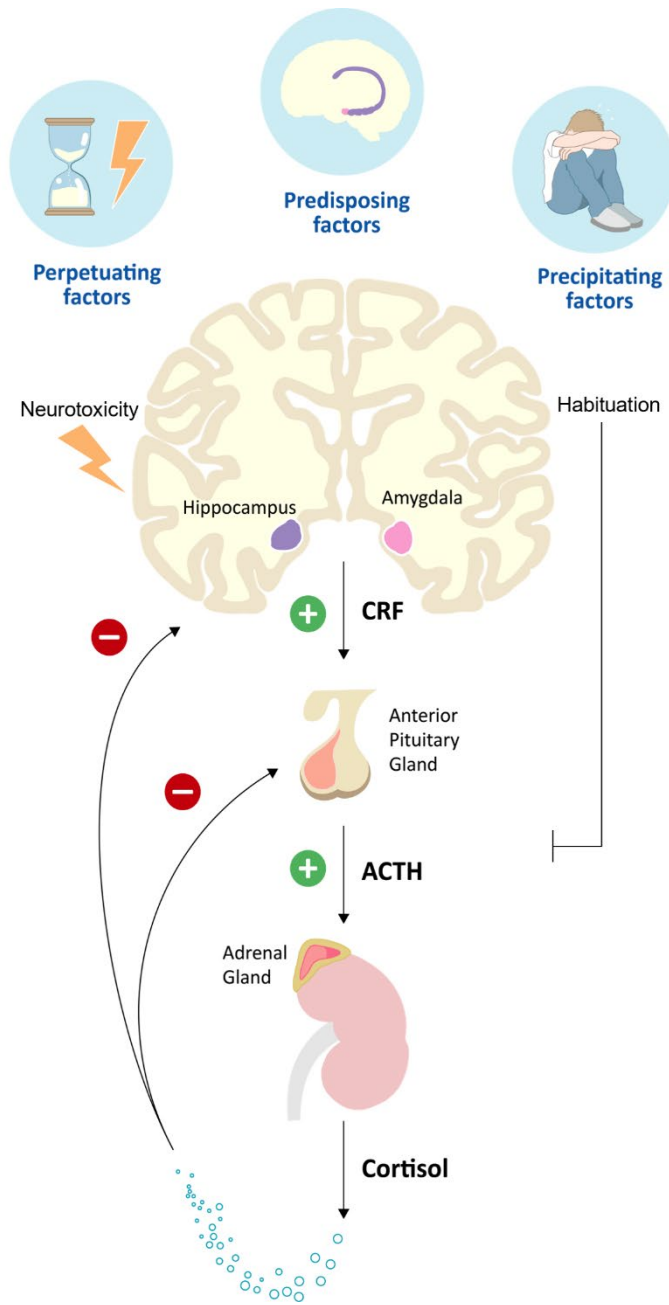


Figure 3.6: The stress-diathesis model in functional neurological disorders. The aetiology of FND is multifactorial and depends on predisposing, precipitating, and perpetuating risk factors. Long-term exposure to stress can exert neurotoxic effects on regions particularly sensitive to cortisol. Moreover, it can alter the HPA-axis in terms of a maladaptive habituation. Distinct predisposing factors, i.e., ‘trait’ markers might influence the individual resilience to stress and the later development of psychopathology. Abbreviations: CRF = corticotropin-releasing factor, ACTH = Adrenocorticotropic hormone.

Additionally – and firstly in FND, we identified an inverse relationship between cortisol measures and various dimensions of emotional neglect (assessed using the TEC), whereas no association with symptom severity or duration of symptoms was detected. As such, a significant multivariate pattern of correlation was found in patients but not in controls, between lower morning cortisol levels and higher duration and severity scores of emotional neglect (measured by the TEC). Specifically for emotional neglect, exposure was in average 4.5 years longer in FND as compared to HC. In general, adverse experiences occurred more frequent in early childhood in FND than in HC, even though this effect was not specific to emotional neglect but was found across all traumatic experiences. This result is consistent with the findings on the CTQ, in which increased neglect and abuse was found in FND across all trauma subscores except for sexual abuse. Particularly, the role of neglect as predisposing factor of FND has been highlighted by the results of a meta-analysis of 34 case-control studies including 1405 patients showing odd ratios (OR) of 5.6 for FND patients compared to control populations, which was higher than for sexual and physical abuse (OR 3.3 and 3.9 respectively) (Ludwig et al., 2018). Our results go further than confirming an association between emotional neglect and FND in demonstrating that both the severity and duration of emotional neglect are more pronounced in FND. The effect of maltreatment on different expressions of psychopathology has been shown to depend on the developmental period, severity, and frequency of trauma exposure (Dunn et al., 2017; Teicher and Samson, 2013). In FND, no clear consensus on the role of trauma type, timing and number of traumatic events is known, with the exception that early-onset FND was rather associated to childhood sexual abuse (Morsy et al., 2021) when late-onset was associated to physical trauma (Stone et al., 2009a). In sum, our results add to previous knowledge that trauma predisposes to FND, highlighting the importance of emotional neglect. Additionally, we first showed that in FND exposure to early and long-lasting emotional neglect might contribute to disrupting the biological regulation of stress, as reflected by the association with blunted CAR. This is further supported by the absence of an association between CAR and symptom severity, as an association between CAR and symptom severity would rather indicate a (subacute) disease-related (‘state’) change of the HPA-axis.

Thereby, dysregulation of morning cortisol secretion might represent a downregulation of the HPA-axis following initial high levels of cortisol in response to long-term stress (Dozier and Peloso, 2006). A proposed mechanism of action is the suppression of the negative feedback inhibition of cortisol (Lupien et al., 2018; McEwen, 2017). Under normal health conditions, an acute stressor would activate the HPA-axis and subsequent cortisol secretion through the amygdala. The amygdala is strongly regulated by the PFC and the hippocampus, which are responsible for the integration of information on threat stimuli. When the stressor is removed, a negative feedback inhibition is induced through the hippocampus and the HPA-axis itself, reducing the cortisol secretion. In a chronic state of hypervigilance to stressors, the HPA-axis is tonically inhibited through the hippocampus, as a result of suppressed negative feedback inhibition due to HPA-axis sensitization (maladaptive habituation) to the stressor. Correspondingly, an overreactive HPA-axis has been observed in early phases of chronic stress,

whereas a downregulation corresponds to subsequent, sustained phases of chronic stress (Guilliams and Edwards, 2010). Hence, the prolonged exposure to emotional neglect in FND patients might reflect a long-term process resulting in the downregulation of the HPA-axis, as represented in the flattened CAR. At the same time, it is suspected that glucocorticoid receptors become more sensitive to enhanced cortisol levels during early phases of chronic stress, and consequently to the increased neurotoxic effects of cortisol (Heim et al., 2000; Herman, 2013; Yehuda and Seckl, 2011). Chronic stress indeed has been repeatedly associated with neuroanatomic alterations in regions expressing a high glucocorticoid receptors density i.e., hippocampus, PFC, and amygdala (for review: Lupien et al., 2018; McEwen, 2017). In FND, a volume reduction of the hippocampus has previously been found to inversely relate to trauma history (Perez et al., 2017a). No data on cortisol was available in this study but it was hypothesized that the hippocampal atrophy might be mediated by changes in stress biomarkers such as cortisol. However, large variation in hippocampal volumes has also been described in healthy populations, irrespective of chronic stress or trauma history, suggesting that reduced hippocampal volume may represent a trait factor rather than a disease-related feature (state) (Lupien et al., 2007). In line with these findings, our results on smaller hippocampal and amygdalar volumes compared to HC, and the absence of a correlation with cortisol measures nor with symptom severity suggest that these anatomical variations rather represent a trait factor for FND, in terms of a biological predisposition. Interestingly, while some studies neither identified a relationship between cortical volumes and symptom severity (Aybek et al., 2014b; Kozłowska et al., 2017a; Nicholson et al., 2014), recent studies inversely correlated symptom severity to lower volumes in regions other than the hippocampus, such as the left insula (Jungilligens et al., 2022; Perez et al., 2017b, 2017a), precentral gyrus (Jungilligens et al., 2022), as well as the temporo-parietal junction (Sojka et al., 2022). Therefore, regional differences in cortical volume might be linked to trait-vulnerability (e.g., hippocampus) while others might be linked to disorder-related pathophysiological changes (state). However, additional research is needed to disentangle the role of regional structural abnormalities in the pathophysiology of FND. On the contrary in HC, the inverse relationship between subcortical volume and cortisol measures may represent a plasticity phenomenon in response to recent stress. In summary, a disease model including HPA-axis sensitization might contribute to the development of FND in terms of maladapting to long-term emotional neglect. Moreover, the here found reduced hippocampal and amygdalar volumes in FND point towards a ‘trait’ biomarker for FND, which potentially decreases the resilience to stress.

Psychosocial stressors, HPA-axis sensitization and biological predisposition might represent transdiagnostic risk factors (McLaughlin et al., 2020) which conjointly contribute to general psychopathology and symptom overlaps in neuropsychiatric disorders (Hornor, 2017). However, by way of example, about 15% of childhood maltreatment survivors do not develop mental health problems (Werner, 2004), and further variations in psychopathology have been explained by individual resilience to stress (Hornor, 2017). Similarly, FND represents a disorder of multifactorial origin (Hallett et al., 2022). Biopsychological risk factors might

interplay with other, yet unknown factors which might explain why a subgroup of vulnerable individuals develop FND and not any other psychopathology. Recently, research on resilience focuses not only on the exploration of eco-phenotypes (i.e., environmental factors), but also genetics and their interplay (endo-phenotypes, i.e., gene \times environment interactions). As such, early life adversities may influence brain development and mental health outcome by means of (epi-) genetic mechanisms. The first two years of development is the critical window for emotional development and has been associated with increased risk for mental disorders and negative impact on the brain structure and function (Lippard and Nemeroff, 2019; Taillieu et al., 2016). Emotional neglect during early childhood is often accompanied by social disentanglement and rejection, which prevents children to learn how to properly process emotions (Gould et al., 2012; Teicher et al., 2014; Yeung et al., 2016), as found in FND populations (Aybek et al., 2015, 2014a; Blakemore et al., 2016; Espay et al., 2018c). In terms of gene \times environment interactions, a genetic variation in the oxytocin receptor (*OXTR*) in subjects with a history of childhood emotional neglect was associated with reduced amygdalar and hippocampal brain volumes (Womersley et al., 2020). The role of oxytocin in emotion processing has been studied in infants (5-7 months old): infants with increased *OXTR* methylation rates showed enhanced response to aversive faces in a functional neuroimaging paradigm (Krol et al., 2019). Epigenetic changes in the oxytocin pathway are as well of particular interest in FND, as increased *OXTR* methylation was demonstrated in a cohort of 16 FND patients compared to 15 HC (Apazoglou et al., 2018). Other genetic/epigenetic changes in FND have been very recently studied: Diez (Diez et al., 2020) linked history of childhood physical abuse to cortico-limbic brain network dysfunction in regions which *in situ* showed an overlap with high expression of genes involved in neuronal morphogenesis. Those findings firstly linked childhood trauma and its potential effects on brain function to a trauma-related functional brain reorganization in the context of a gene \times environment interaction in FND. In the same line of research, tryptophan-hydroxylase 2 (*THP2*) polymorphism was associated with childhood trauma, symptom onset and severity, as well as amygdalar functional connectivity in FND (Spagnolo et al., 2020). In summary, individual resilience factors might explain how early childhood emotional neglect potentially induce (epigenetically mediated) neurodevelopmental delays in individuals who later develop FND affecting brain structure and function of regions involved in emotion regulation which is reflected in a dysfunctional HPA-axis. Further research must be conducted to identify risk factors specific for FND.

Our study has several limitations. First, the measure of cortisol awakening response relies on self-reported diaries and deviations from the protocol cannot be fully controlled. To verify accurate execution of cortisol sampling, objective verification of awakening and sampling times are required (Adam and Kumari, 2009), e.g., using objective electronic monitoring systems, such as polysomnography or wrist actigraphy (Elder et al., 2016). We did not use such objective tools but minimized the risk of error of self-report data by thoroughly instructing our participants, agreeing on an appropriate day for the sampling, and explaining them the importance of properly adhering to the protocol and/or reporting deviations from the protocol.

Second, we collected saliva samples on only one day, thus cortisol alterations might represent fluctuations due to situational aspects rather than a long-term trait (Stalder et al., 2016). Thirdly, salivary cortisol only indirectly measures HPA-axis activity, as it depends on levels of other biological factors such as corticotropin releasing factor, adrenocorticotrophic hormone, or estrogens (Hellhammer et al., 2009). Nonetheless, salivary cortisol is considered to be a good measure of allostatic load, and a useful biomarker in stress research (Hellhammer et al., 2009; Wust et al., 2000). Another limitation in studying the role of trauma lies in methodological issues as self-report questionnaires can have recall bias (Ludwig et al., 2018). Detailed interview technique (Brown and Harris, 1989), are less prone to recall bias but are time-consuming and requires appropriate training of study personnel, which limits its feasibility in larger cohorts of participants. Lastly, our patient cohort has only been compared to HC, which prevents making conclusions on the specificity of the findings to FND in comparison to other stress-related disorders. We, however, corrected for depression and anxiety and excluded severe psychiatric conditions, therefore, we do not expect that the results are biased due to mood disorder comorbidities. The lack of systematic psychiatric evaluation – such as the psychiatric interview (SCID) – does not allow to check if the data could be confounded by a psychiatric co-morbidity (e.g., post-traumatic stress disorder (PTSD)), which is common in FND (Carson and Lehn, 2016; Perez et al., 2017a).

3.4.1. Conclusion

Our findings point towards a multifactorial stress-diathesis model for FND. A flattened CAR might represent a long-term process in direct relation to severity and duration of emotional neglect (state). Reduced subcortical volumes in FND did not relate to HPA-axis dysfunction and rather delineate a predisposing biological vulnerability, than a disease-related feature, thus potentially representing a trait marker for FND. In line with a stress-diathesis model, phenotypical variations in clinical presentation of symptoms must potentially be attributed to different contributions of a variety of diverse eco-phenotypes (e.g., trauma history) and endo-phenotypes (e.g., biological predisposition or trait markers). However, a causal relationship between HPA-axis dysfunction, trauma, and brain functional- and structural stress adaptation remains to be discovered. Longitudinal data would need to be assessed including the collection of behavioural, neuroendocrine, genetic, and neuroimaging data already in early childhood.

CHAPTER 4

Dynamic Functional Connectivity

This chapter is prepared for submission to: BRAIN | Oxford Academic – Oxford University Press

Authors: Samantha Weber, Serafeim Loukas, Janine Bühler, Thomas Bolton, Giorgio A. Vanini, Rupert Bruckmaier, Selma Aybek

Contribution:

I was involved in the conceptualization, experimental design, and project administration. Together with my colleague Janine Bühler, we planned the study execution and collected the data. I performed the pre-processing and analysis of all the demographic-, biological-, and imaging data. For the imaging data, I was supported by PhD Serafeim Loukas and PhD Thomas Bolton. I wrote the original draft of the manuscript.

Abstract

Functional neurological disorder is a neuropsychiatric condition in which patients experience neurological symptoms such as weakness or involuntary movements in the absence of a classical neurological disease. Functional imaging studies linked abnormal motor control to impaired emotion regulation, interoceptive deficits, and increased self-referential processes. The pathophysiological mechanisms, however, remain poorly understood. Analysing large-scale brain network dynamics at rest is promising to explore temporal fluctuations in aberrant brain functions and to identify potential imaging-based biomarkers. As in comparison to static approaches, dynamic functional connectivity approaches better reflect the constantly adapting behaviour of the brain and thus, could provide new insights into clinical characteristics of the fluctuating appearance of functional neurological symptoms.

In this study, we report on resting-state functional magnetic resonance imaging data of 79 functional neurological disorders patients and 74 age- and sex-matched healthy controls. Functional connectivity was computed between 17 resting-state networks, for which we identified aberrant functional connectivity of the salience-limbic network in patients as compared to healthy controls. The salience- and limbic networks encompass regions such as the amygdala and the insula, and are involved in various neuroscientific concepts such as emotion regulation, interoception, and self-referential processes, all of which have been previously linked to the pathology of FND. To further disentangle underlying network dysfunctions, we examined the dynamic properties of these networks using co-activation pattern analysis based on the seed activity of the insula and the amygdala, representing the hubs of the salience-limbic networks. Three dynamic brain states were selected per seed using k-means clustering.

We identified insular co-activation patterns related to the default mode network, the somatosensory network, the dorsal attention network, as well as the interoception network, and amygdalar co-activation patterns related to the default mode network, the basal ganglia network, as well as networks involved in attention and self-referential processes. Furthermore, patients visited the state that was characterized by the insular co-activation of the interoceptive network less frequently than healthy controls. Also, patients entered the amygdalar state with co-deactivation of the default mode network less frequently, and they spent less time in the state that was characterized by insular co-deactivation of the default mode network. Insular-interoception network as well as amygdalar-default mode network temporal dynamics positively correlated with stress biomarkers, and negatively correlated with symptom severity.

In summary, we identified altered functional brain network dynamics in functional neurological disorders supporting concepts of abnormal emotional regulation and interoceptive deficits. Moreover, we narratively reviewed our results by means of the Bayesian model account for FND. Altogether, functional changes involving salience-limbic inter- and intra-network interactions might reflect underlying pathophysiological mechanisms of functional neurological disorders.

4.1. Introduction

Patients diagnosed with a functional neurological disorder (FND; conversion disorder; historically referred to as hysteria) can present with a variety of neurological symptoms (Bennett et al., 2021; Stone and Carson, 2015) which cannot be attributed to a classical neurological disease (Drane et al., 2020; Espay et al., 2018a) but are rather of functional nature. In the late 19th century, Jean-Martin Charcot – known for his exceptional work on *hysteria* – postulated that the symptoms might be produced by a *dynamic* lesion triggered by emotional trauma (Aybek, 2019; Harris, 2005). To date, however, the underlying pathophysiology of FND remains elusive. To study how symptoms are produced in the absence of a neurological disease, efforts have been devoted to investigating brain functional abnormalities in FND patients most commonly using functional MRI. As such, previous research has provided comprehensive evidence of multiple brain function alterations and network dysfunctions in FND (for reviews: Aybek and Vuilleumier, 2016; Conejero et al., 2018; Demartini et al., 2021; Thomsen et al., 2020; Voon et al., 2016). In summary, key regions involve the insula, the amygdala, the prefrontal cortex, the temporo-parietal junction (TPJ), the supplementary motor area (SMA), the hippocampus, as well as basal ganglia structures. Of particular interest are the insula and the amygdala. The insula is an important hub of the salience and limbic network, associated with conscious and unconscious emotion processing (i.e., emotional awareness), as well as with interoception (i.e., the perception of the body's state also in relation to its emotional state (Barrett and Simmons, 2015; Gu et al., 2013)). Moreover, the insula is implicated in the detection of external and internal stimuli and the resulting behavioural response (Uddin, 2017). In FND, the insula has been associated with attentional and interoceptive deficits (Pick et al., 2019) and increased self-monitoring (de Lange et al., 2007; Pareés et al., 2013), and is thought to be implicated in the mediation of emotional influence on motor control (Vuilleumier, 2014). Additionally, the amygdala, a key region of the limbic system, is suggested to play a major role in the pathophysiology of FND. Emotional arousal and enhanced amygdalar activity have been associated with aberrant motor planning (SMA) and motor behaviour (basal ganglia) (Aybek et al., 2015). As such, insular and amygdalar structures might directly alter motor planning and execution, and thus, bypass executive control. Moreover, they closely interact with higher-order regions (e.g., prefrontal cortex, TPJ) associated with self-referential processes and self-agency. These higher-order regions modulate motor actions by integrating external and internal stimuli based on self-relevant information (Aybek and Vuilleumier, 2016; Conejero et al., 2018; Demartini et al., 2021; Thomsen et al., 2020; Voon et al., 2016).

Attentional deficits, increased self-monitoring, and altered self-agency in FND have been explained on the basis of a hierarchical Bayesian model (Edwards et al., 2012; Pareés et al., 2012). Using this model approach, the brain is thought to infer upon sensory inputs based on precise internal models of the behavioural outcome, and further updating the model based on mismatches between prediction and outcome (prediction errors). In FND, patients are thought to overweight their prior beliefs on the expected outcome (e.g., of a movement) and to further

misinterpret the prediction error, strong enough to cause abnormal motor programs and to alter the sensation of the symptoms (Pareés et al., 2013, 2012). In essence, functional brain alterations associated with the pathophysiology of FND entail a combination of aberrant FC between top-down higher-order functions (e.g., self-monitoring and agency) and bottom-up influences which altogether affect proper motor behaviour and sensations.

Most commonly, FC in FND has been assessed using *static* approaches which summarize the temporal correlation between spatially distinct brain regions or networks, assuming their activity remains constant over time. The brain, however, is a dynamic system that fluctuates between different states in order to adapt its behaviour towards intrinsic and extrinsic stimuli (Brembs, 2021). Therefore, assessing dynamic changes in FC might provide a better understanding of the fundamental properties of Charcot's *dynamic* lesion in patients with FND (Hutchison et al., 2013; Preti et al., 2017).

Over the last decades, numerous methods have been developed to study the temporal dynamics of the resting brain (Preti et al., 2017). Up to now, however, only two studies used a dynamic approach: Diez *et al.* (Diez et al., 2019) demonstrated the potential of (static) graph-theory step-wise FC (Sepulcre et al., 2012) as a prognostic biomarker for FND, whereas Marapin *et al.* (Marapin et al., 2020) studied the spatial and temporal characteristics of dynamic brain states in FND patients using a clustering-approach based on sliding-window dynamic FC on brain networks derived from independent component analysis (ICA). Here, we adopt a method based on co-activation pattern (CAP) analysis (Liu et al., 2018, 2013). On a conceptual level, CAP analysis works on a single-volume resolution and thus deviates from the conventional methods applied to the temporal domain such as e.g., FC (Liu and Duyn, 2013). In a first step, volumes in which a seed region of interest (de-)activates above a specific threshold are selected. In a second step, k-means clustering is applied to the remaining selected volumes (with the seed always (de-)active). K-means clustering partitions the volumes into clusters in which each volume belongs to a cluster (i.e., CAPs) with the nearest averaged co-activation pattern. Apart from the spatial information, this method allows us to additionally capture the temporal characteristics of the dynamic brain. In comparison to ICA, which works on the temporal as well as on the spatial domain, CAP analysis does not require independence between components, and is thus more flexible (Liu et al., 2018; Liu and Duyn, 2013). In previous studies, CAP analysis was able to detect very small anatomical regions (e.g., thalamic nucleus or substantia nigra) (Fox et al., 2005), unveiled new insights into the dynamic FC of the brain which could further be associated to symptom severity in bipolar disorders (Rey et al., 2021), helped tracking treatment response in idiopathic normal pressure hydrocephalus (Griffa et al., 2021), or identified cognitive aspects of emotional processes in healthy volunteers (Gaviria et al., 2021). In summary, CAP analysis can account for the dynamic behaviour of the brain, which might reveal new insights into different cognitive processes, has high anatomical precision, and can provide clinically important information.

Hence, a better characterization of dynamic functional alterations in FND patients is desirable, as they potentially underlie the observed clinical presentation of symptoms (the

dynamic lesion). As such, including not only spatial but also temporal features could shed light on the underpinnings of FND, assist as a quantitative biomarker, be associated with clinical scores, or be used as prognostic outcome measure by understanding how dynamic brain networks contribute to normal brain function.

Here, we examine the spatial and temporal characteristics of limbic brain networks in FND patients compared to a cohort of age- and sex matched healthy controls (HC). Furthermore, we investigate the potential relationship between the characteristics of dynamic brain states and symptom presentation in FND patients. To achieve this goal, FND patients and HC enrolled in this study underwent a resting-state fMRI assessment, and patients further underwent a neurological examination. The aims of the study were 1) to identify dynamic functional networks related to FND pathology and to investigate their spatial and temporal characteristics; and 2) to explore the relationship between dynamic fMRI features, clinical scores, and stress biomarkers. Doing so, we aim to provide a deeper understanding of the dynamic characteristics of functional networks and their potential role in the pathophysiology of FND.

4.2. Materials and methods

4.2.1. Participants

The study was carried out at the University Hospital Inselspital Bern, Switzerland. 86 FND patients with motor and sensory symptoms (F44.4 and 44.6), psychogenic non-epileptic seizures (PNES, F44.5), mixed symptom type (F44.7), and persistent postural-perceptual dizziness (PPPD) were recruited. The diagnosis of FND was confirmed by board-certified neurologists according to DSM-5 (American Psychiatric Association, 2013) and using positive signs (Stone and Carson, 2015). In parallel, 76 age- and sex matched HC were recruited through advertisement. Exclusion criteria in both groups were: 1) a current neurological disease or disorder (other than FND), 2) a current severe psychiatric condition (e.g., psychiatric disorder with acute suicidality), 3) alcohol or drug abuse, 4) contraindication to MRI, 5) pregnancy or breast-feeding or 6) insufficient language skills to understand the study procedure. The study was approved by the Competent Ethics Committee of the Canton Bern (SNCTP000002289). Written informed consent was provided by all subjects.

4.2.2. Demographic, behavioural, and clinical characteristics

Symptom severity was evaluated with the Simplified Version of the Psychogenic Movement Disorder Rating Scale (S-FMDRS, Nielsen et al., 2017), as well as with the Clinical Global Impression (CGI) score (0 = no symptoms to 7 = among the most extremely ill). Duration of symptoms was calculated in months from the beginning of first symptoms to the date of study inclusion. Current intake of psychotropic medication (i.e., benzodiazepines, opioids, antidepressants, neuroleptics, and antiepileptics) was assessed. To control for anxiety

and depression, patients and HC completed the Beck's Depression Inventory (BDI, Beck, 1961) and State-Trait Anxiety Inventory (STAI, Spielberger et al., 1983).

4.2.3. Stress biomarkers

To assess stress objectively in FND patients (i.e., hypothalamus-pituitary-adrenal (HPA)-axis activity), salivary cortisol and alpha-amylase samples were collected. The exact procedure can be found in Chapter 3.2.2 Saliva Samples. As an estimate of the CAR, the area-under-the-curve with respect to increase (AUC_i) was computed (Pruessner et al., 2003; Stalder et al., 2016). In comparison to cortisol, which represents a slow stress response (chronic), alpha-amylase can be used as an indicator for the rapid sympathetic stress response and has previously been found to be elevated in FND patients (Apazoglou et al., 2017). Therefore, we collected saliva samples before entering the MRI scanner, in order to assess objective, acute stress levels in patients using alpha-amylase.

4.2.4. Neuroimaging acquisition and pre-processing

MRI data were recorded using a 3 Tesla Scanner (Magnetom Prisma, Siemens, Germany). For anatomical imaging, a sagittal-oriented T1-weighted 3D-MPRAGE sequence (TR = 2330ms, TE = 3.03 ms, TI = 1100ms, matrix 256 × 256, FOV 256 mm × 256 mm, flip angle 8°, resolution 1 mm³ isotropic, TA = 5:27 min) was acquired for all subjects (Gallichan et al., 2016). Functional imaging data were acquired using a whole-brain interleaved multi-slice BOLD echo-planar-imaging (EPI) sequence (TR = 1300ms; TE = 37 ms, flip angle = 52°, FOV = 230 mm, voxel size = 2.2 mm³ isotropic, TA = 6:39 min, for a total of 300 functional volumes. Imaging data were pre-processed using SPM12 (<https://www.fil.ion.ucl.ac.uk/spm/software/spm12/>) in MATLAB (R2017b, MathWork Inc., Natick, USA). Functional volumes were first realigned and co-registered to the structural T1 volume. They were then detrended and covariates of no interest were regressed out (including constant, linear, and quadratic trends, average white matter/cerebrospinal fluid time courses, motion artefacts, and global signal). Functional data were then filtered using a high-pass filter at 0.01 Hz. Lastly, functional volumes were warped into MNI standard space and smoothed using a spatial Gaussian kernel of 5mm FWHM.

As head motion is known to affect FC analyses in a way that FC in large-scale distributed networks decreases, while local FC increases (Van Dijk et al., 2012), functional images were checked for excessive translation and rotation with the framewise displacement (FD) criterion of Power *et al.* (Power et al., 2014) at a threshold of FD > 0.5mm. Subjects, in which more than 50% (i.e., > 150 volumes) of volumes showed too high motion, were excluded from further analysis.

4.2.5. Resting-state functional dynamics

To characterize large-scale brain network dynamics at rest in patients with FND and HC, we applied a two-step data-driven methodological approach. First, a whole-brain FC analysis of within- and between resting-state networks was performed. This analysis identified the salience- and limbic network as particularly differently connected in FND patients as compared to HC (see Chapter 4.3. Results). Second, we analysed the spatial and temporal dynamics of the insula and the amygdala, the hubs of the salience- and limbic network, using a co-activation pattern (CAP) analysis, a method that allows to study the functional dynamics of brain networks (Bolton et al., 2020; Liu et al., 2018, 2013). As such, the insular- and amygdalar co-activations were clustered in time to examine dynamic interactions of these networks and other regions and networks of the brain.

4.2.5.1. Resting-state functional network connectivity

To assess the resting-state FC of the brain, we first parcellated each participant's functional brain data into 17 resting-state networks according to the convention of Yeo *et al.* (Yeo et al., 2011). The network-averaged time courses were extracted, and functional network connectivity was computed using Pearson's correlation coefficient between the time series of each of the networks, producing an individual 17×17 FC matrix for each subject (Figure 4.1). Negative values were removed due to their disputed interpretation (Qian et al., 2018). The correlation coefficients were further z -scored using Fisher- z transformation. Significant differences in functional network connectivity between patients and controls were assessed using multiple t -tests, corrected using false discovery rate (FDR) at a significance threshold $P < \alpha$, where alpha level (α) was set to 0.05.

4.2.5.2. Insular- and amygdalar co-activation patterns

We selected two seed regions (insula and amygdala) representing the hubs of the salience and limbic networks. The seeds were defined using the automatic anatomic labelling (AAL) atlas (Tzourio-Mazoyer et al., 2002). The analysis was restricted to voxels within the grey matter only. The seed time series were scrubbed at 0.5mm, extracted, and z scored in time. To identify those time-points corresponding to high-amplitude events (activation) within our seeds, we thresholded the time-series at 0.84 SD ($\text{CDF}^{-1}(0.80) = 0.84$) (Liu and Duyn, 2013). To generate CAPs, we used a customized version of the TbCAPs toolbox (https://c4science.ch/source/CAP_Toolbox/), which is described in detail in Bolton *et al.* (Bolton et al., 2020). In order to identify the optimal number of clusters K , a consensus clustering approach was performed (Bolton et al., 2020; Monti et al., 2003). Due to the high dimensionality of the data, and the consequential high computational load for the clustering

approaches, an additional principal component analysis (PCA) step was introduced, to reduce the dimensionality of the data. Hence, we concatenated the data of each subject (of size [n dimensions \times t timepoints per subject]), where n is the number of grey matter voxels) into a data matrix X with dimensionality of [N dimensions \times T datapoints], where T is the selected number of timepoints across all subjects. The X matrix was then centred by subtracting the mean of each voxel. X further served as an input to the PCA. The PCA projected data (scores) W (of dimension [$T \times T$]) were used as an input for the consensus clustering. Based on the output of the consensus clusters, the cumulative distribution of consensus values was computed to further calculate the proportion of ambiguously clustered pairs in order to evaluate the stability of the individual cluster sizes (proportion of ambiguous clustering, PAC) (Şenbabaoğlu et al., 2014). The consensus matrices and the stability measure, defined as $1 - \text{PAC}$, can be found in the Appendix C, Supplementary Material for Chapter 4, Figure C.1, Figure C.2 and Figure C.4, Figure C.5. Based on the stability measure and the consensus matrices, the dimensionality-reduced selected fMRI volumes were then clustered into three different states (CAPs) using the k-means algorithm. The individual CAPs were then back reconstructed by multiplying the PC scores with the transposed eigenvectors and adding back the mean. The CAPs were subsequently spatially z -scored, representing the distinct insular- and amygdalar CAPs with positive and negative contributions (Liu and Duyn, 2013). In order to characterize the temporal properties of the obtained CAPs, we calculated the average duration of a CAP (average number of consecutive volumes assigned to one CAP multiplied by the TR), the number of entries (how many times a subject transitioned to a specific CAP), number of volumes corresponding to a CAP (volumes assigned to a CAP), as well as relative temporal occurrence (defined as the number of volumes assigned to one CAP normalized by the number of selected volumes). The analyses were repeated with the second most stable cluster number and can be found in the Appendix C, Supplementary Material for Chapter 4, Figure C.3 and Figure C.6.

4.2.6. Relationship between CAPs, stress biomarkers, and clinical scores

As temporal characteristics of dynamic brain states were often found to be a representative biomarker for neuropsychiatric disorders (Khanna et al., 2014; Michel and Koenig, 2018), we explored the multivariate patterns of correlation between aberrant CAPs temporal measures, stress biomarkers, and clinical scores in FND patients using a partial least squares correlation analysis (PLSC; Krishnan et al., 2011; McIntosh and Lobaugh, 2004). We implemented our analysis using the publicly available PLS toolbox for MATLAB (https://github.com/FND-Research-Group/myPLS_SL.git), the use of which has already been described elsewhere (Loukas et al., 2021; Zöllner et al., 2019). The PLSC thus calculates correlation weights by means of detecting linear combinations of CAPs' temporal characteristics and clinical scores

as such that the covariance is maximized across subjects. The stability of the weights was assessed using bootstrapping (500 bootstrap samples) and statistical significance was evaluated using permutation testing (1000 permutations) at an alpha-level of 0.05. To evaluate that our findings are specific for the FND cohort (with regard to HC), we repeated the analysis in the HC (without symptom severity scores) in the Appendix C, Supplementary Material for Chapter 4, Figure C.8 and Figure C.9, Table C. 2.

4.3. Results

4.3.1. Clinical and demographic characteristics

Data from 86 FND patients and 76 age- and sex matched HC were included in this study. Sensorimotor deficits (38.7%), gait disorders (21.5%), and/or tremors (14.6%) were the most frequent symptoms. FND patients significantly differed in terms of depression and anxiety scores, with higher levels in patients. Demographic, behavioural, and clinical data are presented in Table 4.1.

Table 4.1: Demographic, behavioural, and clinical data

	FND (N = 86)	HC (N = 76)	Statistics
Age, mean (SD), years, [range]	37.7 (14.2), [17 – 77]	33.1 (10.9), [18 – 62]	<i>ns</i>
Sex (females/males)	64/22	55/21	<i>ns</i>
Disease severity (CGI, median, quantile)	2 [1 – 4]	<i>NA</i>	
Disease severity (S-FMDRS, median, quantile)	6 [2 -12.75]	<i>NA</i>	
Duration of illness (in months)	75 (166)		
Symptom type ^a	45 sensorimotor		
	25 gait disorder		
	17 tremor		
	12 myoclonus		
	13 PNES		
	8 dystonia	<i>NA</i>	
	7 PPPD		
	5 speech disorder		
	2 functional deafness		
	1 functional vision loss		
ICD-10 Classification ^b	63 F44.4		
	7 F44.5		
	30 F44.6	<i>NA</i>	
	8 F44.7		
	6 PPPD		
	14 benzodiazepines		
Psychotropic medication	29 antidepressants	0/76	
	6 neuroleptics		
	9 antiepileptics		
	6 opioids		
BDI score, mean (SD)	14.4 (9.96)	4.59 (6.28)	$Z = -7.61, P < 0.0001$ ***
STAI-S score, mean (SD)	37.2 (10.9)	32.1 (7.67)	$t(156.68) = 3.22, P = 0.002$ **
STAI-T score, mean (SD)	45.5 (13.0)	33.9 (7.11)	$t(135.07) = 7.14, P < 0.001$ ***

^aPatients can present with several symptom types

^bDiagnosis of mixed FND (F44.7) was given when F44.4, F44.5, and F44.6 was present

Significance code: $P^{***} < 0.001, P^{**} < 0.01, P^* < 0.05$.

Abbreviations: FND: functional neurological disorders, HC: healthy controls, CGI: Clinical Global Impression Score, S-FMDRS: Simplified Version of the Psychogenic Movement Disorder Rating Scale, BDI: Beck's Depression Inventory, STAI: State-Trait Anxiety Inventory, SD: standard deviation, ns: not significant, NA: not applicable.

4.3.2. Aberrant resting-state network connectivity in FND

For the fMRI analysis, data from one HC and seven FND patients had to be excluded due to too high motion artefacts ($N = 6$), due to a bleeding cyst found during the MRI examination ($N = 1$), or due to drug abuse ($N = 1$). One HC did not finish the resting-state acquisition in the MRI and was thus excluded. This leads to a total sample size of 74 HC and 79 FND patients. Resting-state FC within- and between 17 RSN was computed for each of the remaining subjects.

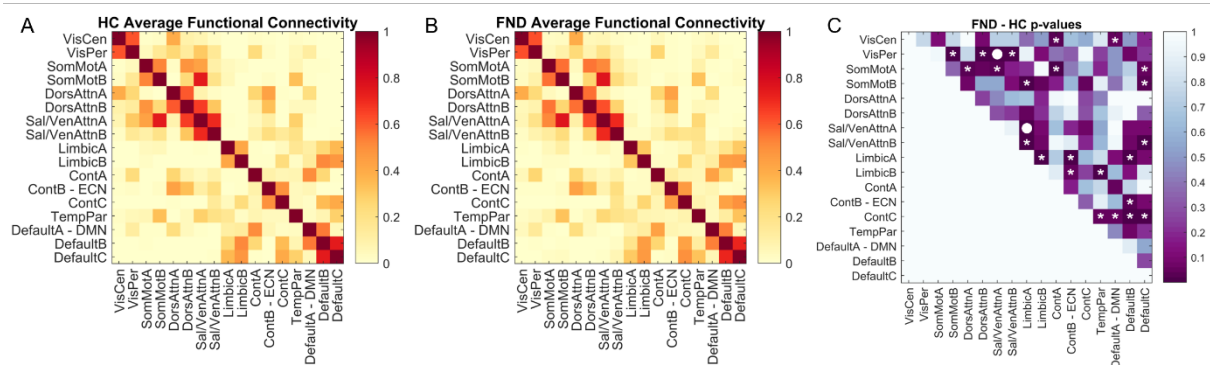


Figure 4.1: Resting-state network connectivity in healthy controls (HC) and FND patients. Average within- and between-RSN FC values in A) HC and B) FND patients; C) p-values for the FND patients-HC group comparisons using multiple t-tests corrected for multiple comparison using FDR. RSN labels follow the convention of Yeo. Significance code: * $P < 0.01$; ● q surviving FDR-correction ($q < 0.01$). Abbreviations: Cont = Executive control, Default = Default mode DorsAttn = Dorsal attention, Sal/VenAttn = Saliency/Ventral attention, SomMot = somatomotor, TempPar = Temporoparietal, VisCen = Central vision, VisPer = Visual perception.

In FND patients, FC between the salience network and the limbic network, as well as the visual perception network was found to be significantly increased as compared to HC ($P < 0.05$, FDR-corrected). Similarly – but not surviving FDR-correction – patients showed increased FC between the somatomotor network and the dorsal attention network (DAN), the executive control network (ECN) and the default mode network (DMN) ($P < 0.05$, not surviving FDR-correction). Lastly, increased FC was found between the ECN and the temporo-parietal network, and the DMN ($P < 0.05$, not surviving FDR-correction).

4.3.3. Distinct dynamic brain networks in FND

4.3.3.1. Insular co-activation patterns

Using the insula as a seed region, we identified three distinct co-activation patterns corresponding to insular activations. The first CAP (CAP1_{Ins}) represents an insular activation pattern with co-activation of the SMA, and a co-deactivation with the DMN, the caudate, and the nucleus accumbens (NAc), reflecting an insular somatomotor-DMN-related CAP. The second CAP (CAP2_{Ins}) exhibited an insular activation pattern with co-activation of the SMA, and a co-deactivation with the dorsal DMN, the precuneus, and the visual network, representing an insular attention network-related CAP. The third CAP (CAP3_{Ins}) denotes an insular activation pattern with co-activation of the cingulate cortex, the superior frontal gyrus, the caudate, and thalamic nuclei (mediodorsal), as well as co-deactivation of the angular gyrus, the inferior parietal lobule (IPL), the hippocampus and parahippocampal regions, and the NAc, to which we refer to as the insular interoception network-related CAP, as it comprises brain regions involved in interoceptive processing (i.e., insula, striatum, cingulate, PFC (Pollatos et al., 2005)) (Figure 4.2). Most functional volumes were assigned to CAP1_{Ins} (41.10%). 10.05% of the volumes were assigned to CAP2_{Ins}, and 28.85% to CAP3_{Ins}, respectively. Group

comparisons of temporal characteristics revealed that FND patients entered CAP3_{Ins} less frequently than HC ($t_{CAP3Ins}(129.5) = -4.84, P < 0.001$) and had a lower relative occurrence of CAP3_{Ins} ($t_{CAP3Ins}(138.8) = -3.03, P = 0.009$). Further, patients had a shorter duration of CAP1_{Ins} as compared to HC ($t_{CAP1Ins}(134.3) = -2.78, P = 0.018$).

4.3.3.2. Amygdalar co-activation patterns

Likewise, three co-activation patterns were identified corresponding to amygdalar co-activation. The first CAP (CAP1_{Amy}) demonstrated an amygdalar activation pattern with co-activation of the cuneus and the SMA, and a co-deactivation with the DMN, the midcingulate cortex, the caudate, cerebellum, and thalamic nuclei (mediodorsal, pulvinar anterior), representing an amygdalar DMN-related CAP. The second CAP (CAP2_{Amy}) characterizes an amygdalar activation pattern with co-activation of the DMN, the angular gyrus, parahippocampal regions, the temporal pole, the NAc, and the ventral tegmental area, as well as a co-deactivation of the insula, the SMA and the DAN (i.e., supramarginal gyrus, TPJ), representing an attention-related CAP. The third CAP (CAP3_{Amy}) represents an amygdalar activation pattern with co-activation of the IPL, the superior temporal lobe, and the inferior frontal gyrus (pars triangularis), as well as co-deactivation of the precentral gyrus, and the precuneus, reflecting a visual network-related CAP (Figure 4.2). 39.13% of the selected volumes were assigned to CAP1_{Amy}, 39.03% of the volumes were assigned to CAP2_{Amy}, and 21.84% to CAP3_{Amy}, respectively. Group comparisons of temporal characteristics revealed that FND patients entered CAP1_{Amy} less frequently than HC ($t_{CAP1Amy}(141.7) = -2.78, P = 0.018$). There were no significant differences in duration nor relative occurrence of CAPs.

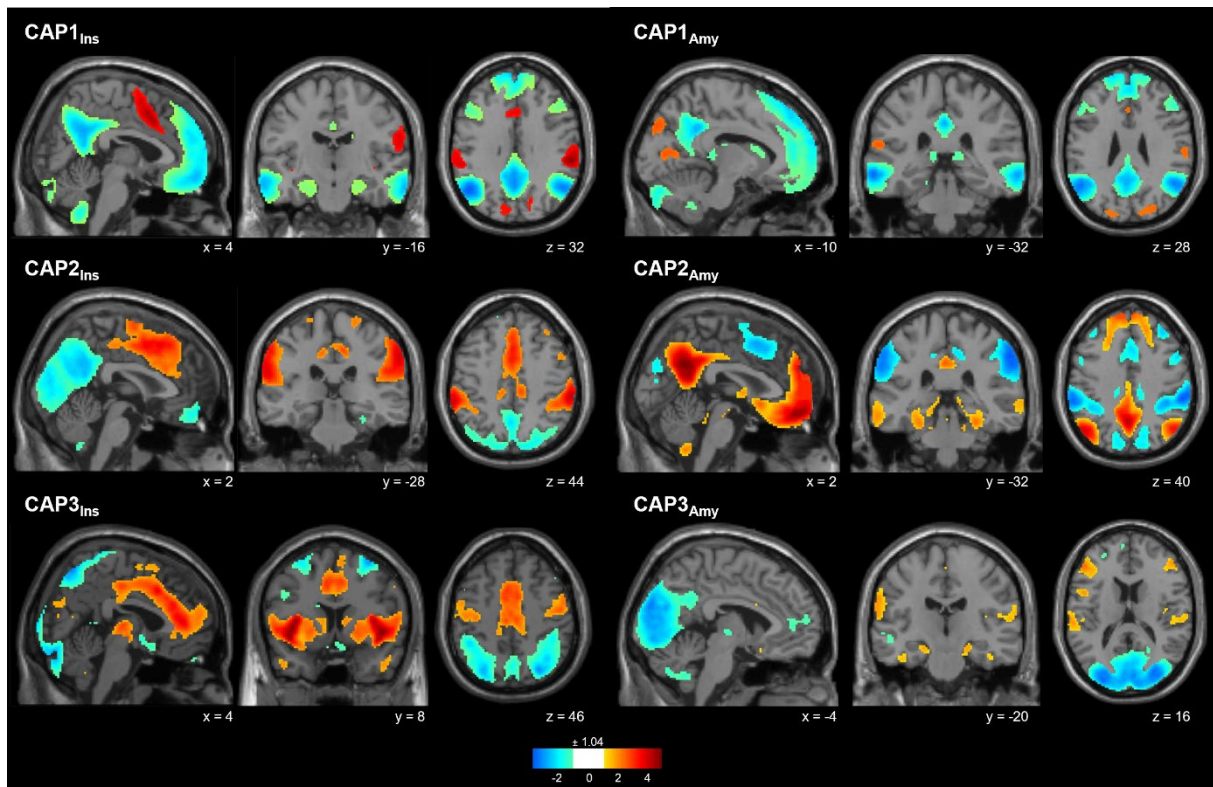


Figure 4.2: Co-activation pattern (CAP) maps based on insular and amygdalar seed activation. For each seed, three CAPs were detected. CAPs were Z-scored and only the 15% largest positive and 15% smallest negative contributions are represented in colour ($Z = \pm 1.04$) with red representing positive contributions and blue negative contributions. Locations are displayed in Montreal Neurological Institute (MNI) standard space coordinates. Abbreviation: Amy = Amygdala, Ins = Insula.

4.3.4. Association with clinical scores and stress biomarkers

To explore the multivariate relationship between aberrant CAPs temporal characteristics in FND patients with clinical scores and stress biomarkers, a partial least squares correlation (PLSC) analysis was conducted using the significantly different CAPs temporal metrics as design variables, and clinical scores and stress biomarkers as outcome variables. Based on permutation testing, one PLSC component was statistically significant ($P = 0.034$). The saliences are shown in Figure 4.3. Saliency weights highlighted in yellow indicate statistical significance and were found to be robust (based on bootstrapping). The data were standardized and thus, weights can be interpreted similarly to correlation coefficients. A significant positive correlation was found between the CAPs temporal metrics (CAP3_{Ins} – Relative Occurrence and Entries, and CAP1_{Amy} – Entries) and stress biomarkers (CAR and amylase) – meaning that the lower levels of cortisol were associated with lesser entries, or fewer occurrences, respectively. A significant negative correlation was found between the CAPs temporal metrics and symptom severity (S-FMDRS) – meaning that lesser entries and fewer occurrences were associated with

a worse symptom severity. No correlations were found between CAPs temporal measures and symptom duration, CGI, psychotropic medication intake, depression nor anxiety.

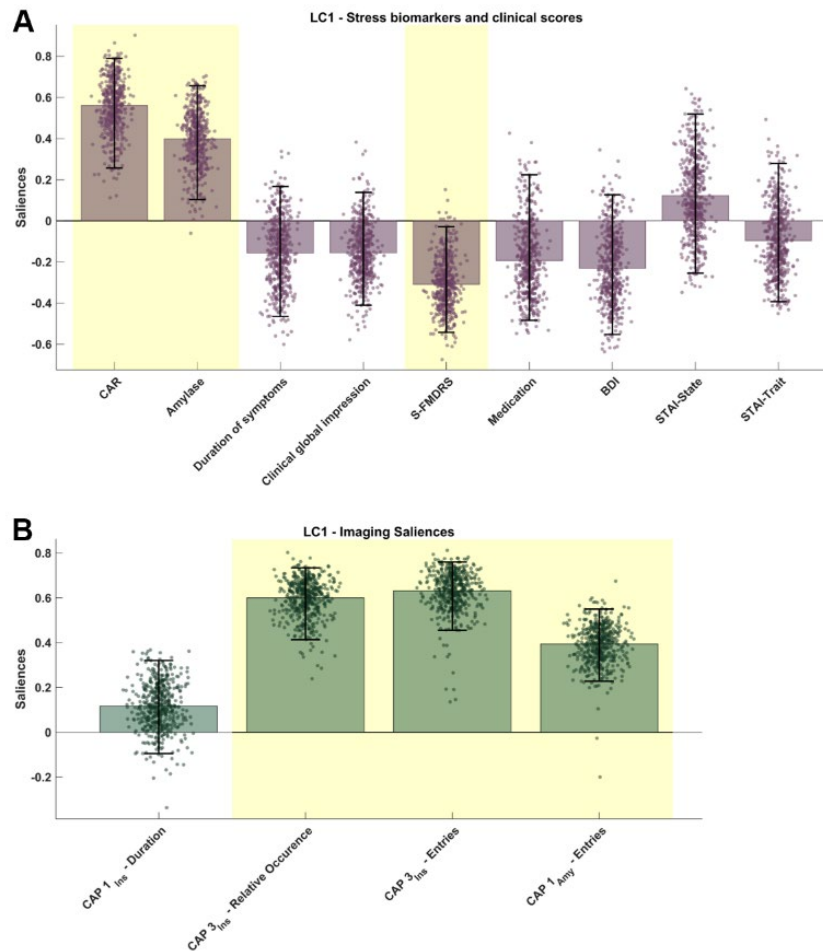


Figure 4.3: Partial least squares correlation (PLSC) results of the CAPs temporal metrics in FND patients. The outcome (A) and imaging saliences (B) of the significant PLSC component ($P = 0.034$) are presented. Error bars represent the 5th to 95th percentiles of bootstrapping and yellow highlighted bars show robustness. The height of the bar represents the salience's weight to the multivariate correlation pattern and can be interpreted analogously to correlation coefficients as the data were standardized. The permutation null distribution and the bootstrap mean percentiles are reported in Supplementary Fig. 7, Supplementary Table 1. Abbreviations: Amy = Amygdala, BDI = Beck's Depression Inventory, CAP = Co-activation pattern, CAR = Cortisol Awakening Response, Ins = Insula, S-FMDRS = Simplified Version of the Psychogenic Movement Disorder Rating Scale, STAI = State-Trait Anxiety Inventory.

4.4. Discussion

For the first time in FND, we applied a novel method investigating dynamic co-(de)activation patterns in the brain and could further link their temporal characteristics to symptom severity and stress biomarkers.

As such, based on a static whole-brain within- and between functional network connectivity analysis, we first highlighted the importance of salience-limbic network connectivity in patients with FND. Moreover, aberrant FC was found between the salience network and the somatomotor network, the DAN, the ECN, and the DMN, which however, did not survive FDR-correction. Second, by applying a co-activation pattern-based approach (CAP), we investigated the temporal characteristics of the salience-limbic networks. We identified three transient insular co-activation patterns involving motor regions (e.g., SMA, caudate), midbrain thalamic nuclei and the mesolimbic dopaminergic system (i.e., NAc), hippocampal- and parahippocampal regions, the visual-perception network and the DMN. Similarly, we found three amygdalar co-activation patterns comprising the attention network, the DMN, motor regions, the midbrain thalamic nuclei and mesolimbic system, temporal memory-related regions, as well as higher-order regions involved in self-referential processes (i.e., angular gyrus, TPJ, frontal gyrus). Furthermore, patients entered these states that were characterized by the insular interoception network activation patterns, as well as amygdalar DMN network patterns less frequently than HC. Also, the CAP characterized by the insular interoception network activation pattern occurred less often in FND patients. Lastly, the insular DMN-related network pattern was found to be activated longer in HC as compared to FND. Eventually, we identified an inverse relationship between the entries and relative occurrences of the insular interoception-related CAP (CAP_{3Ins}), as well as the amygdalar DMN-related CAP (CAP_{1Amy}) with symptom severity, as well as a positive relationship with the stress biomarkers. In sum, FND patients were found to have aberrancies in functional brain dynamics encompassing dynamic insular interoception-related network patterns as well as amygdalar DMN-related patterns. These aberrancies could further be linked to symptom severity and biological stress markers. Hence, reduced appearance of these dynamic network patterns can be associated with worse symptoms and an impaired HPA-axis, as well as sympathetic stress response. In the following sections, we will discuss first our results in the context of previous literature. Then, we will provide a narrative review on our results in the context of the Bayesian model account for FND.

4.4.1. Network disturbances in FND

In this study, we adopted a hierarchical approach in which we analysed whole-brain aberrant network connectivity and then, investigated the specific dynamic characteristics which might be implicated in the pathology of FND. The whole-brain (static) functional network connectivity approach highlighted the importance of functional abnormalities encompassing the salience-limbic network in patients with FND. Functional abnormalities in the limbic network have recurrently been reported in patients with FND and are thought to be involved in the pathophysiological mechanisms underlying symptom production (Aybek and Vuilleumier, 2016; Conejero et al., 2018; Demartini et al., 2021; Thomsen et al., 2020; Voon et al., 2016). Especially, enhanced amygdalar (re-)activity was frequently found in patients, and was linked

to impaired motor behaviour (e.g., SMA) (Aybek et al., 2015, 2014a; Diez et al., 2019; Hassa et al., 2017; Voon et al., 2010a). In addition, the insula was suggested to exert a mediating role in the emotional influence over motor behaviour (Vuilleumier, 2014). These findings imply impaired emotion regulation in patients and underline a direct limbic influence on motor control (Voon et al., 2010a). At the circuit level, many of the limbic emotional processing functions overlap in the salience and interoceptive circuits emphasizing their importance in interrelated network dysfunctions. For instance, patients showed increased attentional bias towards threat-related stimuli (Bakvis et al., 2009a, 2009b). This might be explained by means of heightened salience for emotional relevant contextual cues due to increased bottom-up activation of the amygdala and the periaqueductal grey (Aybek et al., 2014a; Voon et al., 2010a). The insula, on the other hand, is involved in the detection of internal and external stimuli (Uddin, 2017), and has been associated with interoceptive deficits (Pick et al., 2019), and increased self-monitoring in FND patients (de Lange et al., 2007; Pareés et al., 2013). Lastly, aberrant connectivity in FND has also been found between the amygdala and the insula to higher-order regions involved in external- and internal stimulus-driven processes such as self-agency and motor behaviour (Aybek and Vuilleumier, 2016; Maurer et al., 2016; Monsa et al., 2018; Perez et al., 2017b; Voon et al., 2010b; Vuilleumier, 2014; Weber et al., 2022). Our results, thus, support the notion of abnormal salience-limbic activity and connectivity in FND patients, which might underlie dysfunctional emotion regulation and interoceptive deficits.

Further evidence arises from our co-activation pattern analysis (Liu et al., 2018), in which we assessed spatial and temporal connectivity features of the insula and the amygdala, representing key nodes of the salience-limbic network. We identified decreased insular co-activation patterns engaging the interoceptive network, as well as decreased amygdalar co-activation patterns involving the DMN network. Reduced CAP temporal measures can be interpreted as decreased inter- and intra-network coupling (Griffa et al., 2021). As such, patients had a lower relative occurrence and entered the insular-interoception-related CAP (CAP3_{Ins}) less frequently than HC representing decreased intra-network coupling in FND. Similarly, patients entered insular- and amygdalar CAPs related to co-deactivation of DMN less frequently than HC (i.e., CAP1_{Amy}), respectively spent less time in that CAP (i.e., CAP1_{Ins}), pointing towards a reduced inter-network coupling in patients.

Of particular interest are the decreased temporal dynamics in FND patients regarding the CAP1_{Ins} and CAP1_{Amy}, both characterized by co-activation of the somatomotor network as well as co-deactivation of the DMN. The insular- and amygdalar co-activation with the somatomotor network reflects previous findings and hypotheses of limbic influences on motor pathways in FND (Aybek et al., 2015, 2014a; Diez et al., 2019; Hassa et al., 2017; Voon et al., 2010a). Moreover, inter-network synchronization of the somatomotor network and the DMN was found to facilitate execution of motor functions (Wu et al., 2020), and re-organization of somatomotor-DMN connectivity was associated with motor function recovery during neurorehabilitation (Hu et al., 2021). Therefore, a reduced coupling between the DMN and the somatomotor network in FND might be implicated in impaired execution of motor functions.

In general, functional abnormalities in the DMN have frequently been observed in diverse neuropsychiatric disorders (Nair et al., 2020; Whitfield-Gabrieli and Ford, 2012). Its proper functioning is crucial for integrative and self-referential processes (Davey et al., 2016), and reduced functional inter-network coupling of the DMN has been associated with enhanced self-referential processing (van Buuren et al., 2010), which can further affect orientation of attention (S. Zhao et al., 2018; Zhao et al., 2015). Likewise, increased self-referential processing and shifted attention towards self-relevant cues have also been observed in FND (Cojan et al., 2009; Pareés et al., 2012). As such, patients' symptoms were found to worsen when focusing their attention on the affected limb, and to improve when shifting it away, reflecting aberrant dynamic processes in the brain underlying symptom production potentially related to reduced inter-network coupling of the DMN (de Lange et al., 2008; Espay and Lang, 2015; Huys et al., 2021; Pareés et al., 2013).

The second interesting pattern encompasses the insular-interoception network-related CAP (CAP3_{Ins}) and its related temporal measures. The intrinsic connectivity of the insular-salience network has previously been associated with increased interoceptive accuracy (Chong et al., 2017). Noteworthy, the connectivity between the insular interoception/salience network with the right TPJ is implicated in stimulus-driven attention and detection of relevant internal and external cues (Kucyi et al., 2012). In line with our findings, aberrant TPJ activity in particular, was suggested to play a key role in the pathophysiology of FND, and more specifically, has been associated with a decreased self-agency (Aybek and Vuilleumier, 2016; Demartini et al., 2021; Drane et al., 2020; Maurer et al., 2016). Likewise, increased link-step connectivity from the insula to the TPJ was associated with symptom severity in FND patients (Diez et al., 2019). In addition, and firstly in FND, we identified an insular activation pattern with co-activation of the thalamus and co-deactivation of the NAc (CAP3_{Ins}). Previously, it could be shown that the insula, the thalamus, and the NAc play a fundamental role in predictive processing. As such, the thalamus projects goal-driven anticipation signals to the NAc, whereas the insula provides information on emotional valence, thus possibly modulating NAc behaviour (Cho et al., 2013). Our results showed decreased insular-NAc coupling in FND, which might indicate reduced modulating insular influence on the NAc. Simulating reduced NAc activity, dopamine receptor antagonists in the NAc were found to increase latency to motor initiation (Morrison et al., 2017; Nicola, 2010). Reduced motor initiation has also been described in FND (de Lange et al., 2008, 2007; Marshall et al., 1997; Stone et al., 2007; Tiihonen et al., 1995) and was further linked to increased activity of the prefrontal cortex. The prefrontal cortex – as part of the DMN – is active during self-referential processes (Gusnard et al., 2001), thus, linking dysfunctions in motor initiation to increased self-monitoring in FND patients (Cojan et al., 2009).

These results highlight the impaired intrinsic- as well as cross-dynamics of the salience- limbic network in FND (Drane et al., 2020; Pick et al., 2019). In particular, symptom production, misdirected attention, and increased self-referential processing in FND might be reflected by the reduced functional coupling of the DMN in FND with the salience-, limbic-, and somatomotor network, as well as intra-network coupling of the interoception network.

4.4.2. Network dynamics from a Bayesian model perspective

To connect our findings on the aberrancies in DMN and interoceptive network-related CAPs and their associated neuroscientific concepts, we can model somatosensory deficits, impaired interoception, and aberrant self-monitoring in FND as an iterative process during which the brain's expectation on sensory input is based on precise internal models which are continuously updated through incoming sensory information and current internal body states (perceptual inference). Mismatches between the perceptual inference and actual sensory input is calculated as a prediction error (Edwards et al., 2012; Friston, 2010; Paulus et al., 2019). In such a hierarchical Bayesian approach, perceptual inferences can be strongly affected by expectations on the outcome, i.e., prior beliefs. FND patients have previously been suspected to overweight their prior beliefs on sensory input, misapprehend the prediction error, and attribute the abnormal sensation to their supposedly involuntarily produced symptoms (Pareés et al., 2013, 2012). We further narratively review our results on reduced insular interoceptive network coupling and amygdalar DMN coupling in the context of the Bayesian model for FND (Edwards et al., 2012). As such, the insular cortex (interoception) computes the prediction error by integrating internal and external somatosensory stimuli, and - amongst others - receives emotionally valenced information from the amygdala (Clark et al., 2018), at which the amygdala exhibits a biased attention towards threat potentially explained by its judgement of novel sensory input based on past (aversive) life events (Pareés et al., 2012). Subsequent bottom-up integration of somatosensory input biased through salience-limbic hyperpriors can cause a misinterpretation of the contextual information (i.e., the prediction error) in the higher-order regions (Fox et al., 2018). The concept of wrongly delivered somatomotor-limbic information to higher-order integration regions has previously been supported by findings on enhanced functional propagation from motor-limbic information to the multimodal integration network in FND (Diez et al., 2019). Further, insular-TPJ connectivity was related to symptom severity, and increased insular-amygdalar connectivity predicted clinical improvement. In a similar study, patients were found to remain longer in certain brain states associated with attentional- and self-reflective processes, which might result in misinterpretation of the prediction error and excessive precision weighting due to increased attention as an effect of the hyperpriors (Marapin et al., 2020).

According to the Bayesian model account for FND (Edwards et al., 2012), hyperpriors are generated in intermediate steps of the hierarchy and interpretation of the prediction error depends on its precision weight. Furthermore, the precision of the prediction error is encoded as gain of synaptic strength mediated by neurotransmitters such as dopamine (Feldman and Friston, 2010). Firstly, in FND, we described an insular co-deactivation with the NAc (CAP3_{Ins}). In the framework of the Bayesian account for FND, the reduced insular co-deactivation of the NAc might represent impaired mesolimbic dopaminergic neuromodulation as a result of emotionally-valenced hyperpriors. The dopaminergic projections from the NAc further modulate striatal nuclei involved in motor behaviour (Sesack and Grace, 2010),

potentially strong enough to elicit symptoms in FND. This intermediate limbic-striatal local loop might further increase the prediction error and subsequently reinforces prior beliefs as a result of wrongly encoded gain of synaptic strength.

In summary, our results firstly showed that aberrant dynamic brain states in FND encompass the intra-network coupling of the interoceptive circuits as well as inter-network coupling between salience-limbic networks and the DMN using a co-activation pattern analysis. This supports the notion that perception in FND is strongly influenced by the dynamic behaviour of salience-limbic lower-order regions and their influence on higher-order cognitive processes. Second, we hypothesized that mesolimbic dopaminergic activity might directly elicit abnormal motor behaviour mediated by hyperpriors, and thus, bypassing higher-order executive control networks and consequently strengthening hyperpriors in FND. These concepts are visually represented in Figure 4.4.

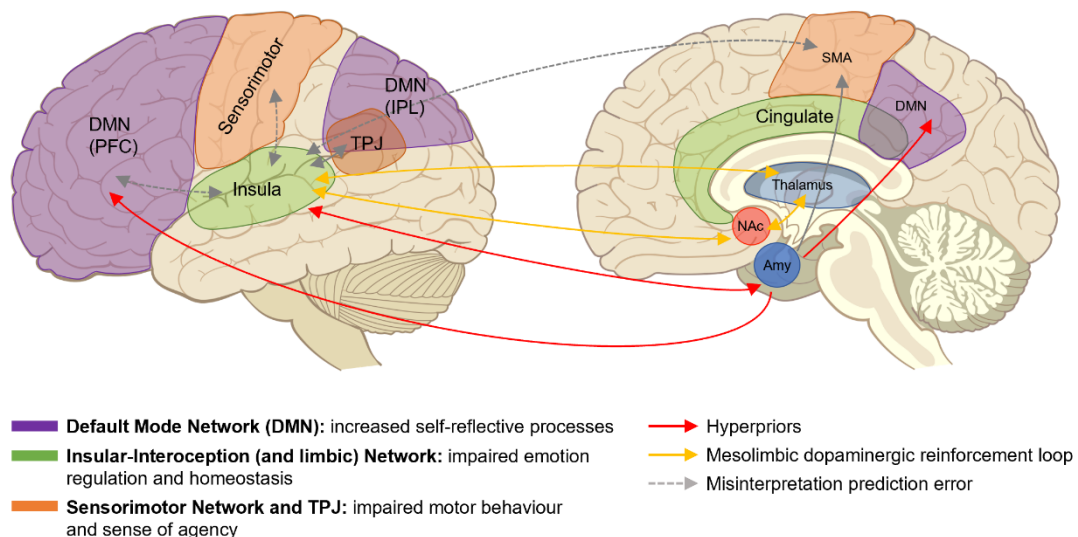


Figure 4.4: Visual representation of the insular- and amygdalar co-activation pattern-related networks and related neuroscientific constructs in functional neurological disorders. The insular cortex is involved in the computation of the prediction error (grey dotted arrows), whereas the amygdala provides information on priors (red arrows). Bottom-up integration of somatosensory input is biased by hyperpriors from the salience-limbic networks, leading to a misinterpretation of the prediction error and excessive precision weighting. The precision of the prediction error is encoded as a gain of synaptic strength, mediated by the mesolimbic dopaminergic system (yellow arrows). The limbic-striatal loop reinforces prior beliefs as a consequence of wrongly encoded gain of synaptic strength in the NAc. Abbreviations: Amy = Amygdala, IPL = Inferior Parietal Lobule, NAc = Nucleus accumbens, PFC = Prefrontal Cortex, TPJ = Temporo-parietal Junction.

4.4.3. Clinical implication and stress biomarkers

In FND patients, the here found differences in temporal characteristics of the insular CAP associated with the interoception network, as well as the amygdalar CAP associated with the DMN further correlated with stress biomarkers and clinical scores. Namely, reduced occurrences and entries are associated with reduced stress biomarkers, as indexed by cortisol,

representing a slow or chronic response to stress, as well as indexed by alpha-amylase, representing the rapid autonomous sympathetic stress response (Apazoglou et al., 2017). Dynamic shifts in DMN-salience connectivity have previously been associated to an altered cortisol stress response (Zhang et al., 2019). As such, increased stress reduced inter- and intra-network coupling of the DMN, whereas it increased intra-network connectivity of the salience network. The salience network, thus, has been suggested to play a pivotal role in the response to acute stress, whereas the DMN has rather been associated to post-stress homeostatic restoration and emotion regulation (van Oort et al., 2017). Likewise, changes in the dynamic interaction of the DMN and salience network were associated with the autonomous stress response (as measured using heart rate variability) upon stress induction, suggesting a carry-over effect of stress on functional brain network dynamics (Chand et al., 2020). Interestingly, CAP3_{Ins} shows substantial overlap with the insular-frontoparietal cognitive control network (insuFPCN) as reported by Gaviria *et al.* (Gaviria et al., 2021), which has been linked to emotion elicitation and adaptive homeostatic regulations after stressful events. In FND, reduced temporal characteristics of the insular and amygdalar co-deactivation of DMN-related CAPs might represent an impairment in the restoration of homeostatic processes in the aftermath of (acute) stressful events (Gaviria et al., 2021) in relation to aberrant self-referential processes (Cojan et al., 2009; Pareés et al., 2012) and emotion regulation (Voon et al., 2010a).

Second, abnormalities in salience-limbic network dynamics showed an inverse relationship with symptom severity, meaning that a reduced appearance of these states was associated with worse functional symptoms. Similarly, for the first time, dynamic changes in the DMN could be linked to symptom severity in major depressive disorder (Sendi et al., 2021). Interestingly, dynamic aberrancies were not associated with depression or anxiety scores in FND patients, but negatively correlated with depressive and anxious behaviour in HC, Appendix C, Supplementary Material for Chapter 4, Figure C.8, Figure C.9, Table C.2. Our study design does not allow to infer upon causal relationships between stress biomarkers, clinical scores, and the time-varying temporal dynamics of distinct brain networks in FND. These findings, however, point towards an interaction between symptom presentation and the appearance of certain brain states related to salience-limbic networks and the DMN, potentially driven by dysfunctional autonomous- and HPA-axis stress response. The fact that in HC interoception-CAP3_{Ins} and DMN-CAP1_{Amy} negatively correlated with depressive and anxious behaviour might delineate that enhanced appearance of these CAPs acts as an intrinsic protection mechanism, as such that reduced appearance might represent a susceptibility factor for neuropsychiatric disorders such as FND.

4.4.4. Limitations

Co-activation pattern analysis represents a novel method to study functional brain network dynamics in FND. However, adopting a seed-based approach might be susceptible to noise. As it works on a single-volume resolution, all selected timepoints show high activity in the seed

region and consequently will the resulting CAPs (Liu et al., 2018). Therefore, co-activation with other regions might occur at change-level, without an actual physiological relevance. Second, although our sample size is considerably large, the FND population is heterogenous in type and severity of symptoms, which impedes the generalizability of the results. In addition, patients often suffer from comorbidities such as panic-, mood-, or anxiety disorders (Carson and Lehn, 2016), which is also reflected in our population. The CAPs temporal characteristics in FND did not correlate with depressive or anxious behaviour, indicating that our results were not necessarily driven by depression and anxiety. In HC, however, the CAPs temporal measures were inversely related to depression and anxiety scores, and this association, and its potential effect on dynamic behaviour of the brain, must be further investigated before drawing final conclusions. Lastly, even though psychotropic medication intake did not correlate with our findings, the effect of patients' diverse medication intake on functional brain dynamics must be evaluated with caution, especially regarding our hypothesis on the mesolimbic dopaminergic system as a positive reinforcement of the prediction error.

4.4.5. Conclusion

Our study firstly explored aberrant dynamic salience-limbic inter-and intra-network connectivity patterns in FND. We identified altered insular co-activation patterns with the DMN, and regions involved in interoception. Moreover, aberrant amygdalar co-activation patterns with the DMN were detected. These dynamic functional alterations could further be linked to stress biomarkers and symptom severity in patients. In line with previous findings on abnormal emotion regulation, interoceptive deficits, and increased self-referential processes these findings firstly investigated dynamic alterations in related networks, which might account for the clinical symptom presentation in FND. Furthermore, these results support the Bayesian account for FND, in which hyperpriors are generated in intermediate steps of the cortical hierarchy. Correspondingly, we firstly introduced the hypothesis of that the mesolimbic dopaminergic synaptic gain might be implicated in the production and reinforcement of the prediction error in FND. In essence, temporal brain dynamics linked to interoception, and self-referential processes was associated with functional symptom presentation and can be linked to abnormal predictive coding in FND. However, causal relationships between brain functional dynamics, symptom severity, and stress regulation in FND remain to be discovered and results must be replicated paying attention to psychotropic medication, and psychiatric comorbidities.

CHAPTER 5

General Discussion and Outlook

5.1. Recap Thesis Background and Aims

Functional neurological disorder (FND) is a condition at the border between neurology and psychiatry (Perez et al., 2020). Born as *hysteria*, FND rose to fame during the 19th century, accompanied by the interest of Charcot and Freud, only to become a relict of antiquity during the 20th century (Fend et al., 2020). FND never actually vanished, thus research had to abandon the mind-body dualism, and neurology and psychiatry were united again in FND. With the efforts to not only understand *why* but also *how* the symptoms develop, a new era started for research in FND (J. Stone et al., 2010b).

Contemporary models of FND focus on the integration of a multifactorial origin of FND (Cretton et al., 2020; Keynejad et al., 2019), including a range of different predisposing, perpetuating, and precipitating factors. As one of the most commonly studied risk factor in FND, childhood trauma – particularly sexual and physical abuse – has repeatedly been found (Kanaan and Craig, 2019; Karatzias et al., 2017; Reuber et al., 2007; Roelofs and Pasman, 2016). More recently, emphasis was put on the significant role of emotional neglect in the development of FND (Ludwig et al., 2018). Nonetheless, only little emphasis has been devoted to the biological consequences of adverse life events in FND. Hence, only few studies investigated a potential dysregulation in the biological stress system – the HPA axis – and results were often contradictory and difficult to interpret.

In addition, multiple brain network dysfunctions have been identified in FND with major impairments in the limbic and salience networks – responsible for emotion processing, awareness and interoception –, as well as fronto-parietal- and sensorimotor networks – involved in attention motor intention and self-agency. As such, symptom production and their neural correlates can be interpreted in the framework of a Bayesian model (Edwards et al., 2012; Friston, 2010), in which symptom presentation is strongly influenced by prior beliefs on their severity rather than on external sensory inputs. Those prior beliefs might arise from past adverse life events, i.e., physical or psychological trauma (Pareés et al., 2012). Locating the attentional focus on the symptoms themselves can then increase expectancy on their severity strong enough to actually cause abnormal motor behaviour.

Connecting the knowledge on diverse network dysfunctions and multifactorial- and integrative models on FND development and symptom production could help translating the knowledge from bench to bedside in terms of identifying latent disease mechanisms and defining potential prognostic and diagnostic biomarkers for FND.

This thesis, therefore, set out to study the link between biological and psychological stress and the neural correlates of FND, in order to advance the understanding of underlying disease mechanisms and to investigate potential objective biomarkers for the disorder. As such, this thesis exposit 1) aberrant FC as a potential imaging-based biomarker for FND in a multi-centre setting, 2) the biological stress axis in FND patients and potential experience-dependent anatomical changes to examine the biological relevance of stress, and 3) how functional brain dynamics relate to clinical symptom presentation, as well as biological stress markers.

5.2. General Findings of the Thesis

5.2.1. Multi-centre classification using resting-state functional connectivity

Aberrant FC in FND patients was previously found to be a strong predictor when classifying against HC (Wegrzyk et al., 2018) using a SVM classifier. In order to work towards a clinical application of aberrant FC as a positive, imaging-based biomarker for FND, the previously found results were replicated within and across different centres using a pooled and a scanner-specific cross-validation approach. First, the results were successfully replicated in other movement disorder centres with overall accuracies at or above 70% (centre I: 73.9%/II: 72.9%/III: 70.8%/ IV: 70.0%), highlighting the robustness against clinical heterogeneity as the different patient populations differed in symptom presentation and severity (intra-centre cross-validation). Second, the classification approach was found to be robust enough when pooling the data from four different centres including different patients and different MRI scanners (pooled cross-validation). Moreover, classification results were not affected by symptom severity, psychological comorbidities nor psychotropic medication. Together with the results on the intra-centre cross-validation, these results strongly suggest that machine learning is a robust tool to detect subtle differences in FC between patients and controls, independent of their clinical symptom presentation, severity of symptoms, or psychological comorbidities. Thus, functional brain abnormalities in patients might represent an FND specific trait. To further confirm this, FND patients must be compared as well to other patient groups with similar symptoms but different diagnoses. Moreover, we must also consider that other predisposing or precipitating factors (Hallett et al., 2022) – such as genetic factors or adverse life events – might underlie these traits and potentially influence classification performance.

As a last step, however, the classification did not succeed, when using $N - 1$ centre as training set, and evaluate on the left-out centre (inter-centre cross-validation). Compared to the previous validation steps, during the inter-centre cross-validation step, the classifier did not possess prior knowledge on scanner-induced confounding factors. Inter-scanner variability (Noble et al., 2017), therefore, represents an obstacle yet to be overcome, as it introduces noise that is fully unrelated to the disorder (Abdulkadir et al., 2011) and thus limits the generalizability across centres. From a clinical perspective, a failure of the inter-centre cross-validation might also be attributed to the different FND symptoms represented in each centre used as test set. For example, centre IV presents with myoclonus in its majority, which could limit the generalizability against other subtypes.

When further investigating the results on the successful pooled cross-validation, we evaluated the contribution of different FC patterns to the classification. We identified regions that were commonly found in the literature in FND, such as 1) limbic regions (Aybek et al., 2015; Espay et al., 2018b, 2018c; Monsa et al., 2018), 2) sensorimotor regions (Baek et al., 2017; Blakemore et al., 2016; Cojan et al., 2009), or 3) right temporal regions (i.e., TPJ (Aybek

et al., 2014a; Espay et al., 2018b; Maurer et al., 2016). Of particular interest is the aberrant functional connections between the temporo-parietal regions to sensorimotor regions. With the TPJ being the key region of the processing of the sensory prediction signal (i.e., sense of agency), aberrant FC to sensorimotor regions might cause an impaired sensorimotor integration and thus, could explain the feeling of symptoms being experienced as if produced involuntarily (Perez et al., 2012; Voon et al., 2010b).

In summary, a machine learning classification approach showed promising results when classifying against healthy controls in a multi-centre setting. The classification was mostly driven by regions commonly found to show impaired activity or FC, independent of symptom presentation and severity, comorbidities, or medication status. Potentially representing a trait marker of FND, aberrant FC in FND patients thus represent a promising potential biomarker for the disorder. Future validation steps focusing on the inclusion of patient groups with similar symptoms, and further technical development to provide generalizability across centres, however, are of utmost importance.

5.2.2. A biopsychological approach to the stress-diathesis model

FND patients are suspected to find themselves in a hyperarousal state, as defined by enhanced sympathetic activity (Bakvis et al., 2009a; Kozłowska et al., 2017b, 2015). Only few studies, however, have investigated the HPA-axis – and in this context cortisol as a marker for stress – and results were inconsistent, what can be mostly explained by the increased variability of cortisol due to diverse confounding factors and different experimental settings (Hellhammer et al., 2009). In order to generalize previous findings, potential dysregulations of the HPA-axis were investigated and its association with psychological-, and neurological correlates of stress were examined – a line of research that has never been pursued before. In a large population of mixed FND patients, a flattened CAR was identified. The here found effect was even more profound in patients with a history of childhood emotional neglect, whereat this effect could not be identified in HC. Generally, patients reported more emotional neglect, which lasted in average 4.5 years longer as compared to HC. When evaluating the association between different dimensions of emotional neglect and the flattened CAR – as observed in patients – it was confirmed that not only the sole fact of having had experienced emotional neglect during childhood but also its severity and duration of the emotional neglect significantly contributes to the multivariate pattern of correlation between emotional neglect and the flattened CAR in FND patients. The acute response to stress is an activation of the HPA axis and a subsequent increase in cortisol levels. Prolonged exposure to stress, however, is suggested to cause a maladaptive habituation, or downregulation of the HPA-axis stress response leading to reduced cortisol levels. Similarly, hypocortisolism has been previously described in patients suffering from PTSD (Pacella et al., 2014; Pan et al., 2018; Rauch et al., 2020; Wahbeh and Oken, 2013;

Wessa et al., 2006). Apart from PTSD - but less intensively studied – hypocortisolism has also been observed in other stress-related functional somatic disorders with a potential relation to trauma, such as burnout with physical complaints, chronic fatigue syndrome, fibromyalgia, or idiopathic chronic pain (for review: Heim et al., 2000). Similarly, a flattened cortisol profile could even be detected in relation to emotional neglect in patients with fibromyalgia (Yeung et al., 2016).

Lastly, alterations in brain volumes of regions particularly sensitive to chronic stress (i.e., hippocampus, amygdala) were examined on the presumption of the neurotoxic effect of chronic cortisol exposure. Patients were found to have a reduced hippocampal and amygdalar volume as compared to healthy controls. These results are consistent with previous findings on patients with PTSD (Heim et al., 2000; Herman, 2013; Yehuda and Seckl, 2011), in which a neurotoxic effect of cortisol has been suggested. A significant multivariate pattern of correlation between cortisol and brain volumes, however, was only detected in HC but not in FND patients. Therefore, the here found results do not point towards a reduction in brain volume due to a neurotoxic effect of cortisol, and rather denotes to be the product of a neurodevelopmental effect of childhood emotional neglect or a biological predisposition (i.e., congenitally smaller brain volumes).

In summary, a flattened CAR in FND patients could be linked to severe and prolonged (childhood) emotional neglect, pointing towards long-term maladaptive habituation of the HPA-axis. Contrarily, reduced subcortical volumes were not directly related to the dysfunctional HPA-axis and thus, might represent a predisposing vulnerability factor (congenital or neurodevelopmental) to FND. Nevertheless, these results do not provide evidence for causal relationships between biological, neurological, and psychological correlates of stress and further studies are needed in order to disentangle specific effects of predisposing, precipitating, and predisposing factors in the aetiology of FND. To conclude, the here found results point towards a multifactorial stress-diathesis model for the pathophysiology of FND. Different phenotypical variations in symptom presentation thus might be ascribed to individual contributions of biological-, and psychological risk factors for FND.

5.2.3. Dynamic functional connectivity

Functional brain abnormalities in patients with FND potentially underlying symptom production have commonly been studied using *static* FC approaches in which brain activity is summarized as the temporal correlation between spatially distinct brain regions. Nowadays, however, it is known that the brain behaves dynamically and changes between different so-called brain states in order to flexibly adapt its behaviour to intrinsic and extrinsic stimuli (Brembs, 2021; Michel and Koenig, 2018). Here, the importance of the salience-limbic network connectivity was highlighted using a static whole-brain within- and between functional network connectivity analysis. As a next step, the dynamic behaviour of the salience- and limbic network – or more specific of the insula and the amygdala as seed regions – was investigated using a

dynamic co-activation pattern (CAP) approach. Conceptually, different CAP maps were detected by means of k-means clustering on those functional volumes showing highest activity in the seed regions. Doing so, three CAPs were identified for each seed regions encompassing insular co-activation patterns with somatomotor regions, the DMN, attention networks, and the interoception network, as well as amygdalar co-activation patterns involving the DMN, attention networks, and higher-order function networks (i.e., self-referential processes).

In particular, patients showed reduced temporal characteristics (i.e., duration, occurrences, entries) of the insular CAPs related to the co-activation of the interoception network and the co-deactivation of the DMN, as well as the amygdalar CAP related to DMN co-deactivation. The DMN plays a crucial role in diverse self-relevant processes (Davey et al., 2016), whereas the insular-interoception network is implicated in somatosensory perception as well as emotional awareness (Barrett and Simmons, 2015; Gu et al., 2013). Reduced insular interoceptive coupling, as well as amygdalar DMN coupling can be put in the context of a Bayesian model account for FND (Edwards et al., 2012), at which hyperpriors on a behavioural outcome are computed in intermediate steps of the cortical hierarchy (i.e., insula, amygdala), which might cause a miscalculation and misinterpretation of the prediction error by higher-order systems (i.e., TPJ) by means of its precision weight. The precision of the prediction error is thought to be encoded as gain of synaptic strength of neuromodulatory neurons (Feldman and Friston, 2010). Such neuromodulatory circuits might encompass the dopaminergic mesolimbic system, for which potential abnormalities are firstly identified within the framework of this thesis. As such, reduced co-activation of the insula and the nucleus accumbens might modulate dopaminergic projections (Cho et al., 2013) which might further impair motor behaviour through striatal pathways (Sesack and Grace, 2010). Intermediate limbic-striatal local loop might enhance the abnormal sensations and consequently reinforces prior beliefs on behavioural outcomes as a result of wrongly encoded gain of synaptic strength.

Abnormal prior beliefs might also arise through a maladaptive attentional process through nocebo-like mechanisms (Fiorio et al., 2022). Particularly, the placebo effect – contrarily to the nocebo effect referring to the improvement of clinical symptoms within a positive psychosocial context – has been associated with an increase of dopamine in the striatum in Parkinson's patients (Lidstone et al., 2010), highlighting the potential involvement of dopaminergic pathways in somatic perception. Similarly, the hypothesis on that a nocebo effect can be learned in the form of a classical conditioning (Van den Bergh et al., 2002) – which as well involves dopaminergic pathways (Galaj and Ranaldi, 2021) – supports the notion of a reinforcement of maladaptive prior beliefs and expectations, strong enough to trigger the misperception of somatic sensations (Beissner et al., 2015).

Lastly, dynamic functional aberrancies could be linked to symptom severity and stress biomarkers. Previously it could be shown that dynamic brain states might be linked to emotion regulation and restoration of homeostasis in the body (Gaviria et al., 2021). As such, this analysis firstly revealed a connection between dynamic brain states, symptom severity, as well

as stress biomarkers, which might explain the fluctuations of functional neurological symptoms as a dynamic interplay between internal and external events.

5.3. General Limitations and Future Directions

One major limitation of this thesis is the generalizability of the findings to specific FND subtypes. With our decision to apply a transdiagnostic approach, we were not limited by being able to only recruit patients with a particular symptom type, but – on the contrary – cannot assign our findings to an individual symptom type. Therefore, the here identified findings rather represent a general “footprint” of FND. Future studies should also aim at replicating the here found results by focusing on only one symptom type by means of a differential diagnostic approach to identify biomarkers specific for that symptom and to be able to focus on a specific neurological pathway.

Apart from using a transdiagnostic approach, the patients were found to suffer from movement disorders most commonly (e.g., tremor, gait disorders) whereas PNES or PPPD was rarer. Consequently, we lack the power to assert whether these findings might be generally FND-related or rather specific to a certain FND type (e.g., motor FND). Moreover, psychiatric or physical comorbidities such as depression, anxiety or pain and fatigue were very common across the patients recruited in this study, which is commonly observed (Carson and Lehn, 2016). Even though we corrected for psychiatric comorbidities, results might not be solely attributed to FND. Analogously, we did not systematically screen for detailed non-motor symptoms such as chronic fatigue or pain. Especially chronic pain might as well lead to substantial changes in the brain (Li and Hu, 2016) and thus, could have influenced the results. Likewise, symptom severity and illness duration differed between the patients. This might impact the results in terms of a long-term adaptations or changes in brain functions or biological data as a consequence of prolonged suffering. Likewise, data from FND patients were compared only to data from HC. However, to translate findings into a clinical routine, results must be robust against other psychiatric conditions or neurological diseases which might overlap in symptom presentation. Thereby, these findings are not necessarily specific to FND, as – for instance – a reduced CAR or smaller hippocampal volumes have also been reported in other neuropsychiatric disorders such as PTSD (Rauch et al., 2020), chronic pain, or fibromyalgia (Heim et al., 2000; Yeung et al., 2016). Therefore, future studies should include patients with more balanced symptom types, and better characterize across neurological and psychological domains in order to define individual implications on the pathophysiology within FND (e.g., motor FND versus PNES) but also between different disorder (e.g., FND versus PTSD). To also provide clinical utility for differential diagnostic approaches, future studies must include psychiatric or neurological control populations. Correspondingly, data should also be compared in a within- and between-group design to evaluate factors such as symptom severity and illness duration (Perez et al., 2021).

Further limitations arise when studying biological data, such as cortisol. Especially hormones strongly interplay within a homeostatic process and alterations in hormonal levels might represent fluctuations due to rapid adaptations to situational aspects rather than disease-specific traits (Stalder et al., 2016). A next step could be to assess RNA levels for mineralocorticoid or glucocorticoid receptors in the brain in order to assess change in expression levels. Generally, to gain a more representative picture of ongoing homeostatic processes within the body, studies should measure several key players by means of hormones or metabolic products, but also genetic or epigenetic data. Moreover, potential confounding factors must be addressed carefully and relationships across other risk factors must be considered (e.g., neurodevelopment, sex differences, social factors).

Generally, data assessed in a cross-sectional manner cannot provide sufficient information on the actual disease development. As such, it cannot be concluded whether the here found results represent a cause (e.g., subsequent consequence of a trauma), a risk factor (e.g., biological-, or psychological predisposing factors), or merely an effect of being ill. This highlights the need of longitudinal studies, which include the assessment of neuroimaging, behavioural, endocrine, and/or genetic data in order to investigate state versus trait markers of FND, as well as to study potential pathophysiological mechanisms.

In terms of the technical limitations, especially resting-state fMRI data can be subject to noise and artefacts, and findings might be result of these, or thorough data cleaning and pre-processing might accidentally remove signal of interest (Bright and Murphy, 2015; Goto et al., 2016). This represents particularly a strong limitation in terms of using multi-centre imaging data, where artefacts and noise can arise from different technical or human sources. Future studies should still aim at collecting multi-centre data but by implementing a quality assurance program which assures collective data acquisition, validation and monitoring (Glover et al., 2012). Particularly for research in FND, no such international data sharing initiative exists. Effort must be devoted to establishing multimodal international databases including standardized data collected across different centres.

In general, numerous studies, including this PhD thesis, identified neural correlates of FND, correlated it to symptom severity, investigated the stress regulation, adapted multifactorial theories, and applied the latest research methods, not only with the aim to better understand the underlying pathological mechanisms, but also to translate the knowledge from bench to bedside by means of identifying objective biomarkers. Such biomarkers could provide additional rule-in criteria and further strengthen the clinical diagnosis. Unfortunately, previous results – or biomarkers – reflect group-level comparisons and cannot yet be applied on an individual basis. Moreover, many network aberrancies and dysfunctions in neuroscientific concepts have been repeatedly identified but thorough replication and validation studies are missing (Thomsen et al., 2020). Similarly, research on biological and/or genetic factors in FND is in its beginnings. Only few studies exist and often reported controversial results, which makes larger and standardized (replication- and validation) studies of need.

In summary, future studies should include different FND phenotypes, but handle neurological and psychological factors with care. Patients must be compared in within- and between group designs using diverse control groups. Moreover, longitudinal studies are of need to disentangle maladaptive adaptations and congenital-, or predisposing factors. Findings must then be replicated and carefully validated in standardized multi-centre studies. Lastly, technical limitations should be approached by unifying methods, for instance in terms of confounding factors. Additionally, studies should encourage the use of multimodal imaging, biological, psychological, or genetic data in order to contextualize the findings into a multi-factorial disease model.

5.4. Contribution to the field

The aim of this thesis was to connect the *how* and the *why* by means of studying the neurological-, biological-, and psychological aspects of FND and thereby advance the understanding of pathophysiological mechanisms. There are several important contributions to the field resulting from the findings of this thesis. Firstly, we could replicate and validate the previous results of (Wegrzyk et al., 2018) using data arising from different movement disorder centres including diverse patients with FND. Even though these results do not represent a final solution, it is a first attempt towards the development of fMRI-based positive biomarkers for FND. In the future, machine learning algorithms could potentially support clinicians by means of a differential or transdiagnostic approaches, predict treatment outcomes or optimize patient management. However, it also highlighted the current technical limitations in the field and further obstacles that must be overcome before clinical utility can be provided.

More importantly, this thesis firstly studied the association between preceding, precipitating, and predisposing risk factors in FND, connecting psychological, biological and neural correlates of FND, a line of research that has never been followed before. As such, it could be shown that an aberrant HPA-axis stress response system coheres with preceding long-term (childhood) emotional neglect, confirming the suggested importance of emotional neglect in the pathology of FND (Ludwig et al., 2018). On the other hand, it could be shown that patients have reduced anatomical volumes of the hippocampus and the amygdala, but however, without an association to cortisol. These results thus, speak against the hypothesis of that prolonged stress exposure (i.e., enhanced cortisol secretion) might exert a neurotoxic effect on certain brain regions particularly sensitive to cortisol due to high glucocorticoid and mineralocorticoid receptor density (Heim et al., 2000; Yehuda and Seckl, 2011). With this – and firstly in FND – we introduced the hypothesis of reduced subcortical volume might represent a biological vulnerability factor in FND. Biological relevance and causal relationship however must be confirmed before making final conclusions.

Moreover, on a functional level, we could show for the first time that patient exert functional abnormalities in the temporal properties of salience and limbic brain networks. These findings firstly highlight the temporal variations of functional brain abnormalities and more

importantly linked them to symptom severity and stress biomarkers. Especially as symptoms can fluctuate, also in the context of acute stress, investigating the functional dynamics of the brain can provide new insights on symptom production and their state-dependent appearance. Therefore, this work firstly presents a way of studying functional brain abnormalities in patients which also integrates the temporal dynamics of the symptoms as a function of the rapid adaptations of the brain to external and internal stimuli. Next, we narratively reviewed our results in the context of the Bayesian model approach for FND and firstly introduced the hypothesis of the mesolimbic dopaminergic system (i.e., insula-thalamus-NAc loop) representing an important relay station reinforcing the prior beliefs on symptoms in FND.

To conclude, this thesis suggests a link between past adverse life events, potential biological predisposition, as well as acute implications of stress on brain functional abnormalities, which might be involved in symptom production. Upon proper validation and replication of these results preferably in longitudinal multi-centre studies, these results could for instance serve the development of a preventative screening marker or as a diagnostic biomarker. Moreover, these findings set path to further research on gene-environment interactions in order to further disentangle individual contributions of diverse risk factors to the pathology of FND. The novel points of view open new directions to study potential pathophysiological pathways in FND highlighting the HPA-axis as well as the dopaminergic system.

5.4.1. Potential clinical applications

FND is the second most common diagnosis in outpatient neurology clinics in the UK (J. Stone et al., 2010a). Nevertheless, patients often feel that they are not taken serious (Crimlisk et al., 2000), and undergo multiple consultations and medical tests (Espay et al., 2009), delaying their diagnosis and impeding an appropriate treatment, which can further worsen their symptoms (Gelauff et al., 2014). Being correctly diagnosed often depends on the subjective clinical evaluation of highly qualified and trained medical personnel, as still only few clinicians are consciously aware of the disorder. On top of that, patients – once diagnosed – are often refused to receive help and support from health insurance companies because the disorder is still highly stigmatized (MacDuffie et al., 2021), as no objective data accompanying the diagnosis can be presented. In addition to the clinical diagnosis thus, objective physiological and imaging-based biomarkers could assist in a medico-legal context (Colombari et al., 2021). Such objective biomarkers could give credibility to the diagnosis and could be assessed in almost every hospital in which MRI scanners or diagnostic laboratories are available.

First, functional imaging-based biomarkers could provide further information on functional abnormalities upon admission of a patient to the neurological ward or emergency unit when ambiguous neurological symptoms are present and no structural cause identified. Particularly resting-state fMRI data can be obtained easily with an average of 5-10 min of acquisition time and additionally, does not depend on the patient's active participation. Therefore, it could

simply be integrated in the clinical protocol upon admission of a patient with neurological symptoms. However, technical limitations such as inter-scanner variability must be overcome. A further limitation is presented as current knowledge on functional abnormalities is based on group level comparisons, as the fMRI signal is represented by a relative change in intensity and cannot be measured as absolute value. For such an application, a potential solution must be found to standardize findings from fMRI studies, and objective read-out options must be implemented and validated.

Second, additional diagnostic procedures could be developed on the basis of objective physiological data such as cortisol. Similarly, cortisol can be easily extracted and is stable upon extraction for a relatively long time. As such, the flattened CAR might serve as a diagnostic marker, as – for example – many infectious, autoimmune, or inflammatory neurological diseases would rather coincide with increased cortisol levels (Barugh et al., 2014; Kern et al., 2013; Ouanes and Popp, 2019). Similarly, cortisol could be used to monitor treatment responses or disease progression. For such an application, cortisol should be studied in longitudinal data in relation to treatment administration, and whether clinical improvement can be reflected in a normalization of the HPA-axis stress response system.

Lastly, the here presented results provide important clinical implications for the development of appropriate therapy programs for patients with FND. As found in Chapter 2, the abnormal connectivity between the right TPJ and sensorimotor regions is one of the most discriminative between patients and controls. With the TPJ representing a key region involved in the sense of agency, future therapies might invest on treatment options targeting the sense of agency, such as e.g., non-invasive brain stimulation (Chambon et al., 2015; Peterson et al., 2018) or neurofeedback training (Sitaram et al., 2017). Results from Chapter 3 suggest an abnormal stress regulation system in patients with FND. Potential treatment options might target stress reduction or stress perception, such as mindfulness-based interventions (Baslet et al., 2020). Finally, Chapter 4 highlighted the role of maladaptive hyperpriors, for which future therapies might adapt cognitive behavioural therapy based approach, which has already been found effective for FND (Richardson et al., 2020, 2018), or attentional bias modification training which directs attention away from illness-relevant stimuli (Mogg and Bradley, 2016).

In summary, multimodal data could support the diagnostic process, monitor treatment outcomes, and could assist the patient management. However, diagnostic utility is only provided if these results can be replicated, validated, and standardized. Subsequently, these techniques could be incorporated in the clinical daily routine, supporting clinicians during the decision-making process, and guide the patients' journey into the correct direction, and eventually help eliminating the societal bias.

5.5. Conclusion

To conclude, these findings significantly contributed to connecting the question on *how* and *why* FND develops and set path to investigate other potential targets in order to understand

FND in the framework of a multifactorial and integrative model, which could help translating the knowledge from bench to bedside and defining potential prognostic, diagnostic and treatment response biomarkers for FND.

List of Tables

Table 2.1: Scanner acquisition parameters.....	32
Table 2.2: Demographic and clinical characteristics of the four centres.....	37
Table 2.3: Classification performance of the intra-centre and pooled validation steps on the four different centres.	38
Table 2.4: Classification performance of the inter-centre cross-validation step on the four different centres.....	42
Table 3.1: Demographic, behavioural, and clinical data	60
Table 3.2: Whole-brain voxel-based morphometric results with total intracranial volume (TIV), age, sex, depression (BDI), and anxiety (STAI) as covariates of no interest.....	65
Table 4.1: Demographic, behavioural, and clinical data	85
Table A.1: Conversion of CGI score.....	149
Table A.2: Mean functional connectivity in controls and patients between pairs of regions showing discriminative functional connectivity.	158
Table A.3: Logistic regression model. Logistic regression models testing the effects of anxiety (STAI), depression (BDI), psychotropic medication (yes/no), and clinical scores (CGI) taken-together and individually in (A) intra-centre cross-validation, and (B) pooled cross-validation.	164
Table B.1: ROI-analysis using an inclusive hippocampus mask. Results with total intracranial volume (TIV), age, gender, depression, and anxiety as covariates.....	172
Table B.2: ROI-analysis using an inclusive amygdala mask. Results with total intracranial volume (TIV), age, gender, depression, and anxiety as covariates.....	172
Table B.3: Whole-brain voxel-based morphometric results with total intracranial volume (TIV), age, and sex, as covariates of no interest.	175

Table B.4: Exact values of mean bootstrap weights and 5th to 95th percentiles for the identified statistically significant PLSC component (LC1, $P = 0.026$). 178

Table B.5: Exact values of mean bootstrap weights and 5th to 95th percentiles for the identified statistically significant PLSC component (LC1, $P = 0.021$). 180

Table B.6: Whole brain analysis in females only. Results with total intracranial volume (TIV), age, depression, and anxiety as covariates. Results did not survive FWE/FDR correction. 187

Table C.1: Exact values of mean bootstrap weights and 5th to 95th percentiles for the identified statistically significant PLSC component (LC1, $P = 0.034$). 198

Table C.2: Exact values of mean bootstrap weights and 5th to 95th percentiles for the identified statistically significant PLSC component (LC1, $P = 0.013$). 201

List of Figures

Figure 1.1: Schematic overview of calculation of functional connectivity. 3D functional brain volumes are acquired across a specific measurement period t and parcellated according to predefined ROIs or network atlases. Region/network-averaged BOLD signal is extracted and temporal cross-correlations (i.e., functional connectivity) is calculated. Whole-brain functional connectivity can be represented using a correlation matrix (functional connectivity matrix). 16

Figure 1.2: Schematic representation of the functional connectivity network. (A) Pearson's correlation coefficient can be calculated between two individual graphs as a measure of functional connectivity. (B) The functional brain network can be represented as a graph consisting of a set of vertices (orange circles) and edges (orange lines). Highly connected nodes are referred to as hubs (green circle). 17

Figure 1.3: Schematic representation of co-activation pattern (CAP) analysis. CAPs are derived by selecting those volumes that highly (de-) coactivate with the selected seed(s). The selected seeds are further grouped into different brain states using a temporal clustering approach. Adapted from (Sokolov et al., 2019))..... 18

Figure 1.4: Workflow voxel-based morphometry. The T1-weighted anatomical image is first segmented, then normalized to a standard (template) space, and smoothed using a Gaussian kernel. Statistical inference is made upon voxel-wise comparison of grey matter using a general linear model (GLM). 21

Figure 1.5: Schematic representation of HPA Axis. Corticotropin-releasing factor (CRF) is released in the paraventricular nucleus of the hypothalamus, resulting in the secretion of adrenocorticotrophic hormone (ACTH) in the pituitary gland, subsequently triggering cortisol release from the adrenal glands. 22

Figure 1.6: Graphical illustration of the circadian rhythm of cortisol. The initial peak in the morning, 30 to 45 minutes upon awakening represents the cortisol awakening response. During the afternoon, the cortisol levels are low. 24

Figure 2.1: Flow chart of the three cross-validation approaches. Flow chart including (A) intra-centre cross-validation, (B) pooled cross-validation, and (C) inter-centre cross-validation. Throughout the training, a leave-one-out cross-validation (LOOCV) approach was applied. 35

Figure 2.2: Classification results of the pooled cross-validation. (A) Overview over the 30 most discriminative features to distinguish FND from HC representing the weights assigned by the classifier (Median LOOCV importance). LOOCV refers to leave-one-out cross-validation. (B) Confusion matrix for the pooled cross-validation. (C) The receiver operating characteristics (ROC) curve, and area-under-the-curve (AUC) for the pooled cross-validation..... 39

Figure 2.3: Regions yielding the most discriminative connections of the pooled classification based on the AAL atlas. Size of the nodes correspond to nodal degree, respectively occurrence within the most discriminative connections. Colour of the nodes corresponds to different lobes of the AAL. Thickness of edges correspond to SVM weights. Thicker edges therefore indicate higher SVM weights, respectively higher discrimination power. The mean functional connectivity values corresponding to this figure can be found in Appendix A, Supplementary Material for Chapter 2, Table A.2. The figures corresponding to each single centre can be found in Appendix A, Supplementary Material for Chapter 2, Figure A.6. 41

Figure 3.1: Traumatic Life Events. (A) For visualization purposes, means and confidence intervals of overall number of experienced traumata (ranging from 0 to 29). (B) Means and confidence intervals of six trauma severity scores (determined by subjective impact and age of trauma, ranging from 0 to 13 for emotional neglect, emotional abuse, physical abuse, sexual harassment, and sexual abuse or from 0 to 24 for bodily threat). (C) Means and confidence intervals of developmental composite scores (across trauma subscores). (D) Means and confidence intervals of duration of trauma. Significance codes: P*** < 0.001, P ** < 0.01, P * < 0.05. Results are FDR-corrected. 62

Figure 3.2: Cortisol Profile of FND patients and healthy. Mean and confidence intervals of daytime cortisol profile in FND patients and HC. Significance code: P* < 0.05. 63

Figure 3.3: Results of voxel-based morphometry analysis. (A) Differential effect of voxel-wise comparison (HC > FND) with smaller grey-matter volume in FND in the hippocampus, parahippocampal gyri, amygdala, and dorsolateral frontal gyri. (B) Differential effect of mean ROI volume using a hippocampal mask (upper panel) and amygdala mask (lower panel) with smaller grey matter volume in FND. For both analyses, total intracranial volume (TIV), age, sex, depression (BDI), and anxiety (STAI) were added as covariates, thresholded on whole-brain level at $P_{FWE} < 0.05$. Significance codes: P*** < 0.001, P** < 0.01, P* < 0.05. A model corrected only for TIV, age, and sex can be found in the Appendix B, Supplementary Material for Chapter 3, Figure B.3, Table B.3. 64

Figure 3.4: Partial least squares correlation (PLSC) results of the different cortisol measures (CARI, PACC, DBCC) in FND patients and healthy controls. The outcome (A) and cortisol saliences (B) of the significant PLSC component (P = 0.033) are presented. 5th to 95th percentiles of bootstrapping are indicated in the error bars and yellow highlighted bars indicate robustness. The height of the bar corresponds to the salience weight to the multivariate correlation pattern and can be interpreted similarly to correlation coefficients as the data was standardized. The permutation null distribution and the bootstrap mean percentiles are reported

in Appendix B, Supplementary Material for Chapter 3, Figure B.4, Table B.4. Abbreviations: EN = Emotional neglect; EA = Emotional abuse; PA = Physical abuse; SH = Sexual harassment; SA = Sexual abuse; BT = Bodily threat. 66

Figure 3.5: Partial least squares correlation (PLSC) results of the imaging data (hippocampal and amygdalar volumes) in FND patients and healthy controls. The outcome (A) and imaging saliences (B) of the significant PLSC component ($P = 0.021$) are presented. 5th to 95th percentiles of bootstrapping are indicated in the error bars and yellow highlighted bars indicate robustness. The height of the bar corresponds to the salience weight to the multivariate correlation pattern and can be interpreted similarly to correlation coefficients as the data was standardized. The permutation null distribution and the bootstrap mean percentiles are reported in Appendix B, Supplementary Material for Chapter 3, Figure B.5. 67

Figure 3.6: The stress-diathesis model in functional neurological disorders. The aetiology of FND is multifactorial and depends on predisposing, precipitating, and perpetuating risk factors. Long-term exposure to stress can exert neurotoxic effects on regions particularly sensitive to cortisol. Moreover, it can alter the HPA-axis in terms of a maladaptive habituation. Distinct predisposing factors, i.e., ‘trait’ markers might influence the individual resilience to stress and the later development of psychopathology. Abbreviations: CRF = corticotropin-releasing factor, ACTH = Adrenocorticotrophic hormone. 70

Figure 4.1: Resting-state network connectivity in healthy controls (HC) and FND patients. Average within- and between-RSN FC values in A) HC and B) FND patients; C) p-values for the FND patients-HC group comparisons using multiple t-tests corrected for multiple comparison using FDR. RSN labels follow the convention of Yeo. Significance code: * $P < 0.01$; • P surviving FDR-correction ($P < 0.05$). Abbreviations: Cont = Executive control, Default = Default mode DorsAttn = Dorsal attention, Sal/VenAttn = Salienc/Ventral attention, SomMot = somatomotor, TempPar = Temporoparietal, VisCen = Central vision, VisPer = Visual perception. 86

Figure 4.2: Co-activation pattern (CAP) maps based on insular and amygdalar seed activation. For each seed, three CAPs were detected. CAPs were Z-scored and only the 15% largest positive and 15% smallest negative contributions are represented in colour ($Z = \pm 1.04$) with red representing positive contributions and blue negative contributions. Locations are displayed in Montreal Neurological Institute (MNI) standard space coordinates. Abbreviation: Amy = Amygdala, Ins = Insula. 88

Figure 4.3: Partial least squares correlation (PLSC) results of the CAPs temporal metrics in FND patients. The outcome (A) and imaging saliences (B) of the significant PLSC component ($P = 0.034$) are presented. Error bars represent the 5th to 95th percentiles of bootstrapping and yellow highlighted bars show robustness. The height of the bar represents the salience’s weight to the multivariate correlation pattern and can be interpreted analogously

to correlation coefficients as the data were standardized. The permutation null distribution and the bootstrap mean percentiles are reported in Supplementary Fig. 7, Supplementary Table 1. Abbreviations: Amy = Amygdala, BDI = Beck's Depression Inventory, CAP = Co-activation pattern, CAR = Cortisol Awakening Response, Ins = Insula, S-FMDRS = Simplified Version of the Psychogenic Movement Disorder Rating Scale, STAI = State-Trait Anxiety Inventory. 89

Figure 4.4: Visual representation of the insular- and amygdalar co-activation pattern-related networks and related neuroscientific constructs in functional neurological disorders. The insular cortex is involved in the computation of the prediction error (grey dotted arrows), whereas the amygdala provides information on priors (red arrows). Bottom-up integration of somatosensory input is biased by hyperpriors from the salience-limbic networks, leading to a misinterpretation of the prediction error and excessive precision weighting. The precision of the prediction error is encoded as a gain of synaptic strength, mediated by the mesolimbic dopaminergic system (yellow arrows). The limbic-striatal loop reinforces prior beliefs as a consequence of wrongly encoded gain of synaptic strength in the NAc. Abbreviations: Amy = Amygdala, IPL = Inferior Parietal Lobule, NAc = Nucleus accumbens, PFC = Prefrontal Cortex, TPJ = Temporo-parietal Junction..... 94

Figure A.1: Workflow of filtering pipelines. For the intra-centre cross-validation settings both pipelines were applied to the data and different classification performances (based on different filtering pipelines) were examined. For pooled- and inter-centre cross-validation, only pipeline 1 (bandpass filter) was used in order to maintain a uniform pre-processing pipeline across all centres..... 151

Figure A.2: Mean Framewise displacement (FD) per centre. FD measures showed a significant main effect of *centre* ($F(3,164) = 5.5, P = 0.001$). Post-hoc multiple comparison of means showed that the difference between centre I and centre III ($P < 0.0001$) and centre IV ($P = 0.0006$), as well as between centre II and centre III ($P = 0.0002$) and IV ($P = 0.008$) were statistically significant. Significance code *** $P \leq 0.001$, ** $P \leq 0.01$, * $P \leq 0.05$ 152

Figure A.3: Results across centres and settings. (A) Accuracy, (B) Sensitivity, and (C) Specificity with 95% confidence interval (95% - CI) of the different classification settings.153

Figure A.4: Area-under-the-curve (AUC) with 95% confidence interval (95% - CI) for the individual classification obtained with each setting. (A) Intra-centre cross-validation classification, and (B) inter-centre cross-validation classification..... 155

Figure A.5: Functional connectivity of regions yielding the most discriminative connections of the pooled classification based on the AAL atlas. Size of the nodes correspond to nodal degree, respectively occurrence within the most discriminative connections. Colour of the nodes corresponds to different lobes of the AAL. Colour of the edges correspond to functional connectivity between the regions, i.e., red displaying hyperconnected and blue hypoconnected in patients compared to controls..... 157

Figure A.6: Regions yielding the most discriminative connections for each centre based on the AAL atlas. Size of the nodes correspond to nodal degree, respectively occurrence within the 200 most discriminative connections. Colour of the nodes corresponds to different lobes of the AAL. Thickness of edges correspond to SVM weights. Thicker edges therefore indicate higher SVM weights, respectively higher discrimination power. **A)** Centre I, **B)** Centre II, **C)** Centre III, and **D)** Centre IV. 159

Figure A.7: Learning Curve of the different centres during the adaptation of the inter-centre cross-validation setting. In this setting one centre was used as test set, whereas the other three centres were used as training set. This setting can be strongly affected by sources of uncontrolled variances across scanners and datasets (Abraham et al., 2017; Noble et al., 2017). Therefore, we specifically tested for the effect of transferring subjects from the training set into the test set. Doing so, the test set won't be fully naïve to uncontrolled variance such as inter-scanner variability, which might benefit classification performance. In each iteration thus, two subjects (1 HC, 1FND) were transferred from the test set to the training set. An increase in classification performance (across accuracy, sensitivity, and specificity could be observed. After the transfer of 16 – 20 subjects, and consequently with a decrease in number of subjects in the test set, the model started overfitting the results. 163

Figure B.1: Graphical Illustration of the different AUC measures. (A) Post-Awakening Cortisol Concentration (PACC), (B) Diurnal Baseline Cortisol Concentration (DBCC), and (C) CARi as a measure of the cortisol awakening response..... 170

Figure B.2: Results of whole-brain analysis. Differential effect of voxel-wise comparison (HC > FND) with smaller grey-matter volume in FND in the hippocampus, parahippocampal gyri, amygdala, and dorsolateral frontal gyri. Total intracranial volume (TIV), age, sex, depression (BDI), and anxiety (STAI) were added as covariates of no interest, thresholded on whole-brain level at $P_{FWE} < 0.05$ **Error! Bookmark not defined.**

Figure B.3: The permutation null distribution. The histogram of the null distribution of the singular values is presented among with the observed (red line) singular value of the significant latent component (permutation testing, $P = 0.026$). Y-axis represents frequency and x-axis the singular values obtained by the permutation testing. **Error! Bookmark not defined.**

Figure B.4: The permutation null distribution. The histogram of the null distribution of the singular values is presented among with the observed (red line) singular value of the significant latent component (permutation testing, $P = 0.021$). Y-axis represents frequency and x-axis the singular values obtained by the permutation testing. 180

Figure C.1: Stability measure (1 – PAC). To assess whether a certain cluster number is good, two given data points should consistently be clustered together or in different clusters across folds. The cumulative distribution of consensus values across all pairs of data points can be

computed which gives a quantification of the goodness of fit. We refer to this distribution as Pkc with $c \in 0,1$. From this, the proportion of ambiguously clustered pairs (PAC) can be computed (Şenbabaoğlu et al., 2014) as $PACk = C = CT1 - CTPkc$ with c_T being a threshold consensus value above which an assignment is judged as not sufficiently homogeneous across folds, and k the cluster number. A lower PAC thus represents a robust cluster. The stability measure is then represented as $1 - PAC$, therefore greater values representing more robust clusters..... 118

Figure C.2: Consensus matrices. The consensus matrices $C_{ki,j}$ for a given number of clusters k and two data points i and j are calculated by averaging over all folds where both data points jointly entered the computations. 192

Figure C.3: Spatial pattern of the second most stable cluster (K = 4) of co-activation patterns (CAPs) based on insular seed activation. Four CAPs were detected. CAPs were Z-scored and only the 15% largest positive and 15% smallest negative contributions are represented in colour ($Z = \pm 1.04$) with red representing positive contributions and blue negative contributions. Locations are displayed in Montreal Neurological Institute (MNI) standard space coordinates. Abbreviations: Ins = Insula..... 193

Figure C.4: Stability measure (1 – PAC). To assess whether a certain cluster number is good, two given data points should consistently be clustered together or in different clusters across folds. The cumulative distribution of consensus values across all pairs of data points can be computed which gives a quantification of the goodness of fit. We refer to this distribution as Pkc with $c \in 0,1$. From this, the proportion of ambiguously clustered pairs (PAC) can be computed (Şenbabaoğlu et al., 2014) as $PACk = C = CT1 - CTPkc$ with c_T being a threshold consensus value above which an assignment is judged as not sufficiently homogeneous across folds, and k the cluster number. A lower PAC thus represents a robust cluster. The stability measure is then represented as $1 - PAC$, therefore greater values representing more robust clusters..... 194

Figure C.5: Consensus matrices. The consensus matrices $C_{ki,j}$ for a given number of clusters k and two data points i and j can then be extracted by averaging over all folds where both data points jointly entered the computations 195

Figure C.6: Spatial pattern of the second most stable cluster (K = 5) of co-activation patterns (CAPs) based on amygdalar seed activation. Five CAPs were detected. CAPs were Z-scored and only the 15% largest positive and 15% smallest negative contributions are represented in colour ($Z = \pm 1.04$) with red representing positive contributions and blue negative contributions. Locations are displayed in Montreal Neurological Institute (MNI) standard space coordinates. Abbreviations: Amy = Amygdala..... 196

Figure C.7: The permutation null distribution. The histogram of the null distribution of the singular values is presented among with the observed (red line) singular value of the significant latent component (permutation testing, $P = 0.034$). Y-axis represents frequency and x-axis the singular values obtained by the permutation testing. 197

Figure C.8: Partial least squares correlation (PLSC) results of the CAPs in HC. The outcome (A) and imaging saliences (B) of the significant PLSC component ($P = 0.013$) are presented. Error bars represent 5th to 95th percentiles of bootstrapping and yellow highlighted bars show robustness. The height of the bar represents the salience’s weight to the multivariate correlation pattern and can be interpreted analogously to correlation coefficients as the data were standardized. Abbreviations: Amy = Amygdala, BDI = Beck’s Depression Inventory, CAP = Co-activation pattern, CAR = Cortisol Awakening Response, Ins = Insula, STAI = State-Trait Anxiety Inventory..... 200

Figure C.9: The permutation null distribution. The histogram of the null distribution of the singular values is presented among with the observed (red line) singular value of the significant latent component (permutation testing, $P = 0.013$). Y-axis represents frequency and x-axis the singular values obtained by the permutation testing. 201

References

- Abdulkadir, A., Mortamet, B., Vemuri, P., Jack, C.R., Krueger, G., Klöppel, S., 2011. Effects of hardware heterogeneity on the performance of SVM Alzheimer's disease classifier. *Neuroimage* 58, 785–792. <https://doi.org/10.1016/j.neuroimage.2011.06.029>
- Abraham, A., Milham, M.P., Di Martino, A., Craddock, R.C., Samaras, D., Thirion, B., Varoquaux, G., 2017. Deriving reproducible biomarkers from multi-site resting-state data: An Autism-based example. *Neuroimage* 147, 736–745. <https://doi.org/10.1016/j.neuroimage.2016.10.045>
- Achard, S., Salvador, R., Whitcher, B., Suckling, J., Bullmore, E., 2006. A resilient, low-frequency, small-world human brain functional network with highly connected association cortical hubs. *J. Neurosci.* 26, 63–72. <https://doi.org/10.1523/JNEUROSCI.3874-05.2006>
- Adam, E.K., Kumari, M., 2009. Assessing salivary cortisol in large-scale, epidemiological research. *Psychoneuroendocrinology* 34, 1423–1436. <https://doi.org/10.1016/j.psyneuen.2009.06.011>
- Adam, E.K., Quinn, M.E., Tavernier, R., McQuillan, M.T., Dahlke, K.A., Gilbert, K.E., 2017. Diurnal cortisol slopes and mental and physical health outcomes: A systematic review and meta-analysis. *Psychoneuroendocrinology* 83, 25–41. <https://doi.org/10.1016/j.psyneuen.2017.05.018>
- Aléman-Gomez, Y.M.-G., Melie-Garcia, L., Valdés-Hernandez, P., 2006. IBASPM: toolbox for automatic parcellation of brain structures. *Annu. Meet. Organ. Hum. Brain Mapping. Florence, Italy* 27.
- Allen, E.A., Erhardt, E.B., Damaraju, E., Gruner, W., Segall, J.M., Silva, R.F., Havlicek, M., Rachakonda, S., Fries, J., Kalyanam, R., Michael, A.M., Caprihan, A., Turner, J.A., Eichele, T., Adelsheim, S., Bryan, A.D., Bustillo, J., Clark, V.P., Ewing, S.W.F., Filbey, F., Ford, C.C., Hutchison, K., Jung, R.E., Kiehl, K.A., Kodituwakku, P., Komesu, Y.M., Mayer, A.R., Pearlson, G.D., Phillips, J.P., Sadek, J.R., Stevens, M., Teuscher, U., Thoma, R.J., Calhoun, V.D., 2011. A baseline for the multivariate comparison of resting-state networks. *Front. Syst. Neurosci.* 5, 1–23. <https://doi.org/10.3389/fnsys.2011.00002>
- Alper, K., Devinsky, O., Perrine, K., Vazquez, B., Luciano, D., 1993. Nonepileptic seizures and childhood sexual and physical abuse. *Neurology* 43, 1950–1953. <https://doi.org/10.1212/wnl.43.10.1950>
- American Psychiatric Association, 2013. *Diagnostic and Statistical Manual of Mental Disorders*. American Psychiatric Association. <https://doi.org/10.1176/appi.books.9780890425596>
- Ancelin, M.-L., Carrière, I., Artero, S., Maller, J., Meslin, C., Ritchie, K., Ryan, J., Chaudieu, I., 2019. Lifetime major depression and grey-matter volume. *J. Psychiatry Neurosci.* 44, 45–53. <https://doi.org/10.1503/jpn.180026>
- Apazoglou, K., Adouan, W., Aubry, J.M., Dayer, A., Aybek, S., 2018. Increased methylation of the oxytocin receptor gene in motor functional neurological disorder: a preliminary study. *J. Neurol. Neurosurg. Psychiatry* 89, 552–554. <https://doi.org/10.1136/jnnp-2017-316469>
- Apazoglou, K., Mazzola, V., Węgrzyk, J., Frasca Polara, G., Aybek, S., 2017. Biological and perceived stress in motor functional neurological disorders. *Psychoneuroendocrinology* 85, 142–150. <https://doi.org/10.1016/j.psyneuen.2017.08.023>
- Ashburner, J., 2007. A fast diffeomorphic image registration algorithm. *Neuroimage* 38, 95–113. <https://doi.org/10.1016/j.neuroimage.2007.07.007>
- Ashburner, J., Friston, K.J., 2005. Unified segmentation. *Neuroimage* 26, 839–851. <https://doi.org/10.1016/j.neuroimage.2005.02.018>
- Ashburner, J., Friston, K.J., 2000. Voxel-based morphometry - The methods. *Neuroimage* 11, 805–821. <https://doi.org/10.1006/nimg.2000.0582>
- Aybek, S., 2019. Corticolimbic fast-tracking in functional neurological disorders: Towards understanding of the “dynamic lesion” of Jean-Martin Charcot. *J. Neurol. Neurosurg. Psychiatry* 90, 845. <https://doi.org/10.1136/jnnp-2019-320597>
- Aybek, S., Nicholson, T.R., O'Daly, O., Zelaya, F., Kanaan, R.A., David, A.S., 2015. Emotion-motion interactions in conversion disorder: An fMRI study. *PLoS One* 10, 1–11. <https://doi.org/10.1371/journal.pone.0123273>
- Aybek, S., Nicholson, T.R., Zelaya, F., O'Daly, O.G., Craig, T.J., David, A.S., Kanaan, R.A., O'Daly, O.G., Craig, T.J., David, A.S., Kanaan, R.A., 2014a. Neural correlates of recall of life events in conversion disorder. *JAMA Psychiatry* 71, 52–60. <https://doi.org/10.1001/jamapsychiatry.2013.2842>
- Aybek, S., Nicholson, T.R.J., Draganski, B., Daly, E., Murphy, D.G., David, A.S., Kanaan, R.A., 2014b. Grey matter changes in motor conversion disorder. *J. Neurol. Neurosurg. Psychiatry* 85, 236–238. <https://doi.org/10.1136/jnnp-2012-304158>
- Aybek, S., Perez, D.L., 2022. Diagnosis and management of functional neurological disorder. *BMJ* o64. <https://doi.org/10.1136/bmj.o64>
- Aybek, S., Vuilleumier, P., 2016. Imaging studies of functional neurologic disorders, in: *Handbook of Clinical Neurology*. pp. 73–84. <https://doi.org/10.1016/B978-0-12-801772-2.00007-2>
- Baek, K., Doñamayor, N., Morris, L.S., Strelchuk, D., Mitchell, S., Mikheenko, Y., Yeoh, S.Y., Phillips, W., Zandi, M., Jenaway, A., Walsh, C., Voon, V., 2017. Impaired awareness of motor intention in functional neurological disorder: Implications for voluntary and functional movement. *Psychol. Med.* 47, 1624–1636. <https://doi.org/10.1017/S0033291717000071>

- Baker, M.G., Kale, R., Menken, M., 2002. The wall between neurology and psychiatry. *Br. Med. J.* 324, 1468–1469. <https://doi.org/10.1136/bmj.324.7352.1468>
- Bakvis, P., Roelofs, K., Kuyk, J., Edelbroek, P.M., Swinkels, W.A.M., Spinhoven, P., 2009a. Trauma, stress, and preconscious threat processing in patients with psychogenic nonepileptic seizures. *Epilepsia* 50, 1001–1011. <https://doi.org/10.1111/j.1528-1167.2008.01862.x>
- Bakvis, P., Spinhoven, P., Giltay, E.J., Kuyk, J., Edelbroek, P.M., Zitman, F.G., Roelofs, K., 2010. Basal hypercortisolism and trauma in patients with psychogenic nonepileptic seizures. *Epilepsia* 51, 752–759. <https://doi.org/10.1111/j.1528-1167.2009.02394.x>
- Bakvis, P., Spinhoven, P., Roelofs, K., 2009b. Basal cortisol is positively correlated to threat vigilance in patients with psychogenic nonepileptic seizures. *Epilepsy Behav.* 16, 558–560. <https://doi.org/10.1016/j.yebeh.2009.09.006>
- Balachandran, N., Goodman, A.M., Allendorfer, J.B., Martin, A.N., Tocco, K., Vogel, V., LaFrance, W.C., Szaflarski, J.P., 2021. Relationship between neural responses to stress and mental health symptoms in psychogenic nonepileptic seizures after traumatic brain injury. *Epilepsia* 62, 107–119. <https://doi.org/10.1111/epi.16758>
- Barrett, L.F., Simmons, W.K., 2015. Interoceptive predictions in the brain. *Nat. Rev. Neurosci.* 16, 419–429. <https://doi.org/10.1038/nrn3950>
- Barsky, A.J., 2002. Nonspecific Medication Side Effects and the Nocebo Phenomenon. *JAMA* 287, 622. <https://doi.org/10.1001/jama.287.5.622>
- Barugh, A.J., Gray, P., Shenkin, S.D., MacLulich, A.M.J., Mead, G.E., 2014. Cortisol levels and the severity and outcomes of acute stroke: a systematic review. *J. Neurol.* 261, 533–545. <https://doi.org/10.1007/s00415-013-7231-5>
- Baslet, G., Ehler, A., Oser, M., Dworetzky, B.A., 2020. Mindfulness-based therapy for psychogenic nonepileptic seizures. *Epilepsy Behav.* 103, 106534. <https://doi.org/10.1016/j.yebeh.2019.106534>
- Beck, A.T., 1961. An Inventory for Measuring Depression. *Arch. Gen. Psychiatry* 4, 561. <https://doi.org/10.1001/archpsyc.1961.01710120031004>
- Beck, A.T., Epstein, N., Brown, G., Steer, R.A., 1988. An inventory for measuring clinical anxiety: Psychometric properties. *J. Consult. Clin. Psychol.* 56, 893–897. <https://doi.org/10.1037/0022-006X.56.6.893>
- Beissner, F., Brünner, F., Fink, M., Meissner, K., Kaptchuk, T.J., Napadow, V., 2015. Placebo-Induced Somatic Sensations: A Multi-Modal Study of Three Different Placebo Interventions. *PLoS One* 10, e0124808. <https://doi.org/10.1371/journal.pone.0124808>
- Benedetti, F., 2013. Placebo and the New Physiology of the Doctor-Patient Relationship. *Physiol. Rev.* 93, 1207–1246. <https://doi.org/10.1152/physrev.00043.2012>
- Bennett, K., Diamond, C., Hoeritzauer, I., Gardiner, P., McWhirter, L., Carson, A., Stone, J., 2021. A practical review of functional neurological disorder (FND) for the general physician. *Clin. Med. J. R. Coll. Physicians London* 21, 28–36. <https://doi.org/10.7861/CLINMED.2020-0987>
- Bernstein, D.P. and F., Laura, Handelsman, L., Foote, J., 1998. Childhood trauma questionnaire. *Assess. Fam. violence A Handb. Res. Pract.* <https://doi.org/https://doi.org/10.1037/t02080-000>
- Betts, T., Boden, S., 1992. Diagnosis, management and prognosis of a group of 128 patients with non-epileptic attack disorder. Part II. Previous childhood sexual abuse in the aetiology of these disorders. *Seizure Eur. J. Epilepsy* 1, 27–32. [https://doi.org/10.1016/1059-1311\(92\)90051-2](https://doi.org/10.1016/1059-1311(92)90051-2)
- Biswal, B., Zerrin Yetkin, F., Haughton, V.M., Hyde, J.S., 1995. Functional connectivity in the motor cortex of resting human brain using echo-planar mri. *Magn. Reson. Med.* 34, 537–541. <https://doi.org/10.1002/mrm.1910340409>
- Biswal, B.B., Kylen, J. Van, Hyde, J.S., 1997. Simultaneous assessment of flow and BOLD signals in resting-state functional connectivity maps. *NMR Biomed.* 10, 165–170. [https://doi.org/10.1002/\(SICI\)1099-1492\(199706/08\)10:4/5<165::AID-NBM454>3.0.CO;2-7](https://doi.org/10.1002/(SICI)1099-1492(199706/08)10:4/5<165::AID-NBM454>3.0.CO;2-7)
- Blakemore, R.L., Sinanaj, I., Galli, S., Aybek, S., Vuilleumier, P., 2016. Aversive stimuli exacerbate defensive motor behaviour in motor conversion disorder. *Neuropsychologia* 93, 229–241. <https://doi.org/10.1016/j.neuropsychologia.2016.11.005>
- Bolton, T.A.W., Tuleasca, C., Wotruba, D., Rey, G., Dhanis, H., Gauthier, B., Delavari, F., Morgenroth, E., Gaviria, J., Blondiaux, E., Smigielski, L., Van De Ville, D., 2020. TbCAPs: A toolbox for co-activation pattern analysis. *Neuroimage* 211, 116621. <https://doi.org/10.1016/j.neuroimage.2020.116621>
- Brass, M., Derrfuss, J., von Cramon, D.Y., 2005. The inhibition of imitative and overlearned responses: a functional double dissociation. *Neuropsychologia* 43, 89–98. <https://doi.org/10.1016/j.neuropsychologia.2004.06.018>
- Brembs, B., 2021. The brain as a dynamically active organ. *Biochem. Biophys. Res. Commun.* 564, 55–69. <https://doi.org/10.1016/j.bbrc.2020.12.011>
- Brewer, J.A., Garrison, K.A., Whitfield-Gabrieli, S., 2013. What about the “Self” is Processed in the Posterior Cingulate Cortex? *Front. Hum. Neurosci.* 7. <https://doi.org/10.3389/fnhum.2013.00647>
- Bright, M.G., Murphy, K., 2015. Is fMRI “noise” really noise? Resting state nuisance regressors remove variance with network structure. *Neuroimage* 114, 158–169. <https://doi.org/10.1016/j.neuroimage.2015.03.070>
- Brown, G., Harris, T., 1989. Life events and illness. New York Guilford Press.
- Brown, L.B., Nicholson, T.R., Aybek, S., Kanaan, R.A., David, A.S., 2014. Neuropsychological function and memory suppression in conversion disorder. *J. Neuropsychol.* 8, 171–185. <https://doi.org/10.1111/jnp.12017>
- Brown, R., 2006. What Is a Brain State? *Philos. Psychol.* 19, 729–742. <https://doi.org/10.1080/09515080600923271>
- Brown, R.J., 2016. Dissociation and functional neurologic disorders, in: *Handbook of Clinical Neurology.* pp. 85–94. <https://doi.org/10.1016/B978-0-12-801772-2.00008-4>

- Carson, A., Lehn, A., 2016. Epidemiology, in: *Handbook of Clinical Neurology*. pp. 47–60. <https://doi.org/10.1016/B978-0-12-801772-2.00005-9>
- Castrillon, J.G., Ahmadi, A., Navab, N., Richiardi, J., 2015. Learning with multi-site fMRI graph data. *Conf. Rec. - Asilomar Conf. Signals, Syst. Comput.* 2015-April, 608–612. <https://doi.org/10.1109/ACSSC.2014.7094518>
- Chambon, V., Moore, J.W., Haggard, P., 2015. TMS stimulation over the inferior parietal cortex disrupts prospective sense of agency. *Brain Struct. Funct.* 220, 3627–3639. <https://doi.org/10.1007/s00429-014-0878-6>
- Chand, T., Li, M., Jamalabadi, H., Wagner, G., Lord, A., Alizadeh, S., Danyeli, L. V., Herrmann, L., Walter, M., Sen, Z.D., 2020. Heart Rate Variability as an Index of Differential Brain Dynamics at Rest and After Acute Stress Induction. *Front. Neurosci.* 14. <https://doi.org/10.3389/fnins.2020.00645>
- Chang, C.-C. and Lin, C.-J., 2011. LIBSVM: A Library for Support Vector Machines. *ACM Trans. Intell. Syst. Technol.* 2, 1–27.
- Chang, C., Glover, G.H., 2010. Time–frequency dynamics of resting-state brain connectivity measured with fMRI. *Neuroimage* 50, 81–98. <https://doi.org/10.1016/j.neuroimage.2009.12.011>
- Chen, A.A., Srinivasan, D., Pomponio, R., Fan, Y., Nasrallah, I.M., Resnick, S.M., Beason-Held, L.L., Davatzikos, C., Satterthwaite, T.D., Bassett, D.S., Shinohara, R.T., Shou, H., 2022. Harmonizing Functional Connectivity Reduces Scanner Effects in Community Detection. *Neuroimage* 256, 119198. <https://doi.org/10.1016/j.neuroimage.2022.119198>
- Chen, H.H., Duan, X., Liu, F., Lu, F., Ma, X., Zhang, Y., Uddin, L.Q., Chen, H.H., 2016. Multivariate classification of autism spectrum disorder using frequency-specific resting-state functional connectivity—A multi-center study. *Prog. Neuro-Psychopharmacology Biol. Psychiatry* 64, 1–9. <https://doi.org/10.1016/j.pnpbp.2015.06.014>
- Cho, Y.T., Fromm, S., Guyer, A.E., Detloff, A., Pine, D.S., Fudge, J.L., Ernst, M., 2013. Nucleus accumbens, thalamus and insula connectivity during incentive anticipation in typical adults and adolescents. *Neuroimage* 66, 508–521. <https://doi.org/10.1016/j.neuroimage.2012.10.013>
- Chong, J.S.X., Ng, G.J.P., Lee, S.C., Zhou, J., 2017. Salience network connectivity in the insula is associated with individual differences in interoceptive accuracy. *Brain Struct. Funct.* 222, 1635–1644. <https://doi.org/10.1007/s00429-016-1297-7>
- Chung, J., Mukerji, S., Kozłowska, K., 2022. Cortisol and α -amylase awakening response in children and adolescents with functional neurological (conversion) disorder. *Aust. New Zeal. J. Psychiatry* 00, 000486742210825. <https://doi.org/10.1177/00048674221082520>
- Clark, J.E., Watson, S., Friston, K.J., 2018. What is mood? A computational perspective. *Psychol. Med.* 48, 2277–2284. <https://doi.org/10.1017/S0033291718000430>
- Clow, A., Hucklebridge, F., Thorn, L., 2010. The Cortisol Awakening Response in Context, in: *Review of Neurobiology* (Vol. 93.) Academic Press Inc. pp. 153–175. [https://doi.org/10.1016/S0074-7742\(10\)93007-9](https://doi.org/10.1016/S0074-7742(10)93007-9)
- Clow, A., Thorn, L., Evans, P., Hucklebridge, F., 2004. The Awakening Cortisol Response: Methodological Issues and Significance. *Stress* 7, 29–37. <https://doi.org/10.1080/10253890410001667205>
- Cojan, Y., Waber, L., Carruzzo, A., Vuilleumier, P., 2009. Motor inhibition in hysterical conversion paralysis. *Neuroimage* 47, 1026–1037. <https://doi.org/10.1016/j.neuroimage.2009.05.023>
- Colombari, M., Di Vico, I.A., Turrina, S., De Leo, D., Tinazzi, M., 2021. Medico-legal aspects of functional neurological disorders: time for an interdisciplinary dialogue. *Neurol. Sci.* 42, 3053–3055. <https://doi.org/10.1007/s10072-021-05162-w>
- Conejero, I., Collombier, L., Lopez-Castroman, J., Mura, T., Alonso, S., Olié, E., Boudousq, V., Boulet, F., Arquizan, C., Boulet, C., Wacongne, A., Heitz, C., Castelli, C., Mouchabac, S., Courtet, P., Abbar, M., Thouvenot, E., 2022. Association between brain metabolism and clinical course of motor functional neurological disorders. *Brain* 145, 3264–3273. <https://doi.org/10.1093/brain/awac146>
- Conejero, I., Thouvenot, E., Abbar, M., Mouchabac, S., Courtet, P., Olié, E., 2018. Neuroanatomy of conversion disorder: Towards a network approach. *Rev. Neurosci.* 29, 355–368. <https://doi.org/10.1515/revneuro-2017-0041>
- Conrad, C.D., 2008. Chronic Stress-induced Hippocampal Vulnerability: The Glucocorticoid Vulnerability Hypothesis. *Rev. Neurosci.* 19, 395–411. <https://doi.org/10.1515/revneuro.2008.19.6.395>
- Cortes, C., Vapnik, V., 1995. Support-vector networks. *Mach. Learn.* 20, 273–297. <https://doi.org/10.1007/BF00994018>
- Cretton, A., Brown, R.J., Lafrance, W.C., Aybek, S., 2020. What does neuroscience tell us about the conversion model of functional neurological disorders? *J. Neuropsychiatry Clin. Neurosci.* 32, 24–32. <https://doi.org/10.1176/appi.neuropsych.19040089>
- Crimlisk, H.L., Bhatia, K.P., Cope, H., David, A.S., Marsden, D., Ron, M.A., 2000. Patterns of referral in patients with medically unexplained motor symptoms. *J. Psychosom. Res.* 49, 217–219. [https://doi.org/10.1016/S0022-3999\(00\)00167-7](https://doi.org/10.1016/S0022-3999(00)00167-7)
- Dansereau, C., Benhajali, Y., Risterucci, C., Pich, E.M., Orban, P., Arnold, D., Bellec, P., 2017. Statistical power and prediction accuracy in multisite resting-state fMRI connectivity. *Neuroimage* 149, 220–232. <https://doi.org/10.1016/j.neuroimage.2017.01.072>
- Daum, C., Gheorghita, F., Spatola, M., Stojanova, V., Medlin, F., Vingerhoets, F., Berney, A., Gholam-Rezaee, M., Maccaferri, G.E., Hubschmid, M., Aybek, S., 2015. Interobserver agreement and validity of bedside ‘positive signs’ for functional weakness, sensory and gait disorders in conversion disorder: a pilot study. *J. Neurol. Neurosurg. Psychiatry* 86, 425–430. <https://doi.org/10.1136/jnnp-2013-307381>
- Davey, C.G., Pujol, J., Harrison, B.J., 2016. Mapping the self in the brain’s default mode network. *Neuroimage* 132, 390–397. <https://doi.org/10.1016/j.neuroimage.2016.02.022>

- de Lange, F.P., Roelofs, K., Toni, I., 2008. Motor imagery: A window into the mechanisms and alterations of the motor system. *Cortex* 44, 494–506. <https://doi.org/10.1016/j.cortex.2007.09.002>
- de Lange, F.P., Roelofs, K., Toni, I., 2007. Increased self-monitoring during imagined movements in conversion paralysis. *Neuropsychologia* 45, 2051–2058. <https://doi.org/10.1016/j.neuropsychologia.2007.02.002>
- Demartini, B., Nisticò, V., Edwards, M.J., Gambini, O., Priori, A., 2021. The pathophysiology of functional movement disorders. *Neurosci. Biobehav. Rev.* 120, 387–400. <https://doi.org/10.1016/j.neubiorev.2020.10.019>
- Dewey, B.E., Zhao, C., Reinhold, J.C., Carass, A., Fitzgerald, K.C., Sotirchos, E.S., Saidha, S., Oh, J., Pham, D.L., Calabresi, P.A., van Zijl, P.C.M., Prince, J.L., 2019. DeepHarmony: A deep learning approach to contrast harmonization across scanner changes. *Magn. Reson. Imaging* 64, 160–170. <https://doi.org/10.1016/j.mri.2019.05.041>
- Di Martino, A., Yan, C.-G.G., Li, Q., Denio, E., Castellanos, F.X., Alaerts, K., Anderson, J.S., Assaf, M., Bookheimer, S.Y., Dapretto, M., Deen, B., Delmonte, S., Dinstein, I., Ertl-Wagner, B., Fair, D.A., Gallagher, L., Kennedy, D.P., Keown, C.L., Keysers, C., Lainhart, J.E., Lord, C., Luna, B., Menon, V., Minshew, N.J., Monk, C.S., Mueller, S., Müller, R.-A.A., Nebel, M.B., Nigg, J.T., O’Hearn, K., Pelphrey, K.A., Peltier, S.J., Rudie, J.D., Sunaert, S., Thioux, M., Tyszka, J.M., Uddin, L.Q., Verhoeven, J.S., Wenderoth, N., Wiggins, J.L., Mostofsky, S.H., Milham, M.P., 2014. The autism brain imaging data exchange: towards a large-scale evaluation of the intrinsic brain architecture in autism. *Mol. Psychiatry* 19, 659–667. <https://doi.org/10.1038/mp.2013.78>
- Diez, I., Larson, A.G., Nakhate, V., Dunn, E.C., Fricchione, G.L., Nicholson, T.R., Sepulcre, J., Perez, D.L., 2020. Early-life trauma endophenotypes and brain circuit–gene expression relationships in functional neurological (conversion) disorder. *Mol. Psychiatry*. <https://doi.org/10.1038/s41380-020-0665-0>
- Diez, I., Ortiz-Terán, L., Williams, B., Jalilianhasanpour, R., Ospina, J.P., Dickerson, B.C., Keshavan, M.S., Lafrance, W.C., Sepulcre, J., Perez, D.L., 2019. Corticolimbic fast-tracking: Enhanced multimodal integration in functional neurological disorder. *J. Neurol. Neurosurg. Psychiatry* 90, 929–938. <https://doi.org/10.1136/jnnp-2018-319657>
- Diez, I., Williams, B., Kubicki, M.R., Makris, N., Perez, D.L., 2021. Reduced limbic microstructural integrity in functional neurological disorder. *Psychol. Med.* 51, 485–493. <https://doi.org/10.1017/S0033291719003386>
- Ding, J.R., An, D., Liao, W., Li, J., Wu, G.R., Xu, Q., Long, Z., Gong, Q., Zhou, D., Sporns, O., Chen, H., 2013. Altered Functional and Structural Connectivity Networks in Psychogenic Non-Epileptic Seizures. *PLoS One* 8. <https://doi.org/10.1371/journal.pone.0063850>
- Dixon, M.L., Thiruchselvam, R., Todd, R., Christoff, K., 2017. Emotion and the prefrontal cortex: An integrative review. *Psychol. Bull.* 143, 1033–1081. <https://doi.org/10.1037/bul0000096>
- Donnelly-Kehoe, P.A., Pascariello, G.O., García, A.M., Hodges, J.R., Miller, B., Rosen, H., Manes, F., Landin-Romero, R., Matallana, D., Serrano, C., Herrera, E., Reyes, P., Santamaria-Garcia, H., Kumfor, F., Pigué, O., Ibanez, A., Sedeño, L., 2019. Robust automated computational approach for classifying frontotemporal neurodegeneration: Multimodal/multicenter neuroimaging. *Alzheimer’s Dement. Diagnosis, Assess. Dis. Monit.* 11, 588–598. <https://doi.org/10.1016/j.dadm.2019.06.002>
- Dozier, M., Peloso, E., 2006. The Role of Early Stressors in Child Health and Mental Health Outcomes. *Arch. Pediatr. Adolesc. Med.* 160, 1300. <https://doi.org/10.1001/archpedi.160.12.1300>
- Drane, D.L., Fani, N., Hallett, M., Khalsa, S.S., Perez, D.L., Roberts, N.A., 2020. A framework for understanding the pathophysiology of functional neurological disorder. *CNS Spectr.* 1–7. <https://doi.org/10.1017/S1092852920001789>
- Dunn, E.C., Nishimi, K., Powers, A., Bradley, B., 2017. Is developmental timing of trauma exposure associated with depressive and post-traumatic stress disorder symptoms in adulthood? *J. Psychiatr. Res.* 84, 119–127. <https://doi.org/10.1016/j.jpsychires.2016.09.004>
- Dyrba, M., Ewers, M., Wegrzyn, M., Kilimann, I., Plant, C., Oswald, A., Meindl, T., Pievani, M., Bokde, A.L.W., Fellgiebel, A., Filippi, M., Hampel, H., Klöppel, S., Hauenstein, K., Kirste, T., Teipel, S.J., 2013. Robust Automated Detection of Microstructural White Matter Degeneration in Alzheimer’s Disease Using Machine Learning Classification of Multicenter DTI Data. *PLoS One* 8. <https://doi.org/10.1371/journal.pone.0064925>
- Eddy, C.M., 2016. The junction between self and other? Temporo-parietal dysfunction in neuropsychiatry. *Neuropsychologia* 89, 465–477. <https://doi.org/10.1016/j.neuropsychologia.2016.07.030>
- Edwards, M.J., Adams, R.A., Brown, H., Pareés, I., Friston, K.J., 2012. A Bayesian account of “hysteria.” *Brain* 135, 3495–3512. <https://doi.org/10.1093/brain/aws129>
- Edwards, M.J., Moretto, G., Schwingenschuh, P., Katschnig, P., Bhatia, K.P., Haggard, P., 2011. Abnormal sense of intention preceding voluntary movement in patients with psychogenic tremor. *Neuropsychologia* 49, 2791–2793. <https://doi.org/10.1016/j.neuropsychologia.2011.05.021>
- Eickhoff, S.B., Constable, R.T., Yeo, B.T.T., 2018. Topographic organization of the cerebral cortex and brain cartography. *Neuroimage* 170, 332–347. <https://doi.org/10.1016/j.neuroimage.2017.02.018>
- Elder, G.J., Ellis, J.G., Barclay, N.L., Wetherell, M.A., 2016. Assessing the daily stability of the cortisol awakening response in a controlled environment. *BMC Psychol.* 4, 3. <https://doi.org/10.1186/s40359-016-0107-6>
- Erickson, B.J., Korfiatis, P., Akkus, Z., Kline, T.L., 2017. Machine Learning for Medical Imaging. *RadioGraphics* 37, 505–515. <https://doi.org/10.1148/rg.2017160130>
- Espay, A.J., Aybek, S., Carson, A., Edwards, M.J., Goldstein, L.H., Hallett, M., LaFaver, K., LaFrance, W.C., Lang, A.E., Nicholson, T., Nielsen, G., Reuber, M., Voon, V., Stone, J., Morgante, F., 2018a. Current concepts in diagnosis and treatment of functional neurological disorders. *JAMA Neurol.* 75, 1132–1141. <https://doi.org/10.1001/jamaneurol.2018.1264>

- Espay, A.J., Goldenhar, L.M., Voon, V., Schrag, A., Burton, N., Lang, A.E., 2009. Opinions and clinical practices related to diagnosing and managing patients with psychogenic movement disorders: An international survey of movement disorder society members. *Mov. Disord.* 24, 1366–1374. <https://doi.org/10.1002/mds.22618>
- Espay, A.J., Lang, A.E., 2015. Phenotype-Specific Diagnosis of Functional (Psychogenic) Movement Disorders. *Curr. Neurol. Neurosci. Rep.* 15, 32. <https://doi.org/10.1007/s11910-015-0556-y>
- Espay, A.J., Maloney, T., Vannest, J., Norris, M.M., Eliassen, J.C., Neefus, E., Allendorfer, J.B., Chen, R., Szaflarski, J.P., 2018b. Dysfunction in emotion processing underlies functional (psychogenic) dystonia. *Mov. Disord.* 33, 136–145. <https://doi.org/10.1002/mds.27217>
- Espay, A.J., Maloney, T., Vannest, J., Norris, M.M., Eliassen, J.C., Neefus, E., Allendorfer, J.B., Lang, A.E., Szaflarski, J.P., 2018c. Impaired emotion processing in functional (psychogenic) tremor: A functional magnetic resonance imaging study. *NeuroImage Clin.* 17, 179–187. <https://doi.org/10.1016/j.nicl.2017.10.020>
- Espay, A.J., Ries, S., Maloney, T., Vannest, J., Neefus, E., Dwivedi, A.K., Allendorfer, J.B., Wulsin, L.R., LaFrance, W.C., Lang, A.E., Szaflarski, J.P., 2019. Clinical and neural responses to cognitive behavioral therapy for functional tremor. *Neurology* 93, e1787–e1798. <https://doi.org/10.1212/WNL.00000000000008442>
- Faul, L., Knight, L.K., Espay, A.J., Depue, B.E., LaFaver, K., 2020. Neural activity in functional movement disorders after inpatient rehabilitation. *Psychiatry Res. Neuroimaging* 303, 111125. <https://doi.org/10.1016/j.psychres.2020.111125>
- Feinstein, A., 2011. Conversion disorder: advances in our understanding. *Can. Med. Assoc. J.* 183, 915–920. <https://doi.org/10.1503/cmaj.110490>
- Fekedulegn, D.B., Andrew, M.E., Burchfiel, C.M., Violanti, J.M., Hartley, T.A., Charles, L.E., Miller, D.B., 2007. Area Under the Curve and Other Summary Indicators of Repeated Waking Cortisol Measurements. *Psychosom. Med.* 69, 651–659. <https://doi.org/10.1097/PSY.0b013e31814c405c>
- Feldman, H., Friston, K.J., 2010. Attention, Uncertainty, and Free-Energy. *Front. Hum. Neurosci.* 4. <https://doi.org/10.3389/fnhum.2010.00215>
- Fend, M., Williams, L., Carson, A.J., Stone, J., 2020. Grey matter the arc de siècle: Functional neurological disorder during the “forgotten” years of the 20th century. *Brain* 143, 1278–1284. <https://doi.org/10.1093/brain/awaa037>
- Fiorio, M., Braga, M., Marotta, A., Villa-Sánchez, B., Edwards, M.J., Tinazzi, M., Barbiani, D., 2022. Functional neurological disorder and placebo and nocebo effects: shared mechanisms. *Nat. Rev. Neurol.* 18, 624–635. <https://doi.org/10.1038/s41582-022-00711-z>
- Fiorio, M., Recchia, S., Corrà, F., Simonetto, S., Garcia-Larrea, L., Tinazzi, M., 2012. Enhancing non-noxious perception: Behavioural and neurophysiological correlates of a placebo-like manipulation. *Neuroscience* 217, 96–104. <https://doi.org/10.1016/j.neuroscience.2012.04.066>
- Fox, K.C.R., Andrews-Hanna, J.R., Mills, C., Dixon, M.L., Markovic, J., Thompson, E., Christoff, K., 2018. Affective neuroscience of self-generated thought. *Ann. N. Y. Acad. Sci.* 1426, 25–51. <https://doi.org/10.1111/nyas.13740>
- Fox, M.D., Snyder, A.Z., Vincent, J.L., Corbetta, M., Van Essen, D.C., Raichle, M.E., 2005. The human brain is intrinsically organized into dynamic, anticorrelated functional networks. *Proc. Natl. Acad. Sci.* 102, 9673–9678. <https://doi.org/10.1073/pnas.0504136102>
- Friedman, L., Glover, G.H., The FBIRN Consortium, 2006. Reducing interscanner variability of activation in a multicenter fMRI study: Controlling for signal-to-fluctuation-noise-ratio (SFNR) differences. *Neuroimage* 33, 471–481. <https://doi.org/10.1016/j.neuroimage.2006.07.012>
- Friston, K., 2010. The free-energy principle: a unified brain theory? *Nat. Rev. Neurosci.* 11, 127–138. <https://doi.org/10.1038/nrn2787>
- Friston, K.J., Frith, C.D., Liddle, P.F., Frackowiak, R.S.J., 1993. Functional Connectivity: The Principal-Component Analysis of Large (PET) Data Sets. *J. Cereb. Blood Flow Metab.* 13, 5–14. <https://doi.org/10.1038/jcbfm.1993.4>
- Friston, K.J., Holmes, A.P., Worsley, K.J., Poline, J.-P., Frith, C.D., Frackowiak, R.S.J., 1994. Statistical parametric maps in functional imaging: A general linear approach. *Hum. Brain Mapp.* 2, 189–210. <https://doi.org/10.1002/hbm.460020402>
- Galaj, E., Ranaldi, R., 2021. Neurobiology of reward-related learning. *Neurosci. Biobehav. Rev.* 124, 224–234. <https://doi.org/10.1016/j.neubiorev.2021.02.007>
- Galli, S., Béreau, M., Magnin, E., Moulin, T., Aybek, S., 2020. Functional movement disorders. *Rev. Neurol. (Paris)*. 176, 244–251. <https://doi.org/10.1016/j.neurol.2019.08.007>
- Gallichan, D., Marques, J.P., Gruetter, R., 2016. Retrospective correction of involuntary microscopic head movement using highly accelerated fat image navigators (3D FatNavs) at 7T. *Magn. Reson. Med.* 75, 1030–1039. <https://doi.org/10.1002/mrm.25670>
- Gao, S., Calhoun, V.D., Sui, J., 2018. Machine learning in major depression: From classification to treatment outcome prediction. *CNS Neurosci. Ther.* 24, 1037–1052. <https://doi.org/10.1111/cns.13048>
- Gaviria, J., Rey, G., Bolton, T., Ville, D. Van De, Vuilleumier, P., 2021. Dynamic functional brain networks underlying the temporal inertia of negative emotions. *Neuroimage* 240, 118377. <https://doi.org/10.1016/j.neuroimage.2021.118377>
- Gelauff, J., Stone, J., Edwards, M., Carson, A., 2014. The prognosis of functional (psychogenic) motor symptoms : a systematic review. *J Neurol Neurosurg Psychiatry* 85, 220–226. <https://doi.org/10.1136/jnnp-2013-305321>
- Gibbons, C.H., 2019. Basics of autonomic nervous system function. pp. 407–418. <https://doi.org/10.1016/B978-0-444-64032-1.00027-8>
- Glasser, M.F., Coalson, T.S., Robinson, E.C., Hacker, C.D., Harwell, J., Yacoub, E., Ugurbil, K., Andersson, J., Beckmann, C.F., Jenkinson, M., Smith, S.M., Van Essen, D.C., 2016. A multi-modal parcellation of human cerebral cortex. *Nature*

- 536, 171–178. <https://doi.org/10.1038/nature18933>
- Glover, G.H., Mueller, B.A., Turner, J.A., Van Erp, T.G.M., Liu, T.T., Greve, D.N., Voyvodic, J.T., Rasmussen, J., Brown, G.G., Keator, D.B., Calhoun, V.D., Lee, H.J., Ford, J.M., Mathalon, D.H., Diaz, M., O’Leary, D.S., Gadde, S., Preda, A., Lim, K.O., Wible, C.G., Stern, H.S., Belger, A., McCarthy, G., Ozyurt, B., Potkin, S.G., 2012. Function biomedical informatics research network recommendations for prospective multicenter functional MRI studies. *J. Magn. Reson. Imaging* 36, 39–54. <https://doi.org/10.1002/jmri.23572>
- Goto, M., Abe, O., Miyati, T., Yamasue, H., Gomi, T., Takeda, T., 2016. Head motion and correction methods in resting-state functional MRI. *Magn. Reson. Med. Sci.* 15, 178–186. <https://doi.org/10.2463/mrms.rev.2015-0060>
- Gould, F., Clarke, J., Heim, C., Harvey, P.D., Majer, M., Nemeroff, C.B., 2012. The effects of child abuse and neglect on cognitive functioning in adulthood. *J. Psychiatr. Res.* 46, 500–506. <https://doi.org/10.1016/j.jpsychires.2012.01.005>
- Greicius, M., 2008. Resting-state functional connectivity in neuropsychiatric disorders. *Curr. Opin. Neurol.* 21, 424–430. <https://doi.org/10.1097/WCO.0b013e328328306f2c5>
- Grier, E.C., 2005. School neuropsychology: A practitioner’s handbook. *Psychol. Sch.* 42, 452–453. <https://doi.org/10.1002/pits.20072>
- Griffa, A., Bommarito, G., Assal, F., Herrmann, F.R., Van De Ville, D., Allali, G., 2021. Dynamic functional networks in idiopathic normal pressure hydrocephalus: Alterations and reversibility by <scp>CSF</scp> tap test. *Hum. Brain Mapp.* 42, 1485–1502. <https://doi.org/10.1002/hbm.25308>
- Gu, X., Hof, P.R., Friston, K.J., Fan, J., 2013. Anterior insular cortex and emotional awareness. *J. Comp. Neurol.* 521, 3371–3388. <https://doi.org/10.1002/cne.23368>
- Guilliams, T.G., Edwards, L., 2010. Chronic stress and the HPA axis: Clinical assessment and therapeutic considerations. *Stand.* 9, 1–12.
- Gupta, A., Lang, A.E., 2009. Psychogenic movement disorders. *Curr. Opin. Neurol.* 22, 430–436. <https://doi.org/10.1097/WCO.0b013e32832832dc169>
- Gusnard, D.A., Akbudak, E., Shulman, G.L., Raichle, M.E., 2001. Medial prefrontal cortex and self-referential mental activity: Relation to a default mode of brain function. *Proc. Natl. Acad. Sci.* 98, 4259–4264. <https://doi.org/10.1073/pnas.071043098>
- Guyon, I., Elisseeff, A., Kaelbling, L.P., 2003. An introduction to variable and feature selection. *J. Mach. Learn. Res.* 3, 1157–1182.
- Haggard, P., 2017. Sense of agency in the human brain. *Nat. Rev. Neurosci.* 18, 196–207. <https://doi.org/10.1038/nrn.2017.14>
- Hahn, T., Marquand, A.F., Ehlis, A.-C., Dresler, T., Kittel-Schneider, S., Jarczok, T.A., Lesch, K.-P., Jakob, P.M., Mourao-Miranda, J., Brammer, M.J., Fallgatter, A.J., 2010. Integrating Neurobiological Markers of Depression. *Arch. Gen. Psychiatry* 68, 361. <https://doi.org/10.1001/archgenpsychiatry.2010.178>
- Hallett, M., 2015. Functional (psychogenic) movement disorders - Clinical presentation. *Park. Relat. Disord.* 8–11. <https://doi.org/10.1016/j.parkreldis.2015.08.036>
- Hallett, M., Aybek, S., Dworetzky, B.A., McWhirter, L., Staab, J.P., Stone, J., 2022. Functional neurological disorder: new subtypes and shared mechanisms. *Lancet Neurol.* 4422. [https://doi.org/10.1016/s1474-4422\(21\)00422-1](https://doi.org/10.1016/s1474-4422(21)00422-1)
- Harris, J.C., 2005. A clinical lesson at the Salpêtrière. *Arch. Gen. Psychiatry* 62, 470–472. <https://doi.org/10.1001/archpsyc.62.5.470>
- Hassa, T., Sebastian, A., Liepert, J., Weiller, C., Schmidt, R., Tüscher, O., 2017. Symptom-specific amygdala hyperactivity modulates motor control network in conversion disorder. *NeuroImage Clin.* 15, 143–150. <https://doi.org/10.1016/j.nicl.2017.04.004>
- Heeger, D.J., Ress, D., 2002. What does fMRI tell us about neuronal activity? *Nat. Rev. Neurosci.* 3, 142–151. <https://doi.org/10.1038/nrn730>
- Heim, C., Ehlert, U., Hellhammer, D.H., 2000. The potential role of hypocortisolism in the pathophysiology of stress-related bodily disorders. *Psychoneuroendocrinology* 25, 1–35. [https://doi.org/10.1016/S0306-4530\(99\)00035-9](https://doi.org/10.1016/S0306-4530(99)00035-9)
- Hellhammer, D.H., Wüst, S., Kudielka, B.M., 2009. Salivary cortisol as a biomarker in stress research. *Psychoneuroendocrinology* 34, 163–171. <https://doi.org/10.1016/j.psyneuen.2008.10.026>
- Herman, J.P., 2013. Neural control of chronic stress adaptation. *Front. Behav. Neurosci.* 7. <https://doi.org/10.3389/fnbeh.2013.00061>
- Hoffmann, M., 2013. The Human Frontal Lobes and Frontal Network Systems: An Evolutionary, Clinical, and Treatment Perspective. *ISRN Neurol.* 2013, 1–34. <https://doi.org/10.1155/2013/892459>
- Honor, G., 2017. Resilience. *J. Pediatr. Heal. Care* 31, 384–390. <https://doi.org/10.1016/j.pedhc.2016.09.005>
- Hu, M., Cheng, H.-J., Ji, F., Chong, J.S.X., Lu, Z., Huang, W., Ang, K.K., Phua, K.S., Chuang, K.-H., Jiang, X., Chew, E., Guan, C., Zhou, J.H., 2021. Brain Functional Changes in Stroke Following Rehabilitation Using Brain-Computer Interface-Assisted Motor Imagery With and Without tDCS: A Pilot Study. *Front. Hum. Neurosci.* 15. <https://doi.org/10.3389/fnhum.2021.692304>
- Hutchison, R.M., Womelsdorf, T., Allen, E.A., Bandettini, P.A., Calhoun, V.D., Corbetta, M., Della Penna, S., Duyn, J.H., Glover, G.H., Gonzalez-Castillo, J., Handwerker, D.A., Keilholz, S., Kiviniemi, V., Leopold, D.A., de Pasquale, F., Sporns, O., Walter, M., Chang, C., 2013. Dynamic functional connectivity: Promise, issues, and interpretations. *Neuroimage* 80, 360–378. <https://doi.org/10.1016/j.neuroimage.2013.05.079>
- Huys, A.C.M.L., Haggard, P., Bhatia, K.P., Edwards, M.J., 2021. Misdirected attentional focus in functional tremor. *Brain* 144, 3436–3450. <https://doi.org/10.1093/brain/awab230>

- Ingram, R.E., Luxton, D.D., 2005. Vulnerability-Stress Models, in: *Development of Psychopathology: A Vulnerability-Stress Perspective*. SAGE Publications, Inc., 2455 Teller Road, Thousand Oaks California 91320 United States, pp. 32–46. <https://doi.org/10.4135/9781452231655.n2>
- Jack, C.R., Bernstein, M.A., Fox, N.C., Thompson, P., Alexander, G., Harvey, D., Borowski, B., Britson, P.J., Whitwell, J.L., Ward, C., Dale, A.M., Felmlee, J.P., Gunter, J.L., Hill, D.L.G., Killiany, R., Schuff, N., Fox-Bosetti, S., Lin, C., Studholme, C., DeCarli, C.S., Krueger, G., Ward, H.A., Metzger, G.J., Scott, K.T., Mallozzi, R., Blezek, D., Levy, J., Debbins, J.P., Fleisher, A.S., Albert, M., Green, R., Bartzokis, G., Glover, G., Mugler, J., Weiner, M.W., L. Whitwell, J., Ward, C., Dale, A.M., Felmlee, J.P., Gunter, J.L., Hill, D.L.G., Killiany, R., Schuff, N., Fox-Bosetti, S., Lin, C., Studholme, C., DeCarli, C.S., Gunnar Krueger, Ward, H.A., Metzger, G.J., Scott, K.T., Mallozzi, R., Blezek, D., Levy, J., Debbins, J.P., Fleisher, A.S., Albert, M., Green, R., Bartzokis, G., Glover, G., Mugler, J., Weiner, M.W., 2008. The Alzheimer’s disease neuroimaging initiative (ADNI): MRI methods. *J. Magn. Reson. Imaging* 27, 685–691. <https://doi.org/10.1002/jmri.21049>
- Janardhanan, P., L., H., Sabika, F., 2015. Effectiveness of Support Vector Machines in Medical Data mining. *J. Commun. Softw. Syst.* 11, 25. <https://doi.org/10.24138/jcomss.v11i1.114>
- Jiang, R., Abbott, C.C., Jiang, T., Du, Y., Espinoza, R., Narr, K.L., Wade, B., Yu, Q., Song, M., Lin, D., Chen, J., Jones, T., Argyelan, M., Petrides, G., Sui, J., Calhoun, V.D., 2018. SMRI Biomarkers Predict Electroconvulsive Treatment Outcomes: Accuracy with Independent Data Sets. *Neuropsychopharmacology* 43, 1078–1087. <https://doi.org/10.1038/npp.2017.165>
- Jungilligens, J., Popkirov, S., Perez, D.L., Diez, I., 2022. Linking gene expression patterns and brain morphometry to trauma and symptom severity in patients with functional seizures. *Psychiatry Res. - Neuroimaging* 326, 111533. <https://doi.org/10.1016/j.psychres.2022.111533>
- Jungilligens, J., Wellmer, J., Kowoll, A., Schlegel, U., Axmacher, N., Popkirov, S., 2021. Microstructural integrity of affective neurocircuitry in patients with dissociative seizures is associated with emotional task performance, illness severity and trauma history. *Seizure* 84, 91–98. <https://doi.org/10.1016/j.seizure.2020.11.021>
- Kadmiel, M., Cidowski, J.A., 2013. Glucocorticoid receptor signaling in health and disease. *Trends Pharmacol. Sci.* 34, 518–530. <https://doi.org/10.1016/j.tips.2013.07.003>
- Kanaan, R., Armstrong, D., Barnes, P., Wessely, S., 2009. In the psychiatrist’s chair: how neurologists understand conversion disorder. *Brain* 132, 2889–2896. <https://doi.org/10.1093/brain/awp060>
- Kanaan, R.A.A., 2016. Freud’s hysteria and its legacy, in: *Handbook of Clinical Neurology*. pp. 37–44. <https://doi.org/10.1016/B978-0-12-801772-2.00004-7>
- Kanaan, R.A.A., Craig, T.K.J., 2019. Conversion disorder and the trouble with trauma. *Psychol. Med.* 49, 1585–1588. <https://doi.org/10.1017/S0033291719000990>
- Karatzias, T., Howard, R., Power, K., Socherel, F., Heath, C., Livingstone, A., 2017. Organic vs. functional neurological disorders: The role of childhood psychological trauma. *Child Abuse Negl.* 63, 1–6. <https://doi.org/10.1016/j.chiabu.2016.11.011>
- Kern, S., Krause, I., Horntich, A., Thomas, K., Aderhold, J., Ziemssen, T., 2013. Cortisol Awakening Response Is Linked to Disease Course and Progression in Multiple Sclerosis. *PLoS One* 8, e60647. <https://doi.org/10.1371/journal.pone.0060647>
- Keynejad, R.C., Frodl, T., Kanaan, R., Pariante, C., Reuber, M., Nicholson, T.R., 2019. Stress and functional neurological disorders: Mechanistic insights. *J. Neurol. Neurosurg. Psychiatry* 90, 813–821. <https://doi.org/10.1136/jnnp-2018-318297>
- Khanna, A., Pascual-Leone, A., Farzan, F., 2014. Reliability of Resting-State Microstate Features in Electroencephalography. *PLoS One* 9, e114163. <https://doi.org/10.1371/journal.pone.0114163>
- King, H., 1993. 1. Once upon a Text: Hysteria from Hippocrates, in: *Hysteria Beyond Freud*. University of California Press, pp. 1–90. <https://doi.org/10.1525/9780520309937-002>
- Kozłowska, K., 2007. The Developmental Origins of Conversion Disorders. *Clin. Child Psychol. Psychiatry* 12, 487–510. <https://doi.org/10.1177/1359104507080977>
- Kozłowska, K., Griffiths, K.R., Foster, S.L., Linton, J., Williams, L.M., Korgaonkar, M.S., 2017a. Grey matter abnormalities in children and adolescents with functional neurological symptom disorder. *NeuroImage Clin.* 15, 306–314. <https://doi.org/10.1016/j.nicl.2017.04.028>
- Kozłowska, K., Melkonian, D., Spooner, C.J., Scher, S., Meares, R., 2017b. Cortical arousal in children and adolescents with functional neurological symptoms during the auditory oddball task. *NeuroImage Clin.* 13, 228–236. <https://doi.org/10.1016/j.nicl.2016.10.016>
- Kozłowska, K., Palmer, D.M., Brown, K.J., McLean, L., Scher, S., Gevirtz, R., Chudleigh, C., Williams, L.M., 2015. Reduction of autonomic regulation in children and adolescents with conversion disorders. *Psychosom. Med.* 77, 356–370. <https://doi.org/10.1097/PSY.0000000000000184>
- Krishnan, A., Williams, L.J., McIntosh, A.R., Abdi, H., 2011. Partial Least Squares (PLS) methods for neuroimaging: A tutorial and review. *Neuroimage* 56, 455–475. <https://doi.org/10.1016/j.neuroimage.2010.07.034>
- Krol, K.M., Puglia, M.H., Morris, J.P., Connelly, J.J., Grossmann, T., 2019. Epigenetic modification of the oxytocin receptor gene is associated with emotion processing in the infant brain. *Dev. Cogn. Neurosci.* 37, 100648. <https://doi.org/10.1016/j.dcn.2019.100648>
- Kucyi, A., Hodaie, M., Davis, K.D., 2012. Lateralization in intrinsic functional connectivity of the temporoparietal junction

- with salience- and attention-related brain networks. *J. Neurophysiol.* 108, 3382–3392. <https://doi.org/10.1152/jn.00674.2012>
- LaFaver, K., 2020. Treatment of Functional Movement Disorders. *Neurol. Clin.* 38, 469–480. <https://doi.org/10.1016/j.ncl.2020.01.011>
- LaFaver, K., Lang, A.E., Stone, J., Morgante, F., Edwards, M., Lidstone, S., Maurer, C.W., Hallett, M., Dwivedi, A.K., Espay, A.J., 2020. Opinions and clinical practices related to diagnosing and managing functional (psychogenic) movement disorders: changes in the last decade. *Eur. J. Neurol.* 27, 975–984. <https://doi.org/10.1111/ene.14200>
- LaFrance, W.C., Baker, G.A., Duncan, R., Goldstein, L.H., Reuber, M., 2013. Minimum requirements for the diagnosis of psychogenic nonepileptic seizures: A staged approach: A report from the International League Against Epilepsy Nonepileptic Seizures Task Force. *Epilepsia* 54, 2005–2018. <https://doi.org/10.1111/epi.12356>
- LeDoux, J., Iwata, J., Cicchetti, P., Reis, D., 1988. Different projections of the central amygdaloid nucleus mediate autonomic and behavioral correlates of conditioned fear. *J. Neurosci.* 8, 2517–2529. <https://doi.org/10.1523/JNEUROSCI.08-07-02517.1988>
- Li, X., Hu, L., 2016. The Role of Stress Regulation on Neural Plasticity in Pain Chronification. *Neural Plast.* 2016, 1–9. <https://doi.org/10.1155/2016/6402942>
- Lidstone, S.C., Schulzer, M., Dinelle, K., Mak, E., Sossi, V., Ruth, T.J., de la Fuente-Fernández, R., Phillips, A.G., Stoessl, A.J., 2010. Effects of Expectation on Placebo-Induced Dopamine Release in Parkinson Disease. *Arch. Gen. Psychiatry* 67, 857. <https://doi.org/10.1001/archgenpsychiatry.2010.88>
- Lippard, E.T.C., Nemeroff, C.B., 2019. The Devastating Clinical Consequences of Child Abuse and Neglect: Increased Disease Vulnerability and Poor Treatment Response in Mood Disorders. *Am. J. Psychiatry* 177, 20–36. <https://doi.org/10.1176/appi.ajp.2019.19010020>
- Liu, F., Guo, W., Yu, D., Gao, Q., Gao, K., Xue, Z., Du, H., Zhang, J., Tan, C., Liu, Z., Zhao, J., Chen, H., 2012. Classification of Different Therapeutic Responses of Major Depressive Disorder with Multivariate Pattern Analysis Method Based on Structural MR Scans. *PLoS One* 7, e40968. <https://doi.org/10.1371/journal.pone.0040968>
- Liu, X., Chang, C., Duyn, J.H., 2013. Decomposition of spontaneous brain activity into distinct fMRI co-activation patterns. *Front. Syst. Neurosci.* 7, 1–11. <https://doi.org/10.3389/fnsys.2013.00101>
- Liu, X., Duyn, J.H., 2013. Time-varying functional network information extracted from brief instances of spontaneous brain activity. *Proc. Natl. Acad. Sci.* 110, 4392–4397. <https://doi.org/10.1073/pnas.1216856110>
- Liu, X., Zhang, N., Chang, C., Duyn, J.H., 2018. Co-activation patterns in resting-state fMRI signals. *Neuroimage* 180, 485–494. <https://doi.org/10.1016/j.neuroimage.2018.01.041>
- Logothetis, N.K., 2003. The Underpinnings of the BOLD Functional Magnetic Resonance Imaging Signal. *J. Neurosci.* 23, 3963–3971. <https://doi.org/10.1523/JNEUROSCI.23-10-03963.2003>
- Longarzo, M., Cavaliere, C., Mele, G., Tozza, S., Tramontano, L., Alfano, V., Aiello, M., Salvatore, M., Grossi, D., 2020. Microstructural Changes in Motor Functional Conversion Disorder: Multimodal Imaging Approach on a Case. *Brain Sci.* 10, 385. <https://doi.org/10.3390/brainsci10060385>
- Loukas, S., Lordier, L., Meskaldji, D.E., Filippa, M., Sa de Almeida, J., Van De Ville, D., Hüppi, P.S., 2021. Musical memories in newborns: A resting-state functional connectivity study. *Hum. Brain Mapp.* 1–18. <https://doi.org/10.1002/hbm.25677>
- Ludwig, J., Speier, P., Seifert, F., Schaeffter, T., Kolbitsch, C., 2021. Pilot tone-based motion correction for prospective respiratory compensated cardiac cine MRI. *Magn. Reson. Med.* 85, 2403–2416. <https://doi.org/10.1002/mrm.28580>
- Ludwig, L., Pasman, J.A., Nicholson, T., Aybek, S., David, A.S., Tuck, S., Kanaan, R.A., Roelofs, K., Carson, A., Stone, J., 2018. Stressful life events and maltreatment in conversion (functional neurological) disorder: systematic review and meta-analysis of case-control studies. *The Lancet Psychiatry* 5, 307–320. [https://doi.org/10.1016/S2215-0366\(18\)30051-8](https://doi.org/10.1016/S2215-0366(18)30051-8)
- Lupien, S.J., Evans, A., Lord, C., Miles, J., Pruessner, M., Pike, B., Pruessner, J.C., 2007. Hippocampal volume is as variable in young as in older adults: Implications for the notion of hippocampal atrophy in humans. *Neuroimage* 34, 479–485. <https://doi.org/10.1016/j.neuroimage.2006.09.041>
- Lupien, S.J., Juster, R.P., Raymond, C., Marin, M.F., 2018. The effects of chronic stress on the human brain: From neurotoxicity, to vulnerability, to opportunity. *Front. Neuroendocrinol.* 49, 91–105. <https://doi.org/10.1016/j.yfrne.2018.02.001>
- Lv, H., Wang, Z., Tong, E., Williams, L.M., Zaharchuk, G., Zeineh, M., Goldstein-Piekarski, A.N., Ball, T.M., Liao, C., Wintermark, M., 2018. Resting-State Functional MRI: Everything That Nonexperts Have Always Wanted to Know. *Am. J. Neuroradiol.* <https://doi.org/10.3174/ajnr.A5527>
- MacDuffie, K.E., Grubbs, L., Best, T., LaRoche, S., Mildon, B., Myers, L., Stafford, E., Rommelfanger, K.S., 2021. Stigma and functional neurological disorder: a research agenda targeting the clinical encounter. *CNS Spectr.* 26, 587–592. <https://doi.org/10.1017/S1092852920002084>
- Mai, F.M., Merskey, H., 1981. Briquet's Concept of Hysteria: An Historical Perspective. *Can. J. Psychiatry* 26, 57–63. <https://doi.org/10.1177/070674378102600112>
- Manjón, J. V., Coupé, P., Martí-Bonmatí, L., Collins, D.L., Robles, M., 2010. Adaptive non-local means denoising of MR images with spatially varying noise levels. *J. Magn. Reson. Imaging* 31, 192–203. <https://doi.org/10.1002/jmri.22003>
- Marapin, R.S., Gelauff, J.M., Marsman, J.B.C., de Jong, B.M., Dreissen, Y.E.M., Koelman, J.H.T.M., van der Horn, H.J., Tijssen, M.A.J., 2021. Altered Posterior Midline Activity in Patients with Jerky and Tremulous Functional Movement Disorders. *Brain Connect.* 11, 584–593. <https://doi.org/10.1089/brain.2020.0779>

- Marapin, R.S., van der Stouwe, A.M.M., de Jong, B.M., Gelauff, J.M., Vergara, V.M., Calhoun, V.D., Dalenberg, J.R., Dreissen, Y.E.M., Koelman, J.H.T.M., Tijssen, M.A.J., van der Horn, H.J., 2020. The chronnectome as a model for Charcot's 'dynamic lesion' in functional movement disorders. *NeuroImage Clin.* 28, 102381. <https://doi.org/10.1016/j.nicl.2020.102381>
- Marshall, J.C., Halligan, P.W., Fink, G.R., Wade, D.T., Frackowiak, R.S.J., 1997. The functional anatomy of a hysterical paralysis. *Cognition* 64, 1–8. [https://doi.org/10.1016/S0010-0277\(97\)00020-6](https://doi.org/10.1016/S0010-0277(97)00020-6)
- Maurer, C.W., LaFaver, K., Ameli, R., Epstein, S.A., Hallett, M., Horovitz, S.G., 2016. Impaired self-agency in functional movement disorders: A resting-state fMRI study. *Neurology* 87, 564–70. <https://doi.org/10.1212/WNL.0000000000002940>
- Maurer, C.W., LaFaver, K., Ameli, R., Toledo, R., Hallett, M., 2015. A biological measure of stress levels in patients with functional movement disorders. *Parkinsonism Relat. Disord.* 21, 1072–1075. <https://doi.org/10.1016/j.parkreldis.2015.06.017>
- McEwen, B.S., 2017. Neurobiological and Systemic Effects of Chronic Stress. *Chronic Stress* 1. <https://doi.org/10.1177/2470547017692328>
- McIntosh, A.R., Lobaugh, N.J., 2004. Partial least squares analysis of neuroimaging data: applications and advances. *Neuroimage* 23, S250–S263. <https://doi.org/10.1016/j.neuroimage.2004.07.020>
- Mckenzie, P.S., Oto, M., Graham, C.D., Duncan, R., 2011. Do patients whose psychogenic non-epileptic seizures resolve , ' replace ' them with other medically unexplained symptoms ? Medically unexplained symptoms arising after a diagnosis of psychogenic non-epileptic seizures 2011–2014. <https://doi.org/10.1136/jnnp.2010.231886>
- McLaughlin, K.A., Colich, N.L., Rodman, A.M., Weissman, D.G., 2020. Mechanisms linking childhood trauma exposure and psychopathology: A transdiagnostic model of risk and resilience. *BMC Med.* 18, 1–11. <https://doi.org/10.1186/s12916-020-01561-6>
- Michel, C.M., Koenig, T., 2018. EEG microstates as a tool for studying the temporal dynamics of whole-brain neuronal networks: A review. *Neuroimage* 180, 577–593. <https://doi.org/10.1016/j.neuroimage.2017.11.062>
- Mogg, K., Bradley, B.P., 2016. Anxiety and attention to threat: Cognitive mechanisms and treatment with attention bias modification. *Behav. Res. Ther.* 87, 76–108. <https://doi.org/10.1016/j.brat.2016.08.001>
- Monroe, S.M., Cummins, L.F., 2015. Diathesis-Stress Models, in: *The Encyclopedia of Clinical Psychology*. John Wiley & Sons, Inc., Hoboken, NJ, USA, pp. 1–6. <https://doi.org/10.1002/9781118625392.wbecp466>
- Monsa, R., Peer, M., Arzy, S., 2018. Self-reference, emotion inhibition and somatosensory disturbance: preliminary investigation of network perturbations in conversion disorder. *Eur. J. Neurol.* 25, 888-e62. <https://doi.org/10.1111/ene.13613>
- Monti, S., Tamayo, P., Mesirov, J., Golub, T., 2003. Consensus Clustering: A Resampling-Based Method for Class Discovery and Visualization of Gene Expression Microarray Data. *Mach. Learn.* 52, 91–118. <https://doi.org/10.1023/A:1023949509487>
- Mori, Y., Miyata, J., Isobe, M., Son, S., Yoshihara, Y., Aso, T., Kouchiyama, T., Murai, T., Takahashi, H., 2018. Effect of phase-encoding direction on group analysis of resting-state functional magnetic resonance imaging. *Psychiatry Clin. Neurosci.* 72, 683–691. <https://doi.org/10.1111/pcn.12677>
- Morris, L.S., To, B., Baek, K., Chang-Webb, Y.-C., Mitchell, S., Strelchuk, D., Mikheenko, Y., Phillips, W., Zandi, M., Jenaway, A., Walsh, C., Voon, V., 2017. Disrupted avoidance learning in functional neurological disorder: Implications for harm avoidance theories. *NeuroImage Clin.* 16, 286–294. <https://doi.org/10.1016/j.nicl.2017.08.007>
- Morrison, S.E., McGinty, V.B., du Hoffmann, J., Nicola, S.M., 2017. Limbic-motor integration by neural excitations and inhibitions in the nucleus accumbens. *J. Neurophysiol.* 118, 2549–2567. <https://doi.org/10.1152/jn.00465.2017>
- Morsy, S.K., Aybek, S., Carson, A., Nicholson, T.R., Stone, J., Kamal, A.M., Abdel-Fadeel, N.A., Hassan, M.A., Kanaan, R.A.A., 2021. The relationship between types of life events and the onset of functional neurological (conversion) disorder in adults: a systematic review and meta-analysis. *Psychol. Med.* 1–18. <https://doi.org/10.1017/S0033291721004669>
- Mueller, K., Růžička, F., Slovák, M., Forejtová, Z., Dušek, Petr, Dušek, Pavel, Jech, R., Serranová, T., 2022. Symptom-severity-related brain connectivity alterations in functional movement disorders. *NeuroImage Clin.* 34, 102981. <https://doi.org/10.1016/j.nicl.2022.102981>
- Munk, A., Guyre, P.M., Holbrook, N.J., 1984. Physiological Functions of Glucocorticoids in Stress and Their Relation to Pharmacological Actions*. *Endocr. Rev.* 5, 25–44. <https://doi.org/10.1210/edrv-5-1-25>
- Myers, L., Trobliger, R., Lancman, M., 2021. Patients with late onset psychogenic non-epileptic seizures (PNES): How do they compare to those with younger onset? *Seizure* 88, 153–157. <https://doi.org/10.1016/j.seizure.2021.04.013>
- Nachev, P., Kennard, C., Husain, M., 2008. Functional role of the supplementary and pre-supplementary motor areas. *Nat. Rev. Neurosci.* 9, 856–869. <https://doi.org/10.1038/nrn2478>
- Nair, A., Jolliffe, M., Lograsso, Y.S.S., Bearden, C.E., 2020. A Review of Default Mode Network Connectivity and Its Association With Social Cognition in Adolescents With Autism Spectrum Disorder and Early-Onset Psychosis. *Front. Psychiatry* 11. <https://doi.org/10.3389/fpsy.2020.00614>
- Nakano, T., Takamura, M., Ichikawa, N., Okada, G., Okamoto, Y., Yamada, M., Suhara, T., Yamawaki, S., Yoshimoto, J., 2020. Enhancing Multi-Center Generalization of Machine Learning-Based Depression Diagnosis From Resting-State fMRI. *Front. Psychiatry* 11. <https://doi.org/10.3389/fpsy.2020.00400>
- Natu, V.S., Lin, J.-J., Burks, A., Arora, A., Rugg, M.D., Lega, B., 2019. Stimulation of the Posterior Cingulate Cortex Impairs

- Episodic Memory Encoding. *J. Neurosci.* 39, 7173–7182. <https://doi.org/10.1523/jneurosci.0698-19.2019>
- Nemiah, J.C., 1996. Breuer, Josef and Freud, Sigmund (1895/1995), *Studies on Hysteria*. In James Strachey (Ed.) *The Standard Edition of the Complete Psychological Works of Sigmund Freud*. London: Hogarth Press, Vol.2, xxxii, pp. 1–335. *Am. J. Clin. Hypn.* 38, 234–237. <https://doi.org/10.1080/00029157.1996.10403343>
- Nicholson, T.R., Aybek, S., Kempton, M.J., Daly, E.M., Murphy, D.G., David, A.S., Kanaan, R.A., 2014. A structural MRI study of motor conversion disorder: evidence of reduction in thalamic volume. *J. Neurol. Neurosurg. Psychiatry* 85, 227–229. <https://doi.org/10.1136/jnnp-2013-305012>
- Nicholson, T.R.J., Stone, J., Kanaan, R.A.A., 2011. Conversion disorder: a problematic diagnosis. *J. Neurol. Neurosurg. Psychiatry* 82, 1267–1273. <https://doi.org/10.1136/jnnp.2008.171306>
- Nicola, S.M., 2010. The Flexible Approach Hypothesis: Unification of Effort and Cue-Responding Hypotheses for the Role of Nucleus Accumbens Dopamine in the Activation of Reward-Seeking Behavior. *J. Neurosci.* 30, 16585–16600. <https://doi.org/10.1523/jneurosci.3958-10.2010>
- Nielsen, A.N., Barch, D.M., Petersen, S.E., Schlaggar, B.L., Greene, D.J., 2020. Machine Learning With Neuroimaging: Evaluating Its Applications in Psychiatry. *Biol. Psychiatry Cogn. Neurosci. Neuroimaging* 5, 791–798. <https://doi.org/10.1016/j.bpsc.2019.11.007>
- Nielsen, G., Ricciardi, L., Meppelink, A.M., Holt, K., Teodoro, T., Edwards, M., 2017. A Simplified Version of the Psychogenic Movement Disorders Rating Scale: The Simplified Functional Movement Disorders Rating Scale (S-FMDRS). *Mov. Disord. Clin. Pract.* 4, 710–716. <https://doi.org/10.1002/mdc3.12475>
- Nijenhuis, E.R.S., Van der Hart, O., Kruger, K., 2002. The psychometric characteristics of the traumatic experiences checklist (TEC): first findings among psychiatric outpatients. *Clin. Psychol. Psychother.* 9, 200–210. <https://doi.org/10.1002/cpp.332>
- Noble, S., Scheinost, D., Finn, E.S., Shen, X., Papademetris, X., McEwen, S.C., Bearden, C.E., Addington, J., Goodyear, B., Cadenhead, K.S., Mirzakhani, H., Comblatt, B.A., Olvet, D.M., Mathalon, D.H., McGlashan, T.H., Perkins, D.O., Belger, A., Seidman, L.J., Thermenos, H., Tsuang, M.T., van Erp, T.G.M., Walker, E.F., Hamann, S., Woods, S.W., Cannon, T.D., Constable, R.T., 2017. Multisite reliability of MR-based functional connectivity. *Neuroimage* 146, 959–970. <https://doi.org/10.1016/j.neuroimage.2016.10.020>
- Nunes, A., Schnack, H.G., Ching, C.R.K., Agartz, I., Akudjedu, T.N., Alda, M., Alnæs, D., Alonso-Lana, S., Bauer, J., Baune, B.T., Bøen, E., Bonnin, C. del M., Busatto, G.F., Canales-Rodríguez, E.J., Cannon, D.M., Caseras, X., Chaim-Avancini, T.M., Dannlowski, U., Diaz-Zuluaga, A.M., Dietsche, B., Doan, N.T., Duchesnay, E., Elvsåshagen, T., Emden, D., Eyster, L.T., Fatjó-Vilas, M., Favre, P., Foley, S.F., Fullerton, J.M., Glahn, D.C., Goikolea, J.M., Grotegerd, D., Hahn, T., Henry, C., Hibar, D.P., Houenou, J., Howells, F.M., Jahanshad, N., Kaufmann, T., Kenney, J., Kircher, T.T.J., Krug, A., Lagerberg, T. V., Lenroot, R.K., López-Jaramillo, C., Machado-Vieira, R., Malt, U.F., McDonald, C., Mitchell, P.B., Mwangi, B., Nabulsi, L., Opel, N., Overs, B.J., Pineda-Zapata, J.A., Pomarol-Clotet, E., Redlich, R., Roberts, G., Rosa, P.G., Salvador, R., Satterthwaite, T.D., Soares, J.C., Stein, D.J., Temmingh, H.S., Trappenberg, T., Uhlmann, A., van Haren, N.E.M., Vieta, E., Westlye, L.T., Wolf, D.H., Yüksel, D., Zanetti, M. V., Andreassen, O.A., Thompson, P.M., Hajek, T., 2020. Using structural MRI to identify bipolar disorders – 13 site machine learning study in 3020 individuals from the ENIGMA Bipolar Disorders Working Group. *Mol. Psychiatry* 25, 2130–2143. <https://doi.org/10.1038/s41380-018-0228-9>
- Oakley, R.H., Cidlowski, J.A., 2013. The biology of the glucocorticoid receptor: New signaling mechanisms in health and disease. *J. Allergy Clin. Immunol.* 132, 1033–1044. <https://doi.org/10.1016/j.jaci.2013.09.007>
- Ogawa, S., Lee, T.-M., Nayak, A.S., Glynn, P., 1990. Oxygenation-sensitive contrast in magnetic resonance image of rodent brain at high magnetic fields. *Magn. Reson. Med.* 14, 68–78. <https://doi.org/10.1002/mrm.1910140108>
- Orrù, G., Pettersson-Yeo, W., Marquand, A.F., Sartori, G., Mechelli, A., 2012. Using Support Vector Machine to identify imaging biomarkers of neurological and psychiatric disease: A critical review. *Neurosci. Biobehav. Rev.* 36, 1140–1152. <https://doi.org/10.1016/j.neubiorev.2012.01.004>
- Oster, H., Challet, E., Ott, V., Arvat, E., de Kloet, E.R., Dijk, D.J., Lightman, S., Vgontzas, A., Van Cauter, E., 2017. The functional and clinical significance of the 24-hour rhythm of circulating glucocorticoids. *Endocr. Rev.* 38, 3–45. <https://doi.org/10.1210/er.2015-1080>
- Ouanes, S., Popp, J., 2019. High Cortisol and the Risk of Dementia and Alzheimer’s Disease: A Review of the Literature. *Front. Aging Neurosci.* 11. <https://doi.org/10.3389/fnagi.2019.00043>
- Pacella, M.L., Feeny, N., Zoellner, L., Delahanty, D.L., 2014. The impact of PTSD treatment on the cortisol awakening response. *Depress. Anxiety* 31, 862–869. <https://doi.org/10.1002/da.22298>
- Pan, X., Wang, Z., Wu, X., Wen, S.W., Liu, A., 2018. Salivary cortisol in post-traumatic stress disorder: A systematic review and meta-analysis. *BMC Psychiatry* 18, 1–10. <https://doi.org/10.1186/s12888-018-1910-9>
- Pareés, I., Kassavetis, P., Saifee, T.A., Sadnicka, A., Davare, M., Bhatia, K.P., Rothwell, J.C., Bestmann, S., Edwards, M.J., 2013. Failure of explicit movement control in patients with functional motor symptoms. *Mov. Disord.* 28, 517–523. <https://doi.org/10.1002/mds.25287>
- Pareés, I., Saifee, T.A., Kassavetis, P., Kojovic, M., Rubio-Agusti, I., Rothwell, J.C., Bhatia, K.P., Edwards, M.J., 2012. Believing is perceiving: mismatch between self-report and actigraphy in psychogenic tremor. *Brain* 135, 117–123. <https://doi.org/10.1093/brain/awr292>
- Patel, M.J., Andreescu, C., Price, J.C., Edelman, K.L., Reynolds, C.F., Aizenstein, H.J., 2015. Machine learning approaches for integrating clinical and imaging features in late-life depression classification and response prediction. *Int. J. Geriatr.*

- Psychiatry 30, 1056–1067. <https://doi.org/10.1002/gps.4262>
- Paulus, M.P., Feinstein, J.S., Khalsa, S.S., 2019. An Active Inference Approach to Interoceptive Psychopathology. *Annu. Rev. Clin. Psychol.* 15, 97–122. <https://doi.org/10.1146/annurev-clinpsy-050718-095617>
- Perez, D.L., Aybek, S., Nicholson, T.R., Kozłowska, K., Arciniegas, D.B., LaFrance, W.C., 2020. Functional Neurological (Conversion) Disorder: A Core Neuropsychiatric Disorder. *J. Neuropsychiatry Clin. Neurosci.* 32, 1–3. <https://doi.org/10.1176/appi.neuropsych.19090204>
- Perez, D.L., Barsky, A.J., Daffner, K., Silbersweig, D.A., 2012. Motor and somatosensory conversion disorder: A functional unawareness Syndrome? *J. Neuropsychiatry Clin. Neurosci.* 24, 141–151. <https://doi.org/10.1176/appi.neuropsych.11050110>
- Perez, D.L., Matin, N., Barsky, A., Costumero-Ramos, V., Makaretz, S.J., Young, S.S., Sepulcre, J., LaFrance, W.C., Keshavan, M.S., Dickerson, B.C., 2017a. Cingulo-insular structural alterations associated with psychogenic symptoms, childhood abuse and PTSD in functional neurological disorders. *J. Neurol. Neurosurg. Psychiatry* 88, 491–497. <https://doi.org/10.1136/jnnp-2016-314998>
- Perez, D.L., Matin, N., Williams, B., Tanev, K., Makris, N., LaFrance, W.C., Dickerson, B.C., 2018. Cortical thickness alterations linked to somatoform and psychological dissociation in functional neurological disorders. *Hum. Brain Mapp.* 39, 428–439. <https://doi.org/10.1002/hbm.23853>
- Perez, D.L., Nicholson, T.R., Asadi-Pooya, A.A., Bègue, I., Butler, M., Carson, A.J., David, A.S., Deeley, Q., Diez, I., Edwards, M.J., Espay, A.J., Gelauff, J.M., Hallett, M., Horovitz, S.G., Jungilligens, J., Kanaan, R.A.A., Tijssen, M.A.J., Kozłowska, K., LaFaver, K., LaFrance, W.C., Lidstone, S.C., Marapin, R.S., Maurer, C.W., Modirrousta, M., Reinders, A.A.T.S., Sojka, P., Staab, J.P., Stone, J., Szaflarski, J.P., Aybek, S., 2021. Neuroimaging in Functional Neurological Disorder: State of the Field and Research Agenda. *NeuroImage Clin.* 30. <https://doi.org/10.1016/j.nicl.2021.102623>
- Perez, D.L., Williams, B., Matin, N., Curt LaFrance, W., Costumero-Ramos, V., Fricchione, G.L., Sepulcre, J., Keshavan, M.S., Dickerson, B.C., 2017b. Corticolimbic structural alterations linked to health status and trait anxiety in functional neurological disorder. *J. Neurol. Neurosurg. Psychiatry* 88, 1052–1059. <https://doi.org/10.1136/jnnp-2017-316359>
- Pessoa, L., 2008. On the relationship between emotion and cognition. *Nat. Rev. Neurosci.* 9, 148–158. <https://doi.org/10.1038/nrn2317>
- Peterson, K.T., Kosior, R., Meek, B.P., Ng, M., Perez, D.L., Modirrousta, M., 2018. Right Temporoparietal Junction Transcranial Magnetic Stimulation in the Treatment of Psychogenic Nonepileptic Seizures: A Case Series. *Psychosomatics* 59, 601–606. <https://doi.org/10.1016/j.psym.2018.03.001>
- Pick, S., Goldstein, L.H., Perez, D.L., Nicholson, T.R., 2019. Emotional processing in functional neurological disorder: A review, biopsychosocial model and research agenda. *J. Neurol. Neurosurg. Psychiatry* 90, 704–711. <https://doi.org/10.1136/jnnp-2018-319201>
- Planès, S., Villier, C., Mallaret, M., 2016. The nocebo effect of drugs. *Pharmacol. Res. Perspect.* 4. <https://doi.org/10.1002/prp2.208>
- Pollatos, O., Kirsch, W., Schandry, R., 2005. Brain structures involved in interoceptive awareness and cardioafferent signal processing: A dipole source localization study. *Hum. Brain Mapp.* 26, 54–64. <https://doi.org/10.1002/hbm.20121>
- Power, J.D., Mitra, A., Laumann, T.O., Snyder, A.Z., Schlaggar, B.L., Petersen, S.E., 2014. Methods to detect, characterize, and remove motion artifact in resting state fMRI. *Neuroimage* 84, 320–341. <https://doi.org/10.1016/j.neuroimage.2013.08.048>
- Preti, M.G., Bolton, T.A., Van De Ville, D., 2017. The dynamic functional connectome: State-of-the-art and perspectives. *Neuroimage* 160, 41–54. <https://doi.org/10.1016/j.neuroimage.2016.12.061>
- Pruessner, J.C., Dedovic, K., Khalili-Mahani, N., Engert, V., Pruessner, M., Buss, C., Renwick, R., Dagher, A., Meaney, M.J., Lupien, S., 2008. Deactivation of the Limbic System During Acute Psychosocial Stress: Evidence from Positron Emission Tomography and Functional Magnetic Resonance Imaging Studies. *Biol. Psychiatry* 63, 234–240. <https://doi.org/10.1016/j.biopsych.2007.04.041>
- Pruessner, J.C., Kirschbaum, C., Meinlschmid, G., Hellhammer, D.H., 2003. Two formulas for computation of the area under the curve represent measures of total hormone concentration versus time-dependent change. *Psychoneuroendocrinology* 28, 916–931. [https://doi.org/10.1016/S0306-4530\(02\)00108-7](https://doi.org/10.1016/S0306-4530(02)00108-7)
- Pruessner, J.C., Wolf, O.T., Hellhammer, D.H., Buske-Kirschbaum, A., Von Auer, K., Jobst, S., Kaspers, F., Kirschbaum, C., 1997. Free cortisol levels after awakening: A reliable biological marker for the assessment of adrenocortical activity. *Life Sci.* 61, 2539–2549. [https://doi.org/10.1016/S0024-3205\(97\)01008-4](https://doi.org/10.1016/S0024-3205(97)01008-4)
- Qian, J., Diez, I., Ortiz-Terán, L., Bonadio, C., Liddell, T., Goñi, J., Sepulcre, J., 2018. Positive Connectivity Predicts the Dynamic Intrinsic Topology of the Human Brain Network. *Front. Syst. Neurosci.* 12. <https://doi.org/10.3389/fnsys.2018.00038>
- Rajapakse, J.C., Giedd, J.N., Rapoport, J.L., 1997. Statistical approach to segmentation of single-channel cerebral MR images. *IEEE Trans. Med. Imaging* 16, 176–186. <https://doi.org/10.1109/42.563663>
- Rauch, S.A.M., King, A., Kim, H.M., Powell, C., Rajaram, N., Venners, M., Simon, N.M., Hamner, M., Liberzon, I., 2020. Cortisol awakening response in PTSD treatment: Predictor or mechanism of change. *Psychoneuroendocrinology* 118, 104714. <https://doi.org/10.1016/j.psyneuen.2020.104714>
- Raynor, G., Baslet, G., 2021. A historical review of functional neurological disorder and comparison to contemporary models. *Epilepsy Behav. Reports* 16, 100489. <https://doi.org/10.1016/j.ebr.2021.100489>
- Redlich, R., Opel, N., Grotegerd, D., Dohm, K., Zaremba, D., Bürger, C., Munker, S., Mühlmann, L., Wahl, P., Heindel, W.,

- Arolt, V., Alferink, J., Zwanzger, P., Zavorotnyy, M., Kugel, H., Dannlowski, U., 2016. Prediction of Individual Response to Electroconvulsive Therapy via Machine Learning on Structural Magnetic Resonance Imaging Data. *JAMA Psychiatry* 73, 557. <https://doi.org/10.1001/jamapsychiatry.2016.0316>
- Reuber, M., Howlett, S., Khan, A., Grünewald, R.A., 2007. Non-epileptic seizures and other functional neurological symptoms: Predisposing, precipitating, and perpetuating factors. *Psychosomatics* 48, 230–238. <https://doi.org/10.1176/appi.psy.48.3.230>
- Rey, G., Bolton, T.A.W., Gaviria, J., Piguët, C., Preti, M.G., Favre, S., Aubry, J.M., Van De Ville, D., Vuilleumier, P., 2021. Dynamics of amygdala connectivity in bipolar disorders: a longitudinal study across mood states. *Neuropsychopharmacology* 46, 1693–1701. <https://doi.org/10.1038/s41386-021-01038-x>
- Richardson, M., Isbister, G., Nicholson, B., 2018. A Novel Treatment Protocol (Nocebo Hypothesis Cognitive Behavioural Therapy; NH-CBT) for Functional Neurological Symptom Disorder/Conversion Disorder: A Retrospective Consecutive Case Series. *Behav. Cogn. Psychother.* 46, 497–503. <https://doi.org/10.1017/S1352465817000832>
- Richardson, M., Kleinstäuber, M., Wong, D., 2020. Nocebo-Hypothesis Cognitive Behavioral Therapy (NH-CBT) for Persons With Functional Neurological Symptoms (Motor Type): Design and Implementation of a Randomized Active-Controlled Trial. *Front. Neurol.* 11. <https://doi.org/10.3389/fneur.2020.586359>
- Richiardi, J., Eryilmaz, H., Schwartz, S., Vuilleumier, P., Van De Ville, D., 2011. Decoding brain states from fMRI connectivity graphs. *Neuroimage* 56, 616–626. <https://doi.org/10.1016/j.neuroimage.2010.05.081>
- Richiardi, J., Van De Ville, D., Riesen, K., Bunke, H., 2010. Vector space embedding of undirected graphs with fixed-cardinality vertex sequences for classification. *Proc. - Int. Conf. Pattern Recognit.* 902–905. <https://doi.org/10.1109/ICPR.2010.227>
- Roelofs, K., Keijsers, G.P.J., Hoogduin, K.A.L., Näring, G.W.B., Moene, F.C., 2002. Childhood abuse in patients with conversion disorder. *Am. J. Psychiatry* 159, 1908–1913. <https://doi.org/10.1176/appi.ajp.159.11.1908>
- Roelofs, K., Pasman, J., 2016. Stress, childhood trauma, and cognitive functions in functional neurologic disorders, in: Hallett, M., Stone, J., Carson, A. (Eds.), *Handbook of Clinical Neurology*. Elsevier, pp. 139–155. <https://doi.org/10.1016/B978-0-12-801772-2.00013-8>
- Roelofs, K., Spinhoven, P., Sandijck, P., Moene, F.C., Hoogduin, K.A.L., 2005. The Impact of Early Trauma and Recent Life-Events on Symptom Severity in Patients With Conversion Disorder. *J. Nerv. Ment. Dis.* 193, 508–514. <https://doi.org/10.1097/01.nmd.0000172472.60197.4d>
- Rolls, E.T., Huang, C.-C., Lin, C.-P., Feng, J., Joliot, M., 2020. Automated anatomical labelling atlas 3. *Neuroimage* 206, 116189. <https://doi.org/10.1016/j.neuroimage.2019.116189>
- Rozycki, M., Satterthwaite, T.D., Koutsouleris, N., Erus, G., Doshi, J., Wolf, D.H., Fan, Y., Gur, R.E., Gur, R.C., Meisenzahl, E.M., Zhuo, C., Yin, H., Yan, H., Yue, W., Zhang, D., Davatzikos, C., 2018. Multisite Machine Learning Analysis Provides a Robust Structural Imaging Signature of Schizophrenia Detectable Across Diverse Patient Populations and Within Individuals. *Schizophr. Bull.* 44, 1035–1044. <https://doi.org/10.1093/schbul/sbx137>
- Ruiz-Padial, E., Sollers, J.J., Vila, J., Thayer, J.F., 2003. The rhythm of the heart in the blink of an eye: Emotion-modulated startle magnitude covaries with heart rate variability. *Psychophysiology* 40, 306–313. <https://doi.org/10.1111/1469-8986.00032>
- Russel, S.J., Norvig, P., 2009. *Artificial Intelligence: A Modern Approach*, Third Edit. ed. Upper Saddle River NJ; Prentice Hall.
- Schlotz, W., Hammerfald, K., Ehlert, U., Gaab, J., 2011. Individual differences in the cortisol response to stress in young healthy men: Testing the roles of perceived stress reactivity and threat appraisal using multiphase latent growth curve modeling. *Biol. Psychol.* 87, 257–264. <https://doi.org/10.1016/j.biopsycho.2011.03.005>
- Şenbabaoğlu, Y., Michailidis, G., Li, J.Z., 2014. Critical limitations of consensus clustering in class discovery. *Sci. Rep.* 4, 6207. <https://doi.org/10.1038/srep06207>
- Sendi, M.S.E., Zendehrouh, E., Sui, J., Fu, Z., Zhi, D., Lv, L., Ma, X., Ke, Q., Li, X., Wang, C., Abbott, C.C., Turner, J.A., Miller, R.L., Calhoun, V.D., 2021. Abnormal Dynamic Functional Network Connectivity Estimated from Default Mode Network Predicts Symptom Severity in Major Depressive Disorder. *Brain Connect.* 11, 838–849. <https://doi.org/10.1089/brain.2020.0748>
- Sepulcre, J., Sabuncu, M.R., Yeo, T.B., Liu, H., Johnson, K.A., 2012. Stepwise Connectivity of the Modal Cortex Reveals the Multimodal Organization of the Human Brain. *J. Neurosci.* 32, 10649–10661. <https://doi.org/10.1523/jneurosci.0759-12.2012>
- Sesack, S.R., Grace, A.A., 2010. Cortico-Basal Ganglia Reward Network: Microcircuitry. *Neuropsychopharmacology* 35, 27–47. <https://doi.org/10.1038/npp.2009.93>
- Shahid, A., Wilkinson, K., Marcu, S., Shapiro, C.M., 2011. Leeds Sleep Evaluation Questionnaire (LSEQ), in: *STOP, THAT and One Hundred Other Sleep Scales*. Springer New York, New York, NY, pp. 211–213. https://doi.org/10.1007/978-1-4419-9893-4_48
- Sitaram, R., Ros, T., Stoeckel, L., Haller, S., Scharnowski, F., Lewis-Peacock, J., Weiskopf, N., Blefari, M.L., Rana, M., Oblak, E., Birbaumer, N., Sulzer, J., 2017. Closed-loop brain training: the science of neurofeedback. *Nat. Rev. Neurosci.* 18, 86–100. <https://doi.org/10.1038/nrn.2016.164>
- Smith, S.M., Miller, K.L., Salimi-Khorshidi, G., Webster, M., Beckmann, C.F., Nichols, T.E., Ramsey, J.D., Woolrich, M.W., 2011. Network modelling methods for FMRI. *Neuroimage* 54, 875–891. <https://doi.org/10.1016/j.neuroimage.2010.08.063>

- Smith, S.M., Vale, W.W., 2006. The role of the hypothalamic-pituitary-adrenal axis in neuroendocrine responses to stress. *Dialogues Clin. Neurosci.* 8, 383–395.
- Sojka, P., Slovák, M., Věchetová, G., Jech, R., Perez, D.L., Serranová, T., 2022. Bridging structural and functional biomarkers in functional movement disorder using network mapping. *Brain Behav.* 12, 1–5. <https://doi.org/10.1002/brb3.2576>
- Sokolov, A.A., Granziera, C., Fisch-Gomez, E., Preti, M.G., Ryvlin, P., Van De Ville, D., Friston, K.J., 2019. Brain network analyses in clinical neuroscience. *Swiss Arch. Neurol. Psychiatry Psychother.* <https://doi.org/10.4414/sanp.2019.03074>
- Spagnolo, P.A., Norato, G., Maurer, C.W., Goldman, D., Hodgkinson, C., Horovitz, S., Hallett, M., 2020. Effects of TPH2 gene variation and childhood trauma on the clinical and circuit-level phenotype of functional movement disorders. *J. Neurol. Neurosurg. Psychiatry* 1–8. <https://doi.org/10.1136/jnnp-2019-322636>
- Spengler, S., von Cramon, D.Y., Brass, M., 2009. Was it me or was it you? How the sense of agency originates from ideomotor learning revealed by fMRI. *Neuroimage* 46, 290–298. <https://doi.org/10.1016/j.neuroimage.2009.01.047>
- Spielberger, C., Gorsuch, R., Lushene, R., Vagg, P., Jacobs, G., 1983. Manual for the State-Trait Anxiety Inventory (Form Y1 - Y2).
- Spinhoven, P., Roelofs, K., Moene, F., Kuyk, J., Nijenhuis, E., Hoogduin, K., Van Dyck, R., 2004. Trauma and dissociation in conversion disorder and chronic pelvic pain. *Int. J. Psychiatry Med.* 34, 305–318. <https://doi.org/10.2190/YDK2-C66W-CL6L-N5TK>
- Stalder, T., Evans, P., Hucklebridge, F., Clow, A., 2010. Associations between psychosocial state variables and the cortisol awakening response in a single case study. *Psychoneuroendocrinology* 35, 209–214. <https://doi.org/10.1016/j.psyneuen.2009.06.006>
- Stalder, T., Kirschbaum, C., Kudielka, B.M., Adam, E.K., Pruessner, J.C., Wüst, S., Dockray, S., Smyth, N., Evans, P., Hellhammer, D.H., Miller, R., Wetherell, M.A., Lupien, S.J., Clow, A., 2016. Assessment of the cortisol awakening response: Expert consensus guidelines. *Psychoneuroendocrinology* 63, 414–432. <https://doi.org/10.1016/j.psyneuen.2015.10.010>
- Stephen, C.D., Fung, V., Lungu, C.I., Espay, A.J., 2021. Assessment of Emergency Department and Inpatient Use and Costs in Adult and Pediatric Functional Neurological Disorders. *JAMA Neurol.* 78, 88. <https://doi.org/10.1001/jamaneurol.2020.3753>
- Stone, J., Carson, A., 2015. Functional Neurologic Disorders. *Contin. Lifelong Learn. Neurol.* 21, 818–837. <https://doi.org/10.1212/01.CON.0000466669.02477.45>
- Stone, J., Carson, A., Aditya, H., Prescott, R., Zaubi, M., Warlow, C., Sharpe, M., 2009a. The role of physical injury in motor and sensory conversion symptoms: A systematic and narrative review. *J. Psychosom. Res.* 66, 383–390. <https://doi.org/10.1016/j.jpsychores.2008.07.010>
- Stone, J., Carson, A., Duncan, R., Coleman, R., Roberts, R., Warlow, C., Hibberd, C., Murray, G., Cull, R., Pelosi, A., Cavanagh, J., Matthews, K., Goldbeck, R., Smyth, R., Walker, J., MacMahon, A.D., Sharpe, M., 2009b. Symptoms ‘unexplained by organic disease’ in 1144 new neurology out-patients: how often does the diagnosis change at follow-up? *Brain* 132, 2878–2888. <https://doi.org/10.1093/brain/awp220>
- Stone, J., Carson, A., Duncan, R., Roberts, R., Warlow, C., Hibberd, C., Coleman, R., Cull, R., Murray, G., Pelosi, A., Cavanagh, J., Matthews, K., Goldbeck, R., Smyth, R., Walker, J., Sharpe, M., 2010a. Who is referred to neurology clinics?—The diagnoses made in 3781 new patients. *Clin. Neurol. Neurosurg.* 112, 747–751. <https://doi.org/10.1016/j.clineuro.2010.05.011>
- Stone, J., LaFrance, W.C., Brown, R., Spiegel, D., Levenson, J.L., Sharpe, M., 2011. Conversion Disorder: Current problems and potential solutions for DSM-5. *J. Psychosom. Res.* 71, 369–376. <https://doi.org/10.1016/j.jpsychores.2011.07.005>
- Stone, J., LaFrance, W.C., Levenson, J.L., Sharpe, M., 2010. Issues for DSM-5: Conversion Disorder. *Am. J. Psychiatry* 167, 626–627. <https://doi.org/10.1176/appi.ajp.2010.09101440>
- Stone, J., Vermeulen, M., 2016. Functional sensory symptoms, 1st ed, *Functional Neurologic Disorders*. Elsevier B.V. <https://doi.org/10.1016/B978-0-12-801772-2.00024-2>
- Stone, J., Vuilleumier, P., Friedman, J.H., 2010b. Conversion disorder: Separating “how” from “why.” *Neurology* 74, 190–191. <https://doi.org/10.1212/WNL.0b013e3181cb4ea8>
- Stone, J., Zeman, A., Simonotto, E., Meyer, M., Azuma, R., Flett, S., Sharpe, M., 2007. fMRI in Patients With Motor Conversion Symptoms and Controls With Simulated Weakness. *Psychosom. Med.* 69, 961–969. <https://doi.org/10.1097/PSY.0b013e31815b6c14>
- Syed, T.U., LaFrance, W.C., Kahrman, E.S., Hasan, S.N., Rajasekaran, V., Gulati, D., Borad, S., Shahid, A., Fernandez-Baca, G., Garcia, N., Pawlowski, M., Loddenkemper, T., Amina, S., Koubeissi, M.Z., 2011. Can semiology predict psychogenic nonepileptic seizures? A prospective study. *Ann. Neurol.* 69, 997–1004. <https://doi.org/10.1002/ana.22345>
- Szaflarski, J.P., Allendorfer, J.B., Nenert, R., LaFrance, W.C., Barkan, H.I., DeWolfe, J., Pati, S., Thomas, A.E., Ver Hoef, L., 2018. Facial emotion processing in patients with seizure disorders. *Epilepsy Behav.* 79, 193–204. <https://doi.org/10.1016/j.yebeh.2017.12.004>
- Tagliazucchi, E., Siniatchkin, M., Laufs, H., Chialvo, D.R., 2016. The Voxel-Wise Functional Connectome Can Be Efficiently Derived from Co-activations in a Sparse Spatio-Temporal Point-Process. *Front. Neurosci.* 10. <https://doi.org/10.3389/fnins.2016.00381>
- Taillieu, T.L., Brownridge, D.A., Sareen, J., Afifi, T.O., 2016. Childhood emotional maltreatment and mental disorders: Results from a nationally representative adult sample from the United States. *Child Abuse Negl.* 59, 1–12. <https://doi.org/https://doi.org/10.1016/j.chiabu.2016.07.005>

- Takamura, T., Hanakawa, T., 2017. Clinical utility of resting-state functional connectivity magnetic resonance imaging for mood and cognitive disorders. *J. Neural Transm.* 124, 821–839. <https://doi.org/10.1007/s00702-017-1710-2>
- Tasca, C., Rapetti, M., Carta, M.G., Fadda, B., 2012. Women And Hysteria In The History Of Mental Health 110–119.
- Teicher, M.H., Anderson, C.M., Ohashi, K., Polcari, A., 2014. Childhood Maltreatment: Altered Network Centrality of Cingulate, Precuneus, Temporal Pole and Insula. *Biol. Psychiatry* 76, 297–305. <https://doi.org/https://doi.org/10.1016/j.biopsych.2013.09.016>
- Teicher, M.H., Samson, J.A., 2013. Childhood maltreatment and psychopathology: A case for ecophenotypic variants as clinically and neurobiologically distinct subtypes. *Am. J. Psychiatry* 170, 1114–1133. <https://doi.org/10.1176/appi.ajp.2013.12070957>
- Teipel, S.J., Wohler, A., Metzger, C., Grimmer, T., Sorg, C., Ewers, M., Meisenzahl, E., Klöppel, S., Borchardt, V., Grothe, M.J., Walter, M., Dyrba, M., 2017. Multicenter stability of resting state fMRI in the detection of Alzheimer’s disease and amnesic MCI. *NeuroImage Clin.* 14, 183–194. <https://doi.org/10.1016/j.nicl.2017.01.018>
- Thomsen, B.L.C., Teodoro, T., Edwards, M.J., 2020. Biomarkers in functional movement disorders: A systematic review. *J. Neurol. Neurosurg. Psychiatry* 91, 1261–1269. <https://doi.org/10.1136/jnnp-2020-323141>
- Tiihonen, J., Kuikka, J., Viinamäki, H., Lehtonen, J., Partanen, J., 1995. Altered cerebral blood flow during hysterical paresthesia. *Biol. Psychiatry* 37, 134–135. [https://doi.org/10.1016/0006-3223\(94\)00230-Z](https://doi.org/10.1016/0006-3223(94)00230-Z)
- Tohka, J., Zijdenbos, A., Evans, A., 2004. Fast and robust parameter estimation for statistical partial volume models in brain MRI. *Neuroimage* 23, 84–97. <https://doi.org/10.1016/j.neuroimage.2004.05.007>
- Tzourio-Mazoyer, N., Landeau, B., Papathanassiou, D., Crivello, F., Etard, O., Delcroix, N., Mazoyer, B., Joliot, M., 2002. Automated anatomical labeling of activations in SPM using a macroscopic anatomical parcellation of the MNI MRI single-subject brain. *Neuroimage* 15, 273–289. <https://doi.org/10.1006/nimg.2001.0978>
- Uddin, L.Q., 2017. Functions of the Salience Network, in: *Salience Network of the Human Brain*. Elsevier, pp. 11–16. <https://doi.org/10.1016/B978-0-12-804593-0.00003-5>
- Vabalas, A., Gowen, E., Poliakoff, E., Casson, A.J., 2019. Machine learning algorithm validation with a limited sample size. *PLoS One* 14, e0224365. <https://doi.org/10.1371/journal.pone.0224365>
- van Buuren, M., Gladwin, T.E., Zandbelt, B.B., Kahn, R.S., Vink, M., 2010. Reduced functional coupling in the default-mode network during self-referential processing. *Hum. Brain Mapp.* 31, 1117–1127. <https://doi.org/10.1002/hbm.20920>
- Van den Bergh, O., Winters, W., Devriese, S., Van Diest, I., 2002. Learning subjective health complaints. *Scand. J. Psychol.* 43, 147–152. <https://doi.org/10.1111/1467-9450.00280>
- van den Heuvel, M.P., Hulshoff Pol, H.E., 2010. Exploring the brain network: A review on resting-state fMRI functional connectivity. *Eur. Neuropsychopharmacol.* 20, 519–534. <https://doi.org/10.1016/j.euroneuro.2010.03.008>
- van der Kruijs, S.J.M., Bodde, N.M.G., Vaessen, M.J., Lazon, R.H.C., Vonck, K., Boon, P., Hofman, P.A.M., Backes, W.H., Aldenkamp, A.P., Jansen, J.F.A., 2012. Functional connectivity of dissociation in patients with psychogenic non-epileptic seizures. *J. Neurol. Neurosurg. Psychiatry* 83, 239–247. <https://doi.org/10.1136/jnnp-2011-300776>
- Van Dijk, K.R.A., Sabuncu, M.R., Buckner, R.L., 2012. The influence of head motion on intrinsic functional connectivity MRI. *Neuroimage* 59, 431–438. <https://doi.org/10.1016/j.neuroimage.2011.07.044>
- van Oort, J., Tendolkar, I., Hermans, E.J., Mulders, P.C., Beckmann, C.F., Schene, A.H., Fernández, G., van Eijndhoven, P.F., 2017. How the brain connects in response to acute stress: A review at the human brain systems level. *Neurosci. Biobehav. Rev.* 83, 281–297. <https://doi.org/10.1016/j.neubiorev.2017.10.015>
- Vasta, R., Cerasa, A., Sarica, A., Bartolini, E., Martino, I., Mari, F., Metitieri, T., Quattrone, A., Gambardella, A., Guerrini, R., Labate, A., 2018. The application of artificial intelligence to understand the pathophysiological basis of psychogenic nonepileptic seizures. *Epilepsy Behav.* 87, 167–172. <https://doi.org/10.1016/j.yebeh.2018.09.008>
- Voon, V., Brezing, C., Gallea, C., Ameli, R., Roelofs, K., LaFrance, W.C., Hallett, M., 2010a. Emotional stimuli and motor conversion disorder. *Brain* 133, 1526–1536. <https://doi.org/10.1093/brain/awq054>
- Voon, V., Brezing, C., Gallea, C., Hallett, M., 2011. Aberrant supplementary motor complex and limbic activity during motor preparation in motor conversion disorder. *Mov. Disord.* 26, 2396–2403. <https://doi.org/10.1002/mds.23890>
- Voon, V., Cavanna, A.E., Coburn, K., Sampson, S., Reeve, A., Curt LaFrance, W., 2016. Functional neuroanatomy and neurophysiology of functional neurological disorders (Conversion disorder). *J. Neuropsychiatry Clin. Neurosci.* 28, 168–190. <https://doi.org/10.1176/appi.neuropsych.14090217>
- Voon, V., Gallea, C., Hattori, N., Bruno, M., Ekanayake, V., Hallett, M., 2010b. The involuntary nature of conversion disorder. *Neurology* 74, 223–228. <https://doi.org/10.1212/WNL.0b013e3181ca00e9>
- Vuilleumier, P., 2014. Brain circuits implicated in psychogenic paralysis in conversion disorders and hypnosis. *Neurophysiol. Clin.* 44, 323–337. <https://doi.org/10.1016/j.neucli.2014.01.003>
- Wahbeh, H., Oken, B.S., 2013. Salivary Cortisol Lower in Posttraumatic Stress Disorder. *J. Trauma. Stress* 26, 241–248. <https://doi.org/10.1002/jts.21798>
- Walzl, D., Carson, A.J., Stone, J., 2019. The misdiagnosis of functional disorders as other neurological conditions. *J. Neurol.* 266, 2018–2026. <https://doi.org/10.1007/s00415-019-09356-3>
- Weber, S., Heim, S., Richiardi, J., Ville, D. Van De, Aybek, S., 2022. Multi-centre classification of functional neurological disorders based on resting-state functional connectivity 35. <https://doi.org/10.1016/j.nicl.2022.103090>
- Wegrzyk, J., Kebets, V., Richiardi, J., Galli, S., de Ville, D. Van, Aybek, S., 2018. Identifying motor functional neurological disorder using resting-state functional connectivity. *NeuroImage Clin.* 17, 163–168. <https://doi.org/10.1016/j.nicl.2017.10.012>

- Werner, E.E., 2004. Journeys From Childhood to Midlife: Risk, Resilience, and Recovery. *Pediatrics* 114, 492–492. <https://doi.org/10.1542/peds.114.2.492>
- Wessa, M., Rohleder, N., Kirschbaum, C., Flor, H., 2006. Altered cortisol awakening response in posttraumatic stress disorder. *Psychoneuroendocrinology* 31, 209–215. <https://doi.org/10.1016/j.psyneuen.2005.06.010>
- Wheelock, M.D., Harnett, N.G., Wood, K.H., Orem, T.R., Granger, D.A., Mrug, S., Knight, D.C., 2016. Prefrontal cortex activity is associated with biobehavioral components of the stress response. *Front. Hum. Neurosci.* 10, 1–12. <https://doi.org/10.3389/fnhum.2016.00583>
- Whitfield-Gabrieli, S., Ford, J.M., 2012. Default Mode Network Activity and Connectivity in Psychopathology. *Annu. Rev. Clin. Psychol.* 8, 49–76. <https://doi.org/10.1146/annurev-clinpsy-032511-143049>
- Winterdahl, M., Miani, A., Vercoe, M.J.H., Ciofica, A., Uber-Zak, L., Rask, C.U., Zak, P.J., 2017. Vulnerability to psychogenic non-epileptic seizures is linked to low neuropeptide Y levels. *Stress* 20, 589–597. <https://doi.org/10.1080/10253890.2017.1378638>
- Womersley, J.S., Hemmings, S.M.J., Ziegler, C., Guttridge, A., Ahmed-Leitao, F., Rosenstein, D., Domschke, K., Seedat, S., 2020. Childhood emotional neglect and oxytocin receptor variants: Association with limbic brain volumes. *World J. Biol. Psychiatry* 21, 513–528. <https://doi.org/10.1080/15622975.2019.1584331>
- World Health Organization, 1993. The ICD-10 classification of mental and behavioural disorders. World Health Organization, Genève, Switzerland.
- Wu, C.W., Lin, S.H.N., Hsu, L.M., Yeh, S.C., Guu, S.F., Lee, S.H., Chen, C.C., 2020. Synchrony Between Default-Mode and Sensorimotor Networks Facilitates Motor Function in Stroke Rehabilitation: A Pilot fMRI Study. *Front. Neurosci.* 14, 1–11. <https://doi.org/10.3389/fnins.2020.00548>
- Wulf, G., 2013. Attentional focus and motor learning: a review of 15 years. *Int. Rev. Sport Exerc. Psychol.* 6, 77–104. <https://doi.org/10.1080/1750984X.2012.723728>
- Wust, S., Wolf, J., Hellhammer, D.H., Federenko, I., Schommer, N., Kirschbaum, C., 2000. The cortisol awakening response - normal values and confounds. *Noise Health* 2, 79–88.
- Xia, C.H., Ma, Z., Ciric, R., Gu, S., Betzel, R.F., Kaczkurkin, A.N., Calkins, M.E., Cook, P.A., García de la Garza, A., Vandekar, S.N., Cui, Z., Moore, T.M., Roalf, D.R., Ruparel, K., Wolf, D.H., Davatzikos, C., Gur, R.C., Gur, R.E., Shinohara, R.T., Bassett, D.S., Satterthwaite, T.D., 2018. Linked dimensions of psychopathology and connectivity in functional brain networks. *Nat. Commun.* 9, 3003. <https://doi.org/10.1038/s41467-018-05317-y>
- Xia, M., Wang, J., He, Y., 2013. BrainNet Viewer: A Network Visualization Tool for Human Brain Connectomics. *PLoS One* 8, e68910. <https://doi.org/10.1371/journal.pone.0068910>
- Yamashita, A., Yahata, N., Itahashi, T., Lisi, G., Yamada, T., Ichikawa, N., Takamura, M., Yoshihara, Y., Kunimatsu, A., Okada, N., Yamagata, H., Matsuo, K., Hashimoto, R., Okada, G., Sakai, Y., Morimoto, J., Narumoto, J., Shimada, Y., Kasai, K., Kato, N., Takahashi, H., Okamoto, Y., Tanaka, S.C., Kawato, M., Yamashita, O., Imamizu, H., 2019. Harmonization of resting-state functional MRI data across multiple imaging sites via the separation of site differences into sampling bias and measurement bias. *PLOS Biol.* 17, e3000042. <https://doi.org/10.1371/journal.pbio.3000042>
- Yang, Y., Wang, J.-Z., 2017. From Structure to Behavior in Basolateral Amygdala-Hippocampus Circuits. *Front. Neural Circuits* 11. <https://doi.org/10.3389/fncir.2017.00086>
- Yehuda, R., Ph, D., 2001. Biology of Posttraumatic Stress Disorder *rig ht a du Pr* 62, 41–46.
- Yehuda, R., Seckl, J., 2011. Minireview: Stress-related psychiatric disorders with low cortisol levels: A metabolic hypothesis. *Endocrinology* 152, 4496–4503. <https://doi.org/10.1210/en.2011-1218>
- Yeo, T., Krienen, F.M., Sepulcre, J., Sabuncu, M.R., Lashkari, D., Hollinshead, M., Roffman, J.L., Smoller, J.W., Zöllei, L., Polimeni, J.R., Fischl, B., Liu, H., Buckner, R.L., 2011. The organization of the human cerebral cortex estimated by intrinsic functional connectivity. *J. Neurophysiol.* 106, 1125–1165. <https://doi.org/10.1152/jn.00338.2011>
- Yeung, E.W., Davis, M.C., Ciaramitaro, M.C., 2016. Cortisol Profile Mediates the Relation Between Childhood Neglect and Pain and Emotional Symptoms among Patients with Fibromyalgia. *Ann. Behav. Med.* 50, 87–97. <https://doi.org/10.1007/s12160-015-9734-z>
- Yu, M., Linn, K.A., Cook, P.A., Phillips, M.L., McInnis, M., Fava, M., Trivedi, M.H., Weissman, M.M., Shinohara, R.T., Sheline, Y.I., 2018. Statistical harmonization corrects site effects in functional connectivity measurements from multi-site fMRI data. *Hum. Brain Mapp.* 39, 4213–4227. <https://doi.org/10.1002/hbm.24241>
- Zeng, L.-L.L., Wang, H., Hu, P., Yang, B., Pu, W., Shen, H., Chen, X., Liu, Z., Yin, H., Tan, Q., Wang, K., Hu, D., 2018. Multi-Site Diagnostic Classification of Schizophrenia Using Discriminant Deep Learning with Functional Connectivity MRI. *EBioMedicine* 30, 74–85. <https://doi.org/10.1016/j.ebiom.2018.03.017>
- Zhang, W., Hashemi, M.M., Kaldewaij, R., Koch, S.B.J., Beckmann, C., Klumpers, F., Roelofs, K., 2019. Acute stress alters the ‘default’ brain processing. *Neuroimage* 189, 870–877. <https://doi.org/10.1016/j.neuroimage.2019.01.063>
- Zhao, N., Yuan, L.-X.X., Jia, X.-Z.Z., Zhou, X.-F.F., Deng, X.-P.P., He, H.-J.J., Zhong, J., Wang, J., Zang, Y.-F.F., 2018. Intra- and Inter-Scanner Reliability of Voxel-Wise Whole-Brain Analytic Metrics for Resting State fMRI. *Front. Neuroinform.* 12, 1–9. <https://doi.org/10.3389/fninf.2018.00054>
- Zhao, S., Uono, S., Li, C., Yoshimura, S., Toichi, M., 2018. The Influence of Self-Referential Processing on Attentional Orienting in Frontoparietal Networks. *Front. Hum. Neurosci.* 12. <https://doi.org/10.3389/fnhum.2018.00199>
- Zhao, S., Uono, S., Yoshimura, S., Toichi, M., 2015. Self make-up: the influence of self-referential processing on attention orienting. *Sci. Rep.* 5, 14169. <https://doi.org/10.1038/srep14169>
- Zhuang, H., Liu, R., Wu, C., Meng, Z., Wang, D., Liu, D., Liu, M., Li, Y., 2019. Multimodal classification of drug-naïve first-

episode schizophrenia combining anatomical, diffusion and resting state functional resonance imaging. *Neurosci. Lett.* 705, 87–93. <https://doi.org/10.1016/j.neulet.2019.04.039>

Zöller, D., Sandini, C., Karahanoglu, F.I., Padula, M.C., Schaer, M., Eliez, S., Van De Ville, D., 2019. Large-Scale Brain Network Dynamics Provide a Measure of Psychosis and Anxiety in 22q11.2 Deletion Syndrome. *Biol. Psychiatry Cogn. Neurosci. Neuroimaging* 4, 881–892. <https://doi.org/10.1016/j.bpsc.2019.04.004>

Samantha Weber

Curriculum Vitae

📍 *Werkgasse 57
3018 Bern
Canton of Bern,
Switzerland*

☎ *+41 (79) 547 90 79*

✉ samantha.weber@extern.insel.ch
🌐 [linkedin.com/in/samantha-weber-357470223](https://www.linkedin.com/in/samantha-weber-357470223)



Personal Profile

I am a highly motivated and enthusiastic **Neuroscientist**, who possesses a profound knowledge in the health science related fields. With my inquisitive mind and driven by passion for clinical neuroscience, I aim at continuously growing beyond myself. During my PhD in Neuroscience at the University of Bern, I endeavoured to identify objective biomarkers for individuals suffering from a functional neurological disorder by exploiting my experience with new technologies (e.g., fMRI, genetics, endocrinology, machine learning).

Education

- 05/2019 – now **Doctor of Philosophy**, *University of Bern*, Switzerland (119th in the 2022 World University Ranking), PhD in Neuroscience
Project Title: “The role of stress on neuropathophysiological mechanisms in functional neurological disorders.”
Additional Studies: Postulating to BENEFRI Neuroscience Program
Supervision of three master students in medicine for master thesis
- 09/2017 – 04/2019 **Master of Science**, *ETH Zurich*, Switzerland (8th in the 2022 World University Ranking), Health Science and Technology, Major Neuroscience
GPA: 5.6/6
Focus: Obtaining a broad conceptual and methodological training to solve neuroscientific research question through molecular, cellular as well as systemic approaches.
Department: *Health Science and Technology*
- 09/2013 – 08/2016 **Bachelor of Science**, *ETH Zurich*, Switzerland (8th in the 2022 World University Ranking)
GPA: 4.76/6
Department: *Health Science and Technology*
- 09/2008 – 07/2012 **Matura**, *Stiftsschule Einsiedeln*, Switzerland
GPA: 4.9/6
Major in: Ancient Greek and Latin

Research Experience

- 09/2022 – 09/2022 **External Doctoral Student**
Fundación Pública Galega de Medicina Xenómica, Universidad Santiago de Compostela, Spain (533rd in the 2022 World University Ranking)
Focus: Acquisition of profound knowledge on statistical analyses of genomic data.
Supervisor: Prof. Dr. med. Ángel Carracedo, Juan Ansede-Bermejo
- 10/2018 – 03/2019 **Master Thesis, University Hospital Inselspital Bern, Switzerland**
Title: “Identification of Functional Neurological Disorder by a Support Vector Machine based on the Resting-State Functional Connectivity”
GPA: 5.75/6
Supervisor: Prof. Nicole Wenderoth
Co-Advisor: Prof. Dr. med. Selma Aybek
Location: Functional Neurological Disorders Group, University Hospital Bern, Switzerland
Department: Neurology, Psychosomatic Medicine Unit, Inselspital Bern, Switzerland
- 08/2017 – 03/2018 **Research Internship**
CRPP Sleep and Health Laboratory, University Hospital Zurich, Switzerland
Focus: Acquisition of relevant laboratory techniques, Influence of sleep on animal model (rats) with Traumatic Brain Injury (TBI)
Supervisor: Dr. nat. sci. Daniela Noaín and PhD Filipe Carlos Gonçalves Moreira
- 09/2016 – 01/2017 **Research Internship**
Anatomical Institute, University of Zurich, Switzerland (90th in the 2019 World University Ranking)
Focus: Behavioural experiments on mouse model of Alzheimer’s disease
Supervisor: Prof. Dr. med. David P. Wolfer and PhD Ann-Kristina Fritz

Teaching Experience

- 08/2017 – 03/2019 **Private lessons teacher**
Private and group lectures
- 06/2018 – 06/2018 **Teaching Assistant**
Topic: Laboratory Course in Molecular Biology
Laboratory of Translational Nutrition Biology, ETH Zurich, Switzerland
Department: Health Science and Technology
- 09/2016 – 12/2016 **Teaching Assistant**
Topic: Laboratory Course in Sports Physiology
Exercise Physiology Lab, ETH Zurich, Switzerland
Department: Health Science and Technology
- 02/2016 – 06/2016 **Teaching Assistant**
Topic: Laboratory Course in Eye Physiology
Exercise Physiology Lab, ETH Zurich, Switzerland
Department: Health Science and Technology

02/2021 – 04/2022

Supervision Master students Medicine

Topic: Stress in FND

FND Research Lab

Department of Neurology, Psychosomatic Medicine Unit, Inselspital Bern, Switzerland

Scholarships & Awards

03/2017

Munich Brain Course 2017, Ludwig Maximilian University of Munich, Germany (64th in the 2022 World University Ranking)

12/2019

Top 15% final GPA, Health Science and Technology, *ETH Zürich* (8th in the 2022 World University Ranking)
Average grade: 5.6/6

05/2022

Grant for “Finanzierung zur Anstellungsverlängerung von Nachwuchsforschenden aufgrund von COVID-19”, 2022, *University of Bern* (119th in the 2022 World University Ranking)

Personal Skills

Language(s)

German: Native Language

English: Written and oral advanced (C1/2)

Spanish: Fluent (B2/C1)

*Levels: A1/2: basic user – B1/2: Independent user – C1/2: Proficient user
Common European Framework of References for Languages*

Technical Skills

Simulation:	MATLAB, diverse toolkits for fMRI data analysis, machine learning	●●●●●
Clinical Trial:	Ethical Conduct Regulations, Clinical Trial Design and Ethical Approvals, Academic communication, Good Clinical Practice, RedCap database	●●●●●
Tools:	Magnetic resonance imaging (MRI), neurostimulation (i.e., transcranial magnetic stimulation)	●●●●○
Statistics:	R, Jasp, SPSS	●●●●●
Design:	Adobe Photoshop	●○○○○
Others:	Ethovision, Eppi-Reviewer	●●●○○

Rating: 1: basics, 2: average, 3: good, 4: very good, 5: excellent

Laboratory Skills

DNA/RNA Extraction, Amplification, Purification, and Quantification
Stereological Analyses
Immunohistostaining

Personal Skills

Works efficiently, determined, and goal-oriented
Excellent planning and time management
Autonomous, fast, rather visual learner
High teaching qualities

List of Publications

- Journal article “*Behavioural Differences Across Theta Burst Stimulation Protocols. A Study on the Sense of Agency in Healthy Humans.*” Zito GA, Worbe Y, Lamy JC, Kälin J, Bühler J, **Weber S**, Müri RM & Aybek S (2021). *Frontiers in neuroscience*, 15, 658-688. <https://doi.org/10.3389/fnins.2021.658688> *Published*
- Journal article “*Multivariate classification provides a neural signature of Tourette disorder.*” Zito GA, Hartmann A, Béranger B, **Weber S**, Aybek S, Faouzi J, Roze E, Vidailhet R, Worbe Y (2021). *Psychological Medicine*, 1-9. doi:10.1017/S0033291721004232 *Published*
- Journal article “*Multi-centre classification of functional neurological disorders based on resting-state functional connectivity*” **Weber S**, Heim S, Richiardi J, Van De Ville D, Serranová T, Jech R, Marapin RS, de Koning-Tijssen M, Aybek S (2022). *NeuroImage: Clinical*, 35, <https://doi.org/10.1016/j.nicl.2022.103090> *Published*
- Journal article “*Identification of biopsychological trait markers in functional neurological disorders.*” **Weber S**, Bühler J, Vanini G, Loukas S., Bruckmaier R, Aybek S. *Brain*, 2022 <https://doi.org/10.1093/brain/awac442> *Published*
- Journal article “*Transient Resting-State Co-activation Patterns of Limbic Brain Network in Functional Neurological Disorders.*” **Weber S**, Loukas S., Bühler J, Vanini G, Bolton, T., Bruckmaier R, Aybek S. *In Preparation*
- Journal article “*Local temporal variability during rest in functional neurological disorders.*” Schneider A & **Weber S**, Loukas S, Bühler J, Aybek S. *In Preparation*
- Journal article “*Case-Control Study on Demographic Data in Functional Neurological Disorders.*” Vanini G, Bühler J, **Weber S**, Aybek S. *In Preparation*

Journal article *“The Effect of Transcranial Magnetic Stimulation on Sense of Agency in Functional Neurological Disorders.”* Bühler J, **Weber S**, Loukas S, Gninenko N, Aybek S. *In Preparation*

Declaration of Originality

Last name, first name: Weber, Samantha

Matriculation number: 13-919-030

I hereby declare that this thesis represents my original work and that I have used no other sources except as noted by citations.

All data, tables, figures and text citations which have been reproduced from any other source, including the internet, have been explicitly acknowledged as such.

I am aware that in case of non-compliance, the Senate is entitled to withdraw the doctorate degree awarded to me on the basis of the present thesis, in accordance with the “Statut der Universität Bern (Universitätsstatut; UniSt)”, Art. 69, of 7 June 2011.

Place, date

Signature

Appendix A
Supplementary Material for Chapter 2

Conversion to CGI score

The CGI score of centre II and IV as well as the S-FMDRS score of centre III was converted into the same CGI score as in centre I.

Table A.1: Conversion of CGI score.

CGI (centre I)	CGI (centre II, IV)	S-FMDRS (centre III)
0 = none	0 = none 1	0 = none
1 = mild	2 = mild 3	1 - 9 = mild
2 = moderate	4 = moderate	10 - 18 = moderate
3 = severe	5 = severe 6	19 - 36 = severe
4 = very severe	7 = very severe	37 - 54 = very severe

Optimal Filter

Each centre was pre-processed individually. Based on previous work of Richiardi and colleagues (Richiardi et al., 2011), we calculated a functional atlas based on a structural atlas. The structural atlas only served as a basis to compute the subject-specific low-resolution functional atlas. We extracted the region-averaged time-course from the voxels which correspond to the individual regions. Assuming t timepoints, we have then a tensor matrix for each centre of size

$$X: t \times r \times s, \quad (1)$$

with r equals the number of regions and s equals the number of subjects. For the **intra-centre cross-validation** setting, we decided to explore the different filter options because of the potential differences in the functional connectivity graphs in different frequency subbands. Such differences might arise from the scanners itself such as mechanical resonance, manufacturer and model of the scanner, scanner sequence, etc.). Doing so, we can explore the diversity in classification performance within different filters and subbands, in which the classifier might build a model with substantially different parameters. Therefore, we optimized each centre independently.

To do so, we used two different filtering pipelines Figure A.1. In the first pipeline, the data was filtered in the time domain using a bandpass filter 0.01-0.08 Hz, which is most commonly used for resting-state data. In a second pipeline, the same data was filtered using a discrete wavelet transform along the temporal dimension, as it has been done in the previous project (Wegrzyk et al., 2018). Five frequency subbands were extracted with main bandpass

characteristics at 0.125–0.25 Hz, 0.0625–0.125 Hz, 0.0312–0.0625 Hz, 0.0156 – 0.0312 Hz, and 0.0078 – 0.0156 Hz based on the repetition time (TR) = 2000ms.

During the **pooled- and inter-scanner cross-validation**, however, we used the bandpass-filtered data, in order to maintain a uniform pre-processing pipeline across all the four centres.

Upon filtering, we then used the filtered region-averaged time courses to compute functional connectivity (i.e., Pearson correlation) between different regions of interests (ROIs) leading to an $r \times r$ matrix for each subject. We then used direct graph embedding, as described in (Richiardi et al., 2011), in order to build our feature vectors.

Optimal Filter Selection for Classification

We explored the performance on the classification for the different filters and subbands of filters. The best performance in the intra-centre cross-validation was achieved using bandpass filter for centre I, wavelets filter subband 2 for centre II, and wavelets subband 5 for centre III and IV. These results are presented in Chapter 2: Multi-centre Classification using Resting-state Functional Connectivity.

Figure A.1: Workflow of filtering pipelines. For the intra-centre cross-validation settings both pipelines were applied to the data and different classification performances (based on different filtering pipelines) were examined. For pooled- and inter-centre cross-validation, only pipeline 1 (bandpass filter) was used in order to maintain a uniform pre-processing pipeline across all centres.

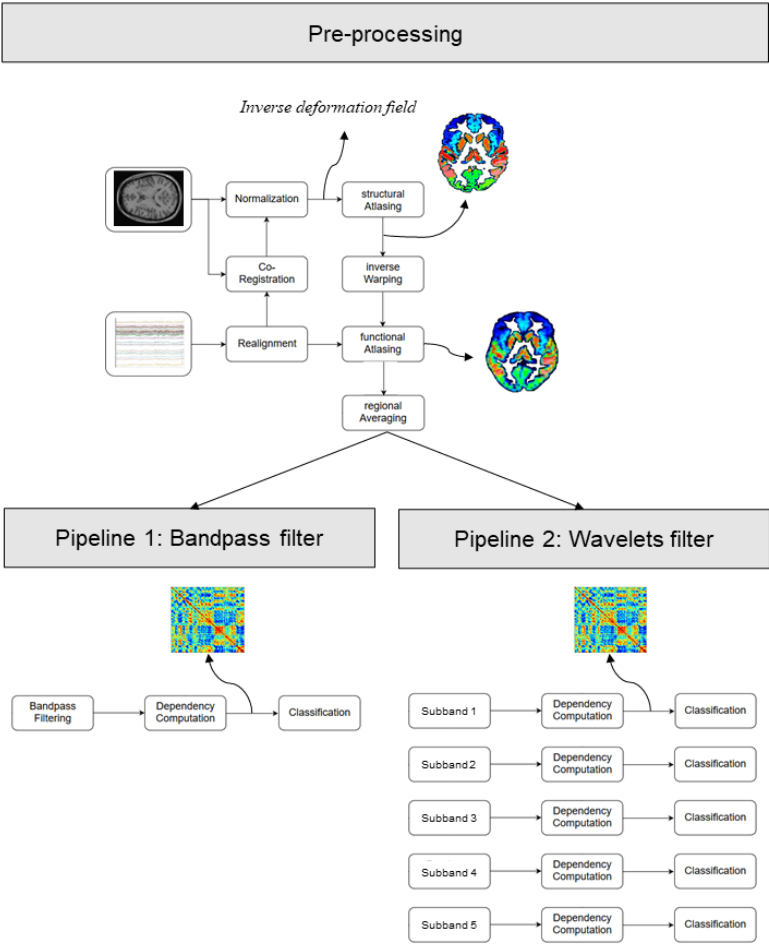


Figure A.2: Mean Framewise displacement (FD) per centre. FD measures showed a significant main effect of *centre* ($F(3,164) = 5.5, P = 0.001$). Post-hoc multiple comparison of means showed that the difference between centre I and centre III ($P < 0.0001$) and centre IV ($P = 0.0006$), as well as between centre II and centre III ($P = 0.0002$) and IV ($P = 0.008$) were statistically significant. Significance code *** $P \leq 0.001$, ** $P \leq 0.01$, * $P \leq 0.05$.

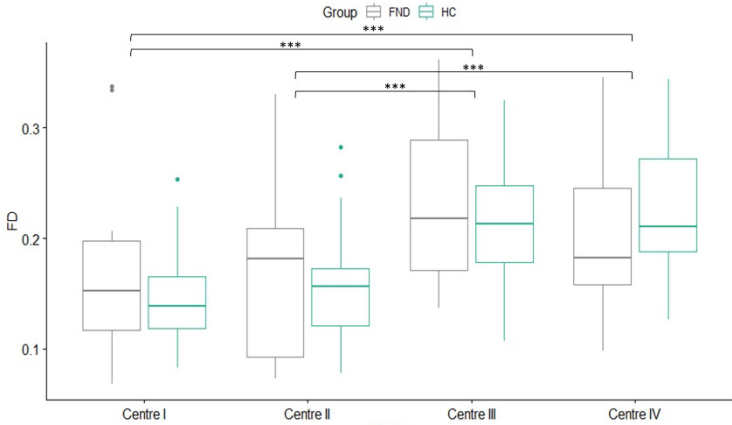
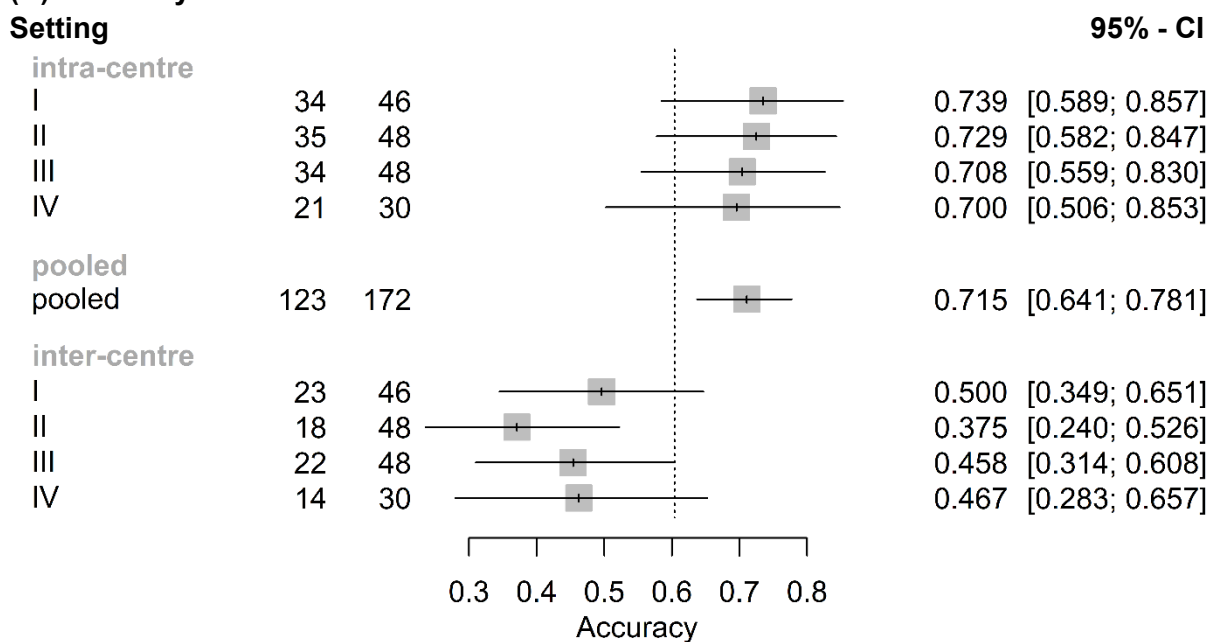
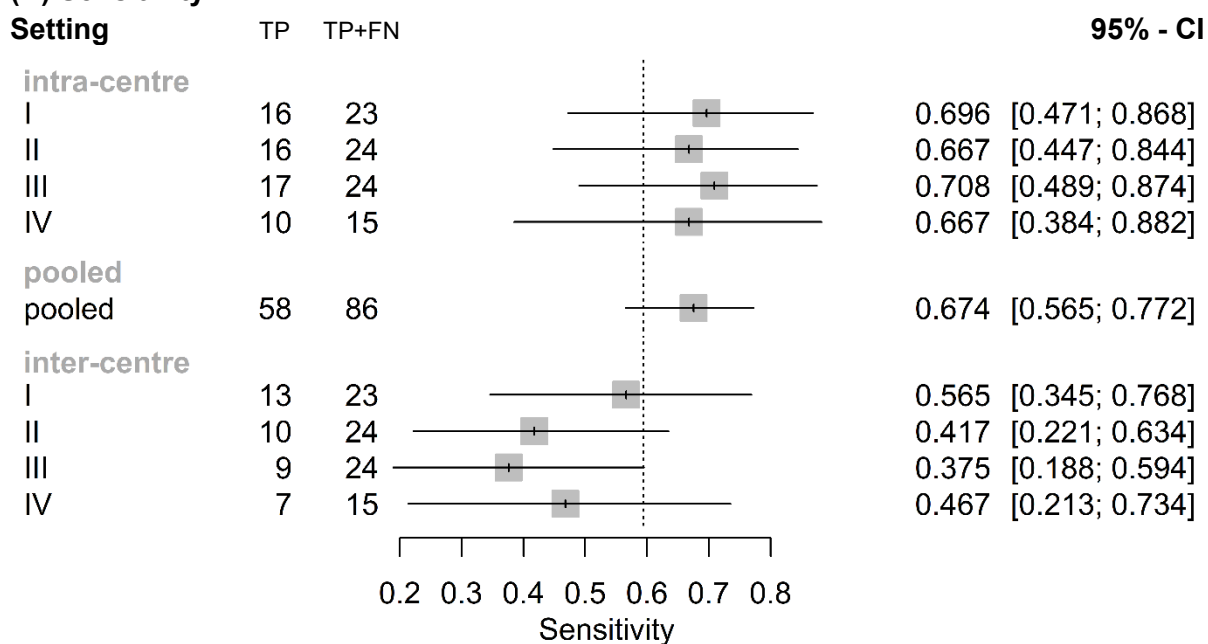


Figure A.3: Results across centres and settings. (A) Accuracy, (B) Sensitivity, and (C) Specificity with 95% confidence interval (95% - CI) of the different classification settings.

(A) Accuracy



(B) Sensitivity



(C) Specificity

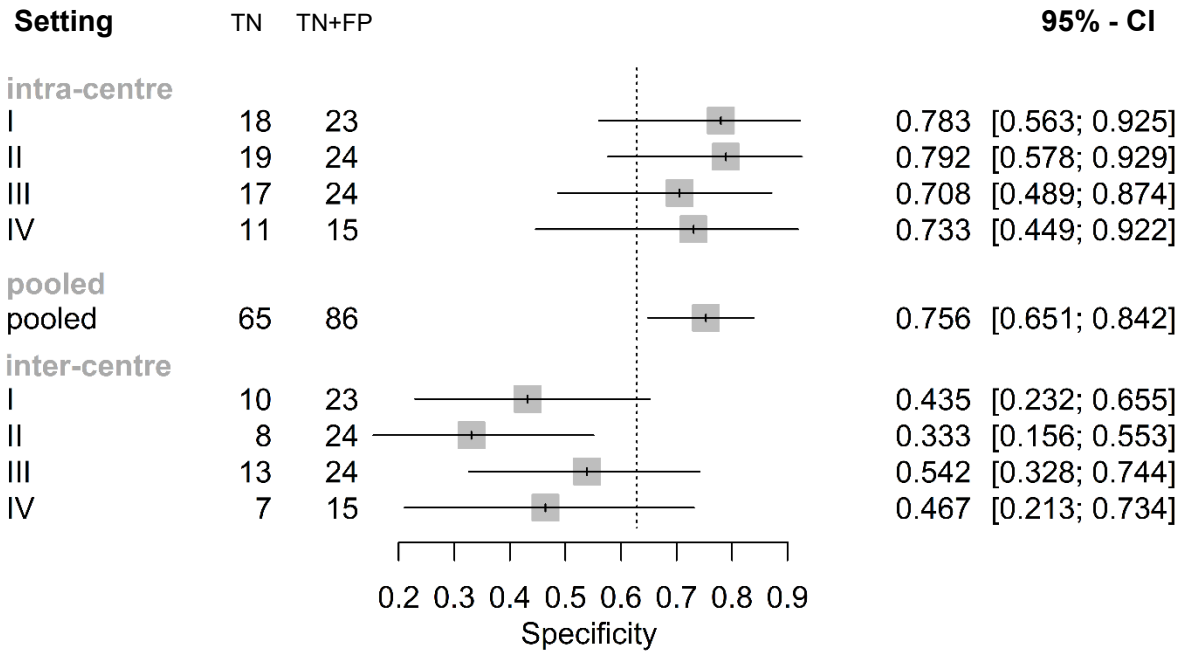
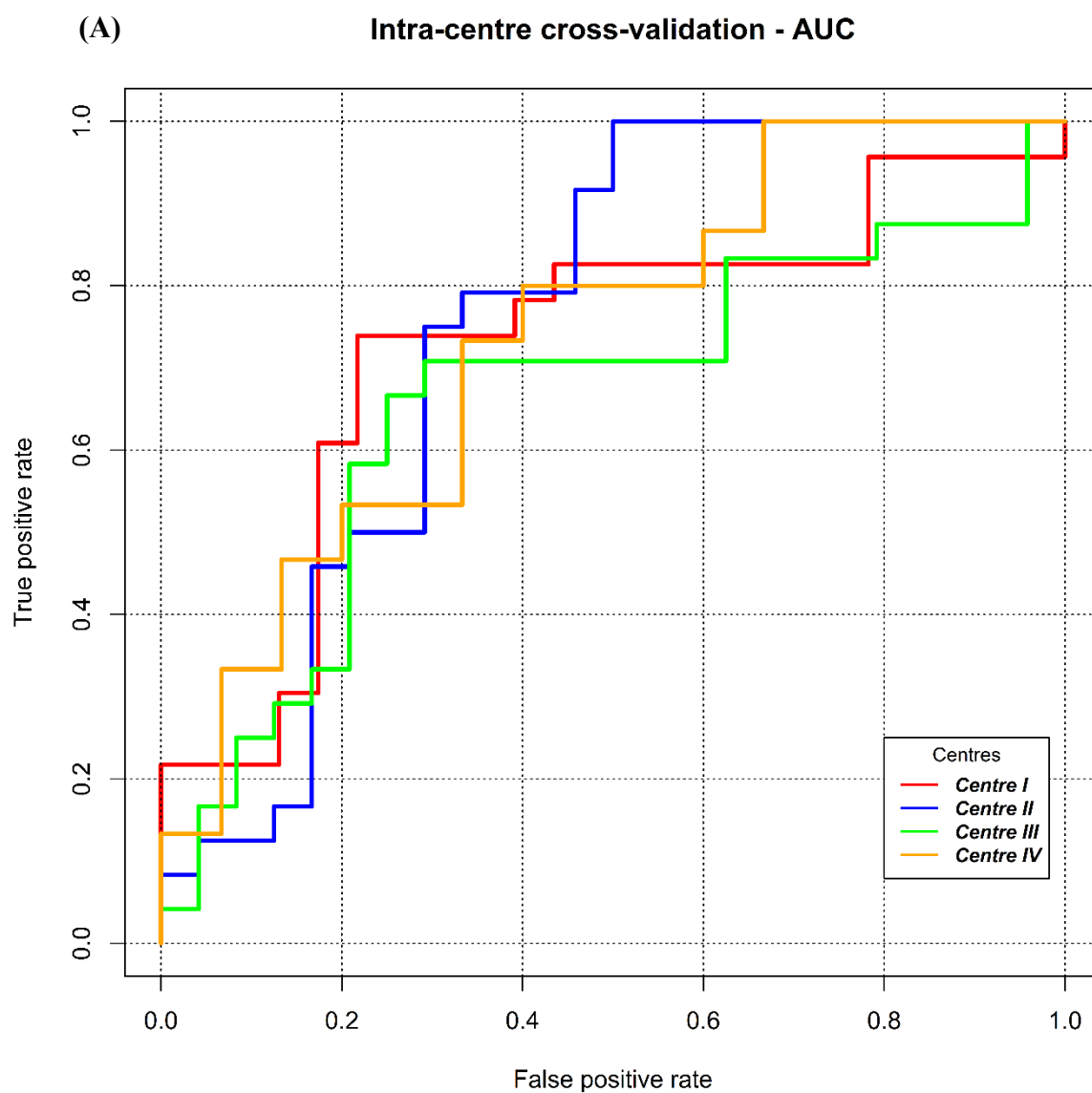


Figure A.4: Area-under-the-curve (AUC) with 95% confidence interval (95% - CI) for the individual classification obtained with each setting. (A) Intra-centre cross-validation classification, and (B) inter-centre cross-validation classification.



(B) Inter-centre cross-validation - AUC

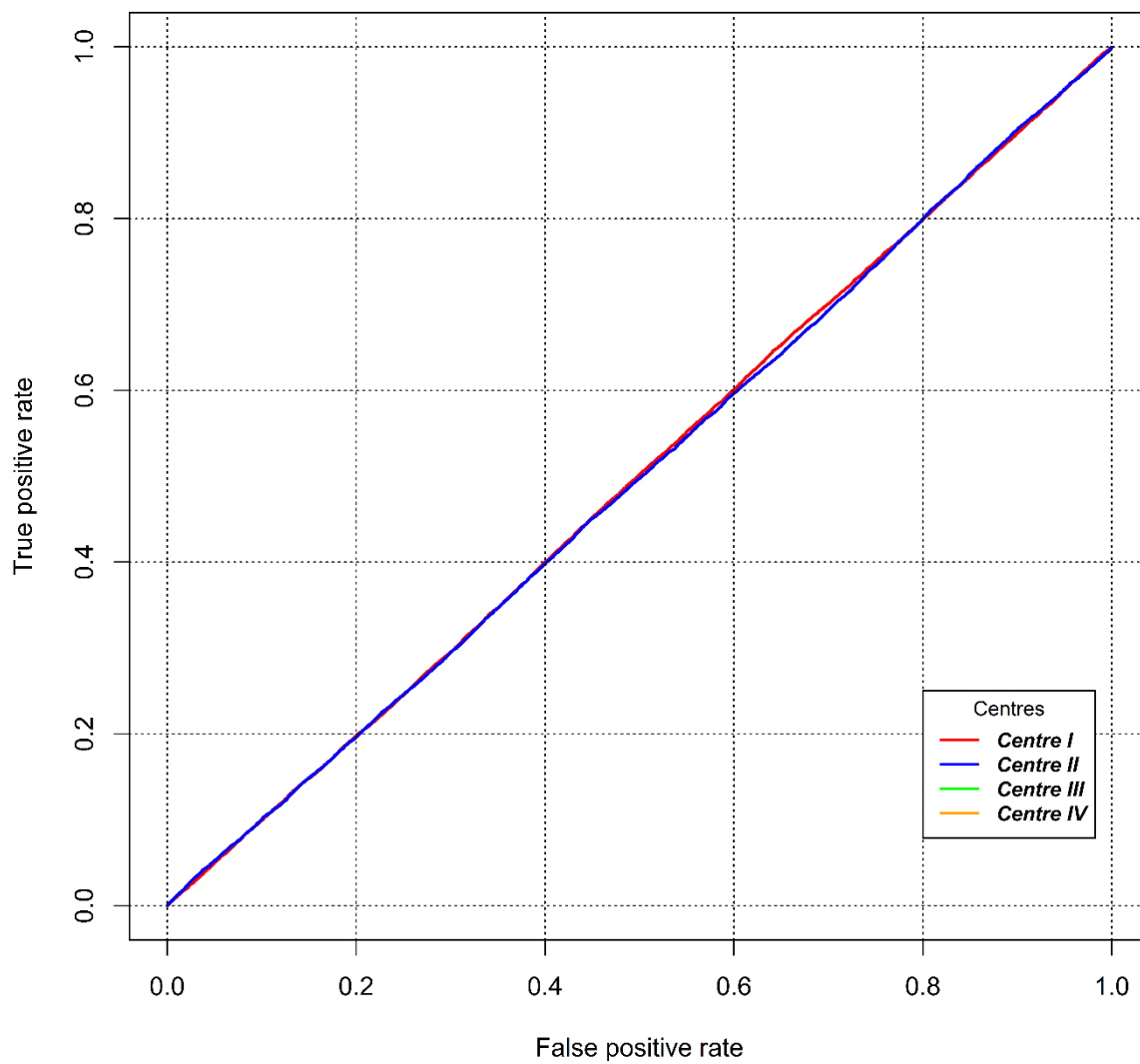


Figure A.5: Functional connectivity of regions yielding the most discriminative connections of the pooled classification based on the AAL atlas. Size of the nodes correspond to nodal degree, respectively occurrence within the most discriminative connections. Colour of the nodes corresponds to different lobes of the AAL. Colour of the edges correspond to functional connectivity between the regions, i.e., red displaying hyperconnected and blue hypoconnected in patients compared to controls.

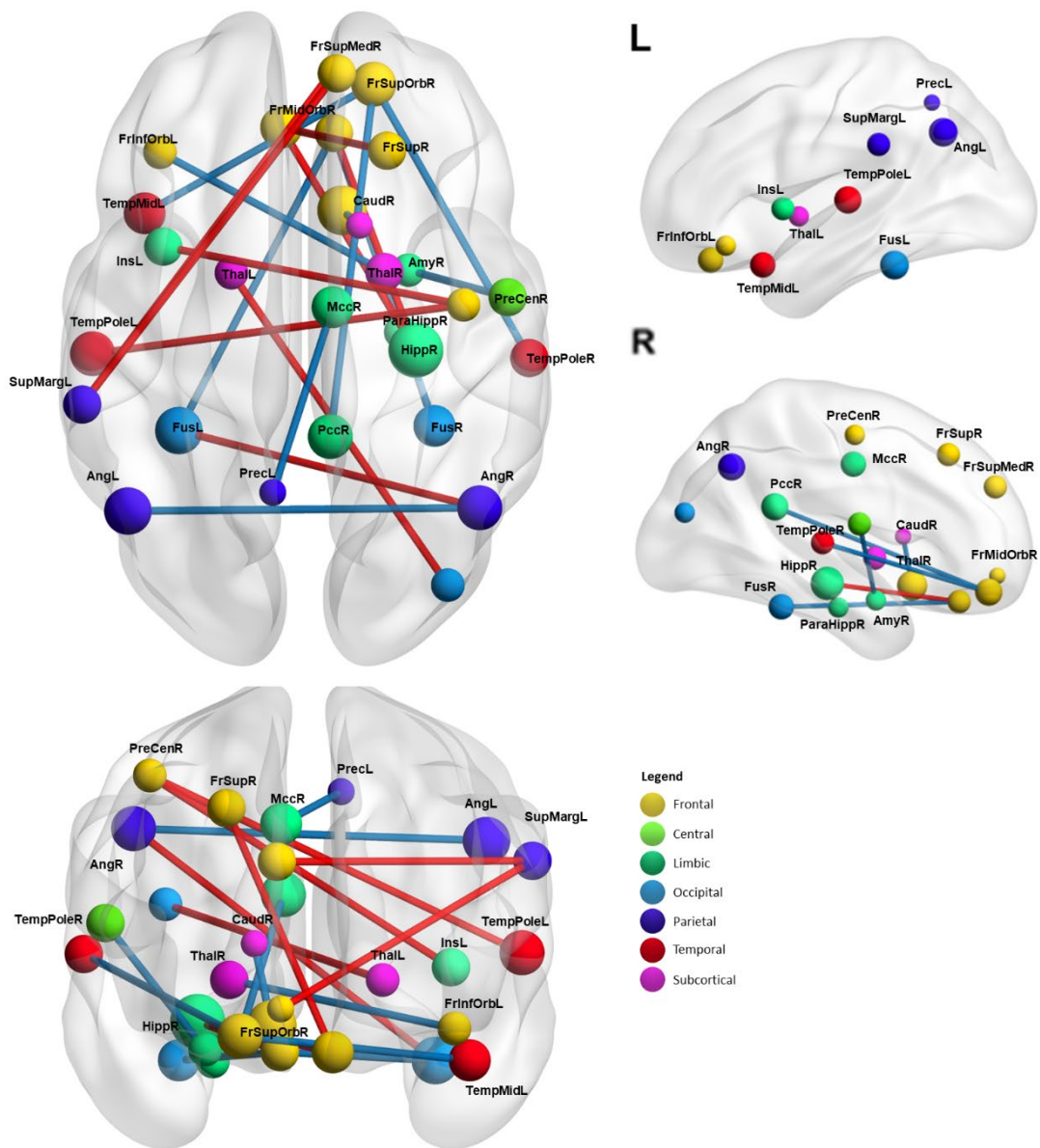
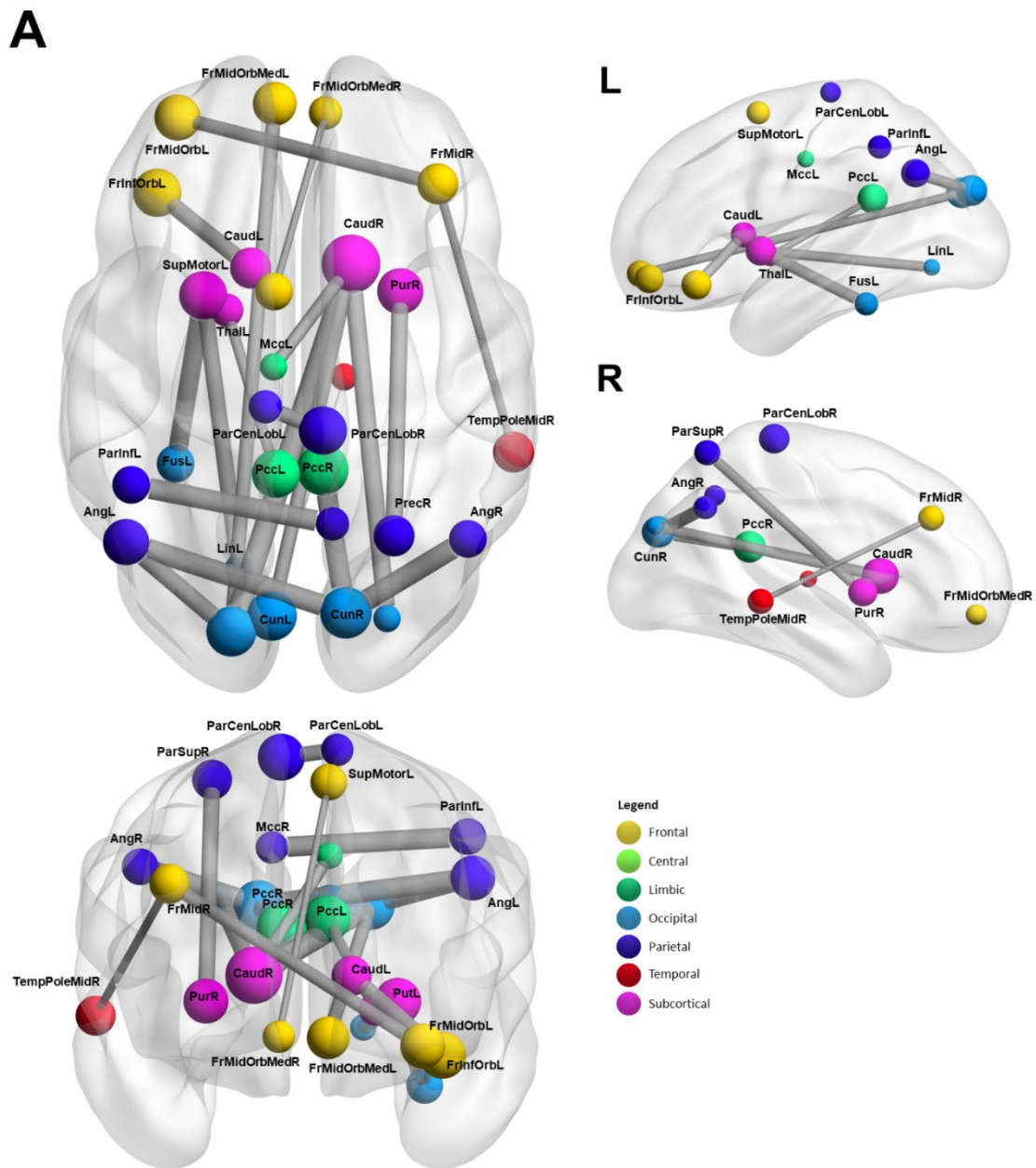


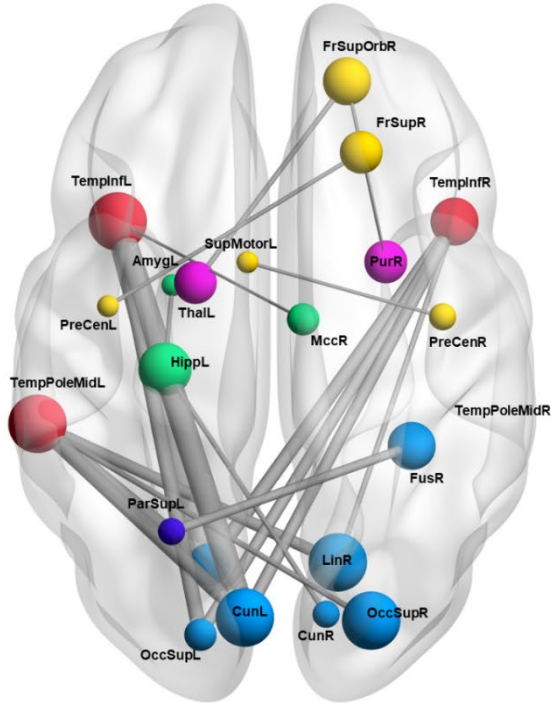
Table A.2: Mean functional connectivity in controls and patients between pairs of regions showing discriminative functional connectivity.

		HC	FND
Hippocampus_R	Rectus_L	0.182	-0.047
	Parahippocampal_R	0.352	0.115
	Rectus_R	0.187	-0.069
	Temporal_Pole_Sup_R	0.218	0.048
	Parahippocampal_L	0.287	0.085
	Frontal_Inf_Orb_R	0.127	-0.028
	Amygdala_L	0.236	0.112
	Putamen_L	0.084	-0.042
	Temporal_Sup_R	0.095	0.401
	Angular_L	Angular_R	0.485
	Occipital_Sup_L	-0.298	0.102
	Frontal_Sup_R	0.322	-0.069
	Lingual_L	-0.270	0.111
	Fusiform_L	-0.210	0.124
	Frontal_Mid_Orb_Medial_L	0.296	0.084
Angular_R	Fusiform_L	-0.184	0.139
	Parietal_Inf_L	0.052	0.269
	Precuneus_R	0.165	0.413
	Fusiform_R	-0.188	0.099
	Postcentral_L	-0.0207	0.128
Cingulum_Mid_R	Precuneus_L	0.018	0.308
	Frontal_Sup_R	0.065	0.279
	Frontal_Mid_Orb_Medial_L	-0.026	0.020
Cingulum_Post_R	Frontal_Sup_Orb_R	-0.126	0.116
	Occipital_Sup_R	-0.187	0.103
	Insula_R	-0.096	-0.139
	Thalamus_R	-0.002	0.182
	Frontal_Sup_Orb_L	-0.063	0.055
	Frontal_Inf_Tri_R	-0.102	-0.056
Cingulum_Ant_R	Caudate_R	0.220	0.023
Amygdala_R	Frontal_Mid_L	-0.061	-0.019
	Temporal_Inf_R	-0.054	0.184
	Amygdala_L	0.346	0.108
Hippocampus_L	Cingulum_Mid_L	-0.015	0.081
	Temporal_Pole_Mid_L	0.068	0.140
	Precuneus_R	-0.009	0.135
	Cingulum_Post_L	0.009	0.213
	Precuneus_L	0.012	0.173
	Amygdala_R	0.203	0.105
	Parahippocampal_R	0.296	0.122
	Temporal_Pole_Mid_R	0.037	0.168
SupraMarginal_R	Frontal_Mid_Orb_R	-0.037	0.101
	Temporal_Mid_L	-0.133	0.064
	Putamen_R	0.009	0.216
SupraMarginal_L	Frontal_Mid_L	0.059	0.053
	Frontal_Inf_Oper_L	0.267	0.171
Fusiform_L	Frontal_Mid_Orb_Medial_L	-0.188	0.191
	Frontal_Mid_Orb_R	-0.178	0.308
	Thalamus_R	-0.032	0.119
	Cingulum_Post_R	-0.120	0.117
	Frontal_Mid_Orb_L	-0.179	0.270

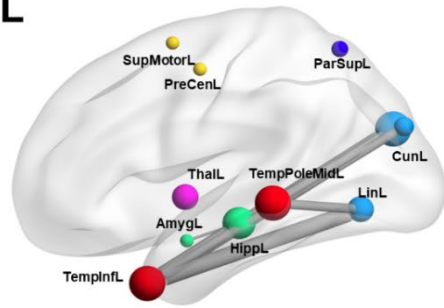
Figure A.6: Regions yielding the most discriminative connections for each centre based on the AAL atlas. Size of the nodes correspond to nodal degree, respectively occurrence within the 200 most discriminative connections. Colour of the nodes corresponds to different lobes of the AAL. Thickness of edges correspond to SVM weights. Thicker edges therefore indicate higher SVM weights, respectively higher discrimination power. **A) Centre I, B) Centre II, C) Centre III, and D) Centre IV.**



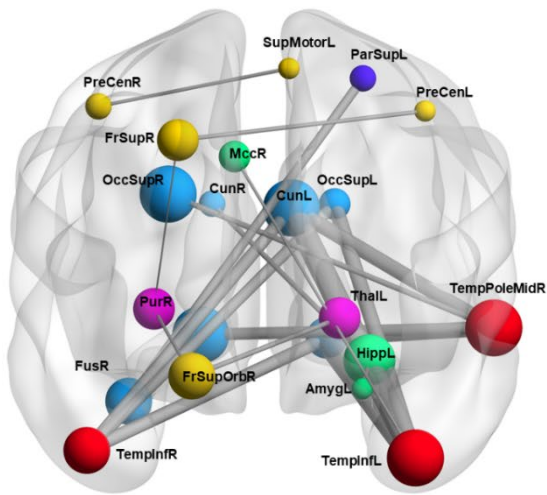
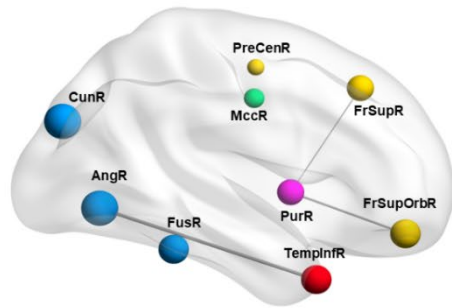
B



L



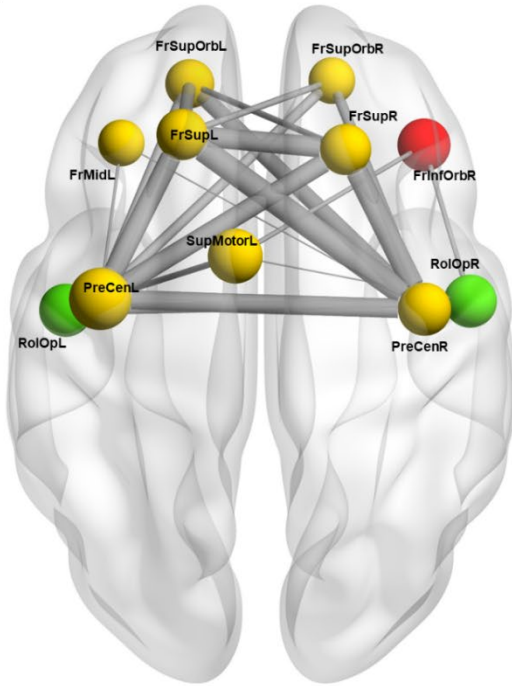
R



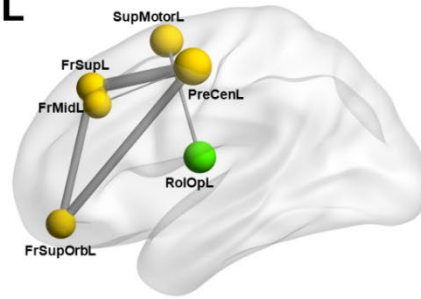
Legend

- Frontal
- Central
- Limbic
- Occipital
- Parietal
- Temporal
- Subcortical

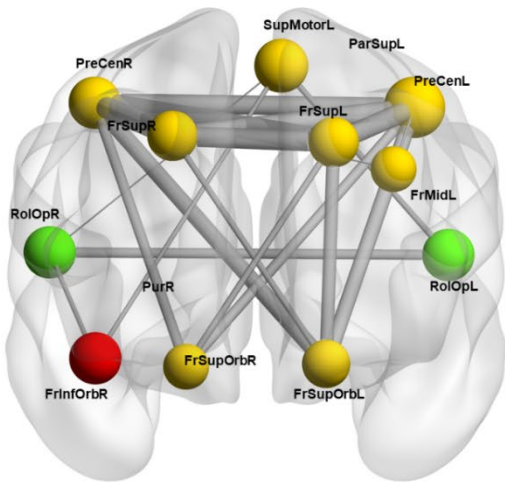
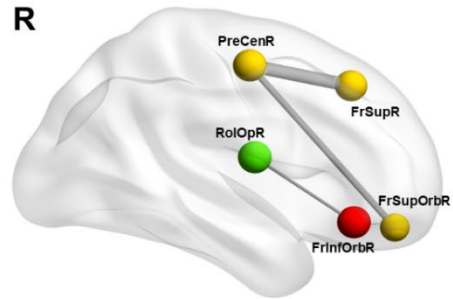
C



L



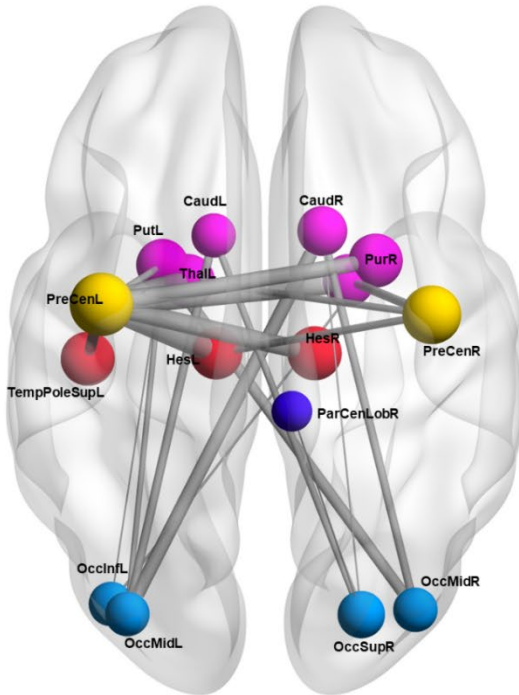
R



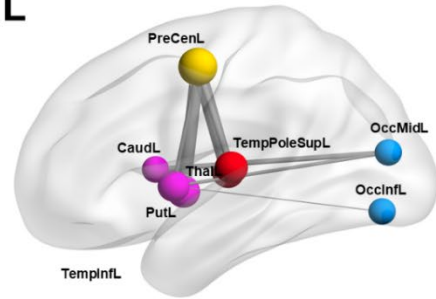
Legend

- Frontal
- Central
- Limbic
- Occipital
- Parietal
- Temporal
- Subcortical

D



L



R

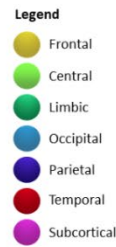
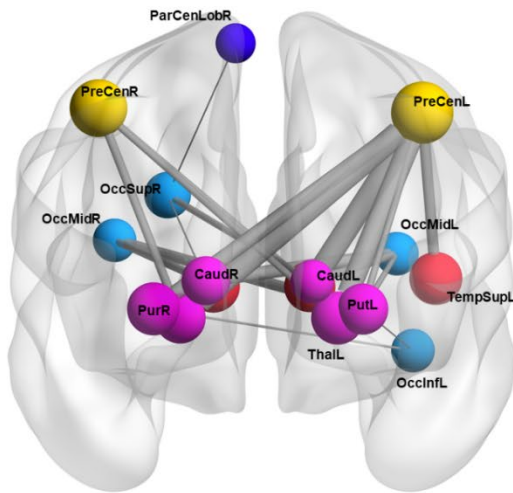
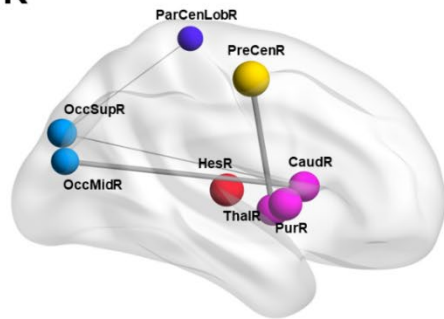


Figure A.7: Learning Curve of the different centres during the adaptation of the inter-centre cross-validation setting. In this setting one centre was used as test set, whereas the other three centres were used as training set. This setting can be strongly affected by sources of uncontrolled variances across scanners and datasets (Abraham et al., 2017; Noble et al., 2017). Therefore, we specifically tested for the effect of transferring subjects from the training set into the test set. Doing so, the test set won't be fully naïve to uncontrolled variance such as inter-scanner variability, which might benefit classification performance. In each iteration thus, two subjects (1 HC, 1FND) were transferred from the test set to the training set. An increase in classification performance (across accuracy, sensitivity, and specificity) could be observed. After the transfer of 16 – 20 subjects, and consequently with a decrease in number of subjects in the test set, the model started overfitting the results.

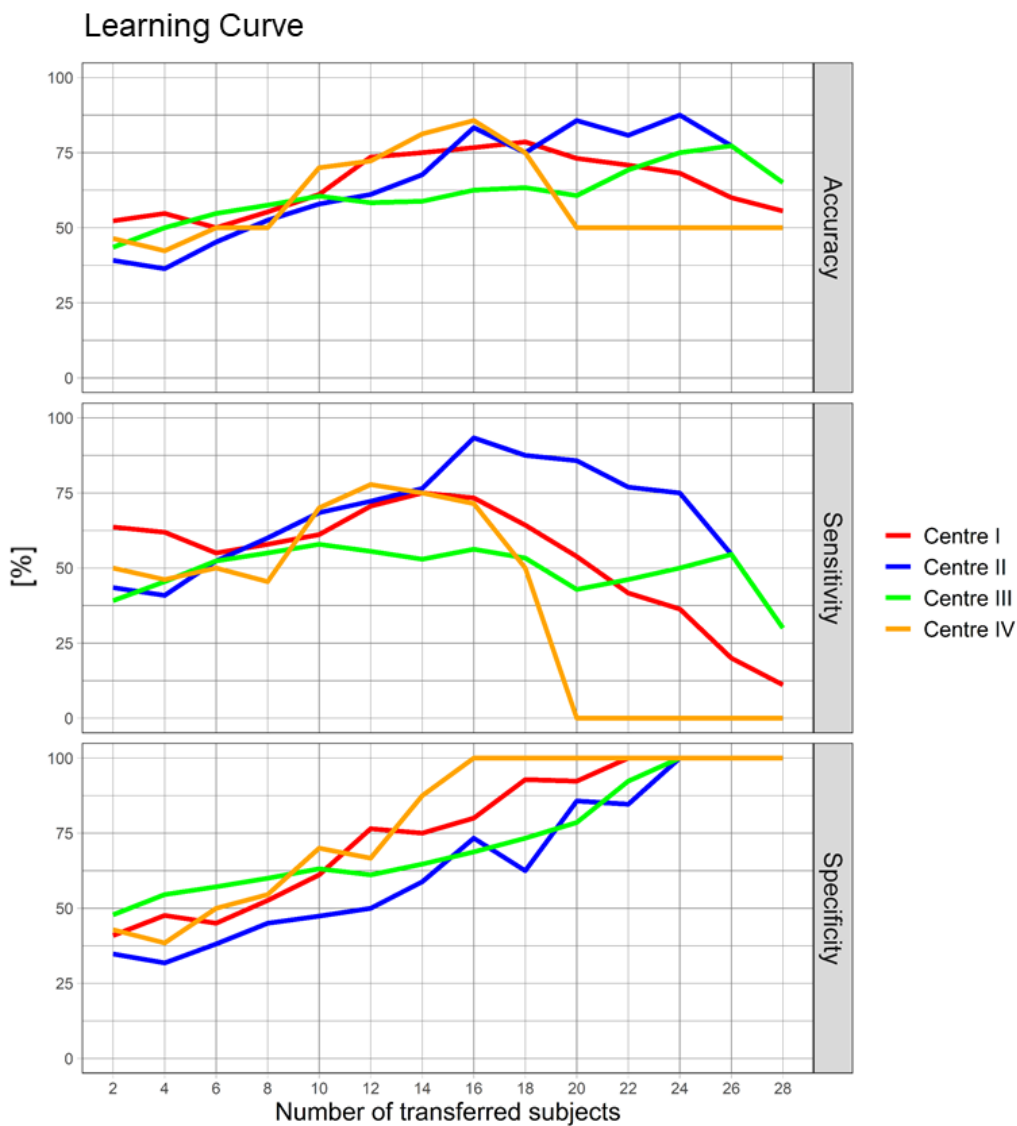


Table A.3: Logistic regression model. Logistic regression models testing the effects of anxiety (STAI), depression (BDI), psychotropic medication (yes/no), and clinical scores (CGI) taken-together and individually in (A) intra-centre cross-validation, and (B) pooled cross-validation.

A) Intra-centre cross-validation					
Centre I	Beta coefficients	p-value	Centre III	Beta coefficients	p-value
<i>intercept</i>	7.0	0.493*	<i>intercept</i>	-1.081	0.753
STAI	-0.075	0.119	STAI	0.04	0.405
BDI	-0.091	0.41	BDI	-0.1	0.298
medication	1.757	0.19	medication	1.66	0.139
CGI	-0.928	0.122	CGI	-0.321	0.673
<i>intercept</i>	3.222	0.034*	<i>intercept</i>	1.174	0.303
STAI	-0.035	0.133	STAI	-0.003	0.792
<i>intercept</i>	1.246	0.04*	<i>intercept</i>	0.843	0.067
BDI	-0.023	0.679	BDI	0.003	0.9
<i>intercept</i>	1.1	0.007**	<i>intercept</i>	0.847	0.033*
medication	-0.182	0.8	medication	0.108	0.87
<i>intercept</i>	1.576	0.08	<i>intercept</i>	1.548	0.146
CGI	-0.434	0.298	CGI	-0.415	0.481
Centre II			Centre IV		
<i>intercept</i>	0.703	0.781	<i>intercept</i>	1.107	0.649
STAI	0.014	0.72	BAI	0.032	0.673
BDI	-0.043	0.646	BDI	-0.868	0.335
medication	-1.32	0.292	medication	-	-
CGI	0.234	0.75	CGI	0.06	0.959
<i>intercept</i>	-0.032	0.979	<i>intercept</i>	1.01	0.309
STAI	0.015	0.4	BAI	0.0001	0.998
<i>intercept</i>	0.737	0.076	<i>intercept</i>	1.5	0.086
BDI	0.039	0.381	BDI	-0.054	0.418
<i>intercept</i>	1.003	0.004**	<i>intercept</i>	-	-
medication	-0.087	0.924	medication	-	-
<i>intercept</i>	1.39	0.126	<i>intercept</i>	0.793	0.705
CGI	-0.123	0.822	CGI	0.087	0.914

B) Pooled cross-validation		
	Beta coefficients	p-value
<i>intercept</i>	0.555	0.603
STAI	-0.007	0.652
BDI	0.007	0.856
medication	0.995	0.08
CGI	0.049	0.87
<i>intercept</i>	0.97	0.102

STAI	-0.002	0.809
<i>intercept</i>	0.835	<0.001***
BDI	0.005	0.787
<i>intercept</i>	0.708	<0.001***
medication	0.496	0.253
<i>intercept</i>	0.179	0.681
CGI	0.317	0.174

Abbreviations: STAI: State-Trait Anxiety Inventory, BDI: Beck's Depression Inventory, CGI: Clinical Global Impression Score. Significance levels with *** $p \leq 0.001$, ** $p \leq 0.01$, * $p \leq 0.05$.

Appendix B
Supplementary Material for Chapter 3

Neuroimaging data acquisition and pre-processing

In order to investigate neuroanatomical differences between patients and controls, we used a voxel-based morphometry approach. For anatomical imaging, a sagittal-oriented T1-weighted 3D-MPRAGE sequence ($TR = 2330$ ms, $TE = 3.03$ ms, $TI = 1100$ ms, matrix 256×256 , FOV 256 mm \times 256 mm, flip angle 8° , resolution 1 mm³ isotropic voxels, $TA = 5:27$ min) was acquired for all subjects except of three FND patients and three healthy controls. Anatomical images were pre-processed and further analysed using the Computational Anatomy Toolbox (CAT12 - <http://www.neuro.uni-jena.de/cat/>) within SPM12 (<https://www.fil.ion.ucl.ac.uk/spm/software/spm12/>). As such, a spatial adaptive non-local means denoising filter (Manjón et al., 2010) was applied, and anatomical images were subsequently resampled, bias-corrected, underwent an affine registration and were segmented using SPM “unified segmentation” algorithm (Ashburner and Friston, 2005). The output images were then further used for skull-stripping of the brain. Local hyperintensities were transformed in order to reduce the effects of local higher grey matter intensities. Eventually, an adaptive maximum a posteriori (AMAP) segmentation (Rajapakse et al., 1997) step was applied and the fractional content for each tissue type per voxel was estimated using a partial volume estimation (Tohka et al., 2004). For the final step, the images were spatially normalized using DARTEL registrations (Ashburner, 2007). Data quality and homogeneity were visually inspected, and images were subsequently smoothed using an isotropic FWHM kernel of 8mm.

Statistical Analysis of Cortisol Data

The dynamic behaviour of cortisol

The dynamic behaviour of the cortisol awakening response (CAR) and the diurnal profile was calculated using a repeated measures ANOVA was used on the fitted data using a linear mixed model (lme4 package) with fixed effect of factor group and timepoint, and using sex, smoking, wake-up time, BDI, STAI, corticosteroid medication, psychotropic medication, hormonal contraception, menstrual cycle, menopause, age, and sleep quality added as covariates of no interest (Pruessner et al., 1997). As the repeated-measures analysis represents an analysis with the concentration m as a function of the time interval t , the time interval between each sample is crucial, subjects with missing samples or extreme delays had to be excluded. As such, we excluded data from eight FND patients and nine HC as they did not properly adhere to the saliva sampling protocol with either missing samples ($N = 1$) or delays ($N = 16$) (strict sampling accuracy margin of $\Delta t > 5$ min for each post-awakening sample and $\Delta t > 15$ min for each afternoon sample (Stalder et al., 2016)).

The area under the curve (AUC)

As a static measure of the CAR, we calculated the Area-under-the-curve with respect to increase (AUC_I). As a measure for the Post-Awakening Cortisol Concentration (PACC) and Diurnal Baseline Cortisol Concentration (DBCC), the area-under-the-curve with respect to ground (AUC_G) was calculated. AUC_G and AUC_I measures were calculated according to Pruessner (Pruessner et al., 2003).

$$AUC_G = \sum_{i=1}^{n-1} \frac{(m_{(i+1)} + m_i) \cdot t_i}{2} \quad (1)$$

$$AUC_I = \left(\sum_{i=1}^{n-1} \frac{(m_{(i-1)} + m_i) \cdot t_i}{2} \right) - (m_1 \cdot \sum_{i=1}^{n-1} t_i) \quad (2)$$

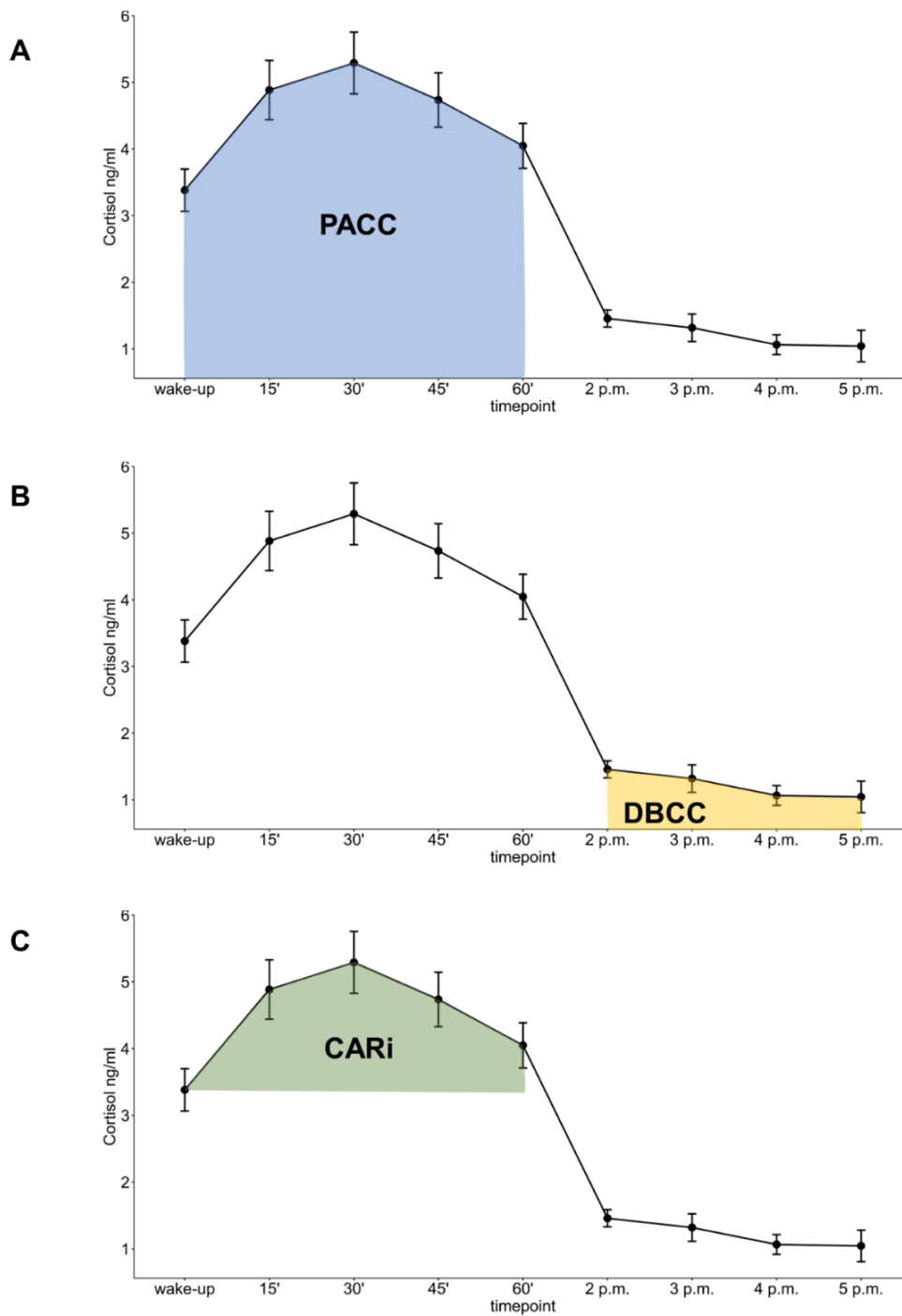
with AUC_I further applying to:

$$AUC_I = AUC_G - (m_1 \cdot \sum_{i=1}^{n-1} t_i) \quad (3)$$

with n = number of samples, t = time point, and m = cortisol value at timepoint i .

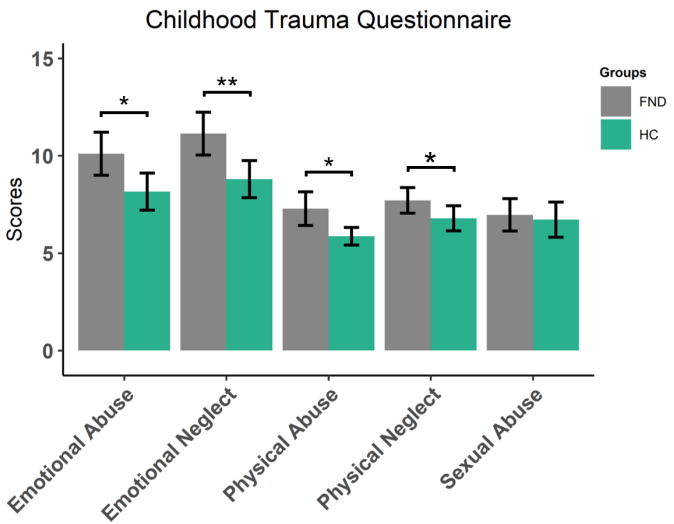
As the AUC formula takes into account the time interval between each measurement, we did not need to exclude subjects with delays and could simply account for them, Figure B.1.

Figure B.1: Graphical Illustration of the different AUC measures. (A) Post-Awakening Cortisol Concentration (PACC), (B) Diurnal Baseline Cortisol Concentration (DBCC), and (C) CARi as a measure of the cortisol awakening response.



Childhood Trauma Questionnaire

Figure B.2: Childhood trauma (CTQ scores). For visualization purposes, means and confidence intervals of childhood trauma questionnaire scores are shown. Significance codes: $P^{***} < 0.001$, $P^{**} < 0.01$, $P^* < 0.05$. Results are FDR-corrected.



Volumetric brain alterations in FND patients

Table B.1: ROI-analysis using an inclusive hippocampus mask. Results with total intracranial volume (TIV), age, gender, depression, and anxiety as covariates.

Cluster-level			Peak-level			<i>Peak coordinates in MNI Space</i>			<i>Cerebral regions</i>
<i>P_{FWE}</i>	<i>P_{FDR}</i>	<i>Cluster extent</i>	<i>P_{FWE}</i>	<i>P_{FDR}</i>	<i>Peak voxel Z-score</i>	<i>x,y,z {mm}</i>			
0.001	0.553	177	0.017	0.875	4.783	-20	-17	-14	Left hippocampus
			0.018	0.875	4.770	-18	-9	-14	
0.035	0.893	6	0.024	0.897	4.700	20	-30	-5	Right hippocampus
0.036	0.893	5	0.035	0.917	4.784	17	-6	-15	Right hippocampus

Table B.2: ROI-analysis using an inclusive amygdala mask. Results with total intracranial volume (TIV), age, gender, depression, and anxiety as covariates.

Cluster-level			Peak-level			<i>Peak coordinates in MNI Space</i>			<i>Cerebral regions</i>
<i>P_{FWE}</i>	<i>P_{FDR}</i>	<i>Cluster extent</i>	<i>P_{FWE}</i>	<i>P_{FDR}</i>	<i>Peak voxel Z-score</i>	<i>x,y,z {mm}</i>			
0.000	0.086	337	0.006	0.667	5.000	-23	-2	-18	Left amygdala
0.028	0.893	12	0.032	0.917	4.809	17	0	-20	Right amygdala

Volumetric brain alterations in FND patients uncorrected for depression and anxiety

Depression and anxiety might not necessarily represent nuisance factors in FND, but rather neural mechanisms implicated in the pathophysiology overlapping with neural circuits implicated in depression and anxiety. Therefore, we report here the findings as well without correction for depression (BDI) and anxiety (STAI).

On a whole-brain level, significant group differences were found between FND patients and female healthy controls in 15 clusters at thresholds of $P_{FWE} = 0.05$, corrected for total intracranial volume, age, and sex, Figure B.3, and Table B.3. These clusters included the following regions with decreased volumes in FND compared to controls: The bilateral nucleus caudate, the superior frontal- and temporal gyri, the supramarginal gyrus, and the angular gyrus.

Interestingly, functional abnormalities in the nucleus caudate has previously been associated with FND (Wegrzyk et al., 2018). A recent meta-analysis, however, reported a significant association between reduced anatomical volume in the nucleus caudate and lifetime major depressive disorder (Ancelin et al., 2019).

Figure B.3: Results of whole-brain analysis corrected for total intracranial volume, age, and sex. (A) Differential effect of voxel-wise comparison (HC > FND) with smaller grey-matter volume in FND in the hippocampus, nucleus caudate, dorsolateral- and orbitofrontal frontal gyri, inferior parietal gyrus, and superior temporal gyrus. Total intracranial volume (TIV), age, and sex were added as covariates. Significance codes: $P^{***} < 0.001$, $P^{**} < 0.01$, $P^* < 0.05$.

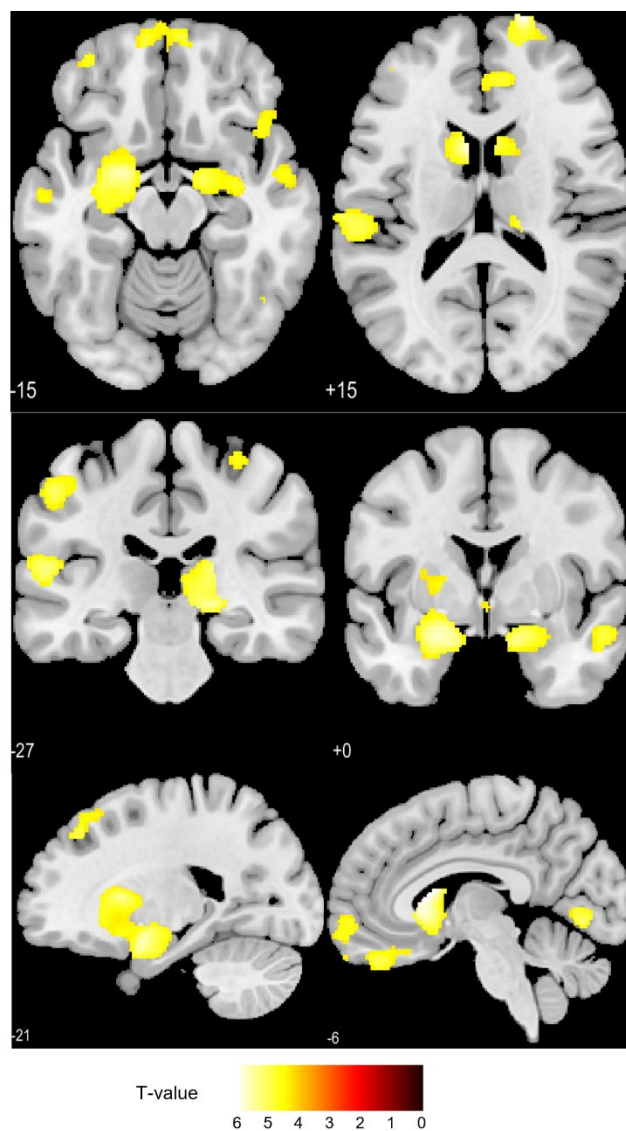


Table B.3: Whole-brain voxel-based morphometric results with total intracranial volume (TIV), age, and sex, as covariates of no interest.

Cluster-level			Peak-level			<i>Peak coordinates in MNI Space</i>			<i>Cerebral regions</i>			
<i>P_{FWE}</i>	<i>P_{FDR}</i>	<i>Cluster extent</i>	<i>P_{FWE}</i>	<i>P_{FDR}</i>	<i>Peak voxel Z-score</i>	<i>x,y,z</i>	<i>{mm}</i>					
0,000	0,000	7208	0,000	0,017	6,024	-6	14	12	Left caudate			
			0,000	0,017	6,019	-5	17	5	Left caudate			
			0,000	0,018	5,934	5	18	5	Right caudate			
0,000	0,001	1239	0,000	0,017	5,991	18	71	14	Right frontal pole			
			0,000	0,024	5,834	20	63	0	Right superior frontal gyrus			
			0,006	0,286	4,952	17	59	17	Right superior frontal gyrus			
0,000	0,000	2062	0,000	0,034	5,704	18	-30	-5	Right thalamus			
			0,000	0,047	5,582	14	3	-23	Right entorhinal area			
			0,001	0,096	5,327	20	-29	11	Right thalamus			
0,000	0,000	1647	0,000	0,061	5,515	3	60	-23	Right gyrus rectus			
			0,003	0,192	5,100	-6	42	-27	Right gyrus rectus			
			0,005	0,253	4,997	-11	60	-15	Right frontal pole			
0,000	0,008	659	0,000	0,070	5,470	-51	-30	48	Left supramarginal gyrus			
			0,002	0,164	5,196	-54	-30	32	Left supramarginal gyrus			
0,000	0,006	784	0,001	0,073	5,446	-15	38	42	Left superior frontal gyrus			
			0,002	0,178	5,158	-29	29	53	Left middle frontal gyrus			
			0,019	0,525	4,680	-17	36	54	Left superior frontal gyrus			
0,000	0,008	679	0,001	0,087	5,397	-53	-66	-36	Left cerebellum			
0,000	0,007	734	0,001	0,087	5,384	-57	-26	12	Left planum temporale			
			0,026	0,632	4,611	-48	-38	9	Left planum temporale			
0,001	0,076	295	0,001	0,095	5,352	-9	-72	2	Left lingual gyrus			
0,000	0,012	584	0,001	0,066	321	0,001	0,121	5,268	3	-12	-6	Right ventral DC
			0,003	0,191	5,117	56	3	-20	Right superior temporal gyrus			
			0,009	0,367	4,846	63	-20	-5	Right superior temporal gyrus			
0,007	0,398	110	0,014	0,454	4,757	63	-9	-9	Right superior temporal gyrus			
			0,004	0,211	5,053	51	-56	23	Right angular gyrus			
0,001	0,046	386	0,004	0,211	5,050	9	42	18	Right superior frontal gyrus			
			0,012	0,419	4,783	2	42	12	Right anterior cingulate cortex			
			0,004	0,218	5,036	44	18	-12	Right anterior insula			
0,001	0,066	324	0,004	0,218	5,036	44	18	-12	Right anterior insula			
			0,005	0,277	4,970	-62	-8	-8	Left superior temporal gyrus			
			0,006	0,286	4,940	-53	-18	-2	Left superior temporal gyrus			
0,001	0,095	262	0,007	0,327	4,898	-56	-14	-17	Left middle temporal gyrus			

0,010	0,504	78	0,008	0,343	4,875	-63	-50	5	Left middle temporal gyrus
0,009	0,454	90	0,008	0,343	4,872	-36	51	-12	Left lateral orbital gyrus
0,005	0,320	134	0,010	0,367	4,825	-41	47	12	Left middle frontal gyrus
0,015	0,625	53	0,010	0,367	4,823	44	-60	-18	Right fusiform gyrus
0,008	0,445	96	0,011	0,367	4,818	60	-12	9	Right central operculum
0,013	0,572	62	0,016	0,484	4,729	32	-27	62	Right postcentral gyrus
0,011	0,520	72	0,019	0,525	4,679	-35	41	36	Left middle frontal gyrus

Relationship between Trauma and Cortisol

Figure B.4: The permutation null distribution. The histogram of the null distribution of the singular values is presented among with the observed (red line) singular value of the significant latent component (permutation testing, $P = 0.026$). Y-axis represents frequency and x-axis the singular values obtained by the permutation testing.

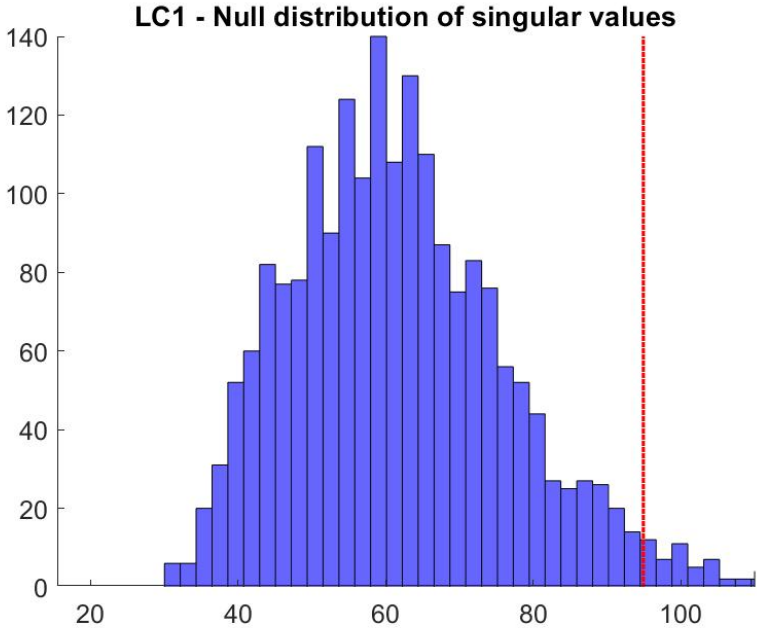


Table B.4: Exact values of mean bootstrap weights and 5th to 95th percentiles for the identified statistically significant PLSC component (LC1, $P = 0.026$).

Mean bootstrapped cortisol salience weights	Lower bound of CI	Upper bound of CI
0.890484567	0.757606185	0.937198006
0.429510963	0.221240297	0.602939479
0.150191772	0.02236804	0.270101913

Mean bootstrapped behavioural salience weights	Lower bound of CI	Upper bound of CI
-0.062020063	-0.201373381	0.12897356
0.002725078	-0.17911563	0.184562863
0.24746152	-0.00128226	0.395081572
0.000158298	-0.170965947	0.163171583
-0.013428309	-0.158624939	0.149784853
-0.055307403	-0.163979531	0.112211131
-0.215246766	-0.318906327	-0.019797615
-0.013858447	-0.211687377	0.17424141
0.152672198	-0.031379595	0.269563264
0.001297286	-0.130442861	0.138805967
-0.009958365	-0.167073143	0.145954885
-0.111976429	-0.243890006	0.083761841
-0.217460013	-0.316646365	-0.015787612
-0.024416503	-0.20645451	0.152307878
0.207862193	0.032788007	0.312500577
-0.00476066	-0.160204742	0.144057729
0.058033017	-0.070310583	0.174273539
0.016710816	-0.13500832	0.175997379
-0.023024908	-0.192136105	0.141574932
0.072244941	-0.093082159	0.224379338
-0.016144072	-0.155907179	0.161003285
-0.128897175	-0.264363266	0.032504371
-0.180740859	-0.287175891	0.013060198
-0.046828325	-0.190663452	0.110712971
-0.066999123	-0.177917042	0.053766233
-0.211229064	-0.320293906	0.028872971
-0.126629926	-0.256169291	0.123013236
0.286782461	-0.086925375	0.391764779
0.034482852	-0.108502572	0.193596472
-0.002577722	-0.15106299	0.137749057
0.031749566	-0.161402437	0.166755261
0.014143368	-0.198888878	0.196378219
0.215546793	-0.061801505	0.345044475
-0.030156543	-0.124091639	0.140696021
0.049792676	-0.101372319	0.202528272
0.130692247	-0.089654025	0.301015599
0.313900387	-0.116849708	0.400331031
0.01034836	-0.184116875	0.2255685
0.159301415	-0.031677359	0.273434138
-0.00498385	-0.137486673	0.167890943
0.135043356	-0.008045032	0.227658127
0.244239795	-0.009928114	0.329576906

0.160748167	-0.094688247	0.296177458
0.223988437	-0.023252013	0.316358418
0.018234707	-0.158415902	0.176885775

Relationship between Cortisol and Brain Volumes

Figure B.5: The permutation null distribution. The histogram of the null distribution of the singular values is presented along with the observed (red line) singular value of the significant latent component (permutation testing, $P = 0.021$). Y-axis represents frequency and x-axis the singular values obtained by the permutation testing.

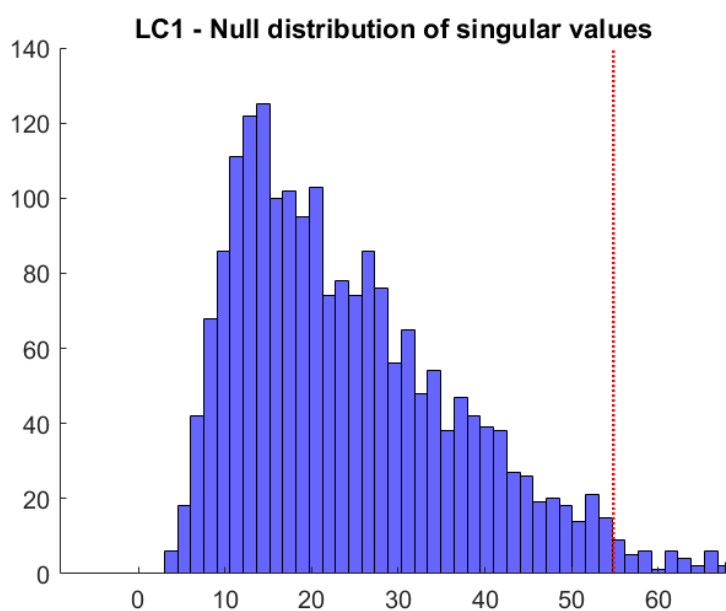


Table B.5: Exact values of mean bootstrap weights and 5th to 95th percentiles for the identified statistically significant PLSC component (LC1, $P = 0.021$).

Mean bootstrapped imaging salience weights	Lower bound of CI	Upper bound of CI
-0.483734277	-0.647126867	-0.23938829
-0.388793738	-0.52701084	-0.079069028
-0.530375888	-0.651062577	-0.291367504
-0.577530948	-0.733911237	-0.398002948

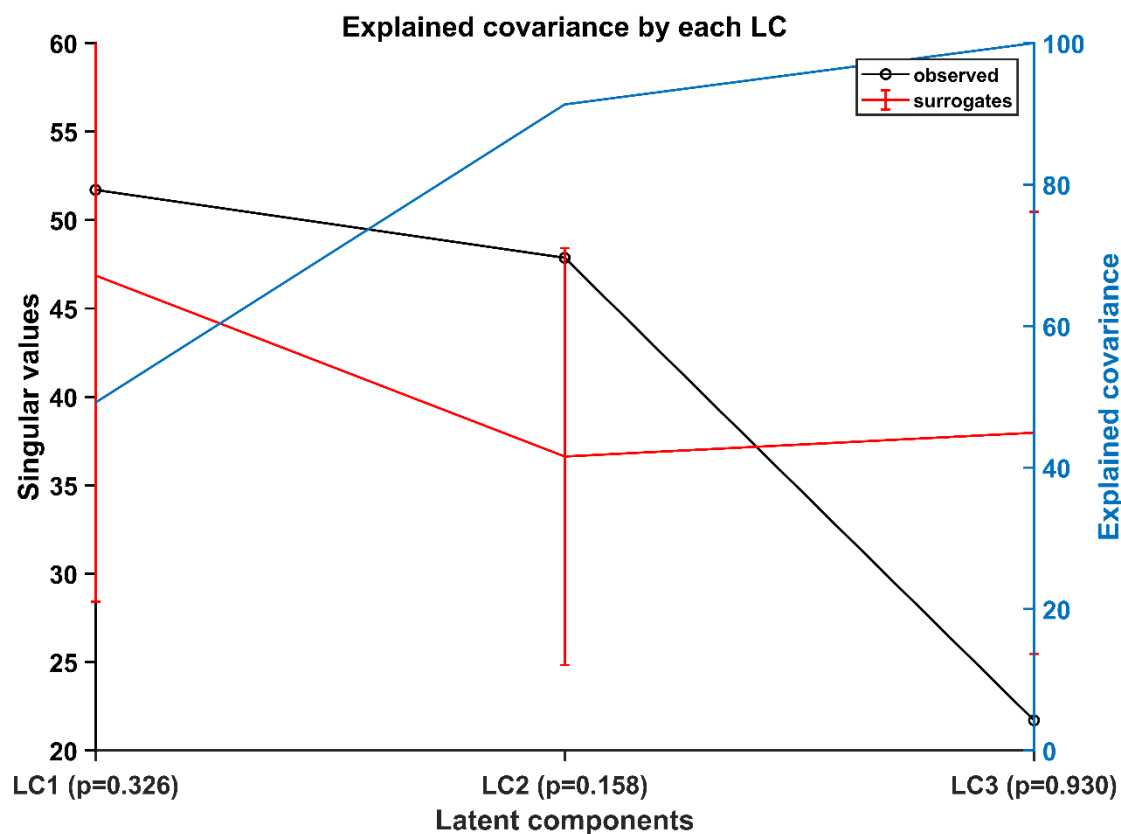
Mean bootstrapped cortisol salience weights	Lower bound of CI	Upper bound of CI
-0.285239902	-0.531519521	0.238988517
0.288737688	-0.180333335	0.603841631
0.007657464	-0.378193738	0.39154701
0.09885699	-0.302670553	0.385083878
-0.169673001	-0.483902179	0.185712182
-0.311603673	-0.54870562	0.072876155
0.712763986	0.329281254	0.808101687
-0.390	-0.520	0.013
0.001	-0.250	0.292

Relationship with symptom severity in FND

No significant multivariate correlation was identified in patients, when using symptom severity as outcome variable, and trauma scores, single estimates of cortisol measures, or brain volumes, independently, as design variables.

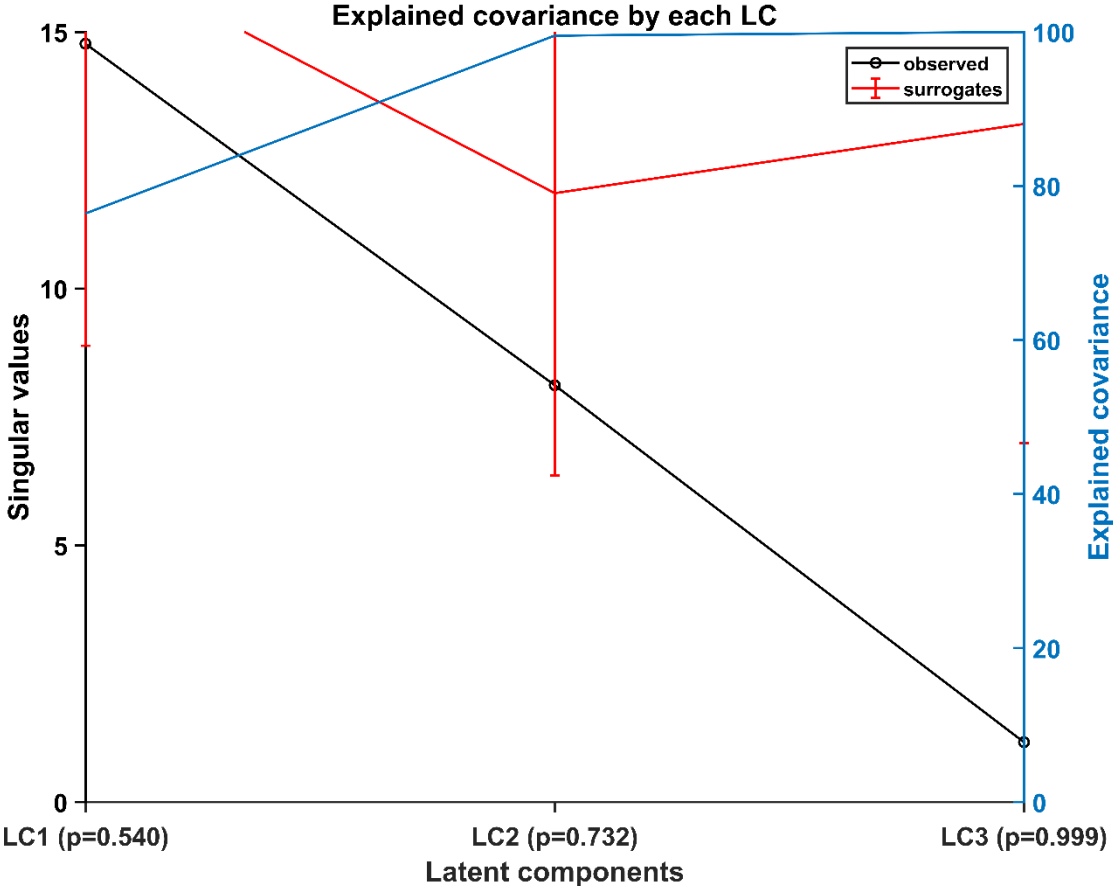
Relationship between symptom severity and trauma history

Figure B.6: Explained covariance by each latent component. In FND patients only, outcome variables were defined as symptom severity (S-FMDRS), clinical global impression score (CGI), and symptom duration (in months). Design variables were defined as the subscores of the TEC questionnaire. None of the latent components (LC) reached significance.



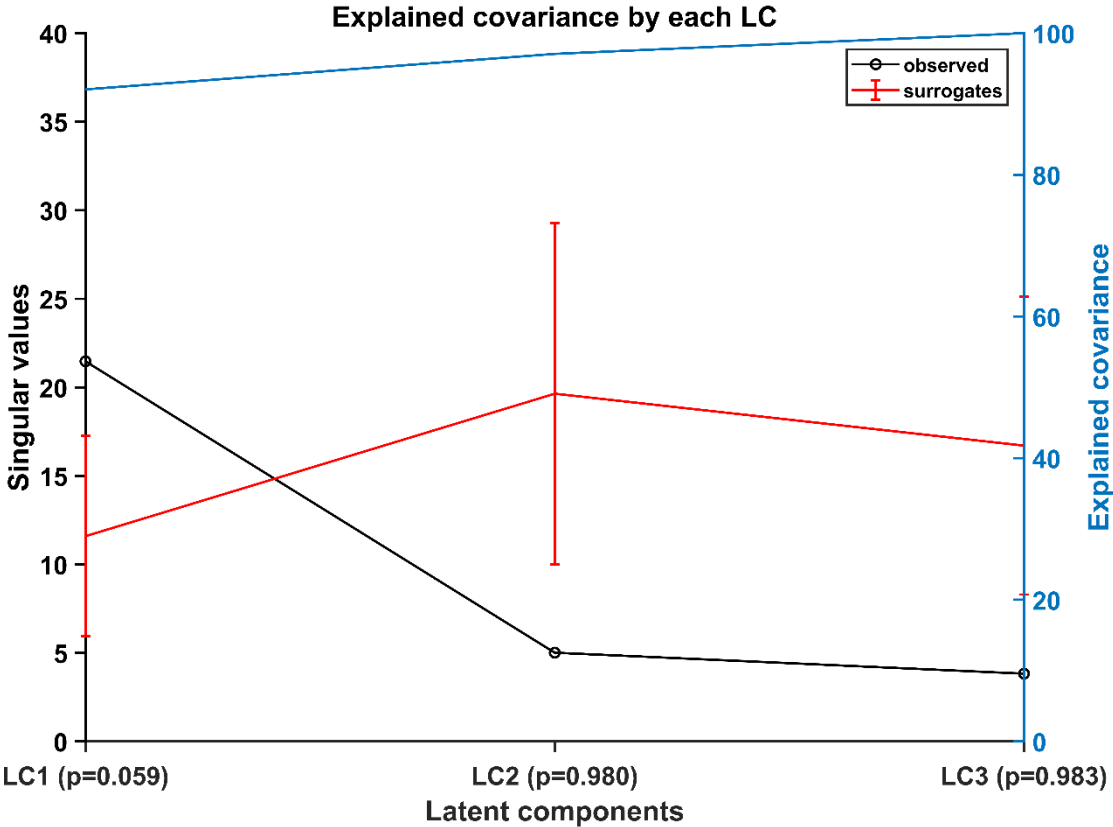
Relationship between symptom severity and cortisol

Figure B.7: Explained covariance by each latent component. In FND patients only, outcome variables were defined as symptom severity (S-FMDRS), clinical global impression score (CGI), and symptom duration (in months). Design variables were defined as the single estimates of the cortisol awakening response (CARi), the post-awakening cortisol concentration (PACC), and the diurnal baseline cortisol concentration (DBCC). None of the latent components (LC) reached significance.



Relationship between symptom severity and cortical volume

Figure B.8: Explained covariance by each latent component. In FND patients only, outcome variables were defined as symptom severity (S-FMDRS), clinical global impression score (CGI), and symptom duration (in months). Design variables were defined as the extracted mean cortical volumes per subject of the left and right hippocampus and amygdala. None of the latent components (LC) reached significance.

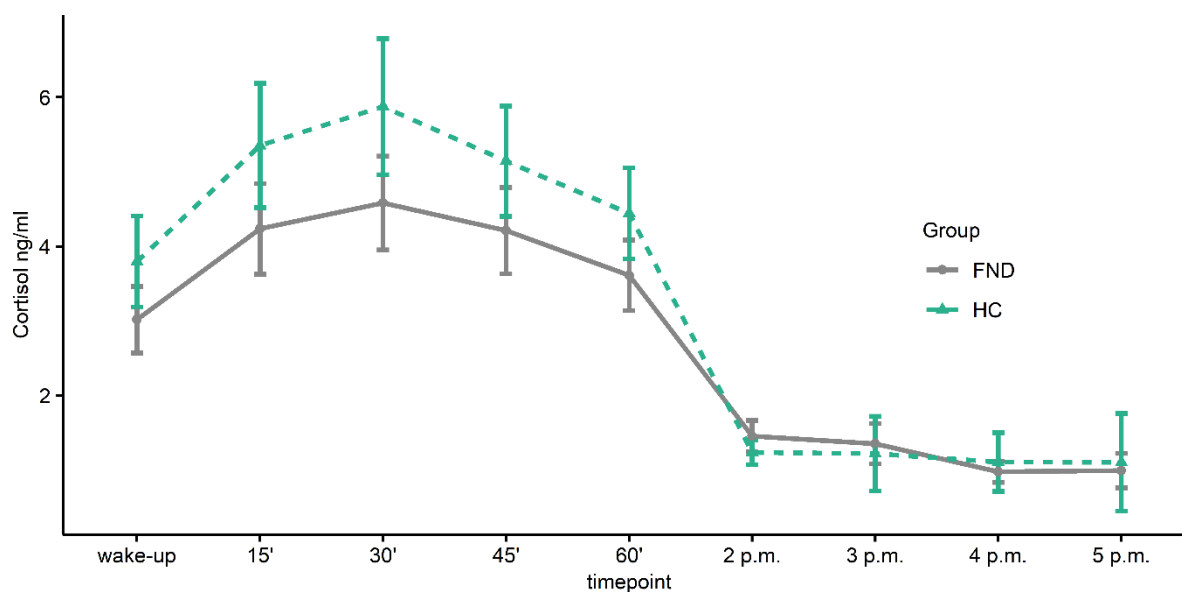


Females only

Salivary cortisol

A significant main effect of group was found for the CAR ($F(1,487) = 31.92, P < 0.0001$) with lower levels in FND than HC. Post-hoc multiple comparisons between group and timepoints, showed that FND patients and HC significantly different in their cortisol levels at timepoints 15' and 30' upon awakening ($P < 0.02$), and almost reached significance at timepoint wake-up, 45', and 60' upon awakening ($P = 0.08$), Figure B.9. No significant differences were found in the diurnal baseline cortisol (afternoon).

Figure B.9: Cortisol Profile of female FND patients and healthy. Mean and confidence intervals of daytime cortisol profile in FND patients and HC. Significance codes: $P^{***} < 0.001$, $P^{**} < 0.01$, $P^* < 0.05$.



Volumetric brain alterations in female FND patients

On a whole-brain level, significant group differences were found between female FND patients and female healthy controls in 18 clusters, corrected for total intracranial volume, age, depression and anxiety. Results did not survive FWE/FDR correction, Figure B.10A and Table B.6. These clusters included the following regions with decreased volumes in FND compared to controls: Left superior temporal gyrus, left gyrus rectus, bilateral amygdala, hippocampal- and parahippocampal gyri, as well as dorsolateral prefrontal gyri.

In line with the results on a whole-brain level, we confirmed our *a priori* hypothesis of a reduced hippocampal- and amygdalar volume in patients with FND using an inclusive brain mask, Figure B.10B. Upon extraction of ROI volumes for external analyses, we found that the hippocampus, as well as amygdala volume were significantly smaller in FND patients compared to HC ($F(1,449) = 55.97$, $P < 0.001$). Post-hoc Tukey's HSD test revealed a significant difference between female FND patients and HC in 1) the left hippocampus ($P < 0.001$), and 2) the right hippocampus ($P < 0.001$). Post-hoc Tukey's HSD test did not reveal significant differences in the amygdala.

Figure B.10: Results of whole-brain analysis in females only. (A) Differential effect of voxel-wise comparison (HC > FND) with smaller grey-matter volume in FND in the hippocampus, nucleus caudate, dorsolateral- and orbitofrontal frontal gyri, inferior parietal gyrus, and superior temporal gyrus. (B) Differential effect of mean ROI volume using a hippocampal mask (upper panel) with smaller grey matter volume in female FND patients. For both analyses, total intracranial volume (TIV), age, depression (BDI), and anxiety (STAI) were added as covariates. Results did not survive FWE/FDR correction for multiple comparisons. Significance codes: $P^{***} < 0.001$, $P^{**} < 0.01$, $P^* < 0.05$.

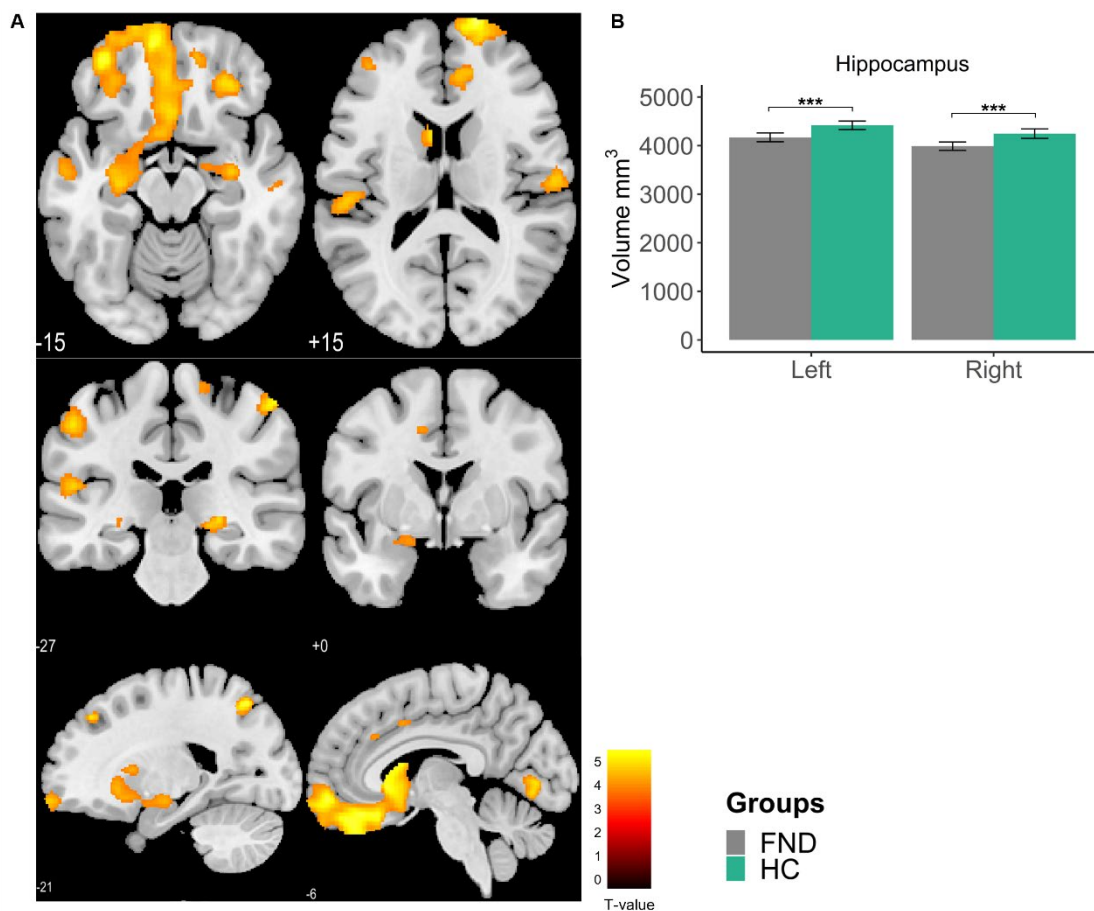


Table B.6: Whole brain analysis in females only. Results with total intracranial volume (TIV), age, depression, and anxiety as covariates. Results did not survive FWE/FDR correction.

Cluster-level			Peak-level			Peak coordinates in MNI Space			Cerebral regions
P_{FWE}	P_{FDR}	Cluster extent	P_{FWE}	P_{FDR}	Peak voxel Z-score	x,y,z {mm}			
0,000	0,000	14181	0,001	0,026	0,001	18 65 0		Right dorsolateral superior frontal gyrus	
			0,003	0,033	0,003	17 74 9		Right dorsolateral superior frontal gyrus	
			0,029	0,147	0,029	-3 17 3		Left nucleus caudate	
0,486	0,452	287	0,067	0,147	0,067	-21 -68 53		Left superior parietal gyrus	
0,060	0,147	884	0,070	0,147	0,070	65 -15 45		Right postcentral gyrus	
			0,207	0,262	0,207	54 -27 59		Right postcentral gyrus	
			0,932	0,753	0,932	53 -12 59		Right postcentral gyrus	
0,016	0,076	1310	0,079	0,147	0,079	-42 39 36		Left middle frontal gyrus	
			0,475	0,386	0,475	-41 35 45		Left middle frontal gyrus	
			0,812	0,598	0,812	-33 27 48		Left middle frontal gyrus	
0,056	0,147	903	0,169	0,249	0,169	-53 -30 47		Left inferior parietal gyrus	
			0,298	0,313	0,298	-53 -33 33		Left supramarginal gyrus	
			0,884	0,683	0,884	-50 -23 59		Left postcentral gyrus	
0,305	0,386	417	0,278	0,313	0,278	60 -14 12		Right superior temporal gyrus	
0,631	0,633	209	0,288	0,313	0,288	-23 38 44		Left dorsolateral superior frontal gyrus	
0,410	0,439	335	0,308	0,313	0,308	27 -26 -5		Right hippocampus	
			0,409	0,352	0,409	20 -32 -6		Right lingual gyrus	
			0,914	0,720	0,914	15 -39 6		Right hippocampus	
0,190	0,334	549	0,379	0,352	0,379	-5 -78 2		Left lingual gyrus	
0,451	0,439	308	0,404	0,352	0,404	-51 -17 -3		Left superior temporal gyrus	
			0,454	0,384	0,454	-54 -14 -18		Left middle temporal gyrus	
0,080	0,160	796	0,417	0,352	0,417	29 38 -15		Right anterior orbital gyrus	
			0,895	0,704	0,895	18 36 -21		Right medial orbital gyrus	
0,773	0,825	141	0,501	0,405	0,501	20 -23 66		Right precentral gyrus	
0,301	0,386	421	0,534	0,421	0,534	-51 -26 14		Left superior temporal gyrus	
			0,946	0,764	0,946	-62 -33 20		Left superior temporal gyrus	
0,439	0,439	316	0,608	0,480	0,608	62 -11 -9		Right middle temporal gyrus	
			0,833	0,598	0,833	62 -18 -6		Right middle temporal gyrus	
			0,977	0,866	0,977	56 -18 -15		Right middle temporal gyrus	

0,705	0,727	173	0,619	0,484	0,619	33	-9	-15	Right hippocampus
			0,977	0,866	0,977	20	-9	-14	Right amygdala
0,279	0,386	442	0,668	0,527	0,668	9	42	15	Right anterior cingulate cortex
0,443	0,439	313	0,685	0,530	0,685	-11	6	41	Left middle cingulate cortex
			0,840	0,598	0,840	-9	27	33	Left middle cingulate cortex
			0,917	0,720	0,917	-11	18	33	Left middle cingulate cortex
0,790	0,825	133	0,930	0,753	0,930	-47	-54	-42	Left crus I cerebellar cortex

Appendix C
Supplementary Material for Chapter 4

CAPs Insula

Figure C.1: Stability measure (1 – PAC). To assess whether a certain cluster number is good, two given data points should consistently be clustered together or in different clusters across folds. The cumulative distribution of consensus values across all pairs of data points can be computed which gives a quantification of the goodness of fit. We refer to this distribution as $P_k(c)$ with $c \in [0,1]$. From this, the proportion of ambiguously clustered pairs (PAC) can be computed (Şenbabaoğlu et al., 2014) as $PAC_k = \sum_{c=c_T}^{1-c_T} P_k(c)$ with c_T being a threshold consensus value above which an assignment is judged as not sufficiently homogeneous across folds, and k the cluster number. A lower PAC thus represents a robust cluster. The stability measure is then represented as $1 - PAC$, therefore greater values representing more robust clusters.

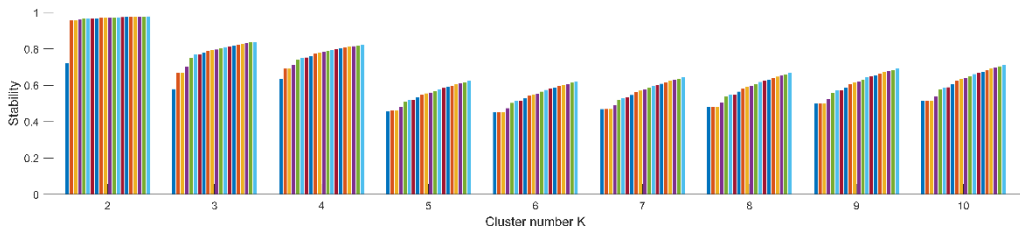


Figure C.2: Consensus matrices. The consensus matrices $[C_k]_{i,j}$ for a given number of clusters k and two data points i and j are calculated by averaging over all folds where both data points jointly entered the computations.

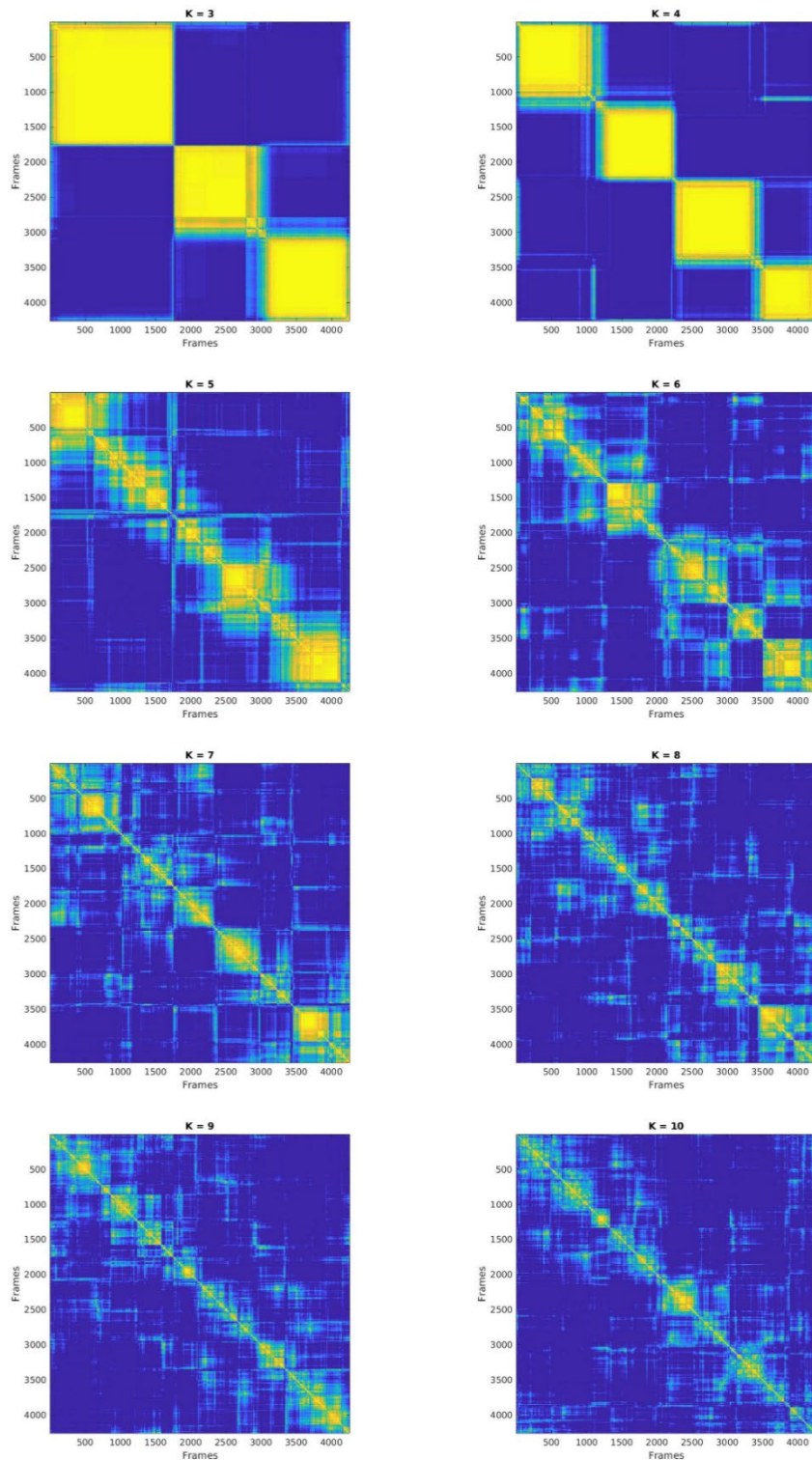
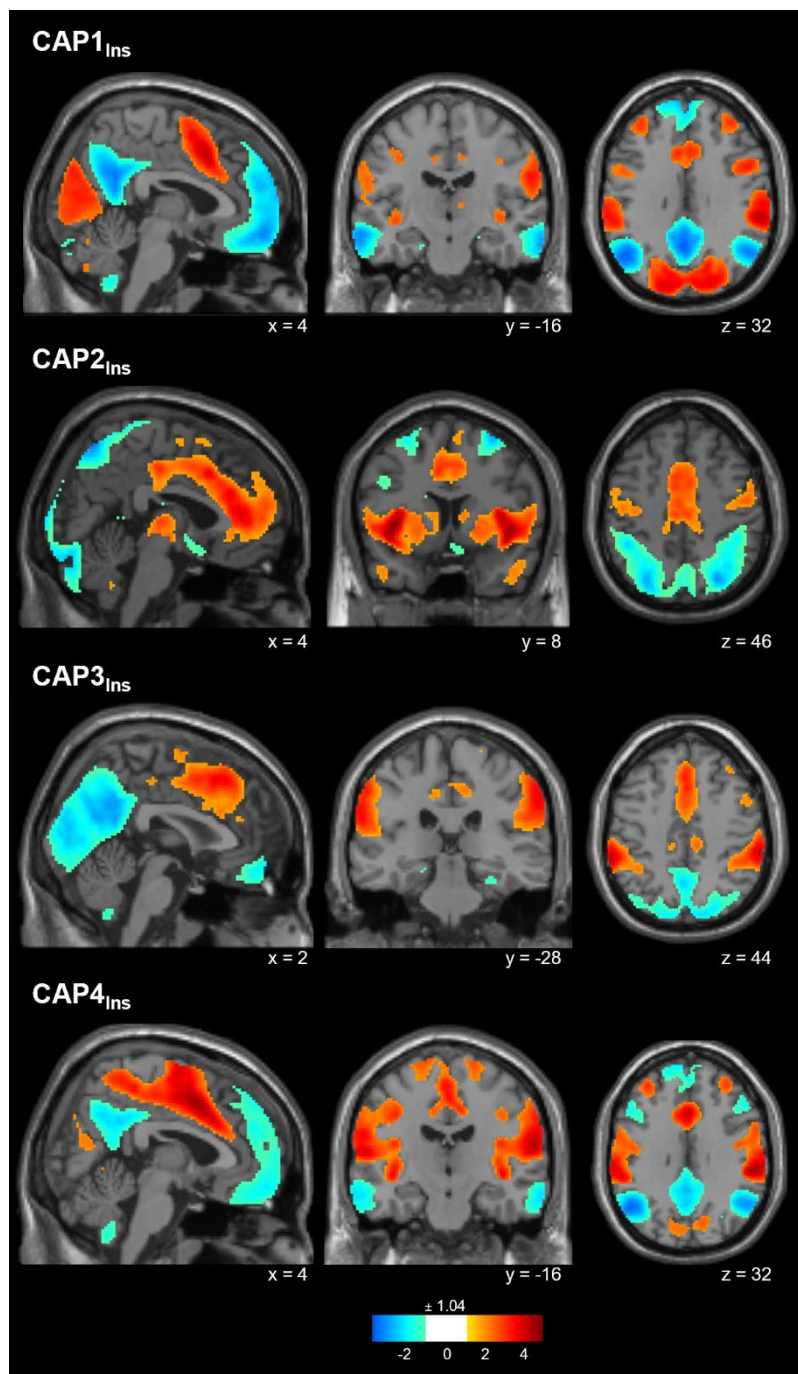


Figure C.3: Spatial pattern of the second most stable cluster ($K = 4$) of co-activation patterns (CAPs) based on insular seed activation. Four CAPs were detected. CAPs were Z-scored and only the 15% largest positive and 15% smallest negative contributions are represented in colour ($Z = \pm 1.04$) with red representing positive contributions and blue negative contributions. Locations are displayed in Montreal Neurological Institute (MNI) standard space coordinates. Abbreviations: Ins = Insula



CAPs Amygdala

Figure C.4: Stability measure (1 – PAC). To assess whether a certain cluster number is good, two given data points should consistently be clustered together or in different clusters across folds. The cumulative distribution of consensus values across all pairs of data points can be computed which gives a quantification of the goodness of fit. We refer to this distribution as $P_k(c)$ with $c \in [0,1]$. From this, the proportion of ambiguously clustered pairs (PAC) can be computed (Şenbabaoğlu et al., 2014) as $PAC_k = \sum_{c=c_T}^{1-c_T} P_k(c)$ with c_T being a threshold consensus value above which an assignment is judged as not sufficiently homogeneous across folds, and k the cluster number. A lower PAC thus represents a robust cluster. The stability measure is then represented as $1 - PAC$, therefore greater values representing more robust clusters.

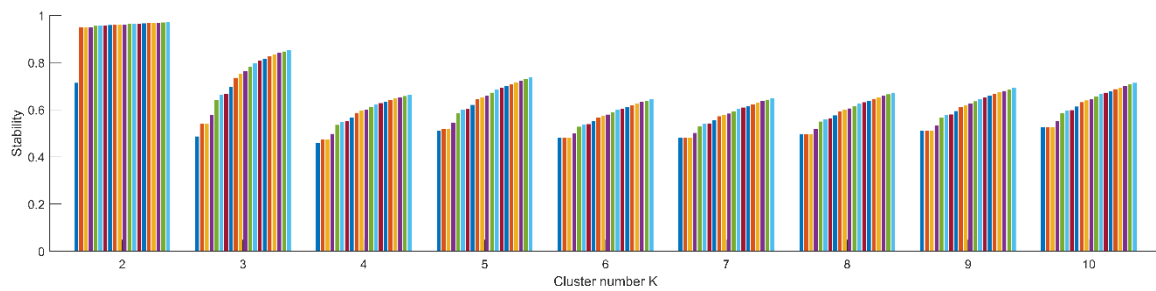


Figure C.5: Consensus matrices. The consensus matrices $[C_k]_{i,j}$ for a given number of clusters k and two data points i and j can then be extracted by averaging over all folds where both data points jointly entered the computations

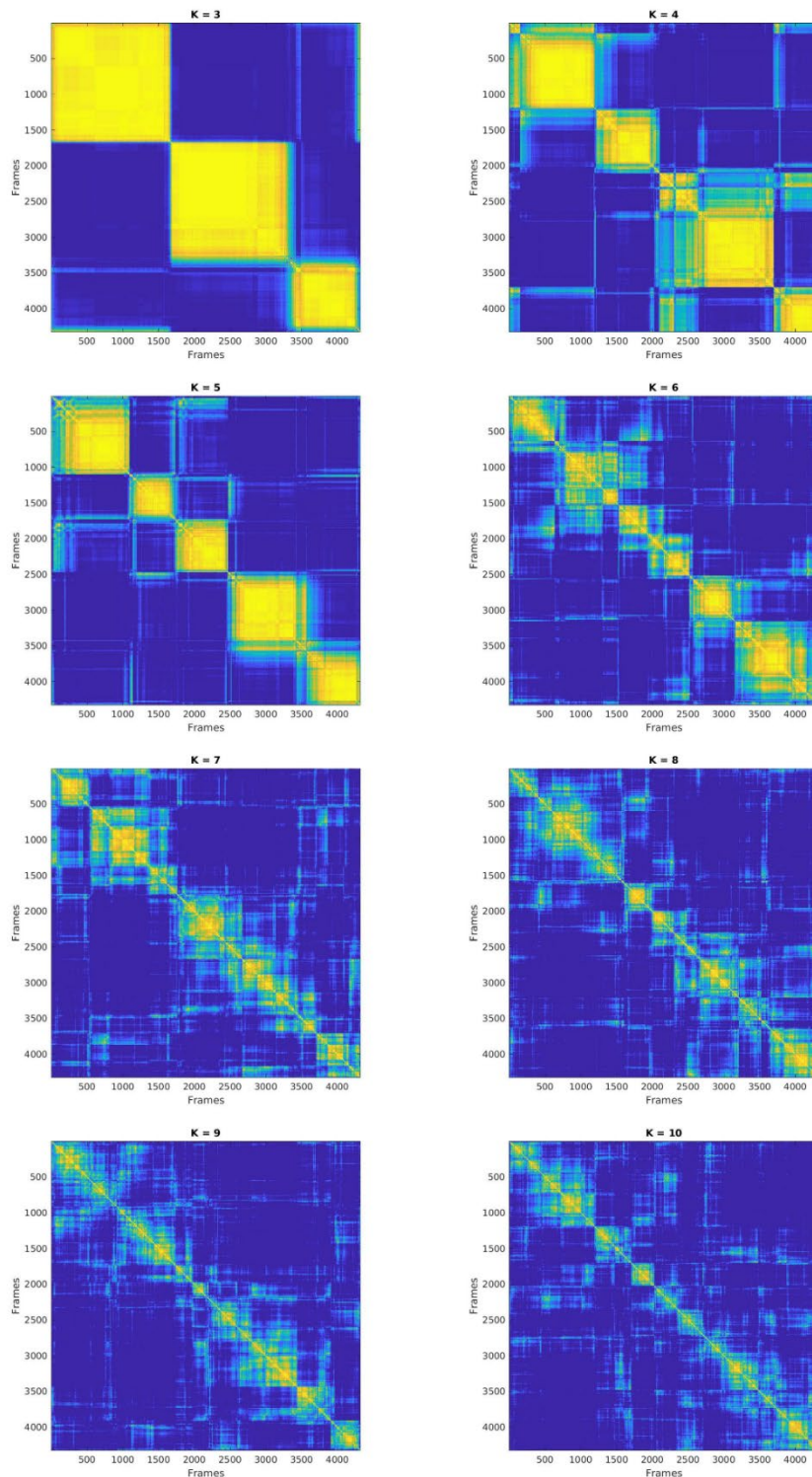
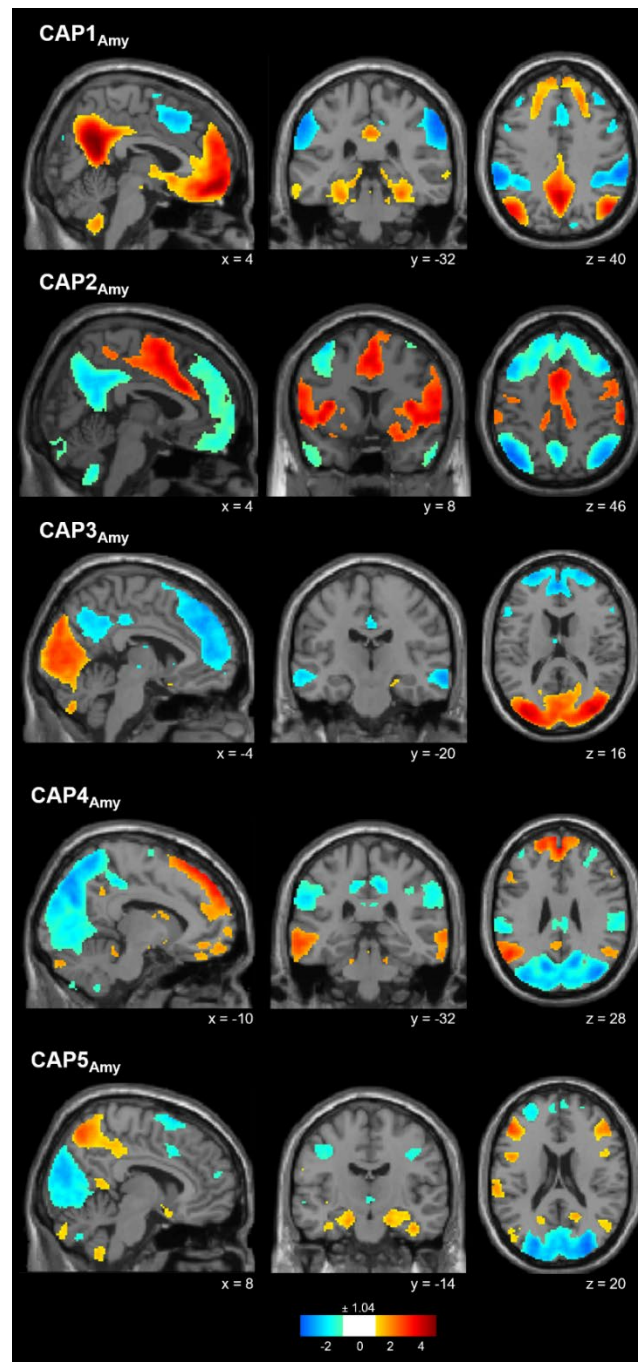


Figure C.8: Spatial pattern of the second most stable cluster ($K = 5$) of co-activation patterns (CAPs) based on amygdalar seed activation. Five CAPs were detected. CAPs were Z-scored and only the 15% largest positive and 15% smallest negative contributions are represented in colour ($Z = \pm 1.04$) with red representing positive contributions and blue negative contributions. Locations are displayed in Montreal Neurological Institute (MNI) standard space coordinates. Abbreviations: Amy = Amygdala



Partial Least Squares Analysis

Data was standardized and a correlation matrix was calculated between CAPs temporal measures and stress biomarkers and clinical variables. To find individual weights of the corresponding data tables (CAPs measures x biomarkers and clinical scores), a single value decomposition (SVD) was used on the correlation matrix. The SVD leads to different correlation components consisting of a set of behavioural weights and outcome weights, indicating the strength of contribution of each weight to the multivariate pattern. The weights were used to calculate two sets of latent variables as such that the covariance was maximized. Significance was evaluated by permutation testing (1000 permutations). Stability of weights was assessed using bootstrapping (500 bootstrapping samples). PLSC allows for examining the relationship between multiple variables with different attributes. The PLSC analysis was conducted using the CAPs measures as design variables, and stress biomarkers and clinical scores as behavioural variables.

Relationship CAPs temporal measures x biomarkers, clinical scores in FND

Figure C.11: The permutation null distribution. The histogram of the null distribution of the singular values is presented among with the observed (red line) singular value of the significant latent component (permutation testing, $P = 0.034$). Y-axis represents frequency and x-axis the singular values obtained by the permutation testing.

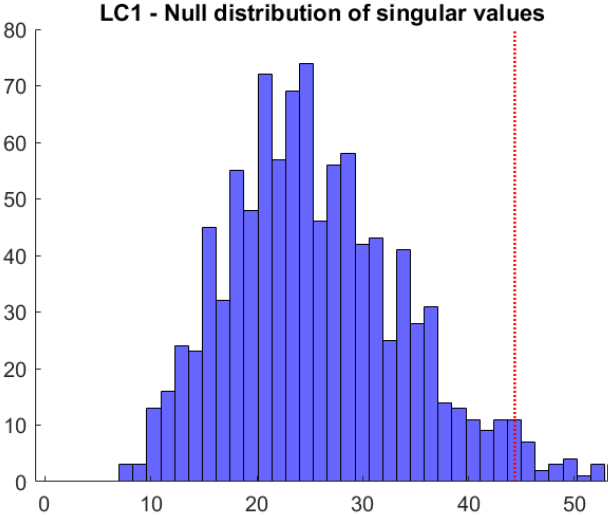


Table C.1: Exact values of mean bootstrap weights and 5th to 95th percentiles for the identified statistically significant PLSC component (LC1, $P = 0.034$).

Mean bootstrapped imaging salience weights	Lower bound of CI	Upper bound of CI
0.13714603	-0.094817643	0.320859038
0.612784758	0.413531433	0.73409599
0.673736196	0.455748473	0.760315576
0.389570719	0.228173721	0.549941799

Mean bootstrapped behavioural salience weights	Lower bound of CI	Upper bound of CI
0.651323184	0.25706752	0.789663852
0.460286958	0.103595302	0.656890509
-0.182253874	-0.464802402	0.166788698
-0.166616165	-0.410701091	0.138379642
-0.36405381	-0.541732457	-0.028674628
-0.260004189	-0.483829265	0.22419939
-0.268379354	-0.552105489	0.127180623
0.126279467	-0.254076632	0.51948551
-0.121759063	-0.392466259	0.279298449

Relationship CAPs temporal measures x biomarkers, clinical scores in HC

To evaluate whether findings were specific for FND (with regard to HC), the multivariate relationship between aberrant CAPs temporal characteristics with clinical scores and stress biomarkers was assessed in HC. A PLSC analysis was conducted using the significantly different CAPs temporal metrics as design variables, and clinical scores and stress biomarkers as outcome variables. Based on permutation testing, one PLSC component was statistically significant ($P = 0.013$). The saliences are shown in Supplementary Fig. 8. Yellow highlighted weights indicate statistical significance and were found to be robust (based on bootstrapping). The data were standardized and thus, weights can be interpreted similarly to correlation coefficients.

A significant negative correlation was found between the CAPs temporal metrics (CAP3_{Ins} – Relative Occurrence and Entries, and CAP1_{Amy} – Entries) and depression and anxiety scores – meaning that the lower the cortisol, the lesser entries, or fewer occurrence, respectively. A significant negative correlation was found between the CAPs temporal metrics and symptom severity (S-FMDRS) – meaning the lower the depression and anxiety scores, the more CAP3_{Ins} occurred, and the more entries happened to CAP3_{Ins} and CAP1_{Amy}, respectively.

Figure C.14: Partial least squares correlation (PLSC) results of the CAPs in HC. The outcome (A) and imaging saliences (B) of the significant PLSC component ($P = 0.013$) are presented. Error bars represent 5th to 95th percentiles of bootstrapping and yellow highlighted bars show robustness. The height of the bar represents the salience's weight to the multivariate correlation pattern and can be interpreted analogously to correlation coefficients as the data were standardized. Abbreviations: Amy = Amygdala, BDI = Beck's Depression Inventory, CAP = Co-activation pattern, CAR = Cortisol Awakening Response, Ins = Insula, STAI = State-Trait Anxiety Inventory.

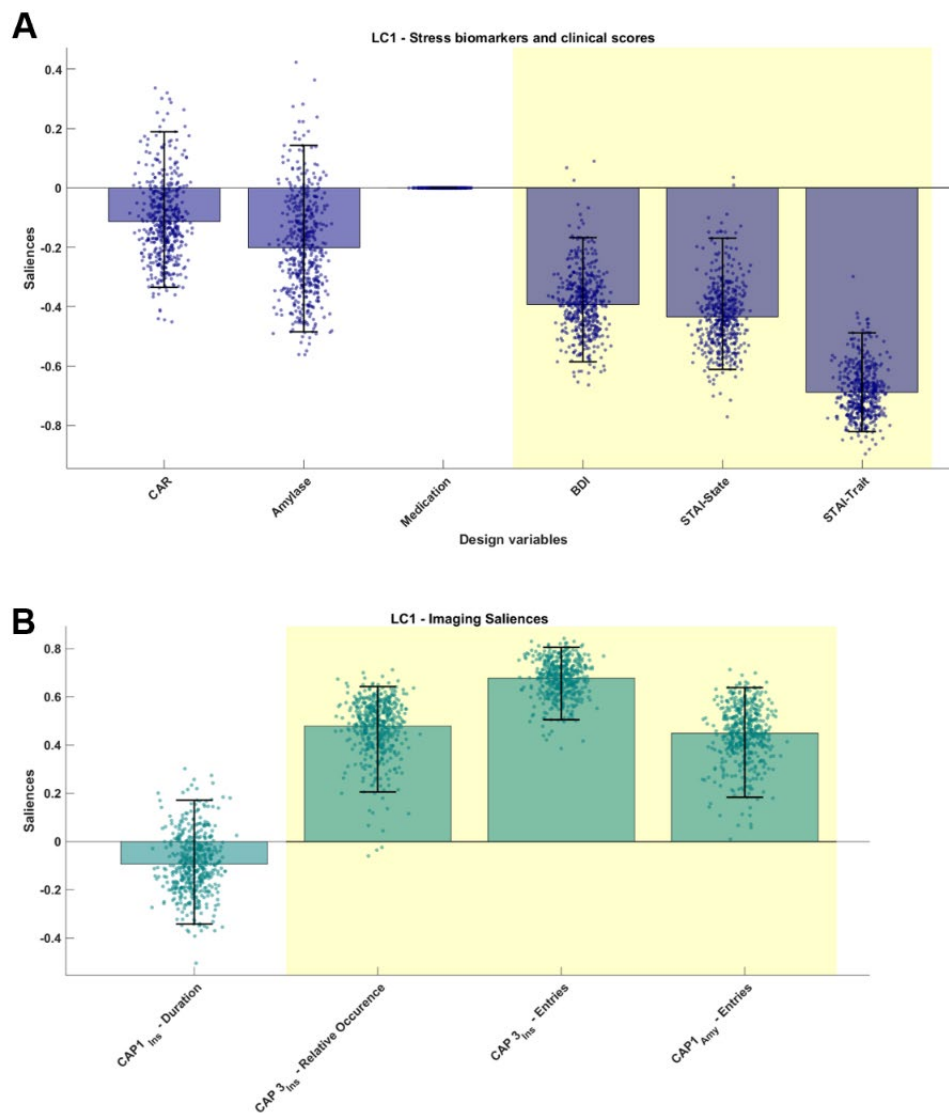


Figure C.17: The permutation null distribution. The histogram of the null distribution of the singular values is presented among with the observed (red line) singular value of the significant latent component (permutation testing, $P = 0.013$). Y-axis represents frequency and x-axis the singular values obtained by the permutation testing.

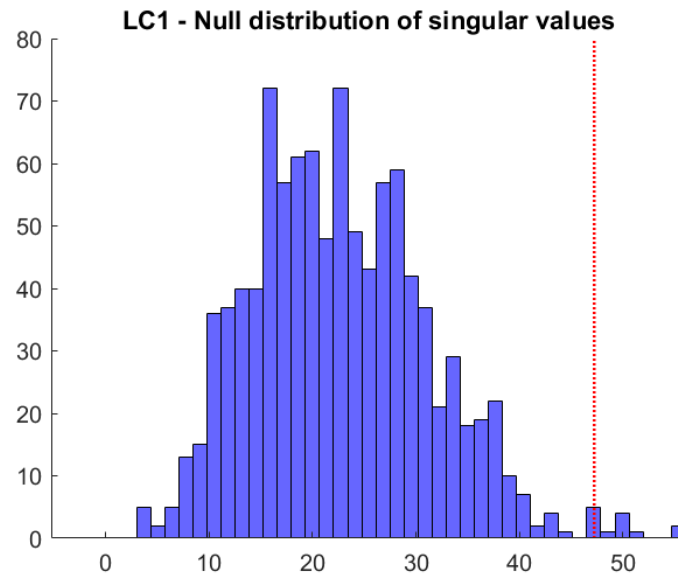


Table C.2: Exact values of mean bootstrap weights and 5th to 95th percentiles for the identified statistically significant PLSC component (LC1, $P = 0.013$).

Mean bootstrapped imaging salience weights	Lower bound of CI	Upper bound of CI
-0.114479649	-0.341975398	0.171481416
0.53494776	0.205666873	0.642978843
0.687501323	0.50544212	0.805806448
0.477563854	0.183728252	0.638667579

Mean bootstrapped behavioural salience weights	Lower bound of CI	Upper bound of CI
-0.125485328	-0.335053365	0.188802552
-0.218409658	-0.484788352	0.142884054
9.30287E-18	-7.73307E-17	9.77817E-17
-0.439410815	-0.585915999	-0.167218105
-0.473747338	-0.611632423	-0.169377828
-0.720438928	-0.821371082	-0.488636988

